Multiple Antibiotic Resistance in Gram-Negative Bacteria: Controlling Cell Envelope Barrier Function

by

Alexandra Elizabeth Trigg

A thesis submitted to the University of Birmingham for the degree of

DOCTOR OF PHILOSOPHY

December 2022

Institute of Microbiology and Infection

School of Biosciences

College of Life and Environmental Sciences

University of Birmingham

Abstract

Antimicrobial resistance is increasingly noted in clinical samples. The multiple antibiotic resistance (*mar*) operon, found in many Gram-negative bacteria, contributes to an increase in susceptibility to a broad range of antibiotics. The *mar* encoded activator, MarA, transcriptionally regulates a range of genes that contribute to multidrug resistance. Multidrug resistance can be caused by loss-of-function mutations in *marR*, encoding the repressor of the *mar* operon. Investigating the mechanisms of MarA-related multiple drug resistance in Gram-negative bacteria is essential to understand widespread antibiotic resistance.

The outer membrane and peptidoglycan layer of Gram-negative bacteria acts as an external barrier to reduce diffusion of antimicrobial agents into the cytoplasm. This work has characterised the regulation of several novel MarA targets involved in outer membrane biosynthesis and peptidoglycan hydrolysis. MarA activates *lpxC*, *lpxL* and *waaY*, which encode enzymes involved in LPS biosynthesis. Additionally, MarA represses *pbpG*, encoding a peptidoglycan hydrolase enzyme.

We hypothesised that MarA-regulated cell envelope genes could act synergistically to improve barrier function. Consistent with this, we found that combining defects in the cell wall and outer membrane barriers significantly changes antibiotic susceptibility. *mlaFEDCB*, encoding an ABC transport system involved in lipid trafficking, has previously been demonstrated to be activated by MarA. Mutating marboxes upstream of *mlaFEDCB*, *waaY* and *pbpG* independently caused no change in antibiotic susceptibility. However, mutating marboxes simultaneously resulted in significantly increased antibiotic susceptibility. Thus, this work predicts that MarA targets multiple cell envelope genes to improve barrier function, reducing antibiotic uptake and resulting in the *mar* phenotype.

Acknowledgments

Thank you so much to all the people who have helped and supported over the last four years. First and foremost, I am incredibly grateful to my supervisor, Professor David Grainger. Thank you for this opportunity, constant guidance, and for being a great supervisor throughout my PhD. I would also like to thank all members of the Grainger lab – I never expected to have such a great and supportive work environment. I'd like to thank Dr. Prateek Sharma for giving up his time to train me in the lab and help out whenever I struggled. Thank you so much to Dr. James Haycocks for helping me troubleshoot FRUIT and provide a lot of laughs along the way. To Dr. David Forrest, Dr. Emily Warman, Dr. Alistair Middlemiss, Dr. Lucas Walker, Dr. Thomas Guest, and Charles Cooper: thank you for all the coffee, the pub trips and the laughter. You've been amazing lab friends over the last four years - it means more than you can ever know.

Many thanks to Dr. Joe Wade and Anne Stringer at the Wadsworth Centre in Albany, New York for sending strains and plasmids required for FRUIT, and for advice with this technique. Thank you also to Professor Stephen Busby, Dr Damon Huber and Dr Jessica Blair for support and advice. I'd also like to thank members of the Chen Group at The University of Warwick for help with LC/MS. Thanks to Dr Yin Chen, Dr. Eleonora Silvano, Dr. Holly Shropshire, Dr. Richard Puxty and Dr. Rebekah Jones for LC/MS training and help with any lab questions I had. Thanks also to Professor Ian Henderson and Dr. Mark Blaskovich for the opportunity to help with CO-ADD (Community for Open Antimicrobial Drug Discovery) at The University of Queensland. Also, to Dr. Alysha Elliot, Dr. Johannes Zuegg, Dr. Karl Hansford, Gabrielle Lowe and Soumya Ramu for help with this internship. My gratitude to the BBSRC for

providing funding for my project through the MIBTP scheme. Thanks also to the EWS Educational Trust for additional help throughout my studies, especially this PhD project.

A final thank you to the people who provided support throughout this time. To the staff at Costa, University of Birmingham: I truly couldn't have got through this without an endless supply of coffee, and I appreciate the kindness along the way. Thank you to friends from the MIBTP scheme, especially Gabrielle Christie and Nicole McFadzean. Gabi – thanks for getting me through the hardest of times and putting up with all the fun of living together for so long. Thanks to my family, Maureen Trigg, Jim Trigg, Samantha Trigg and Lilo, for constant support. I couldn't have done any of this without all of you!

Table of Contents

List of Figures

List of Tables

List of Abbreviations

A	Adenine
ABC	ATP-binding cassette
Amp^R	Ampicillin resistance
AMV	Avian myeloblastosis virus
ANOVA	Analysis of variance
APS	Ammonium persulfate
bp	Base pair
BSA	Bovine serum albumin
C	Cytosine
cAMP	Cyclic AMP
cDNA	Complementary DNA
ChIP-exo	Chromatin immunoprecipitation with exonuclease digestion
ChIP-seq	Chromatin immunoprecipitation with sequencing
Chl^R	Chloramphenicol resistance
Ci	Curie
CIP	Calf intestine alkaline phosphatase
CL	Cardiolipin
CRP	Calf intestine alkaline phosphatase
Cryo-EM	Cryogenic electron microscopy
CTD	C-terminal domain
^oC	Degrees Celsius
dATP	Deoxyadeosine triphosphate

dCTP	Deoxycytidine triphosphate
ddH_2O	Deionised and distilled water
dGTP	Deoxyguanosine triphosphate
DksA	DnaK suppressor
DMSO	Dimethyl sulfoxide
DNA	Deoxyribonucleic acid
dNTP	Deoxyribonucleoside triphosphate
dsDNA	Double-stranded DNA
DTT	Dithiothreitol
dTTP	Deoxythymidine triphosphate
E. coli	*Escherichia coli*
ECA	Enterobacterial common antigen
EDTA	Diaminoethanetetra-acetic acid
EHEC	Enterohaemorrhagic *E. coli*
EMSA	Electrophoretic mobility shift assay
ESBL	Extended-spectrum-beta-lactamase
ETEC	Enterotoxigenic *E. coli*
ExPEC	Extraintesinal pathogenic *E. coli*
Fis	Factor for inversion stimulation protein
FNR	Fumurate and nitrate reduction regulatory protein
FRUIT	Flexible recombineering using integration of *thyA*
G	Guanine
Glc	Glucose
GlcNAc	N-acetyl glucosamine

H-NS	Histone-like nucleoid structuring protein
HCl	Hydrochloric acid
Hep	Heptose
HEPES	4-(2-hydroxyethyl)-1-piperazineethanesulfonic acid
HTH	Helix-turn-helix
IHF	Integration host factor
IM	Inner membrane
InPEC	Intensinal pathogenic *Escherichia coli*
Kan^R	Kanamycin resistance
kb	Kilobase
KDO	3-deoxy-D-manno-octulosonic acid
LB	Luria-Bertani
LC/MS	Liquid chromatography/mass spectrometry
Mar	Multiple antibiotic resistance
MarA	Activator of multiple antibiotic resistance
MarR	Repressor of multiple antibiotic resistance
MATE	Multidrug and toxic compound extrusion
MFS	Major facilitator superfamily
Mg^{2+}	Magnesium ion
MIC	Minimum inhibitory concentration
Mla	Maintenance of lipid asymmetry
mRNA	Messenger RNA
MurNAc	N-acetyl muramic acid
MWCO	Molecular weight cut-off

NAPs	Nucleoid associated protein
NTD	N-terminal domain
NTP	Nucleoside triphosphate
OD	Optical density
OM	Outer membrane
ONPG	Ortho-nitrrophenyl-β-galactosidase
PACE	Proteobacterial antimicrobial compound efflux
PAGE	Polyacrylamide gel electrophoresis
PBS	Phosphate-buffered saline
PCR	Polymerase chain reaction
PE	Phosphatidylethanolamine
PG	Phosphatidylglucosamine
ppGpp	Guanosine tetraphosphate
RNA	Ribonucleic acid
RNAP	RNA polymerase
RND	Resistance nodulation division
Rob	Right of origin binding protein
rRNA	Ribosomal RNA
rut	Rho utilisation site
SDS	Sodium dodecyl sulphate
SDS-PAGE	SDS-polyacrylamide gel electrophoresis
SMR	Small multidrug resistance
SoxS	Superoxide stress protein
ssDNA	Single-stranded DNA

ssRNA	Single-stranded RNA
T	Thymine
T4 PNK	T4 polynucleotide kinase
TBE	Tris-borate EDTA
TEMED	N,N,N′,N′-Tetramethyl ethylenediamine
Tet^R	Tetracycline resistance
T_m	Melting temperature
TNSC	Transcription buffer
Tris	Tris (hydroxymethyl) aminoethane
tRNA	Transfer RNA
TSS	Transcription start site
UTIs	Urinary tract infection
V	Volts
v/v	Volume/volume
W	Watts
w/v	Weight/volume
WHO	World Health Organisation
WT	Wildtype

Chapter 1 - Introduction

1.1. Transcription in prokaryotes

1.1.1. The central dogma of molecular biology

The central dogma of molecular biology describes the flow of genetic information from deoxyribonucleic acid (DNA) to protein (Crick, 1958; Cobb, 2017) (Figure 1.1). Firstly, RNA polymerase (RNAP) catalyses transcription by copying information from the genes within DNA into messenger RNA (mRNA) (Brenner, Jacob and Meselson, 1961). mRNAs are then translated into proteins by ribosomes. Both transcription and translation are highly regulated (Cases, de Lorenzo and Ouzounis, 2003; Tollerson and Ibba, 2020). Thus, protein expression is tightly controlled in response to environmental stimuli, which modify patterns of gene expression.

1.1.2. Transcription in bacteria

Transcription in *Escherichia coli* is catalysed by RNAP, a DNA-dependent enzyme consisting of five subunits: $\alpha_2\beta\beta'\omega$ (Zhang *et al*., 1999). The core enzyme interacts with a sigma factor to form the RNAP holoenzyme (Murakami and Darst, 2003). The first stage of transcription is initiation, and this is followed by elongation and termination (Figure 1.2).

1.1.2.1. The bacterial promoter

The RNAP holoenzyme recognises promoters, which are located upstream of the transcription start site (TSS). Promoter elements are denoted relative to the TSS at +1. Transcription begins with the recognition of specific promoter elements, allowing RNAP to form the 'closed complex'. The sigma factor is vital in enabling promoter recognition; it makes specific interactions with a conserved -35 element (5′-TTGACA-3′) and non-specific backbone interactions with a conserved -10 element (5′-TATAAT-3′) (Campbell *et al*., 2002; Chen *et al*., 2020). The spacer region between the -10 and -35 sites is 17 base pairs (bp) and is important

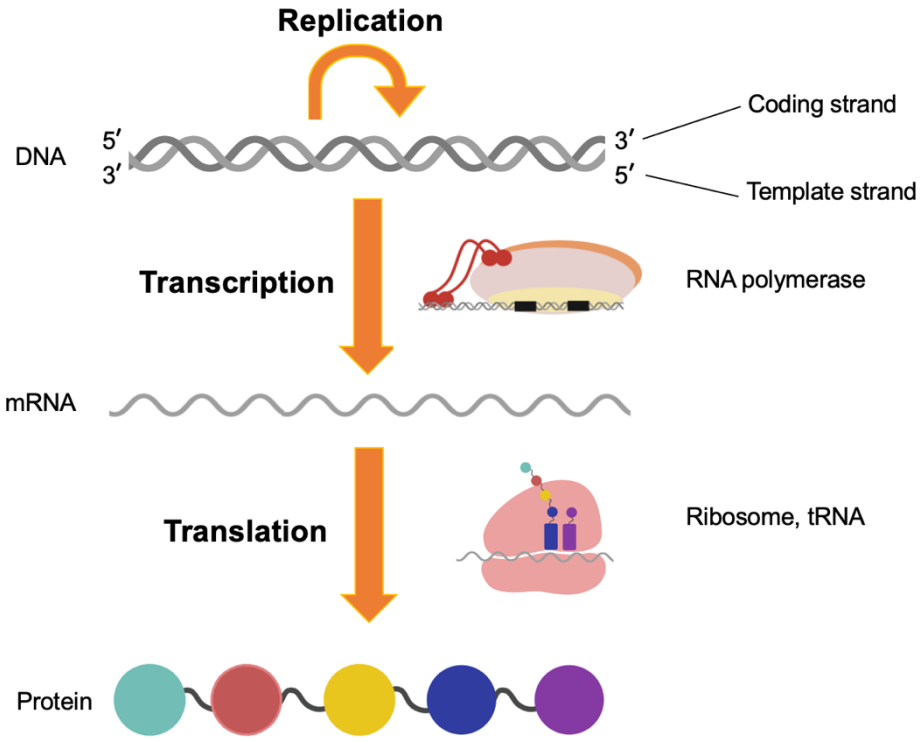

Figure 1.1. The central dogma of molecular biology.

This describes the flow of genetic information from DNA to proteins. DNA and mRNA are shown in grey. Amino acids are shown as coloured circles, separated by grey peptide bonds. The pale pink and orange oval is RNAP. Pink shapes show the ribosome and coloured shapes within the ribosome show tRNA. Created with Biorender.

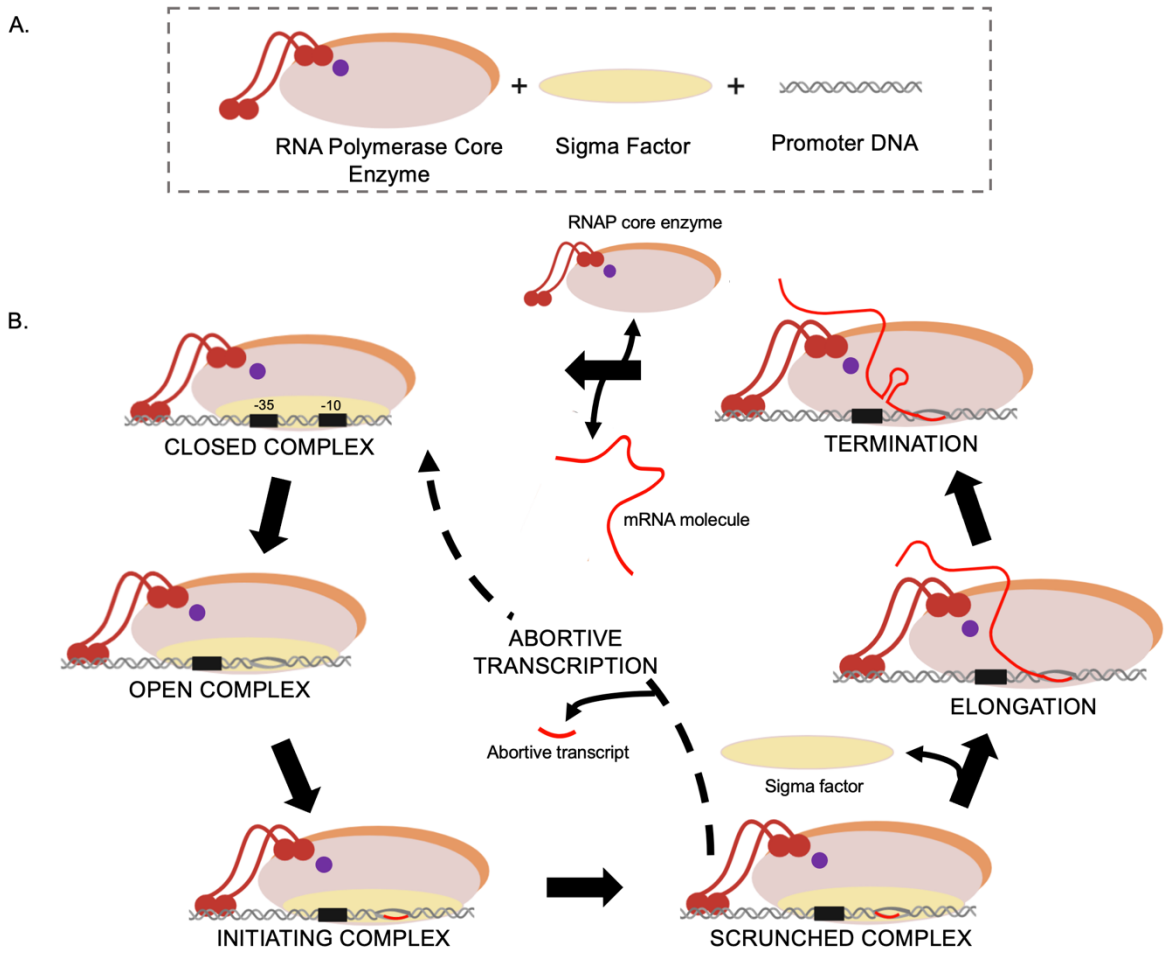

Figure 1.2. Transcription cycle of bacteria.

A. Separate components required for transcription include the RNAP core enzyme, the sigma factor and the promoter DNA. B. Schematic showing transcription initiation, elongation and termination. Promoter recognition by the RNAP holoenzyme and subsequent binding induces the formation of the closed complex. The DNA unwinds to form the open complex, and the initiating NTP is added to form the initiating complex. RNA synthesis begins by the formation of phosphodiester bonds between nucleotides. RNA may be released in abortive transcription or continue to elongation, and finally termination (adapted from Browning and Busby, 2016). Created with Biorender.

in enhancing promoter strength (Walker and Osuna, 2002; Typas and Hengge, 2006). The sigma factor makes contacts with the -18 position, and the β′ subunit of RNAP is thought to make interactions with the spacer region around the -21 position (Singh *et al*., 2011; Yuzenkova *et al*., 2011; Warman *et al*., 2021). Additional promoter elements enhance promoter strength. The extended -10 element (5′-TG-3′) immediately upstream of the -10 element interacts with the sigma factor to stabilise polymerase:DNA interactions (Barne *et al*., 1997). The UP element, found upstream of the -35 element, is found at some promoters. The UP element (5′- AAAWWTWTTTNNNAAANN -3′), targeted by the α subunit C-terminal domain (αCTD), is the only specific promoter element that is recognised by core RNAP (Ross *et al*., 1993; Estrem *et al*., 1998). UP elements increase promoter activity up to 30-fold (Rao *et al*., 1994).

1.1.2.2. Initiation

DNA downstream of the -10 element, notably the region of -2 to +2, interacts with RNAP to introduce a 17 º bend in the DNA, positioning the downstream promoter DNA above the DNA-binding cleft of RNAP (Chen *et al*., 2020). Melting, or unwinding, of around 12 bp of the DNA surrounding the TSS then occurs to produce the 'open complex' (deHaseth, Zupancic and Record, 1998; Tsujikawa, Tsodikov and deHaseth 2002; deHaseth, 2003). During open complex formation, the -10 element is recognised specifically, with the adenine of position 2 and thymine of position 6 being flipped into a specific pocket of the sigma factor (Feklistov and Darst, 2011; Bae *et al*., 2015). Promoter melting is coupled with the downstream DNA duplex moving into the RNAP cleft, whilst the single stranded template DNA of the transcription bubble is loaded into the RNAP active site (Boyaci *et al*., 2019). This allows the TSS to be positioned at the catalytic centre of the active site. Recent work has shown that the transition between the closed complex and open complex can proceed in a single step or involve

a short-lived intermediate state (Malinen *et al*., 2022). The intermediate arises due to an incompatible conformation regarding loading the template strand into the active site cleft.

The initiating nucleoside triphosphate (NTP) is placed into the active site to form the 'initiating complex' (Kapanidis *et al.* 2006; Revyakin *et al.* 2006). Ribonucleic acid (RNA) synthesis begins with the formation of phosphodiester bonds between adjacent NTPs (Steitz, 1998). As phosphodiester bond formation continues, the template strand of DNA moves into the active site 1 bp at a time and is accommodated there, a process known as 'scrunching' (Kapanidis *et al.* 2006). This continues to produce longer RNA transcripts. The mechanism is similar to a spring, in which the 'scrunched' DNA eventually springs out to release free energy and RNAP is returned to the promoter open complex state (abortive initiation) or escapes the promoter (elongation) (Arnaud-Barbe *et al.,* 1998; Feklístov *et al*., 2014; Henderson *et al*., 2017). Abortive initiation, whereby small RNA molecules are released, may occur repeatedly before the elongation phase of transcription is reached. The elongation phase is reached when the RNA molecule extends beyond approximately ten nucleotides, and the polymerase forms the 'elongation complex' (Korzheva *et al.,* 2000). Conformational changes then occur in the holoenzyme to allow release of the sigma factor (Murakami and Darst, 2003).

1.1.2.3. Elongation

Polymerase translocates along the DNA to catalyse elongation of the RNA chain by acting as a 'ratchet' device alongside substrate DNA (Averall *et al*., 2001). The transcription elongation complex is extremely stable, and transcription can proceed at 30-100 nucleotides per second (Levin, Krummel and Chamberlin, 1987). The rate of elongation is regulated by additional elongation factors known as NusA and NusG (Borukhov, Lee and Laptenko, 2005). These two proteins are essential in *E. coli* and have been demonstrated to have opposing effects on the

rate of elongation: NusG increases the rate of elongation, whereas elongation is slowed by NusA.

Both NusA and NusG physically interact with the RNAP core and Rho factor (Burns, Richardson and Richardson, 1998; Strauß *et al*., 2016). NusA, a 55 kDa protein, decreases the elongation rate by increasing polymerase pausing at natural pause sites, as well as Rho-dependent pause sites (Kassavetis and Chamberlin, 1981; Keseler *et al*., 2017). Additionally, NusA has been found to increase the efficiency of termination (Schmidt and Chamberlin, 1987). NusG, a 21 kDa protein, forms part of the antitermination complex (Li *et al*., 1992). The complex prevents premature termination of RNA synthesis by disregarding numerous intrinsic termination signals in favour of Rho-dependent termination sites (Weisberg and Gottesman, 1999; Said *et al*., 2017). The opposing activities of NusA and NusG have been demonstrated to be non-competitive and therefore the proteins interact with different sites of RNAP and Rho (Burns, Richardson and Richardson, 1998; Strauß *et al*., 2016).

1.1.2.4. Termination

Elongation continues until RNAP encounters a termination signal (Yarnell and Roberts, 1999). This can either be an intrinsic termination signal or a protein termination factor. Intrinsic termination, also known as factor-independent termination, involves a GC-rich hairpin structure within the mRNA (Yarnell and Roberts, 1999). The high proportion of guanine and cytosine bases result in the formation of hydrogen bonds and a stable hairpin structure. The GC-rich sequence is closely followed by a chain of uracil bases. As a result of a temporary pause at the hairpin, and weak uracil-adenine bonds, RNAP dissociates completely from the DNA to terminate transcription.

Termination factors include Rho, NusA, Tau and Mfd (Roberts, 1969; Whalen, Ghosh and Das, 1988; Briat *et al*., 1987; Park, Marr and Roberts 2002). Rho-dependent termination is an important mechanism in Gram-negative bacteria. Rho, an ATPase-dependent helicase, binds to the rho utulisation site (rut) in the mRNA (Hart and Roberts, 1994; Zhu and von Hippel, 1998). This site is an extended region of single-stranded RNA (ssRNA) that is rich in cytosine and poor in guanine. Recent cryogenic electron microscopy (cryo-EM) structures of the pre-termination complex reveal that Rho contains a central channel that accommodates mRNA (Molodtsov *et al*., 2022). Sequence-specific interactions are made between mRNA and Rho: 6 bp interact with the central channel and an additional 60 bp interact specifically with the exterior of Rho. The protein factor is oriented relative to RNAP to allow mechanical translocation along the mRNA, towards the 3′ end. Rho reaches the RNA-DNA hybrid and uses helicase activity to unwind the duplex structure. The RNA transcript is released from the DNA and RNAP is removed. In both cases, once polymerase dissociates from the DNA, it can re-bind a sigma factor to begin the transcription cycle once again (Murakami and Darst, 2003).

1.1.3. RNA polymerase

In Gram-negative bacteria, the RNAP core enzyme has a total molecular mass of around 400 kDa, and is made up of five subunits: β, β' ω, and two α subunits (Figure 1.3) (Buck *et al*., 2000a). The multi-subunit molecule has a crab-claw structure formed of the large β and β′ subunits (1342 and 1407 residues, respectively) (Korzheva *et al*., 2000). The claw structure is also known as the β-clamp and can switch from an open conformation to a closed conformation with the help of the hinge region located at the base of the clamp. The pincer opens for DNA loading and closes for transcription initiation. The active site channel, which accommodates the DNA double helix, is found within the β-clamp. Within the active site is a catalytic Mg^{2+}

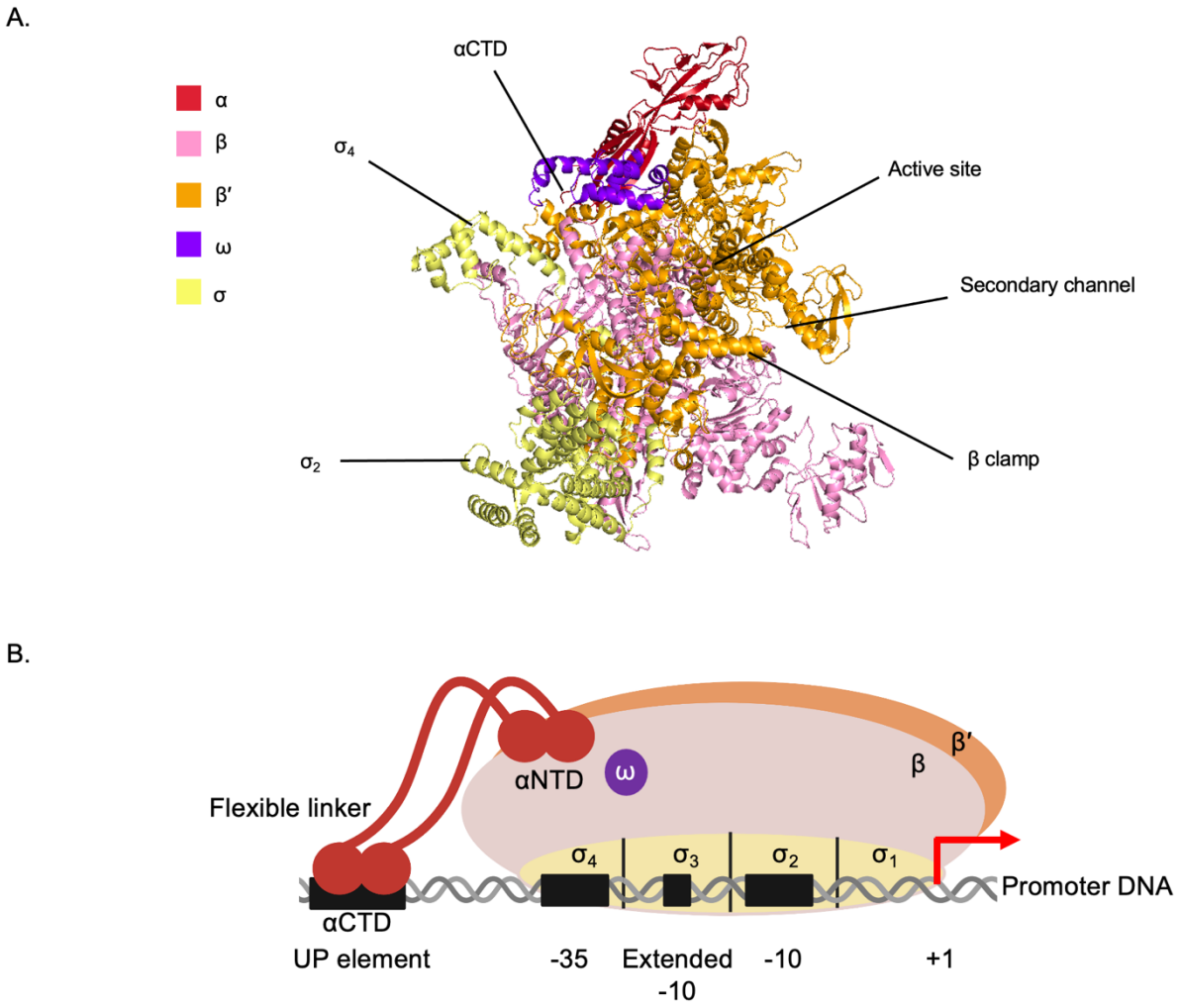

Figure 1.3. Schematic showing subunits of the RNAP holoenzyme.

A. Crystal structure of RNAP complexed with σ^{70} (Murakami *et al.*, 2013). Subunits are coloured according the the key. Image generated using PYMOL. B. The β and β' subunits are shown in pink and orange, respectively. The α are in red. αCTD interacts with the UP element found in some promoters. The ω subunit is shown in purple. The sigma factor is shown in pale yellow and consists of 4 subunits. σ_4 and σ_2 interact with the -35 and -10 elements, respectively. σ_3 binds to the extended -10 element. Adapted from Browning and Busby, 2004. Part B created with Biorender.

ion held in place by three aspartate (Asp) residues (Darst *et al*., 1989; Zhang *et al*., 1999; Murakami *et al*., 2002; Murakami, 2013). The active site contains a bridge helix that, alongside substrate DNA, acts as a 'ratchet' device (Averell *et al*., 2001). The 'ratchet' allows movement of the β-subunits to drive elongation (Bar-Nahum *et al*. 2005; Hein and Landick, 2010).

The identical α subunits (329 residues) are comprised of two independently folded domains (αNTD and αCTD). These domains are joined by a flexible linker of 13 to 15 amino acids (Jeon *et al.* 1997). αNTD (residues 8-235) is involved in the assembly of the core enzyme: the two αNTD domains form a dimer and the other polymerase subunits assemble around them (Igarashi, Fujita and Ishihama, 1991). As noted above, αCTD (residues 249-329) plays a role in promoter recognition (Burgess *et al*., 1969; Gourse, Ross and Gaal, 2000). αCTD dimerises and can recognise UP elements of promoters by binding of residue R265 to the minor groove of DNA (Ross *et al*., 1993; Blatter *et al*., 1994). It should be noted that, although the α subunits play a role in promoter recognition, the sigma factor is still required. Thus, sequence-specific transcription initiation can only occur with the full holoenzyme.

In comparison, the small ω subunit (91 residues) has no direct role in transcription. Instead it acts as a chaperone to assist correct folding of the β′ subunit (Hampsey, 2001). Many studies have demonstrated that ω is not essential (Gentry and Burgess, 1989; Kojima *et al*., 2002; Mathew and Chatterji D, 2006). However, the ω subunit has been demonstrated to facilitate small molecule ppGpp binding to RNAP. Therefore, ω has an important role in gene expression patterns during the stringent response in certain bacteria (Martucci *et al*., 2012; Gunnelius *et al*., 2014; Weiss *et al*., 2017).

1.1.4. Sigma factors

Bacteria have a range of sigma factors that recognise distinct sets of promoters in response to different environmental stimuli (Gruber and Gross 2003; Feklístov *et al*. 2014). This is important in stress-response, allowing rapid alteration of transcriptional output. The predominant sigma factor is known as the housekeeping sigma factor. This is essential for viability of the cell and recognises the majority of promoters under 'normal' conditions. Alternative sigma factors bind a smaller set of promoters.

Recognition of -10 and -35 elements is an important activity of the housekeeping sigma factor and is the vital step in promoter recognition (Figure 1.4). At the -35 site, the sigma factor interacts with the major groove of DNA from -37 to -30 (Campbell *et al*., 2002). Sequence-specific interactions are important in positioning and fixing the RNAP holoenzyme at the promoter. Conversely, the -10 element interacts with the sigma factor non-specifically by phosphate-backbone interactions (Feklistov and Darst, 2011; Chen *et al*., 2020). Specific interactions occur after DNA opening.

1.1.4.1. The housekeeping sigma factor in *E. coli*

The housekeeping sigma factor in *E. coli* is σ^{70}, also known as RpoD (Gruber and Gross, 2003). There are 1643 binding targets of σ^{70} on the *E. coli* genome (Helmann and Chamberlin, 1988; Cho *et al*., 2014). σ^{70} is formed of 4 domains, connected by flexible linker regions (Campbell *et al.,* 2002). Each domain interacts with specific promoter elements.

Domain 1 (σ^{1}) interacts with the discriminator region, located between the -10 element and the TSS (Mekler *et al*., 2002). Binding of the discriminator region induces a conformational change in the holoenzyme facilitating DNA access to the active site only after promoter recognition.

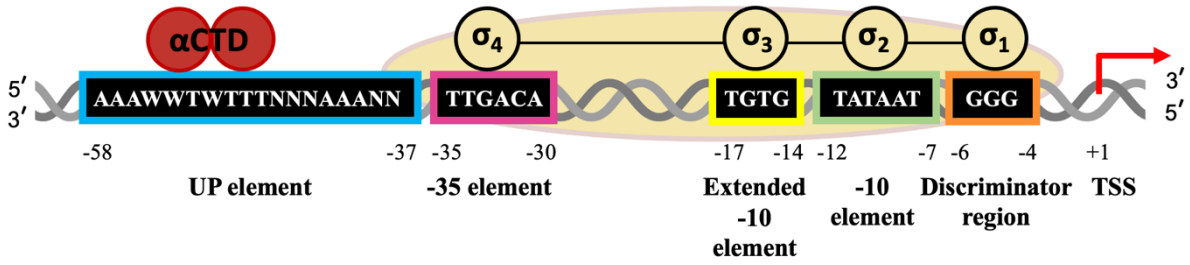

Figure 1.4. Promoter elements in bacteria.

The consensus sequence of each promoter element is shown, as well as their relative position compared to the TSS (+1). Sigma factor is shown in yellow. Binding of the sigma factor domains to promoter element is demonstrated: domains 1-4 interact with the discriminator region, -10 element, extended -10 element and -35 element, respectively. The αCTD of RNAP (red) interacts with the UP element found in some promoters.

Domain 2 (σ^2) is used in non-specific interactions with the -10 element, in which the -10 element DNA is attracted to a basic channel on the surface of the holoenzyme (Chen *et al*., 2020). Domain 3 (σ^3) interacts with an extended -10 element (Gross *et al.,* 1998). Domain 4 (σ^4) forms the important sequence-specific interactions with the -35 element (Chen *et al*., 2020). Binding of σ^{70} to the core RNAP enzyme is facilitated by σ^2 and σ^4. Firstly, a hydrophobic pocket of σ^4 interacts with a conserved α-helix of the β-subunit (Campbell *et al*., 2002; Murakami and Darst, 2003). Following this, σ^2 interacts with a coiled-coil of the β-subunit.

1.1.4.2. Alternative sigma factors of *E. coli*

E. coli has 6 alternative sigma factors, which respond to different environmental stimuli and recognise distinct subsets of promoters (Table 1.1). All sigma factors, with the exception of σ^{54}, are members of the σ^{70} family (Merrick, 1993). The σ^{70} family sigma factors are structurally related, and often have overlapping but distinct groups of promoter recognition sites. The number of promoters recognised by alternative sigma factors differs greatly, between 7 promoters (σ^{19}) and 903 promoters (σ^{38}) (Gruber and Gross, 2003; Maeda, Fujita and Ishihama, 2000; Cho *et al*., 2014). It should be noted that σ^{19} was originally thought to bind 1 promoter. Recent evidence suggests that this alternative sigma factor actually binds 7 promoters (Cho *et al*., 2014).

σ^{38}, or RpoS, is a key alternative sigma factor of *E. coli*, and is important in adaptation to stationary phase of growth and starvation response (Lange and Hengge-Aronis 1994, Mandel and Silhavy 2005; Rahman *et al*., 2006). Environmental stresses, such as nutrient availability or entry into stationary phase growth, cause an increase in σ^{38} activity, due to an interaction with sigma factor binding protein Crl (Figure 1.5) (Pratt and Silhavy 1998; Bougdour, Lelong

Table 1.1. σ factors produced by *E. coli*.

The alternative name for each sigma factor is included, along with function and the reported number of binding site (Maeda *et al*., 2000; Gruber and Gross, 2003). Note that FecI has been hypothesised to only have 1 binding site, but newer ChIP-chip evidence suggests 7 FecI binding sites (Cho *et al*., 2014).

σ factor	Function	Number of binding sites
σ^{70} / RpoD	Housekeeping σ factor for general gene expression	1643
σ^{38} / RpoS	Starvation / stationary phase	903
σ^{32} / RpoH	Heat shock	312
σ^{54} / RpoN	Nitrogen metabolism	180
σ^{24} / RpoE	Extracytoplasmic stress e.g. heat, extracellular proteins	65
σ^{28} / RpoF	Flagellar assembly	51
σ^{19} / FecI	Iron starvation	7

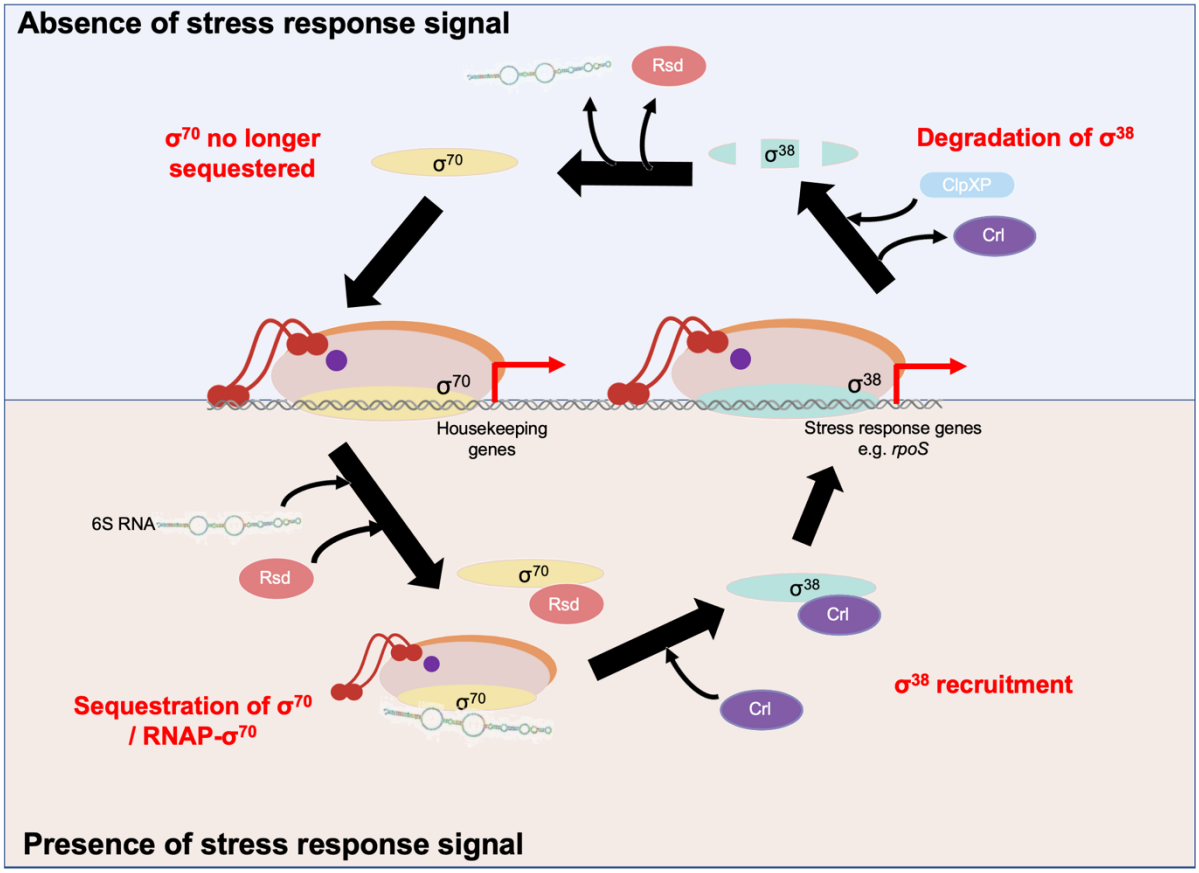

Figure 1.5. Regulation of sigma factor switching between σ^{70} and σ^{38} under starvation or stationary phase conditions.

In the presence of a stress response signal, σ^{70} is sequestered by binding of protein Rsd to free σ^{70} and binding of RNAP-σ^{70} to 6S RNA. Simultaneously, σ^{38} is recruited by sigma factor binding protein Crl. σ^{38} binds to RNAP to activate stress response genes, including *rpoS* in a positive feedback mechanism. Once the stress response signal is absent, free σ^{38} is degraded by protease ClpXP (Zhou and Gottesman, 1998). σ^{70} is released from Rsd and 6S RNA and remaining σ^{38} is outcompeted for RNAP binding. Transcription of housekeeping genes is resumed. Created with Biorender.

and Geiselmann, 2004). Simultaneously, σ^{70} activity is reduced via an interaction with anti-sigma factor Rsd (Jishage and Ishihama, 1998). It has been suggested that sequestration of σ^{70} by Rsd requires crosstalk with non-coding 6S RNA, as Rsd alone appears to only have a minor effect on transcription (Lal, Krishna and Seshasayee, 2018; Rahman, Hasan and Shimizu, 2006). Crl and Rsd proteins redirect transcription towards stress response genes. Studies have demonstrated that σ^{38} regulates approximately 23 % of the *E. coli* genome (Wong *et al.,* 2017).

σ^{54} is structurally unrelated to the other sigma factors in *E. coli*. σ^{54} does not interact with -10 or -35 elements, but instead interacts with -12 and -24 positions on specific promoters (Wigneshweraraj *et al.,* 2008). The σ^{54} holoenzyme requires additional DNA-binding proteins; integration host factor (IHF) and enhancer binding proteins (Buck *et al*., 2000b; Colland *et al*., 2000). IHF binds to specific DNA sequences to cause bending of the DNA (Friedman, 1998). Bending of the DNA allows the σ^{54} holoenzyme to interact with an upstream ATP-dependent enhancer to allow the formation of an open complex (Yang *et al*., 2015).

1.2. Regulation of transcription

1.2.1. Molecular mechanisms of transcriptional regulation

Transcription in bacteria must be highly regulated to allow variation in the expression of genes at the appropriate time. There are various mechanisms by which transcription is regulated: chromosomal structure, promoter sequence, sigma factors, small molecules, and transcription factors (Figure 1.6).

1.2.1.1.Chromosomal structure

Most bacteria contain a single circular chromosome of double-stranded DNA (dsDNA) (Holmes and Jobling, 1996). In a relaxed form, DNA is usually negatively supercoiled and one

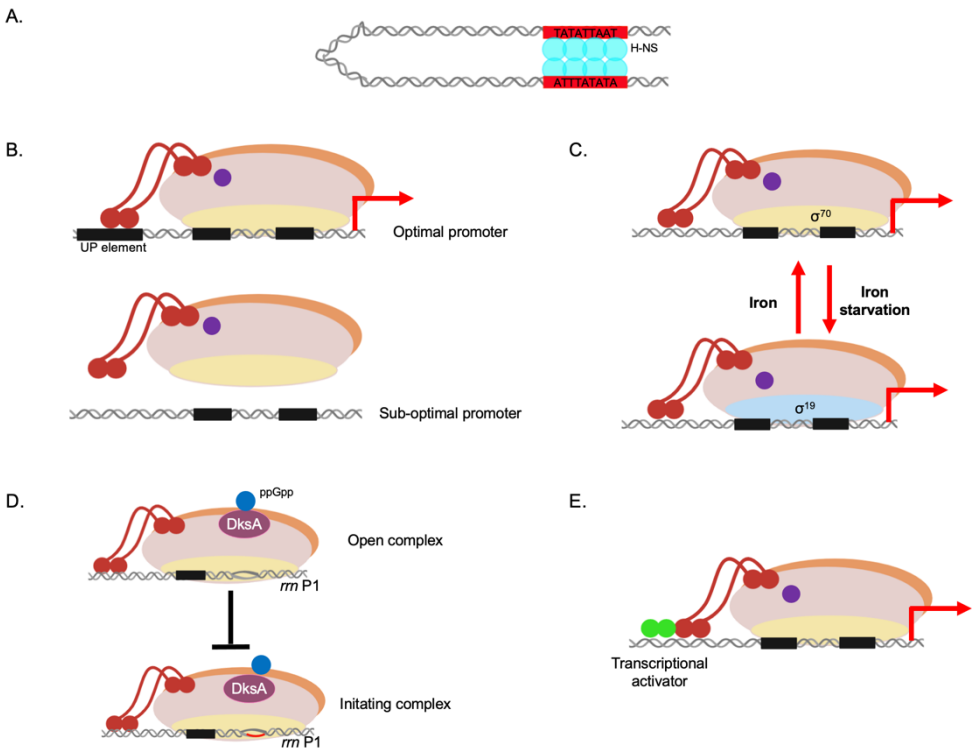

Figure 1.6. Schematic demonstrating different transcription regulatory mechanisms in bacteria.

A. Chromosomal structure can affect transcription from promoters due to DNA bending, wrapping and supercoiling. Nucleoid-associated proteins (NAPs) (e.g. H-NS) bind to sequences within DNA to change DNA topology and further genome condensation. H-NS is shown in cyan to bind AT-rich sequences. B. Promoter sequences themselves act to regulate transcription. Some promoters have optimal promoter elements and additional promoter elements to recruit RNAP. Other promoters do not have optimal promoter elements and are not favoured by RNAP. These promoters often require additional regulators to increase transcription. C. Sigma factors have specific sets of promoters that they bind. The housekeeping sigma factor may be displaced by an alternative sigma factor under environmental stress to cause a change in transcription. σ^{19} (blue) displaces σ^{70} (yellow) under iron starvation conditions to redirect RNAP towards transcription of iron starvation genes. D. Small molecules can bind to RNAP to affect activity. ppGpp (blue) interacts with RNAP bound to DnaK suppressor (DksA) (purple) to destabilise open complex formation at certain genes, including *rrn* P1 which encodes ribosomal RNA (Gaal *et al.*, 1997; Dalebroux and Swanson, 2012). E. Transcription factors can interact with RNAP to affect the rate of transcription. A transcriptional activator is shown in green to recruit RNAP by binding αCTD.

complete turn of the DNA helix is 10.5 bp (Rhodes and Klug, 1981). Negative supercoiling is advantageous as it aids in compaction of DNA into the bacterial cell, as well as facilitating strand unwinding during replication and transcription (Stuger *et al*., 2002; Witz and Stasiak, 2010). The shape of DNA can be changed by further supercoiling, bending or wrapping. Nucleoid-associated proteins (NAPs) interact with DNA to change DNA topology (Dorman and Dillon, 2010). Examples of NAPs include Factor for Inversion Stimulation (Fis) and histone-like nucleoid-structuring (H-NS) protein. H-NS binds to AT-rich regions and oligomerises, resulting in bending of the double helix (Navarre *et al*., 2006; Lang *et al*., 2007). Clusters of H-NS are able to interact to cause genome condensation. Variable DNA supercoiling is a fundamental principle in controlling gene expression, likely due to changes in the distribution of RNAP.

1.2.1.2. Promoter sequences

Promoter sequences act themselves as regulators of genes. Genes are expressed at different levels because some promoters have low basal activity, or no activity at all. This is largely based on the sequences of the -10 and -35 element sequences (Campbell *et al*., 2002). Additional promoter elements increase promoter activity; many of the strongest bacterial promoters contain UP elements whereas weak promoters have UP elements with low consensus sequence or no UP element at all (Gourse, Ross and Gaal, 2000; Browning and Busby, 2016). The strength of promoters determines the distribution of RNAP, therefore determining the extent of gene expression. This type of regulation is a static mechanism that allows genes to be expressed correctly under ‘normal’ conditions. It does not enable gene expression changes in response to environmental stimuli.

1.2.1.3.Sigma factors

Sigma factors alter the binding specificity of polymerase by alternating between the housekeeping sigma factor and alternative sigma factors. Sigma factor regulation is an excellent example of how gene expression changes in response to environmental stimuli. Sigma factors themselves can be regulated by anti-sigma factors and non-coding RNA molecules, which sequester σ^{70}, enabling an alternative sigma factor to bind polymerase (Lal, Krishna and Seshasayee, 2018; Rahman, Hasan and Shimizu, 2006). It has recently been determined that phosphorylation of alternative sigma factors acts as an additional regulation mechanism. It is proposed that some alternative factors are in an inactive state until they are phosphorylated (Iyer *et al*., 2020). Once phosphorylation occurs, the sigma factor can bind RNAP.

1.2.1.4. Small molecules

Small ligands are able to contact RNAP to cause changes in transcriptional patterns. For example, ppGpp, a small molecule that plays a role in stringent response, interacts with RNAP and works by destabilising the open complex at some promoters (Ross *et al*., 2013; Barker *et al*., 2001). The promoters targeted by ppGpp are mainly those that express genes required for the ribosome, the translation machinery. By preventing transcription of such genes, translation of all RNA in downregulated.

Additionally, the availability of nucleotides can act as a regulatory mechanism. For instance, the genes encoding curli fibres, which are involved in extracellular adhesion and cell aggregation, have been reported to be modulated by the intracellular nucleotide concentration (Garavaglia, Rossie and Landini, 2012). This may act through additional sensor proteins, or through a signalling molecule, such as c-di-GMP (Weber *et al*., 2006). Another example is that

of ribosomal RNA (rRNA), which encodes the RNA component of the ribosome. Transcription of rRNA requires a high concentration of NTPs, and therefore a low availability of NTPs acts as a limiting step in transcription of rRNA, and therefore translation of other genes (Gaal *et al*., 1997).

1.2.1.5. Transcription factors

Transcription factors are important proteins that interact with the promoter and cause up- or downregulation of transcription (Babu and Teichmann, 2003). *E. coli* contains an estimated 314 different transcription factors (Pérez-Rueda and Collado-Vides, 2000). The proteins bind specific binding sites within the promoter DNA, known as 'operator' sequences (Robison, McGuire and Church, 1998). Binding to a specific operator sequence allows regulation of specific promoters only, similar to regulation by sigma factors. Transcription factors often bind as multimers (Robison, McGuire and Church, 1998). The proteins can cause activation or repression of transcription initiation. Some transcription factors can act as both an activator and repressor depending on the promoter and operator sequence they bind (Pérez-Rueda and Collado-Vides, 2000).

Some transcription factors bind a wide range of promoters, thereby regulating large numbers of genes. In *E. coli*, it is estimated that 50 % of regulated genes are controlled by 7 global transcription factors (CRP, FNR, IHF, Fis, ArcA, NarL and Lrp) (Vicente, Chater and De Lorenzo, 1999; Martinez-Antonio and Collado-Vides, 2003; Perrenoud and Sauer, 2005). In contrast, specific transcription factors regulate only a small set of promoters, with only 24 single-target regulators reported in *E. coli* K-12 (Shimada *et al*., 2018; Shimada *et al*., 2021).

Transcription factors are grouped into families based on sequence, structure and function (Pérez-Rueda and Collado-Vides, 2000). Common families include the LuxR family, OmpR family, LacI family, LysR family, AraC/XylS family, and CRP family. Briefly, the CRP family will be discussed as this family are the best-studied transcription factors and have historically been known as the paradigm of transcriptional regulators, as well as AraC family transcription factors, which are the topic of research throughout this work (Kolb *et al*., 1993).

CRP family: The cyclic AMP receptor protein (CRP) family of transcription factors respond to a variety of stress signals, including temperature and oxidative stress (Jeong, Baumlerb and Kaspar, 2006; Uppal *et al*., 2011; Li *et al*., 2002). The best-known member of the CRP family is CRP, which has a regulon of around 200 genes in *E. coli* (Figure 1.7) (Zheng *et al.,* 2004). Many CRP-regulated genes encode proteins involved in catabolism. Fumarate and nitrate reductase regulator protein (FNR) is another member of the CRP family, which regulates genes involved in the response to a lack of oxygen (Shaw, Rice and Guest, 1983). These transcription factors are characterised by a C-terminal helix-turn-helix (HTH) DNA-binding motif and an N-terminal domain to bind effector molecules, such as cyclic AMP (cAMP) (Weber and Steitz, 1987; Korner, Sofia and Zumft, 2003). CRP forms dimers of two identical subunits (Lawson *et al*., 2004). Dimerisation requires hydrophobic interactions between amino acids in the N-terminal domain. Subsequently, the dimer binds cAMP to bring the C-terminal domain into an optimal position to interact with DNA. CRP-cAMP interacts with the major groove of DNA (Lawson *et al*., 2004). There are three activating regions (AR1-3) on the surface of CRP, which make contacts with the RNAP holoenzyme (Busby and Ebright, 1999; Benoff *et al*., 2002). Thus, activation by CRP results in increased RNAP binding, and therefore elevated promoter activity.

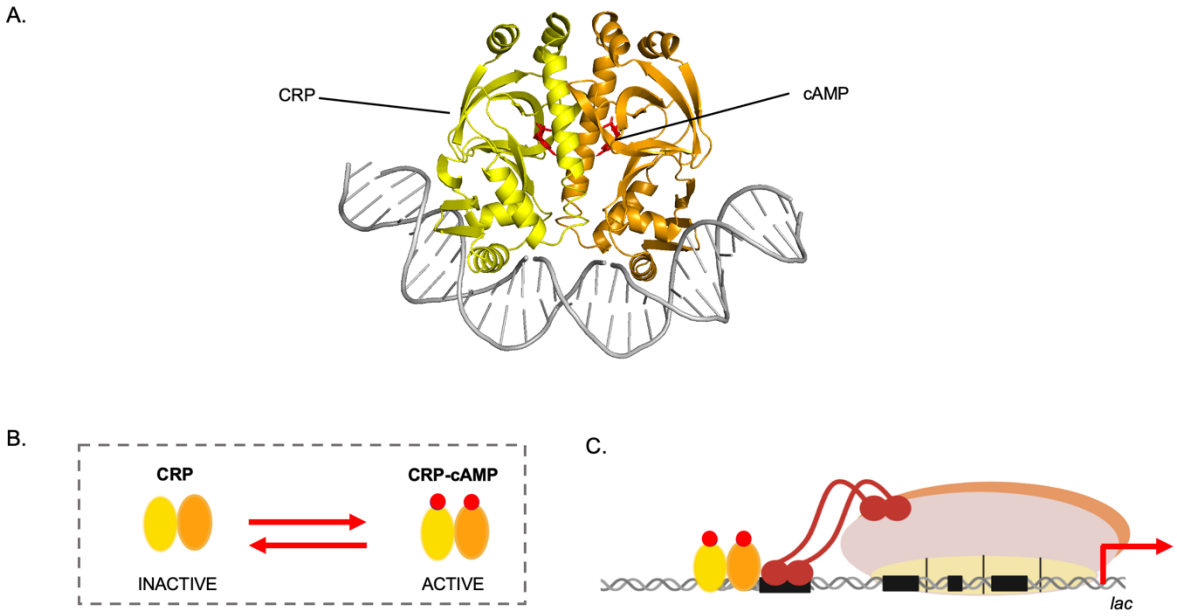

Figure 1.7. The CRP transcription factor.

CRP is shown in yellow and orange. cAMP is shown in red. A. Crystal structure of CRP complexed with cAMP and DNA (Schultz, Shields and Steitz, 1991). CRP-cAMP binds with DNA as a dimer. DNA shown in grey. Image generated using PYMOL. B. cAMP binding to CRP causes activation of the transcription factor. C. CRP bound to DNA can recruit RNAP for activation of transcription. An example of this is the *lac* operon. Panel C created with Biorender.

AraC/XylS family: The AraC family constitutes 830 members across a wide range of Gram-negative bacteria (Egan, 2002). Some of these transcription factors are specific and some regulate a vast array of genes. The proteins are involved in stress response, pathogenesis, and carbon metabolism. In *E. coli,* there are several well-characterised AraC family transcription factors: AraC, MelR, MarA, SoxS and Rob (Greenblatt and Schleif, 1971; Howard *et al.,* 2002, Duval and Lister, 2013). MarA, SoxS and Rob are multidrug resistance regulators, which play a vital role under antimicrobial stress. RamA is an additional multidrug resistance regulator that is not found in *E. coli*, but is important in other Gram-negative bacteria (George, Hall and Stokes, 1995; van der Straaten *et al*., 2004). Typically, these regulatory proteins are characterised by a conserved 100 amino acid C-terminal DNA-binding domain containing two HTH motifs that bind asymmetrical sites (Rhee *et al.,* 1998; Grainger *et al*., 2003). The N-terminal domain is approximately 200 amino acids, and acts to sense ligands. These DNA-binding proteins are highly similar and recognise the same DNA target site, although Rob differs in that it contains an additional C-terminal domain and binds more degenerate sequences (Martin *et al*., 1999; Kwon *et al*., 2000). Some AraC family proteins contain an additional N-terminal dimerisation domain to enable oligomerisation (Soisson *et al.,* 1997).

1.2.2. Transcriptional activation

Transcriptional activators stimulate transcription by increasing RNAP binding to promoters. They often target promoters with low, or no, basal activity. There are four main mechanisms by which activators recruit RNAP: Class I and Class II activation, indirect mechanisms, including remodelling of promoter DNA, and anti-repression (Figure 1.8).

1.2.2.1.Class I activation

Class I activation targets operator sequences upstream of the -35 element (Ebright, 1993).

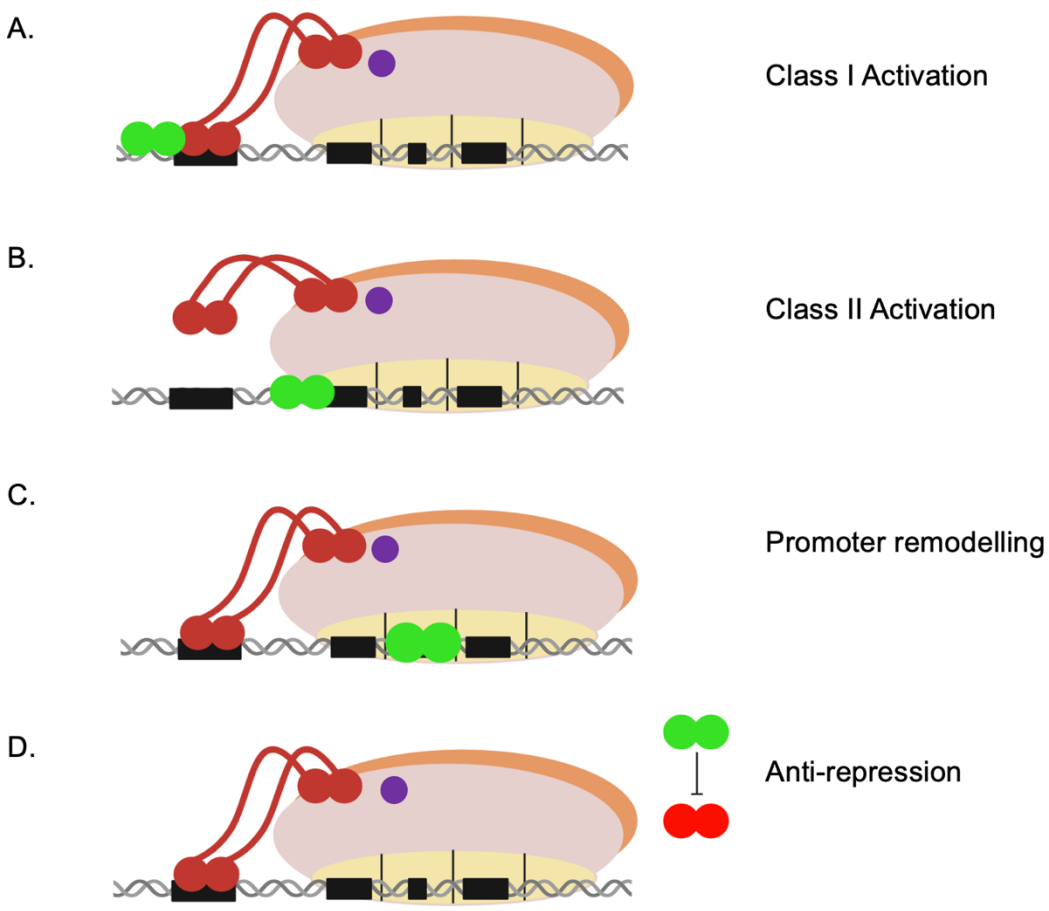

Figure 1.8. Schematic demonstrating mechanisms of activation in bacteria.
Activator proteins are shown in green, and in the schematic we are assuming they are binding as dimers. Repressor proteins are shown in red. A. Class I Activation: the activator binds to a site upstream of the -35 element and is able to contact αCTD of RNAP. B. Class II activation: the activator binds next to, or overlapping with, the -35 element and contacts domain 4 of the sigma factor within the RNAP holoenzyme. C. Promoter remodelling: activators, including NAPs, can bind to the promoter to remodel the -10 and -35 elements into an optimal structure for binding polymerase. D. Anti-repression: activators can bind to transcriptional repressors to inhibit their repressing activity. Adapted from Browning and Busby, 2004. Created with Biorender.

The activator recruits RNAP by direct contact with αCTD (Chen, Tang and Ebright, 2003). An example of Class I activation is CRP activation of the *lac* promoter (Gaston *et al*., 1990; Landis, Xu and Johnson, 1999). It has been noted that Class I activation is more efficient with an optimal UP element (Zhou *et al*., 2014).

1.2.2.2. Class II activation

Class II activation targets operator sequences overlapping with the -35 element. The activator contacts σ^4 and, often, the αCTD and αNTD of RNAP (Belyaeva *et al*., 1996; Busby and Ebright, 1999; Dove, Darst, and Hochschild, 2003). This interaction results in recruitment of RNAP to the promoter. The DNA-activator interaction means that αCTD cannot bind to the usual binding site and may bind further upstream. An example of Class II activation is CRP activation of the *gal* promoter (Gaston *et al*., 1990).

1.2.2.3. Class III activation

Class III promoters require multiple activators for full activation. Two transcription factors may work together to activate transcription, and this can be a combination of Class I and Class II mechanisms. This easily permits a response to multiple environmental stimuli. An example of Class III activation is of the *ansB* promoter. Co-activation is achieved by binding of CRP and FNR to binding sites at -91 and -41 bp, respectively (Scott, Busby and Beacham, 1995). Binding induces promoter activity by RNAP recruitment by both Class I and Class II mechanisms.

1.2.2.4.Indirect activation

Class I and Class II activation require a direct interaction between the activator and polymerase. However, there are mechanisms that indirectly recruit polymerase. One such mechanism has

been previously discussed: NAPs can induce changes in DNA topology to enable a change in RNAP activity. Bending, wrapping or looping of the chromosome may increase access to RNAP by enabling optimal spacing of promoter elements. An example of this is integration host factor (IHF), which is known as a DNA-bending protein (Parekh and Hatfield, 1996). IHF binds an upstream activating sequence within the *ilvPG* promoter to alter to structure of the DNA helix surrounding the -10 element. This is proposed to increase the efficiency of open complex formation at this promoter.

Another mechanism of indirect activation is anti-repression. In this case, activators can interact with transcriptional repressors to lift repression. For instance, the YcgF activator binds to repressor protein YcgE to release it from the promoter of YcgE-regulated genes, including *ymgA* and *ymgB*, which activate biofilm formation through a complex phosphorelay system (Tschowri, Busse and Hengge, 2009).

1.2.3. Transcriptional repression

There are four key ways that transcriptional repressors inhibit or decrease gene expression: steric hindrance, remodelling of promoter DNA, interaction with RNAP and anti-activation (Figure 1.9). Repression can be caused by one, or a combination, of these mechanisms (Browning and Busby, 2004).

1.2.3.1.Steric hindrance

Predominantly, transcriptional repression is via steric hindrance, in which a repressor protein blocks DNA access to RNAP by binding over the -10 or -35 elements (Browning and Busby, 2004). An example of steric hindrance is seen with the LacI repressor (Lewis, 1996). There may be multiple adjacent binding sites, increasing repression of that particular promoter.

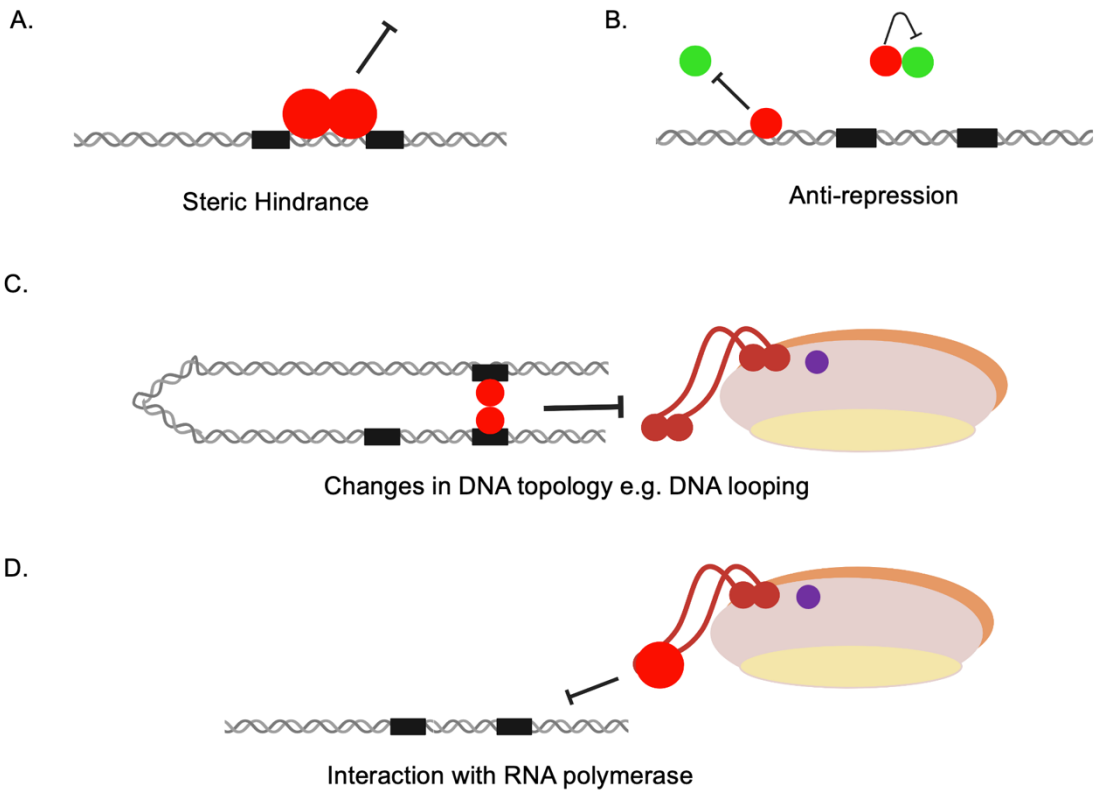

Figure 1.9. Schematic demonstrating mechanisms of repression in bacteria.
Repressor proteins are shown in red and activator proteins are shown in green. A. Repression by steric hindrance: promoter recognition sites are blocked by the repressor. B. Repression by anti-repression: Repressor proteins can bind to activators directly or to promoter DNA, blocking the activator operator sequence. C. Repression by changes in DNA topology: DNA remodelling is important in giving RNAP access to the promoter. One mechanism that causes repression is DNA looping. D. Repression by a direct interaction with polymerase: some repressors can directly bind RNAP to block activity. Adapted from Browning and Busby, 2004. Created with Biorender.

1.2.3.2.DNA looping

Alternatively, there can be operator sequences at distal sites; repressors bound to distal sites can interact with each other to cause DNA looping, thereby blocking RNAP access to the promoter. The combination of steric hindrance and DNA looping increases the strength of the transcriptional repressor (Swint-Kruse and Matthews, 2009). The GalR repressor causes such DNA looping. Repression by chromosomal rearrangement, via the activity of NAPs, is also a form of repression by DNA looping.

1.2.3.3. Repression by polymerase binding

Repressors can directly interact with RNAP to inhibit transcription (Adhya, 2001). One example of this is protein Gp2 encoded by phage T7, which infects *E. coli (*Cámara *et al*., 2010; Bae *et al*., 2013*)*. The protein interacts with the σ^1 subunit and β′ jaw of the RNAP holoenzyme to occupy part of the active site channel. This sterically blocks the correct positioning of DNA in the channel to prevent open complex formation. As some repressors directly interact with polymerase, they may also target transcription elongation, as well as initiation. NusA and NusG are examples of transcription factors that interact with RNAP (Burns, Richardson and Richardson, 1998). As previously discussed, NusA interacts with RNAP to decrease the elongation rate.

1.2.3.4. Anti-activation

Some transcriptional repressors act as anti-activators; that is, they bind to transcriptional activators to block their activity (Browning and Busby, 2004). The CytR repressor can simultaneously interact with DNA and CRP to block the activator binding to αCTD of RNAP (Valentin-Hansen *et al*., 1996).

1.3. Antibiotic resistance in Gram-negative bacteria

The introduction of antibiotics into the clinic has revolutionised medicine and increased life expectancy (Adedeji, 2016). Administration of antimicrobial agents, alongside vaccination, has led to a significant reduction in the morbidity and mortality rates of communicable diseases. Unfortunately, bacteria can acquire resistance to drugs due to spontaneous mutations or acquisition of novel DNA. This can increase their ability to resist the inhibitory or killing effects of antibiotics and, due to selection pressure, these bacteria multiply to lead to widespread resistance. Increasing multidrug resistance has been accelerated by the overuse of antibiotics in the healthcare and agriculture settings, as well as a decrease in drug development by largescale pharmaceutical companies. It is estimated that by the year 2050, there will be approximately 10 million deaths per year attributable to antimicrobial resistance (O'Neill, 2014). The antibiotic resistance phenomenon is an increasing problem in both the community and hospital settings (Ventola, 2015). In particular, Gram-negative bacteria form the majority of multidrug resistant bacteria; this is especially prominent in the hospital setting where 'superbugs' have arisen that are resistant to all known antibiotics (Boucher *et al.,* 2009; Hampton, 2013).

1.3.1. The definition of clinical resistance

Bacteria can be divided into three categories based on their level of susceptibility to any particular antibiotic (Rodloff *et al*., 2008). These categories, or clinical breakpoints, are" susceptible", "intermediate" and "resistant". Clinical breakpoint concentrations consider both the minimum inhibitory concentration (MIC) and pharmacokinetics to establish the true effectiveness of clinical use (EUCAST, 2023). A bacterial strain is "susceptible" to an antibiotic when it is effectively inhibited with therapeutic success. Microorganisms are deemed "intermediate" when the level of antimicrobial activity of a given antibiotic is associated with

uncertain therapeutic effect. "Resistant" strains are defined as having a high likelihood of therapeutic failure for a particular antibiotic, or a range of antibiotics in the case of multidrug resistant isolates.

1.3.1.1. Resistance and tolerance

Resistance results in the ability of a microorganism to grow at high concentrations of an antibiotic, and therefore the MIC is high. In contrast, "tolerant" bacteria can survive antibiotic treatment for prolonged periods (Balaban *et al*., 2013). This may be due to slowing down an essential bacterial process. For instance, tolerance to β-lactams can occur in slow-growing bacteria, associated with slower cell wall biosynthesis (Tuomanen *et al*., 1986). This results in a longer treatment duration regardless of the antimicrobial concentration. Hence, the MIC can remain unchanged. Tolerance can be acquired by environmental conditions, such as nutrient deprivation that slows cell growth, or through mutations (Brauner *et al*., 2016; Levin-Reisman *et al*., 2019).

1.3.1.2. Intrinsic and acquired resistance

Bacteria can be intrinsically resistant to an antibiotic, or they may acquire resistance due to mutations or horizontal gene transfer (Nikaido, 1994; Cox and Wright, 2013). Intrinsic resistance is defined as resistance due to pre-existing characteristics. For instance, the outer membrane of Gram-negative bacteria provides a permeability barrier that some molecules are unable to penetrate (Vance and Vance, 1996). Another example of intrinsic resistance is the activity of efflux pumps that actively remove antibiotics from the cytoplasm (Livermore, 2003; Randall *et al*., 2013). As well as intrinsic resistance, bacteria can acquire resistance to antibiotics due to the acquisition of genetic material that confers resistance. Mechanisms of acquired resistance are explored below.

1.3.2. Mechanisms of multidrug resistance

There are several major mechanisms by which bacteria can resist the activity of antibiotics: inactivation of the drug, alteration of the drug target, decreased accumulation of the drug, protection of the drug target and target bypass (Jovanović *et al*., 2008; Darby *et al*., 2023). Multidrug resistance is most often caused by a combination of mechanisms, providing high levels of resistance to multiple antibiotics.

1.3.2.1. Inactivation of antibiotics

Bacteria can produce enzymes that modify the structure of antibiotics or destroy them completely. For instance, resistance to ciprofloxacin, and other quinolone antibiotics, is often caused by a plasmid-encoded acetyltransferase that can inactivate the drug by acetylation (Tran and Jacoby, 2002). Inactivation may also occur through other modifications, such as phosphorylation or adenylation (Munita and Arias, 2016).

1.3.2.2. Alteration of the drug target

Alteration of the target of the antibiotic is a common mechanism of resistance in bacteria. Resistance to glycopeptide antibiotics, such as vancomycin, is often achieved by the activity of enzymes encoded by the *vanA* and *vanB* gene clusters. The enzymatic activity of these proteins modifies the peptidoglycan precursor D-Ala-D-Ala to D-Ala-D-Lac, which vancomycin binds with much lower affinity. The presence of these gene clusters is being increasingly noted in clinical isolates of a range of bacteria (Hashimoto *et al*., 2018; Kutkowska *et al*., 2019; Shanmugakani *et al.,* 2020).

1.3.2.3. Decreasing intracellular antibiotic concentration

Another mechanism of resistance is to decrease the intracellular antibiotic concentration, through either reduced uptake of a drug or increased efflux. It should be noted that Gram-negative bacteria already have an advantage due to their outer membrane (OM) acting as an additional barrier.

Reducing antimicrobial uptake: Resistance to β-lactam antibiotics, such as penicillin, is often due to loss of porins OmpF and OmpC. These proteins form pores through cellular membranes to allow small hydrophilic molecules into the cytoplasm (Nikaido, 1992). Therefore, downregulation of the *ompF* and *ompC* genes leads to decreased membrane permeability and reduced accumulation of β-lactams. This mechanism of resistance has been understood for many years but has recently been noted increasingly in clinical strains (Harder, Nikaido and Matsuhashi, 1981; Majewski *et al*., 2020; Chetri *et al*., 2020). Of significance, some clinical isolates that are resistant to carbapenems, current last resort antimicrobials, have been demonstrated to downregulate *ompF* and *ompC* (Majewski *et al*., 2020).

Removal of antibiotics from the cytoplasm by efflux pumps: Efflux of drugs, and other small molecules, is executed by specialised protein translocation systems known as membrane-spanning efflux pumps (Marshall and Piddock, 1997). There are six major families of efflux pumps: the ATP-binding cassette (ABC) superfamily, the small multidrug resistance (SMR) superfamily, the multidrug and toxic compound extrusion (MATE) superfamily, the resistance nodulation division (RND) superfamily, and the major facilitator superfamily (MFS), and the proteobacterial antimicrobial compound efflux (PACE) family (Sun, Deng and Yan, 2014; Hassan *et al*., 2015). Efflux pumps can be single-component inner membrane transporters or tripartite complexes that span the inner and outer membranes (Neuberger, Du and Luisi, 2018).

The majority of tripartite efflux pumps are members of the RND family. Some RND efflux pumps have a broad specificity and are therefore responsible for the removal of multiple classes of antibiotics, dyes and detergents via active transport (Nikaido and Pagès, 2012). It should be noted that these molecules are not the natural substrates of efflux pumps (Piddock, 2006). It is suggested that the natural role of efflux pumps is in virulence and biofilm formation, but they have evolved to remove antimicrobial agents due to a combination of their natural role and selective pressure. Efflux pumps contribute to the basal level of resistance of Gram-negative bacteria. Efflux-associated resistance is mainly due to altered regulation of genes encoding efflux pumps, resulting in overexpression (Yasufuku *et al*., 2011).

1.3.2.4. Target Protection

Bacteria can produce protection proteins that bind to the drug target and prevent drug action. Tetracycline resistance can be caused by the TetM and TetO proteins, which interact with the ribosome and cause release of tetracycline (Connell *et al*., 2003). Additionally, a conformational change occurs in the ribosome to prevent re-binding of tetracycline (Dönhöfer *et al*., 2012).

1.3.2.5. Target Bypass

Evolution of new targets that lead to an alternative pathway and redundancy of the original pathway is another mechanism that causes resistance. The alterative pathway accomplishes similar biochemical functions but is not targeted by the antibiotic (Munita and Arias, 2016). For instance, resistance to methicillin, a β-lactam antibiotic that binds to penicillin-binding proteins (PBPs) can be caused by the acquisition of an exogenous PBP (PBP2a) (Ubukata *et al*., 1989). PBP2a has low affinity to β-lactam antibiotics and therefore is not inhibited by them.

1.3.3. The impact of antimicrobial resistance in Gram-negative bacteria

In 2017, the World Health Organisation (WHO) published a list of antibiotic resistant priority pathogens, and the majority of this list are Gram-negative bacteria (WHO, 2017). Those noted as in critical need for new antibiotics include carbapenem-resistant *Acinetobacter baumannii*, *Pseudomonas aeruginosa* and Enterobacteriaceae, which include *E. coli*, *Salmonella* and *Klebsiella pnuemoniae*, amongst others.

1.3.3.1. Multidrug resistance in *Escherichia coli*

E. coli is a genetically diverse species that is divided into five phylogroups: A, B1, B2, D and E (Wirth *et al*., 2006; Chaudhuri and Henderson, 2012). This classification is based on seven housekeeping genes (Wirth *et al*., 2006). Human commensal strains, which can inhabit the intestine without causing disease, mainly belong to group A (Escobar-Páramo *et al*., 2006; Li *et al*., 2010). This includes the model organism *E. coli* K-12. Pathogenic *E. coli* are divided into two main groups: intestinal pathogenic *E. coli* (InPEC) and extraintestinal pathogenic *E. coli* (ExPEC) (Méndez-Moreno *et al*., 2022). The groups are sub-divided into several virotypes, each of which encode distinct virulence factors and cause a variety of infections. For instance, there are six known virotypes of InPEC and four known virotypes of ExPEC (Bhunia, 2018; Pokharel, Dhakal and Dozois, 2023). Interestingly, these virotypes do not always cluster together into phylogroups. For example, enterohaemorrhagic *E. coli* (EHEC) strain O157:H7 is classified into phylogroup E but EHEC strain O103:H2 is classified into phylogroup B1 (Wirth *et al*., 2006). Estimates suggest that the *E. coli* core genome contains between 867 and 2200 genes (Touchon *et al*., 2009; Yang *et al*., 2019). However, the pan-genome may contain up to 43,415 genes (Yang *et al*., 2019).

Pathogenic *E. coli* are a major causative agent of gastroenteritis and urinary tract infections (UTIs), as well as meningitis and septicaemia and a range of other infections (Johnson *et al*., 2003; Kaper, Nataro and Mobley, 2004). Pathogenic *E. coli* remain a huge problem due to their low infectious dose, transmission in ubiquitous mediums; such as food and water; and high morbidity and mortality worldwide. These pathogens are the major cause of infant and traveller's diarrhoea in developing countries, with Enterotoxigenic *E. coli* (ETEC) estimated to cause 2.5 million cases and 700,000 deaths in infants aged below 5 annually (Lamberti *et al*., 2014).

Multidrug resistant *E. coli* strains are of critical priority. Those encoding extended-spectrum-beta-lactamases (ESBLs) appear to be on the rise and are a major concern in UTIs (Ukah *et al.* 2018). Additionally, the *mcr-1* gene, conferring resistance to colistin, has been identified in *E. coli* clinical isolates (Liu *et al.,* 2016; Velasco *et al*., 2020). This antimicrobial resistance has been accelerated by the distribution of antibiotics without prescription in developing countries, often those where ETEC is endemic (Chuc and Tomson, 1999).

1.3.4. The multiple antibiotic resistance (*mar*) phenotype

Multiple antibiotic resistance in Gram-negative bacteria is often controlled by the *mar* locus. Although the *mar* locus alone generally does not cause clinical resistance; with the exception of resistance to tetracycline, nalidixic acid and rifampicin; it can cause decreased sensitivity to a large number of antibiotic classes (Alekshun and Levy 1997; Randall and Woodward 2002). This accelerates the development of further changes in antimicrobial tolerance or acts together with an existing resistance mechanism to increase resistance to antimicrobial agents (Cohen *et al*., 1989; Tavio *et al*., 2010). For instance, it has been demonstrated that *E. coli* strains with *mar* mutations develop resistance to fluoroquinolones at a faster rate than wildtype strains

(Cohen *et al*., 1989). Thus, the *mar* locus plays a significant role in the development of clinical antibiotic resistance. The *mar* locus regulates a variety of activities, including drug efflux and porin expression. These mechanisms combined cause a reduced accumulation of antimicrobial agents in the cytoplasm.

1.4. The *marRAB* operon

The *mar* locus is comprised of two divergent transcriptional units, *marRAB* and *marC* (Figure 1.10) (Alekshun and Levy, 1997). A central operator *marO* is positioned between the two units, and regulates *marRAB* expression via two promoters (Cohen, Hachler and Levy, 1993). The operon is repressed by MarR and activated by MarA (Seoane and Levy, 1995). MarR binds as a dimer to two 21 bp palindromic sequences within the *marO* operator (Martin, Nyantakyi and Rosner, 1995). Tetracycline, the phenolic compound salicylate, and the acidic compound 1,4-dihydroxy-2-naphthoic acid can all bind and inactivate MarR (Seoane and Levy, 1995; Doukyu, Fujisawa and Saito, 2022). MarA binds as a monomer to a 15 bp DNA-binding sequence known as the marbox (Jair *et al*., 1995; Martin *et al*., 1996).

The marbox is located further upstream of the MarR operator sequence. Fis is an accessory activator that binds upstream of the marbox and results in further activation through DNA looping (Martin and Rosner, 1997). MarA is also regulated post-translationally by Lon protease, which rapidly degrades MarA to ensure a quick response to environmental signals (Griffith, Shah and Wolf, 2004). Recent research has demonstrated that Lon protease degrades free H-NS but not DNA-bound H-NS in *Salmonella enterica* (Choi and Groisman, 2020). It is likely, albeit unconfirmed, that Lon protease degrades MarA by a similar mechanism throughout Gram-negative bacteria.

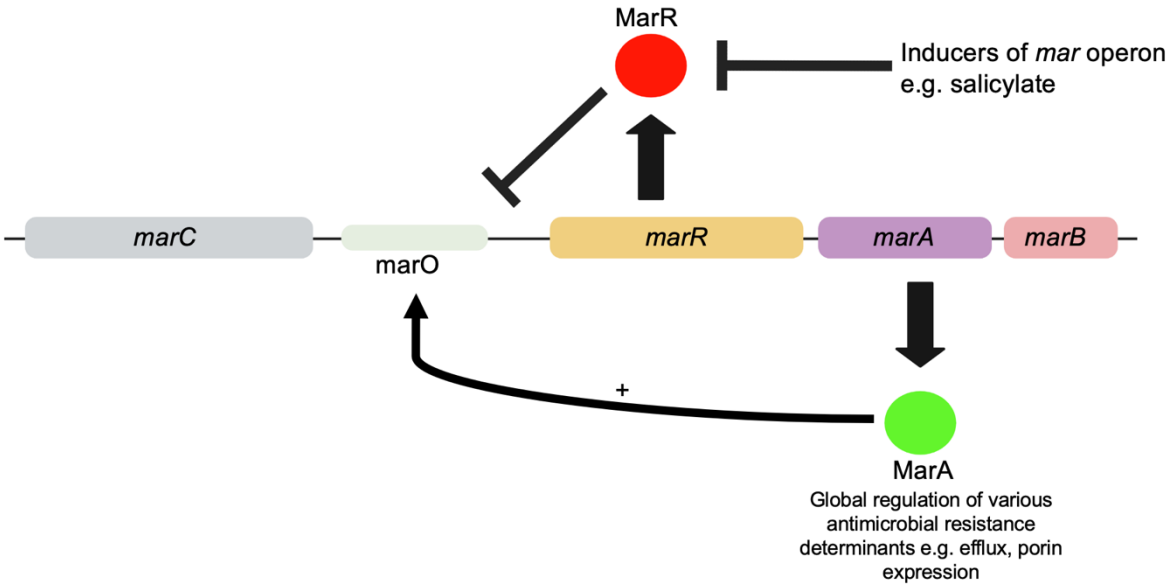

Figure 1.10. *mar* operon of Gram-negative bacteria.

The *mar* operon is formed of divergent transcriptional units – *marC* and *marRAB*. *marO* is a central promoter containing recognition sites. The operon is regulated by a negative feedback loop, in which MarR acts as a repressor of the operon and binds *marO* as a dimer. MarR itself is repressed by small molecules, such as salicylate. Displacement of MarR leads to activation of the operon, and expression of the multiple antibiotic resistance regulator MarA. It is assumed in the schematic that MarA is acting as an activator, but it can also repress gene expression. Multiple antibiotic resistance in clinical samples is often achieved due to mutations in *marR* to cause constitutive expression.

MarB is a periplasmic protein of unknown function. Some research has suggested that it acts to indirectly repress *marRAB*, but the mechanism remains unknown (Vinué, McMurry and Levy 2013). MarC is an inner membrane (IM) protein of unknown function. As it is divergently transcribed, it is not required for the *mar* phenotype (McDermott *et al.,* 2008).

Constitutive expression of the *marRAB* operon is caused by mutations in *marR* or *marO* (Cohen, Hachler and Levy, 1993; Ariza *et al*., 1994). These mutations allow expression of *marA*, a positive feedback loop of *marRAB* expression, and constitutive activation of the *mar* phenotype. Clinical isolates with mutations in the *mar* locus are increasingly noted (Keeney et al., 2007; Pérez *et al*., 2012; Majewski *et al*., 2020; Goodarzi *et al*., 2021; Albarri *et al*., 2022). These studies demonstrate constitutive overexpression of MarA due to the mutations identified. Additionally, mutations that cause overexpression of other AraC family global regulators, including *soxS*, *rob* and *ramA*, are also associated with multidrug resistance (Pérez *et al*., 2012; Majewski *et al*., 2020; Goodarzi *et al*., 2021; Albarri *et al*., 2022). Overexpression of the multidrug resistance regulators lead to constitutive activation or repression of the genes they regulate. In turn, this contributes to a decrease in the susceptibility to numerous antibiotics by targeting important cellular processes, including efflux and porin expression.

1.4.1. The MarA regulator

MarA is a member of the AraC/XylS family of transcription factors. MarA contains two HTH binding motifs, which insert into the major groove of DNA (Figure 1.11). (Rhee *et al*., 1998). The protein binds as a monomer. Conserved residues R46, T93 and R96, at the N-terminus form important electrostatic interactions with the DNA backbone (Rhee *et al*., 1998). Other amino acids, Y39, S40, H43 and K49, have been noted to make non-specific phosphate interactions with the DNA backbone and, alongside the conserved arginine residues, are the

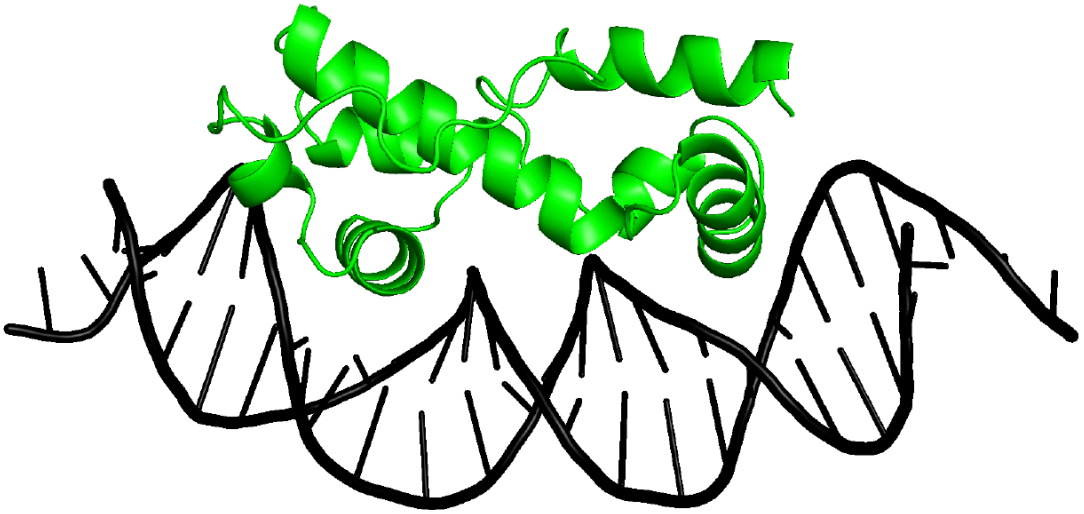

Figure 1.11. Crystal structure of MarA complexed with the marbox.

Diagram made in PYMOL using crystal structure data (Rhee *et al*., 1998). The DNA double helix is shown in black and MarA is shown in green. MarA is a 129-residue protein comprised of 7 α-helices. The N-terminal HTH motif is formed of helices 2 and 3. The C-terminal motif is formed on helices 5 and 6. The major DNA binding elements, helix 3 and helix 6, bind two adjacent major grooves and cause bending of the DNA.

major contributors towards marbox affinity. It is predicted that MarA makes 15 contacts with DNA. Binding results in bending of the DNA by 35 º. NMR analysis suggests that the N-terminal tail may also be involved in DNA-binding (Dangi *et al*., 2001). Due to the non-specific backbone interactions, MarA can bind divergent sequences.

1.4.2. The marbox

The marbox is bound by MarA, as well as SoxS and Rob in *E. coli* (Martin *et al.,* 1999; Chollet *et al*., 2004). Due to this, it is often also called a 'soxbox' or 'robbox" but hereafter will be referred to as a marbox, regardless of which other factors bind to the operator sequence (Fawcett and Wolf, 1995; Jair *et al*., 1996). The marbox is a non-palindromic and highly degenerate sequence of 15-20 bp (Figure 1.12) (Rhee *et al*., 1998; Sharma *et al*., 2017). The marbox is characterised by two important conserved motifs, a 5' GCA motif and a 3' AAA motif, separated by a poorly conserved sequence (Sharma *et al*., 2017). Within the *E. coli* genome, there are approximately 13,000 copies of the marbox (Griffith *et al.,* 2002). However, most are not bound by MarA *in vivo* and it is suggested that MarA regulates around 100 genes (Barbosa and Levy, 2000).

The marbox is generally found in one of two positions, and therefore promoters regulated by MarA can be divided into two classes. At Class I promoters, the marbox is found in the backwards orientation and is located upstream of the -35 element (Martin *et al*., 1999). An interaction with αCTD of RNAP is required (Jair *et al*., 1995; Jair *et al*., 1996). Surface residues D18, W19, D22 and R36 of MarA play an important role in this interaction (Dangi *et al*., 2004). At Class II promoters, the marbox is oriented in a forward position and overlaps with the -35 element (Martin *et al*, 1999). An interaction with domain 4 of the sigma factor may be involved (Zafar, Sanchez-Alberola and Wolf, 2011).

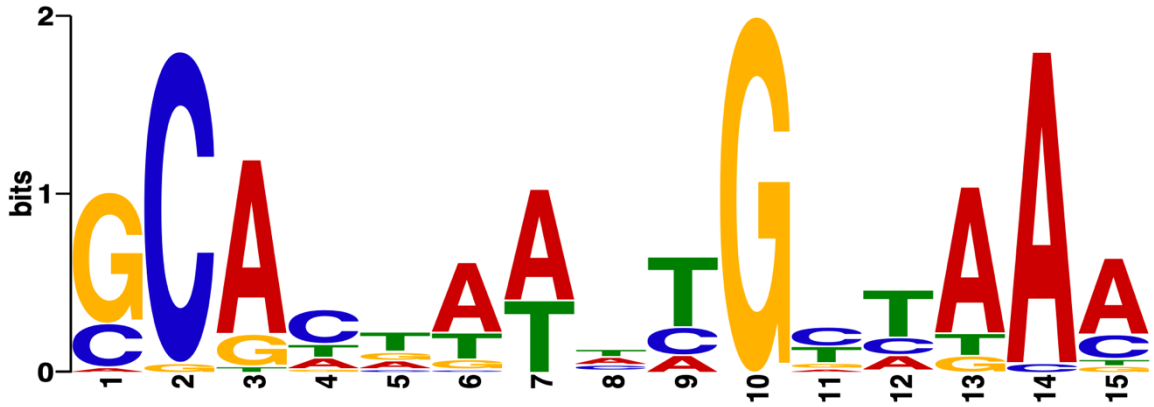

Figure 1.12. The marbox consensus sequence.

Sequence generated by a ChIP-seq experiment (Sharma *et al*., 2017).

1.4.3. Regulation of antibiotic resistance by MarA

The *mar* phenotype is associated with decreased sensitivity to a range of antibiotic classes and stresses, including oxidative stress. The phenotype is induced once MarA binds to the marbox of target promoters and regulates gene expression accordingly. An important focus of the *mar* phenotype is the increased levels of resistance to a range of antibiotics. This is achieved through increased efflux and decreased uptake of drugs (George, 1996; Cohen *et al.,* 1989).

For instance, MarA is a known activator of the *acrAB* operon and the *tolC* gene. Together these genes encode the clinically relevant AcrAB-TolC efflux pump, which is widely distributed in Gram-negative bacteria (Okusu, Ma and Nikaido 1996). This efflux pump is a tripartite complex formed of an IM transporter (AcrB), a periplasmic adapter protein (AcrA) and OM channel (TolC) (Yamasaki *et al*., 2011). The complex has a broad specificity and is responsible for removing a range of antibiotics from the cytoplasm, including fluoroquinolones and β-lactam antibiotics (Blair, Richmond and Piddock, 2014). Overexpression of these genes is commonly found in clinical isolates of multidrug resistant Gram-negative bacteria (Buckley *et al.,* 2006; Blair *et al*., 2009; Swick *et al*., 2011; Majewski *et al*., 2020).

Additionally, the *mar* phenotype is achieved by decreased uptake of antimicrobial agents through the OmpF and OmpC porins (Cohen *et al*., 1989). These proteins form pores in the OM to allow passive diffusion of small molecules into the periplasm (Nikaido and Vaaro, 1985). MarA indirectly downregulates *ompF* and *ompC* expression through activating transcription of the non-coding RNA *micF* (Miller and Sulavik, 1996; Delihas and Forst, 2001). *micF* RNA binds to target mRNA to inhibit translation and accelerate degradation. Downregulation of these broadly specific major OM proteins results in less passive diffusion

of molecules into the bacterial cell and is noted increasingly in clinical isolates (Chetri *et al*., 2019; Majewski *et al*., 2020).

Many additional genes have been proposed to be MarA targets. It has been determined that MarA activates the *mlaFEDCB* operon (Sharma *et al.,* 2017). It is hypothesised that this regulation controls OM permeability to reduce antimicrobial uptake. Furthermore, other MarA targets include the *ycgZ-ymgABC* operon and *xseA*, which inhibit biofilm formation and control DNA repair, respectively (Kettles *et al*., 2019; Sharma *et al*., 2017). In *Salmonella*, MarA represses *flhDC* involved in the production of flagella, to reduce motility (Thota and Chubitz, 2019). Other genes confirmed to be regulated by MarA in a range of Gram-negative bacteria include *inaA*, a stress response gene; *ybjC,* encoding a putative IM protein; and *zwf*, involved in glucose metabolism (Rosner and Slonczewski 1994, Jair *et al*., 1995, Martin *et al*., 2002). It remains unclear if these genes play a role in the *mar* phenotype.

1.4.4. MarA as a transcriptional repressor

Binding of MarA to a marbox usually results in activation of promoter activity. However, it should be noted that MarA may also act as a repressor. For instance, at the *rob* promoter MarA binds in a backward orientation overlapping with both the -10 and -35 promoter elements to repress by steric hindrance (Schneiders *et al*., 2004; McMurry and Levy, 2010). Alternatively, at the *hdeA* and *purA* promoters, MarA binds to a site overlapping with the -35 element in the backward orientation. This is different to Class II activation whereby MarA binds to the site in the forward orientation. It has been proposed that repression occurs due to DNA bending (Schneiders and Levy, 2006; McMurry and Levy, 2010).

1.4.5. Pre-recruitment of RNAP

Recruitment of RNAP usually occurs via a traditional method, as previously discussed: Class I and Class II activation require an activator to first bind an operator sequence, followed by RNAP recruitment (Browning and Busby, 2004). Conversely, MarA activates via a pre-recruitment mechanism, in which the activator first binds RNAP (Martin *et al*., 2002). This complex scans the DNA to bind a marbox only in the correct orientation and position relative to the -10 and -35 elements. Considering the high frequency of marboxes in the *E. coli* genome, the pre-recruitment model partly explains why the majority of these operator sequences are not bound by MarA, and why there are only a comparatively small number of genuine MarA targets. SoxS has also been demonstrated to activate via a pre-recruitment mechanism (Griffith *et al*., 2002). The role of pre-recruitment in repression by steric hindrance, as with the *rob* promoter, remains unclear (McMurry and Levy, 2010).

1.4.6. MarA as a potential target for new antimicrobial therapy

Considering the increasing propensity of MarA in clinical resistance, MarA could be an interesting target for new therapeutics. Artesunate, primarily used as an anti-malarial drug, has been demonstrated to bind MarA (Pan *et al*., 2020). This inhibits MarA binding to the *marA* promoter to prevent activation. Interestingly, artesunate binding to MarA does not directly prevent MarA binding to other marboxes. Thus, the drug appears to specifically target self-regulation of MarA to prevent further regulatory activity. Independently, artesunate has no direct antibacterial effect but, in combination with β-lactams antibiotics, has a synergistic effect. This antimicrobial enhancement could prolong the usefulness of current antibiotics.

1.5. AraC/XylS regulators SoxS, Rob and RamA

As previously mentioned, there are three MarA paralogues throughout Gram-negative bacteria. *E. coli* contains two of these homologs, whereas RamA is found in most other Gram-negative bacteria. These transcription factors share the degenerate binding site, meaning that all are capable of binding to the marbox. This explains the overlap in the regulons of these proteins. Despite this, the regulators respond to different environmental stimuli.

1.5.1. SoxS

Much like MarA, SoxS binds to promoter sequences as a monomer using two HTH motifs that bind to the major groove of DNA (Li and Demple, 1994). SoxS shares 41 % sequence identity with MarA. In contrast to *marA*, *soxS* is divergently transcribed from the gene encoding its own regulator *soxR (*Wu and Weiss, 1991). SoxR binds as a dimer to the *soxS* promoter to repress transcription. Oxidative stress agents, such as paraquat, oxidise a [2Fe-S] cluster of SoxR by redox-cycling, which consequently turns it into an activator of *soxS* (Wu and Weiss, 1992; Hidalgo *et al.,* 1998). Thus, regulation of *soxS* expression is determined by a redox-regulated transcriptional switch by use of allosteric regulation.

1.5.2. Rob

Despite Rob sharing 51 % sequence identity with MarA, the protein binds DNA by a different mechanism (Kwon *et al*., 2000; Taliaferro *et al*., 2012). Although Rob binds as a monomer and contains two HTH motifs, it is hypothesised that one of the motifs interacts with the DNA backbone instead of inserting into the major groove of DNA. Due to this, Rob can bind sequences with greater degeneracy. Notably, Rob contains a C-terminal domain not found in the other paralogues (Kwon *et al*., 2000). This domain is involved in the sequestration of Rob

into inactive foci that are protected from Lon protease degradation and are unable to contact promoter DNA (Griffith *et al*., 2009). This post-translational regulation of Rob means that it can be constitutively expressed. Inducers of Rob, including fatty acids and dipyridyl, interact with the C-terminal domain to mediate dispersal of Rob foci (Rosner *et al*., 2002; Griffith *et al*., 2009). Individual Rob proteins can interact with promoter DNA to regulate activity.

1.5.3. Crosstalk between MarA and the paralogues

There are many genes activated by several MarA paralogues. For example, MarA, SoxS, and Rob have all been reported to activate the *acrAB* operon, as well as activate the *micF* promoter (Rosner and Slonczewski, 1994; Martin, Gillette and Rosner, 2000; Nikaido *et al*., 2011). Additionally, several other genes have been reported to be regulated by more than one of these transcription factors, including *fumC*, *sodA* and *zwf*, which are associated with respiratory and oxidative stress (Duval and Lister, 2013). The transcription factors are also able to regulate each other. In *E. coli*, MarA, SoxS and Rob can activate *marA* and repress *rob* and *soxS* (Martin and Rosner, 1997; Michán, Manchado and Pueyo, 2002; Schneiders and Levy 2006; Chubiz, Glekas and Rao 2012). The full extent of cross talk between MarA, SoxS, Rob and RamA remains poorly understood.

1.6. Objectives of this project

In recent years, a number of novel MarA targets have been identified by ChIP-seq analysis. This works aims to follow up on one of these novel targets, as well as find additional MarA targets. Furthermore, this work looks to understand how different MarA regulated genes can work together. This will allow further characterisation of the MarA regulon in order to understand the mechanisms by which MarA elucidates the multiple antibiotic resistance phenotype.

Chapter 2 – Materials and Methods

2.1. Materials

2.1.1. Buffers, reagents and solutions

All solutions were made with deionised and distilled water (ddH_2O) unless stated. Solutions were autoclaved for 20 minutes at 121 ºC.

Polymerase chain reaction (PCR)

- 100 mM dNTP mix (Bioline): made up of 25 mM dATP, dGTP, dCTP and dTTP. The mix was diluted to 10 mM in ddH_2O.
- Velocity DNA polymerase (Bioline)
- 5 x Hi-Fi Buffer (Bioline)
- MyTaq™ Red mix (Bioline)

Restriction digests

- 10 x CutSmart® Buffer (New England Biolabs): made up of 50 mM potassium acetate, 20 mM Tris-acetate, 10 mM magnesium acetate and 100 µg/ml BSA pH 7.9.
- Calf Intestinal Alkaline Phosphatase (CIP) (New England Biolabs)

Agarose gel electrophoresis

- Powdered agarose (Bioline)
- SYBR Safe (Thermo Fisher Scientific)
- 5 x TBE (Thermo Fisher Scientific): made up of 0.445 M Tris borate pH 8.3 and 10 mM Na_2EDTA. Diluted to a 1 x stock in ddH_2O.
- 6 x gel loading dye (New England Biolabs): made up of 10 mM EDTA 3.3 mM Tris-HCl, 2.5 % Ficoll®-400, pH 8, 0.02 % pink/red dye and 0.001 % blue dye.

Phenol-chloroform extraction/ ethanol precipitation

- Phenol/chloroform/isoamyl alcohol pH 8 (25:25:1)
- 100 % (v/v) ethanol
- 70 % (v/v) ethanol
- 3 M sodium acetate pH 4.8

Ligation of PCR roducts in plasmid vectors

- T4 DNA ligase (New England Biolabs)
- 10 x T4 DNA ligase buffer (New England Biolabs): made up of 50 mM Tris-HCl, 10 mM $MgCl_2$, 10 mM DTT pH 7.5 and 1 mM ATP.

Preparation of chemically competent cells

- 100 mM $CaCl_2$ (Sigma-Aldrich)
- 50 % (v/v) glycerol

Preparation of electrocompetent cells

- 15 % (v/v) glycerol

Polyacrylamide gel electrophoresis (PAGE) and denaturing sequencing gels

- UreaGel® Dilulent (National Diagnostics): made up of 7.5 M urea.
- UreaGel® Concentrate (National Diagnostics): made up of 237.5 g acrylamide, 12.5 g methylene bisacrylamide and 7.5 M urea (per litre).
- UreaGel® Buffer (National Diagnostics): made up of 0.89M Tris-Borate, 20 mM EDTA pH 8.3 and 7.5 M urea.

- 10% (w/v) ammonium persulfate (APS) (Sigma-Aldrich): made up by dissolving 100 mg APS in 1 ml ddH_2O.
- TEMED (N,N,N′,N′-Tetramethyl ethylenediamine) (Sigma-Aldrich)
- ProtoGel® 30% (National Diagnostics): made up of 37:5:1 acrylamide:bisacrylamide

Purification of recombinant proteins

- 1 M IPTG solution
- Lysis buffer: 50 mM Tris-HCl (pH 7.5), 1 mM EDTA, 1 M NaCl
- Wash buffer: 50 mM Tris-HCl (pH 8.5). 4 M urea
- Denaturing buffer: 50 mM Tris-HCl (pH 8.5), 6 M guanidinium-HCl
- Buffer A: 50 mM Tris-HCl (pH 8.5), 1 m NaCl
- Buffer B: Buffer A + 1 M imidazole
- Buffer X: 1 M NaCl, 50 mM HEPES, 1 mM dithiothreitol, 5 mM EDTA, 0.1 mM Triton X-100
- Thrombin Sepharose beads (BioVision): 6 % cross-linked Sepharose beads in 50 % slurry with glycerol

Radiolabelling of DNA fragments for EMSA

- G-50 sephadex beads (Sigma-Aldrich): these were re-suspended with Tris-EDTA (TE) to form a 12% (v/v) slurry.
- Tris-EDTA (Sigma-Aldrich): made up of 10 mM Tris-HCl and 1 mM EDTA pH 8.0
- T4 polynucleotide kinase (New England Biolab)
- 10 x T4 polynucleotidekinase buffer (New England Biolabs): made up of 70 mM Tris-HCl, 10 mM $MgCl_2$ and 5 mM DTT pH 7.6.
- [γ-^{32}P]-ATP (Perkin Elmer): 10 µCi/µl

Electrophoretic mobility shift assay (EMSA)

- 10 x Transcription buffer (TNSC buffer): made up of 400 mM Tris acetate pH 7.9, 10 mM $MgCl_2$, 1 M KCl, 10 mM DTT.

β-galactosidase assays

- Z-buffer: made up of 8.53 g Na_2HPO_4, 4.87 g $NaH_2PO_4.2H2O$ 0.75 g KCl, 0.25 g $MgSO_4$ per litre of ddH_2O, then autoclaved.
- 1 % (w/v) sodium deoxycholate (Sigma-Aldrich)
- 100% (v/v) toluene
- 13 mM 2-Nitrophenyl β-D-galactopyranosidase (ONPG) (Sigma-Aldrich): made up in 'Z-buffer'
- β-mercaptoethanol (Sigma-Aldrich): added to ONPG/Z-buffer solution immediately before use to make a final ONPG concentration of 13 mM (e.g. 100 mg ONPG dissolved in 250 ml Z-buffer, 677 µl β-mercaptoethanol).
- 1 M sodium carbonate (Sigma-Aldrich)

In vitro transcription assays

- NTP mix: 1 mM ATP/GTP/CTP and 50 µM UTP (Thermo Fisher Scientific), final concentrations in assay 200 µM ATP/CTP/GTP and 10 µM UTP.
- 1 mg/ml bovine serum albumin (BSA) (Sigma-Aldrich)
- 10 x Transcription buffer (TNSC buffer): made up of 400 mM Tris acetate pH 7.9, 10 mM $MgCl_2$, 1 M KCl, 10 mM DTT.
- STOP solution: made up of 97.5 % (v/v) deionised formamide, 10 mM EDTA, 0.3 % (v/v) bromophenol blue and 0.3 % xylene cyanol.

- [α-^{32}P]-UTP (Perkin Elmer): 10 µCi/µl
- *E. coli* RNA polymerase core enzyme (New England Biolabs)

Generation of 'G+A' ladder

- DNase I blue: 5 M urea, 20 mM NaOH, 1 mM EDTA, 0.025 % (v/v) bromophenol blue, 0.025 % (v/v) xylene cyanol.
- 10 M piperidine (Sigma-Aldrich)
- 100 % (v/v) formic acid (Sigma-Aldrich)
- 0.3 M sodium acetate (Sigma-Aldrich)
- 20 mg/ml glycogen (Sigma-Aldrich)

Generation of M13 T7 sequencing reactions

- 2 M sodium hydroxide (Sigma-Aldrich)
- 3 M sodium acetate pH 4.8 (Sigma-Aldrich)
- Annealing buffer (USB): made up of 1 M Tris-HCl pH 7.5, 100 mM $MgCl_2$ and 160 mM DTT.
- 'A' mix short (USB): made up of 840 µM dCTP, dGTP and dTTP each, 93.5 µM dATP, 14 µM ddATP, 40 mM Tris-HCl pH 7.5 and 50 mM NaCl
- 'C' mix short (USB): made up of 840 µM dATP, dGTP and dTTP each; 93.5 µM dCTP; 17 µM ddCTP; 40 mM Tris-HCl pH 7.5 and 50 mM NaCl.
- 'G' mix short (USB): made up of 840 µM dATP, dCTP and dTTP each; 93.5 µM dGTP; 14 µM ddGTP; 40 mM Tris-HCl pH 7.5 and 50 mM NaCl.
- 'T' mix short (USB): made up of 840 µM dATP, dCTP and dGTP each; 93.5 µM dTTP; 14 µM ddTTP; 40 mM Tris-HCl pH 7.5 and 50 mM NaCl.

- Label mix 'A' (USB): made up of 1.375 mM of dCTP, dGTP, and dTTP each and 333.5 mM NaCl.
- T7 polymerase dilution buffer: made up of 25 mM Tris-HCl pH 7.5, 5 mM DTT, 100 µg BSA/ml and 5% glycerol.
- T7 DNA polymerase (USB): 8 units/µl in glycerol solution.
- STOP solution: made up of 97.5 % (v/v) deionised formamide, 10 mM EDTA, 0.3 % (v/v) bromophenol blue and 0.3 % xylene cyanol.
- [α-^{32}P]-UTP (Perkin Elmer): 10 µCi/µl

Primer extension assays

All solutions DEPC-treated or made up with DEPC-treated H_2O.

- 1 x hybridisation buffer: made up of 20 mM HEPES, 0.4 M NaCl and 80 % (v/v) formamide
- 100 % (v/v) ethanol
- 70 % (v/v) ethanol
- 3 M sodium acetate pH 4.8 (Sigma-Aldrich)
- 3 M sodium acetate pH 7.0 (Sigma-Aldrich)
- T4 polynucleotide kinase (New England Biolab)
- 10 x T4 polynucleotidekinase buffer (New England Biolabs): made up of 70 mM Tris-HCl, 10 mM $MgCl_2$ and 5 mM DTT pH 7.6.
- AMV (Avian myeloblastosis virus) Reverse Transcriptase (Promega)
- Reverse Transcriptase Buffer (Promega): made up of 250 mM Tris-HCl pH 8.3, 250 mM KCl, 50 mM $MgCl_2$, 2.5 mM spermidine, 50 mM DTT.
- RNasin ® (Promega)
- 10 mg/ml RNase A (Thermo Fisher Scientific)

- DTT (Sigma-Aldrich)
- STOP solution: made up of 97.5 % (v/v) deionised formamide, 10 mM EDTA, 0.3 % (v/v) bromophenol blue and 0.3 % xylene cyanol.
- [γ -^{32}P]-ATP (Perkin Elmer): 10 μCi/μl

Crystal violet accumulation assays

- 10 μg/ml crystal violet ($C_{25}H_{30}N_3Cl$) solution; 0.001 % (w/v) crystal violet aqueous solution (Sigma-Aldrich)
- 0.05 mM phosphate-buffered saline pH 7.4 (Thermo Fisher Scientific)

Membrane separation

- 10 mM HEPES buffer (Thermo Fisher Scientific)
- 10 x cOmplete™ Protease Inhibitor Cocktail (Sigma-Aldrich)
- DNase I and DNase I buffer (Thermo Fisher Scientific)
- 20 % (v/v) sucrose (Sigma-Aldrich)

Sodium dodecyl sulphate (SDS) -PAGE

- NUPAGE™ LDS Sample Buffer (Thermo Fisher Scientific)
- 5 x SDS loading dye: made up of 5 % β-Mercaptoethanol (5 %), 0.02 % Bromophenol blue, 30 % glycerol, 10 % sodium dodecyl sulfate (SDS) and 250 mM Tris-Cl pH 6.8.
- Mini-PROTEAN TGX gel 4-15% (Bio-Rad)
- 10 x Tris-Glycine SDS running buffer (Bio-Rad)
- InstantBlue™ Protein Stain (Sigma Aldrich)
- Colour Prestained Protein Standard, Broad Range (10-250 kDa) (New England Biolabs)

Lipid extraction

- 100% (v/v) methanol (Sigma-Aldrich)
- 100% (v/v) chloroform (Sigma-Aldrich)
- 100% (v/v) acetonitrile (Sigma-Aldrich)

Liquid chromatography/mass spectrometry

- 100% (v/v) 2-propanol (Sigma-Aldrich)
- 100% (v/v) acetonitrile (Sigma-Aldrich)
- 10 mM ammonium acetate (Sigma-Aldrich)

Flexible recombineering using integration of thyA (FRUIT)

- L-arabinose (Sigma-Aldrich)
- Trimethoprim (Sigma-Aldrich)

2.1.2. Strains and plasmids

All bacterial strains used in this study are shown in Table 2.1. All plasmid vectors used in this study are shown in Table 2.2.

2.1.3. Oligonucleotides

Oligonucleotides were produced by Thermo Fisher Scientific, Merck or Eurofins Genomics. All oligonucleotides used in this study are shown in Table 2.3.

2.1.4. Media

LB broth (Sigma-Aldrich), LB agar (Sigma-Aldrich), MacConkey agar (Oxoid) and M9 minimal media agar were used for bacterial growth. Media was dissolved and autoclaved. Agar

plates were dried for 20 minutes before use. M9 minimal agar was not autoclaved but all components were autoclaved separately prior to preparation.

LB broth: 20 g powdered broth dissolved in 1 L ddH_2O.

LB agar: 35 g powdered agar dissolved in 1 L ddH_2O.

MacConkey agar: 52 g powdered agar dissolved in 1 L ddH_2O.

M9 minimal agar: 100 ml M9 salts (made up of 60g Na_2HPO_4, 35 g KH_2PO_4, 5 g NaCl and 10 g NH_4Cl per litre of ddH_2O), 1 ml 1 M $MgSO_4$, 1 ml 100 mM $CaCl_2$, 10 ml 20 % fructose, 5 ml 20 % casamino acids, 875 ml agarose.

Table 2.1. Strains used in this study.

The genotype and source of each strain is depicted. All strains are derivatives of *E. coli* K-12 MG1655 (F- lambda- *ilvG*- *rfb*-50 *rph*-1).

Strain	Description	Source
JCB387	Δ*nirB* Δ*lac*	Typas and Hengge, 2006
JCB387 Δ*thyA*	Δ*nirB* Δ*lac* Δ*thyA*	This work
JCB387 Δ*thyA waaY* M*	Δ*nirB* Δ*lac* Δ*thyA* P*waaY* -48:-46 GCA → TGT	This work
JCB387 Δ*thyA pbpG* M*	Δ*nirB* Δ*lac* Δ*thyA* P*pbpG* -27:-25 GCA → TGT	This work
JCB387 Δ*thyA mlaF* M*	Δ*nirB* Δ*lac* Δ*thyA* P1*mlaF* -37:-35 CCA → TGT	This work
JCB387 Δ*thyA pbpG* M* *mlaF* M*	Δ*nirB* Δ*lac* Δ*thyA* P*pbpG* -27:-25 GCA → TGT, P1*mlaF* -37:-35 CCA → TGT	This work
JCB387 Δ*thyA waaY* M* *mlaF* M*	Δ*nirB* Δ*lac* Δ*thyA* P*waaY* -48:-46 GCA → TGT, P1*mlaF* -37:-35 CCA → TGT	This work
JCB387 Δ*thyA pbpG* M* *waaY* M* *mlaF* M*	Δ*nirB* Δ*lac* Δ*thyA* P*pbpG* -27:-25 GCA → TGT, *PwaaY* -48:-46 GCA → TGT, P1*mlaF* -37:-35 CCA → TGT	This work
MG1655 Δ*thyA* FLAG$_3$-*araC* FLAG$_3$-*thyA*	Δ*thyA* FLAG$_3$ inserted at C-terminus of *araC*, FLAG$_3$ inserted at C-terminus of *thyA*	Kindly donated by Professor Joseph Wade and Anne Stringer

BW25113	*rrnB3 ΔlacZ4787 hsdR514 Δ(araBAD)567 Δ(rhaBAD)568 rph-1*	Datsenko and Wanner, 2000; Baba *et al*., 2006
Δ*pbpG*	*rrnB3 ΔlacZ4787 hsdR514 Δ(araBAD)567 Δ(rhaBAD)568 rph-1 pbpG::kan*	Baba *et al*., 2006
Δ*mlaE*	*rrnB3 ΔlacZ4787 hsdR514 Δ(araBAD)567 Δ(rhaBAD)568 rph-1 mlaE::kan*	Baba *et al*., 2006
Δ*mlaF*	*rrnB3 ΔlacZ4787 hsdR514 Δ(araBAD)567 Δ(rhaBAD)568 rph-1 mlaF::kan*	Baba *et al*., 2006
NCTC 10418	Reference strain	London, 1965
ATCC 25922	Reference strain	Minogue *et al*. 2014 (Human clinical sample, Seattle, 1946)
T7 Express	*fhuA2 lacZ::T7 gene1 [lon] ompT gal sulA11 R(mcr73::miniTn10--T etS)2 [dcm] R(zgb-210::Tn10--TetS) endA1 Δ(mcrCmrr)114::IS10*	New England Biolabs

Table 2.2. Plasmid vectors used in this study.

Plasmid	Size	Description	Map	Source
pRW50	16.9 kb	Contains a cloning site upstream of a *lacZ* fusion. This is flanked by EcoRI and HindIII restriction sites. Encodes Tet^R. Used for β-galactosidase assays.	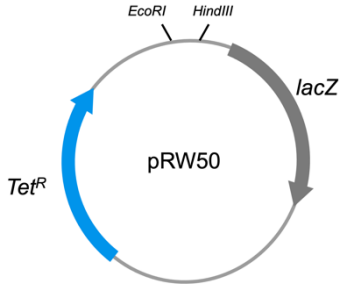	Lodge *et al.*, 1992
pSR	4 kb	Contains a cloning site upstream of a λoop terminator site. This is flanked by EcoR1 and HindIII restriction sites. Derived from pBR322. Encodes Amp^R. Used for *in vitro* transcription.	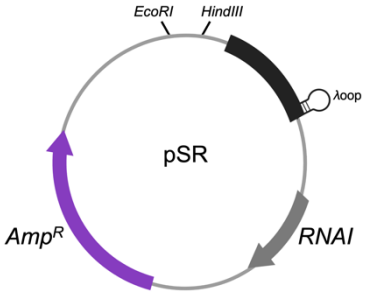	Kolb, 1995
pJ203 + *marA*	5.3 kb	A derivative of pJ203 containing *marA* with a strong constitutive promoter cloned into NdeI and HindIII restriction sites. Derived from pBR322. Encodes Cam^R.	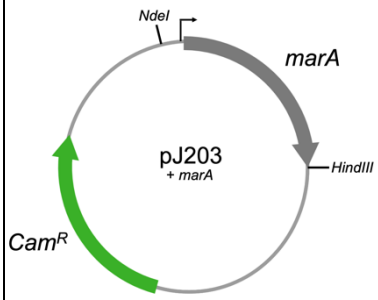	Backbone from Atum Bio. Constructed by Dr Prateek Sharma, The University of Birmingham
pJ203 + *pbpG*	5.9 kb	A derivative of pJ203 containing the MG1655 *pbpG* gene with a strong constitutive promoter cloned into NdeI and HindIII restriction sites. Derived from pBR322. Encodes Cam^R.	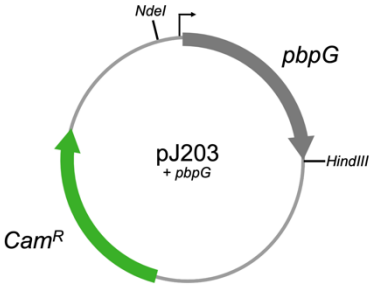	This work

pAM + *soxS*	3.1 kb	A derivative of pJ201 containing an N-terminal $FLAG_3$ tag and the *Salmonella* Typhimurium SL1144 *soxS* gene with a strong modified *lacUV5* promoter cloned into HindIII and KpnI restriction sites. Derived from pBR322. Encodes Kan^R.	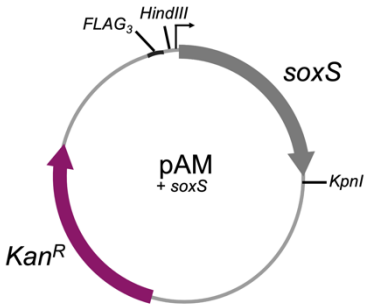	Backbone from Atum Bio. Constructed by Alistair Middlemiss, The University of Birmingham
pAM + *lpxC/L*	4.6 kb	A derivative of pJ201 containing a C-terminal $FLAG_3$ tag and the MG1655 *lpxC* and *lpxL genes* with a strong modified *lacUV5* promoter cloned into HindIII and KpnI restriction sites. Derived from pBR322. Encodes Kan^R.	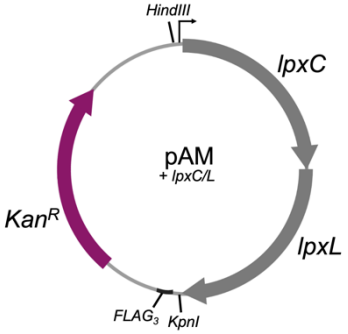	Backbone from Atum Bio. This work
pACBSR	7.3 kb	Recombination plasmid containing arabinose inducible λ Red genes. Encodes Cam^R. Used for FRUIT.	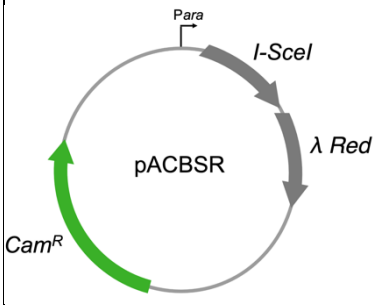	Herring *et al.*, 2003
pAMD001	3.8 kb	pGEM-T containing the MG1655 *thyA* gene with a strong constitutive promoter. Encodes Amp^R. Used for FRUIT.	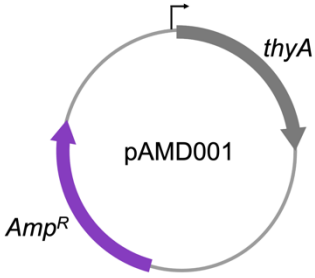	Stringer *et al.*, 2012

Table 2.3. Oligonucleotides used in this study.

Name (F- forward, R- reverse)	Sequence (5' → 3') Restriction sites are shown in bold
Oligonucleotides for amplification of *lpxC* regulatory region	
lpxC.1-F and *lpxC*.1M-F was used alongside *lpxC*-R to generate derivates of the *lpxC* promoter region	
lpxC.1-F	GGCTG**GAATTC**TGCGTAAGCAAGCTGATTAAGAAT
lpxC.1^{M}-F	GGCTG**GAATTC**TGCGTAAGCAAGCTGATTAAGAATTGACTG GAATTTGGGTTTCGAGTGTGTTTGTGCTAAACTGGCCCG
lpxC-R	GCCCG**AAGCTT**CATCGTATTATCTCGCCAAATTACCTAT
Oligonucleotides for amplification of regulatory regions of potential MarA targets identified using bioinformatics	
wbbK.1-F	GGCTG**GAATTC**ATTGGCCAGAGGGTTTGGTTG
wbbK.1-R	GCCCG**AAGCTT**CATAATTTGGTCTCATGATTG
wzxC.1-F	GGCTG**GAATTC**GCGCATAACGAACAGTATCG
wzxC.1-R	GCCCG**AAGCTT**CATATCAATATGCCGCTTTGTTAACG
waaU.1-F	GGCTG**GAATTC**GTAGGGATTTATTCAAAATATTG
waaU.1-R	GCCCG**AAGCTT**CATTTTTATACCATATTATTTTAG
wcaD.1-F	GGCTG**GAATTC**GGTGATTGCCACCCATAG
wcaD.1-R	GCCCG**AAGCTT**CATACTCCTCCAGCATC

wzc.1-F	GGCTG**GAATTC**ATGCTGTTTGGTCACTGGG
wzc.1-R	GCCCG**AAGCTT**CATTCTTATACCTGCTCTGCG
rfaJ.1-F	GGCTG**GAATTC**GCAATCAATTAAGATATAGCGC
rfaJ.1-R	GCCCG**AAGCTT**CACAATGCTACCCTTATATC
waaA.1-F	GGCTG**GAATTC**GGGCCGAGTTTCAATGAATC
waaA.1-R	GCCCG**AAGCTT**CATAGTAAATAGCTGACTTATGG
rffA.1-F	GGCTG**GAATTC**GGACGCGGTGCAGGTG
rffA.1-R	GCCCG**AAGCTT**CATGTGATCACCTGTATAACC
rfaD.1-F	GGCTG**GAATTC**GCACTATTCACATGCAAAACCAAC
rfaD.1-R	GCCCG**AAGCTT**CATAACTGTAACCTTCGAATTATG
waaY.1-F	GGCTG**GAATTC**TGCAACTAAACCGTGG
waaY.1^{M}-F	GGCTG**GAATTC**TGCAACTAAACCGTGGCACAAATGGGCAA TTTATCCATCGGTAAAATACTATAAAATAGCTTTAGAAAATT CCCCCTGGAAAGATGACTCTCCACGAGATCGGCCCTCAA
waaY.1-R	GCCCG**AAGCTT**CATAATAAACCAGTTAAATG
lpxL.1-F	GGCTG**GAATTC**CATGGTGTACGGTTCCTG
lpxL.1^{M1}-F	GGCTGG**AATTCC**ATGGTGTACGGTTCCTGCGAGATGGGAAA GTAAAAATCCGCGGCATGATATATGTATTATCGATAATTAA CATCC

lpxL.1^{M2}-F	GGCTGG**AATTCC**ATGGTGTACGGTTCCTGCGAGATGGGAAA GTAAAAATCCGCGGCATGATATAGCAATTATCGATAATTAA CATCCACACATTTTACGCTACATTACAGCATTAAAAATTATT TG
lpxL.1^{M3}-R	GCCCG**AAGCTT**CATATCAATCCTGTTTTTCAACCTATTCGGG CAATTGTATGTATTGTCGCATTTTTTCGCCCGCAACCAAAAT TTGTGGCTGAAGACTGGCGGCCCTTGCCG
*lpxL.*1-R	GCCCG**AAGCTT**CATATCAATCCTGTTTTTCAACC
*amiC.*1-F	GGCTG**GAATTC**GTAAATTTTATGCGAGAGCGAC
*amiC.*1-R	GCCCG**AAGCTT**CATGCCTCTCCCG
*pbpG.*1-F	GGCTG**GAATTC**GGCGTAAATGTCAGCAATGC
*pbpG.*1^{M}-F	GGCTG**GAATTC**GGCGTAAATGTCAGCAATGCAGCATTTCCT CACGATTCTCCTTTGACGATCTGTCTTTTTGCTCGT
*pbpG.*1-R	GCCCG**AAGCTT**CATGATGAGCATTCAGATAG
*dacB.*1-F	GGCTG**GAATTC**CCTCTTGAATATTCCTGATGG
*dacB.*1-R	GCCCG**AAGCTT**CATAATCTCGCGCTAACAAC
*mepA.*1-F	GGCTG**GAATTC**GCATTACCGTGCCGG
*mepA.*1-R	GCCCG**AAGCTT**CATTTTTTACCAGCGTGGAATATC

Oligonucleotides for sequencing and amplification of DNA fragments from pRW50 and pSR

pSR-F	CCATATATCAGGGTTATTGTCTC
pSR-R	CATCACCGAAACGCGCGAGG
pRW50-F	GTTCTCGCAAGGACGAGAATTTC
pRW50-R	AATCTTCACGCTTGAGATAC

Oligonucleotides for primer extension

Universal primer	GTAAAACGACGGCCAGT
D49724	GGTTGGACGCCCGGCATAGTTTTTCAGCAGGTCGTTG

Oligonucleotides for generation of *pbpG* overexpression plasmid (pJ203 + *pbpG*)

The pbpG gene was ligated into pJ203 using ligation with NdeI and HindIII restriction sites. Flanking primers were used for amplification and sequencing

pbpG-ORF-F	GGCTG**CATATG**ATGCCGAAATTTCGAGTTTC
pbpG-ORF-R	GCCCG**AAGCTT**TTAATCGTTCTGTGCCGTCT
pbpG-flank-F	GGCTGCTACGGTTATCGTTTGTTCTAG
pbpG-flank-R	GCCCGGAACTGCTACAGCAG

Oligonucleotides for generation of *lpxC and lpxL* overexpression plasmid (pJ203 + *lpxC/L*)

The lpxC and lpxL genes were ligated into pJ203 using ligation with NdeI and HindIII restriction sites. The genes were ligated together with the EcoRI restriction site. Flanking primers were used for amplification and sequencing

lpxC-ORF-F	GCCCG**GAATTC**TTATGCCAGTACAGCTGAAG

lpxC-ORF-R	GGCTG**GAATTC**ATGACGAATCTACCCAAGTTC
lpxL-ORF-F	GCCCG**AAGCTT**TTAATAGCGTGAAGGAACGC
lpxL-ORF-R	CGTCCTGAAATCACTCTGGTGACCA
lpxC-flank-F	GATAATACAAAATATAATACAA
lpxC-flank-R	GTGCGACGATAGATGACCCCGGTGT
lpxL-flank-F	TACACTCGCCCAAAAACATTCAGCG
lpxL-flank-R	ACGTTACTTGTCATCGTCATC

Oligonucleotides for generation of *Escherichia coli* Δ*thyA* JCB387 used in FRUIT

JW472	CCGACGCGCAGTTTA
JW473	CACGTTGTGTTTTCATGC

Oligonucleotides for amplification of thyA cassettes and amplification of mutagenesis cassettes for FRUIT

Regions that anneal to pAMD001 are underlined

Targeting upstream *waaY*	AAGACAAAACACATCAAAACTATAAAAAGCTGATTACAGA AAGTACTCTTCTTATTCATTATACAGGTGCAACTAAACCGTA GACAGCTGCATGCAT
Targeting downstream *waaY*	GGAGAGTCATCTTTCCAGGGGGAATTTTCTAAAGCTATTTTA TAGTATTTTACCGATGGATAAATTGCCCATTTGTGCCAGTGT AGGCTGGAGCTG

Mutagenesis upstream *waaY*	GATGACATTATTTTGCCTCGTGAG
Mutagenesis downstream *waaY*	GCTATAATTCCTGAGATATAATGATGTTGCAC
Targeting upstream *pbpG*	GTTCTAGAAAGTTCTTTGACGTTGCATTGCTGGCGTAAATGT CAGCAATGCAGCATTTCCTCACGATTCTCCTTTGACGATAGA CAGCTGCATGCAT
Targeting downstream *pbpG*	TTCACGCGCACGGGTTGCGCACCGCCGGAGTAAGGATTTAC TGAGGCTAGCGACGCCATCATAACGAGCAAAAAGTGCGAG TGTAGGCTGGAGCTG
Mutagenesis upstream *pbpG*	CTTAGCTTCTCTAGTTCGACGCTGG
Mutagenesis downstream *pbpG*	CTGCGGTGCAAAAGGCACAGCCAGCA
Targeting upstream *mlaF*	TTTCTTCAGGTATACTCGCCGGTCCGCTGAAGATTTTCAGAA AGCCGTAACGGATGCTTAATTTTGACTTTATGCGGCTATAGA CAGCTGCATGCATCTTTGTTATGGTGTGTTC
Targeting downstream *mlaF*	CTCAATTTAACCTTGAACCCAACATATTTACAGAATATTACC CGCCGTGGTTAGCGAAAGCTGGCATTTGTTTTACTTTTGTGT AGGCTGGAGCTGTTAGATAGCCACCGGCGCTT
Mutagenesis upstream *mlaF*	CTTAGCTTCTCTAGTTCGACGCTGG
Mutagenesis downstream *mlaF*	CGCATATCGACTAAATTCGC

Targeting upstream *lpxC*	TGCGCCGCAAACTGCGAAAGAGCCGGATTATCTGGATATCC CAGCATTCCTGCGTAAGCAAGCTGATTAAGAATTGACTGTA GACAGCTGCATGCAT
Targeting downstream *lpxC*	CGCCAAATTACCTATCCAACCGAAGTGTACTATACATTCGG CGGGCCAGTTTAGCACAAAGAGCCTCGAAACCCAAATTC GTGTAGGCTGGAGCTG
Targeting downstream *lpxC*-promoter	TCGCCTGAACGATACGTTTAAGTGTCCTTTGTTTGATcatCGT ATTATCTCGCCAAATTACCTATCCAACCGA*ATTATAGCACAGA TGCTGGATCTGTGTA*GGTGTAGGCTGGAGCTG
Targeting upstream *lpxL*	CGCGTCGTTGGAAATGCGGTTGTGTAACACTGGCATGGTGT ACGGTTCCTGCGAGATGGGAAAGTAAAAATCCGCGGCATTA GACAGCTGCATGCAT
Targeting downstream *lpxL*	GCTTGTAAATAACAAATAATTTTTAATGCGCAAATGTAGCG TAAAATGTGTGGATGTTAATTATCGATAATTGCTATATCGTG TAGGCTGGAGCTG
Targeting downstream *lpxL*-promoter	TGCGGTGGAGAACTTGGGTAGATTCGTcatATCAATCCTGTTT TTCAACCTATTCGGGCAATTGTATGTATT*ATTATAGCACAGAT GCTGGATCTGTGTA*GGTGTAGGCTGGAGCT

Gene strand sequences for introducing point mutations using FRUIT

Point mutations are underlined

waaY M*	GATGACATTATTTTTGCCTCGTGAGTACAATACAATTTATAC AATTAAAAGTGAATTAAAAGACAAAACACATCAAAACTAT AAAAAGCTGATTACAGAAAGTACTCTTCTTATTCATTATACA GGTGCAACTAAACCGTGTGTAAATGGGCAATTTATCCATCG GTAAAATACTATAAAATAGCTTTAGAAAATTCCCCCTGGAA AGATGACTCTCCACGAGATGCGAAATCAATTATTGAATTTA

	AAAAAAGATATAAACATCTTTTAGTGCAACATCATTATATC TCAGGAATTATAGC
pbpG M*	CTTAGCTTCTCTAGTTCGACGCTGGCGATTGGCGTGCTGGTA CTGGAAGTGCTGCTCGCCCTAACCGTTATACTATGGGGCTA CGGTTATCGTTTGTTCTAGAAAGTTCTTTGACGTTGCATTGC TGGCGTAAATGTCAGCAATGCAGCATTTCCTCACGATTCTCC TTTGACGATCTGTCTTTTTGCTCGTTATGATGGCGTCGCTAG CCTCAGTAAATCCTTACTCCGGCGGTGCGCAACCCGTGCGC GTGAACCACTATCTGAATGCTCATCATGCCGAAATTTCGAG TTTCTTTATTTAGCCTGGCCCTGATGCTGGCTGTGCCTTTTGC ACCGCAG
mlaF M*	CAGGCGGTCGGCACTGTAAACGACCAAAAGTAAACCAACA ATTAACAGTGCCGTAGCTAAAAGCATCTAACGTCCTTTCTTC AGGTATACTCGCCGGTCCGCTGAAGATTTTCAGAAAGCCGT AACGGATGCTTAATTTTGACTTTATGCGGCTAAAAAGTAAA ACAAATGTGTGCTTTCGCTAACCACGGCGGGTAATATTCTGT AAATATGTTGGGTTCAAGGTTAAATTGAGCGCCATGCTTAG AAAATCAACGCAAGACGAAGGGTGAATTATGGAGCAGTCT GTGGCGAATTTAGTCGATATGCG

Oligonucleotides for colony PCR and sequencing confirmation for FRUIT

waaY-amplify-F	GGCTGCTAACAGAAAAAGCGTTGTC
waaY-amplify-R	GCCCGGATCTTGCTCTTCTGAATCAT
pbpG-amplify-F	TGGTATTCCGAGCTTCCTGAATATC
pbpG-amplify-R	CGCAACGGCCTGCGGTGCAAAAGGC
mlaF-amplify-F	ATCAGCGGCGGGATGCCAAAGGTTC

mlaF-amplify-R	CATCGCGCATATCGACTAAATTCGC
lpxC-amplify-F	CGTCCTGAAATCACTCTGGTGACCA
lpxC-amplify-R	GTGCGACGATAGATGACCCCGGTGT
lpxL-amplify-F	TACACTCGCCCAAAAACATTCAGCG
lpxL-amplify-R	AGCAGTGCGGTGGAGAACTTGGGTA

2.1.5. Antibiotics

Antibiotics were added to media to select for specific plasmids and strains. Bicyclomycin and rifampicin were for additional experiments. The stock solutions as follows were stored at -20 ^{o}C:

Ampicillin: 100 mg/ml (dissolved in water). Final concentration in media was 100 µg/ml.

Bicyclomycin: Unknown concentration, obtained from lab in America.

Chloramphenicol: 35 mg/ml (dissolved in ethanol). Final concentration in media was 35 µg/ml.

Doxycycline: 1 mg/ml (dissolved in water). Final concentration in media was 1 µg/ml.

Kanamycin: 50mg/ml (dissolved in water). Final concentration in media was 50 µg/ml.

Rifampicin: 50 mg/ml (dissolved in methanol). Final concentration in media was 50 µg/ml.

Tetracycline: 35mg/ml (dissolved in methanol). Final concentration in media was 35 µg/ml.

Trimethoprim: 20 mg/ml (dissolved in DMSO). Final concentration in media was 20µg/ml.

2.2. Methods

2.2.1. Polymerase chain reaction (PCR)

PCR reactions were done in a 50 µl volume with 0.5 mM deoxynucleotide triphosphates (dNTPs), 1 µl Velocity DNA polymerase, 10 µl reaction buffer, 20 pmol of each primer and 50-200 ng template DNA. For colony PCR, MyTaq™ Red Mix was used with dH_2O and 20 pmol each primer in a 50 µl final volume. The template was derived from a bacterial boilprep, genomic DNA preparation or a colony dilution in dH_2O. The annealing temperature varied and were calculated as 5 ^{o}C below the T_m of the lowest primer T_m. A typical PCR cycle is shown in Table 2.4.

Table 2.4. Typical PCR cycling conditions used throughout.

Stage	Description	Temperature	Time	Number of cycles
1	Initial denaturation	95 ºC	5 minutes	1
2	Denaturation	95 ºC	30 seconds	35
	Annealing	50 ºC - 72 ºC	30 seconds	
	Elongation	72 ºC	30 seconds	
3	Final elongation	72 ºC	10 minutes	1

2.2.2. PCR purification

PCR products were purified using the Qiagen PCR Purification Kit, according to the manufacturer's instruction.

2.2.3. Restriction digests

Following PCR purification, the products were digested with appropriate restriction enzymes supplied by New England Biolabs. DNA was digested by addition of sterile water, appropriate restriction enzyme(s) and CutSmart® buffer. This was incubated at 37 °C for 3 hours. 4 µl Calf Intestinal Alkaline Phosphatase was added to digested plasmids for the final 30 minutes to prevent self-ligation.

2.2.4. Gel extraction

To further purify DNA, either gel extraction or phenol-chloroform extraction was used. DNA was first separated on a 1 % agarose gel. Briefly, the agarose gel was prepared by dissolving 1 g of agarose in 100 ml 1 x TBE. The agarose was dissolved by microwaving for 1 minute. SYBR Safe was added just before the gel was poured. Separation was achieved by running the gel at 150 V for approximately 30 minutes in 1 x TBE buffer. After separation, the appropriate band was cut out using a razor blade. DNA was extracted from this section of gel using the Qiagen Gel Extraction Kit, according to the manufacturer's instructions.

2.2.5. Phenol-chloroform extraction/ ethanol precipitation of DNA

An equal volume of phenol-chloroform was added to the plasmid preparation. This was vortexed for 15 seconds before centrifugation at 17,000 x g for 3 minutes. The upper aqueous phase was transferred to a new tube, and 3 x volume of ice-cold 100 % ethanol and 0.1 x volume of 3 M sodium acetate pH 5.2 was added. The sample was precipitated at -80 °C for 30

minutes, followed by centrifugation at 17,000 x g for 30 minutes at 4 °C. The pellet was dried under a vacuum, washed in 750 µl ice-cold 70 % ethanol and centrifuged at 17,000 x g for 20 minutes at 4 °C. The pellet was dried under a vacuum and re-suspended in dH_2O.

2.2.6. Ligation of PCR products in plasmid vectors

DNA fragments were ligated with vectors containing complementary 5' and 3' overhangs. Ligation reactions were done in a 20 µl reaction with approximately 50 ng vector, 100-200 ng purified insert, 2 µl 10 x DNA ligase buffer and 2 µl T4 DNA ligase (New England Biolabs). Note that vectors smaller than 10 kb were purified using gel extraction as described above. Vectors larger than 10 kb were purified using phenol-chloroform extraction and ethanol precipitation, as described above. Ligation reactions were left at room temperature for 2 hours. A vector-only reaction was used as a negative control.

2.2.7. Nucleic acid extraction using Qiagen kits

All nucleic acid extractions were done using the Qiagen kits, in which DNA is bound to a silica column, washed with a high salt solution and eluted with water. The Qiagen miniprep kit was used to extract plasmids of high copy number (such as pSR) for cloning vectors. The Qiagen maxiprep kit was used to extract plasmids of low copy number (such as pRW50). 5 ml overnight cultures were used for miniprep extraction, compared with 250 ml cultures for a maxiprep. The Qiagen RNeasy kit was used to extract RNA for use in primer extension assays.

2.2.8. Sequencing of plasmids and DNA fragments

All sequencing was carried out by the Functional Genomics Facility at The University of Birmingham by Sanger sequencing. Each reaction had a total volume of 10 µl and contained 1 µl 10 µM primer and approximately 200 ng of DNA.

2.2.9. Growth of bacterial cultures

Overnight cultures were grown in LB broth at 37 ºC with 200 rpm shaking for 16 – 18 hours.

2.2.10. Preparation of chemically competent cells

1 ml of an overnight culture was used to inoculate 50 ml fresh LB medium. This was incubated at 37 ºC with 200 rpm shaking until the OD_{650} was between 0.4 and 0.5. Cultures were chilled on ice for 20 minutes and harvested by centrifugation at 1,600 x g for 10 minutes at 4 ºC. Cells were re-suspended in 25 ml 100 mM ice-cold calcium chloride, incubated on ice for 30 minutes and re-harvested by centrifugation at 1,600 x g for 10 minutes at 4 ºC. The pellet was re-suspended in 3.3 ml ice-cold 100 mM calcium chloride and was left on ice overnight. Cells were mixed with 50 % glycerol, aliquoted into microfuge tubes and stored at -80 ºC.

2.2.11. Preparation of electrocompetent cells

1 ml of an overnight culture was used to inoculate 50 ml fresh LB medium. This was incubated at 37 ºC with 200 rpm shaking until the OD_{650} was between 0.4 and 0.5. Cultures were chilled on ice for 20 minutes and harvested at 1,600 x g for 10 minutes at 4 ºC. Cells were re-suspended in 50 ml 15 % ice-cold glycerol and re-harvested by centrifugation at 1,600 x g for 10 minutes at 4 ºC. The glycerol wash was repeated 3 times. Finally, cells were re-suspended in 500 µl 15 % glycerol, aliquoted into microfuge tubes and stored at -80 ºC.

2.2.12. Transformation of bacterial cells

To transform bacterial cells with circular plasmid DNA, the ligation reaction or 10 ng plasmid DNA were incubated on ice with 100 µl chemically competent cells for 1 hour. Cells were heat shocked at 42 ºC for 2 minutes, then transferred to ice for 5 minutes. 1 ml LB broth was added to the cells. The reaction was incubated at 37 ºC with 200 rpm shaking for 1 hour. The cells

were pelleted by centrifugation at 2,400 x g for 3 minutes. The pellet was re-suspended in 100 µl LB and plated onto selective agar. To transform bacterial cells with linear DNA, 200 ng DNA was incubated on ice with 45 µl electrocompetent cells for 1 hour. Cells were transferred to a pre-chilled 1 mm electroporation cuvette and subjected to an electric field of 1700 V. 1 ml LB broth was added to the cells and the reaction was incubated, centrifuged and plated as previously described.

2.2.13. Purification of recombinant proteins

MarA, SoxS and Rob were purified using an adapted protocol (Jair *et al*., 1995). Purification of MarA was carried out by Dr Rachel Kettles and purification of SoxS and Rob was carried out by Dr Alistair Middlemiss, both at The University of Birmingham. The open reading frame encoding the appropriate protein was amplified by PCR, digested with NdeI and BamHI and ligated with pET28a downstream of the T7*lac* promoter, inducible with IPTG. Constructs were used to transform *E. coli* T7 Express cells. Recombinant proteins were overexpressed by growth in LB with 0.4 mM IPTG to an OD_{650} of 0.8 – 1.2. Cells were harvested by centrifugation at 1,600 x g for 10 minutes at 4 ^{o}C. Pellets were washed with 25 ml lysis buffer and incubated at -80 ^{o}C for 16 hours.

Frozen pellets were re-suspended in 40 ml lysis buffer. Cells were lysed using an Avestin Emulsiflex C3 high pressure motorised homogeniser. Cells were pelleted by centrifugation at 75,000 x g for 30 minutes and re-suspended in 40 ml wash buffer. Centrifugation was repeated and the pellets were re-suspended in 40 ml denaturing buffer. A final centrifugation step was carried out and the supernatant was loaded onto a HisTrap^{TM} 1 ml pre-charged Ni Sepharose High Performance column. Unbound protein was washed away using Buffer A and bound protein was eluted with buffer B. An elution peak was noted at 0.22 M imidazole, fractions

were confirmed using SDS-PAGE and the desired fractions were dialysed against Buffer X overnight.

Following dialysis, the proteins were concentrated to 1 mg/ml using a 5000 MWCO (molecular weight cut-off) Vivaspin 20 column. The His tag was removed by adding 15 µl of thrombin Sepharose beads per mg protein and incubating at room temperature for 5 hours with gentle rocking. Removal of the His tag was confirmed by SDS-PAGE. Thrombin beads were removed by centrifugation of 1,600 x g for 5 minutes. Digested His tags were removed using the HisTrap^{TM} column with flow-through retained and dialysed with Buffer X + 20 % glycerol overnight. Recombinant proteins were stored at -20 ^{o}C.

2.2.14. Radiolabelling of DNA fragments for EMSA

DNA fragments for use in electrophoretic mobility shift assays (EMSA) were prepared by PCR amplification and purification, digestion with EcoRI and gel extraction. Fragments were radiolabelled at the 5' end by addition of 16 µl digested DNA, 1 µl T4 polynucleotide kinase, 2 µl 10 x T4 polynucleotide kinase and 1 µl [γ-^{32}P]-ATP. Unincorporated nucleotides were removed by passing labelled DNA through two G-50 Sephadex columns.

2.2.15. Electrophoretic mobility shift assay (EMSA)

Approximately 30 counts of [γ-^{32}P]-ATP labelled DNA fragments were mixed with 1 x TNSC buffer and 12.5 µg/ml Herring sperm DNA, in a final volume of 10 µl. This was incubated with 10 µl MarA/1 x TNSC mix for 20 minutes at 37 ^{o}C. Reactions were loaded onto a 7.5 % polyacrylamide gel. The gel was run at 150 V for 1-2 hours and vacuum dried and exposed to a phosphorscreen overnight. It was visualised using a Biorad FX® phosphoimager.

2.2.16. β-galactosidase assays

Promoter fragments of interest were ligated into pRW50 upstream of *lacZ*. *E. coli* JCB387 was transformed with these plasmids and used for β-galactosidase assays. Three overnight cultures were set up for each construct. 100 µl of each overnight culture was sub-cultured into 5 ml LB broth with selective antibiotics. Cultures were grown to mid-log phase (OD_{650} = 0.3 – 0.6). Cells were lysed by adding 3 drops of 100 % (v/v) toluene and 3 drops of 1 % (w/v) sodium deoxycholate, followed by vigorous vortexing. Lysates were aerated at 37 ºC for 20 minutes to allow for toluene evaporation. The reaction was started by adding 100 µl lysate to 2.5 ml ONPG solution at timed intervals. The solutions were incubated at 37 ºC for 15 minutes, or until they turned yellow. Reactions were stopped at timed intervals by the addition of 1 ml 1 M sodium carbonate. The absorbance at OD_{420} was measured.

β-galactosidase activity was calculated using the following formula:

$$\text{Promoter activity (Miller units)} = 1000 \times \frac{OD420 \times total\ reaction\ volume}{OD650 \times lysate\ volume \times reaction\ time}$$

Data shown is the mean from three technical replicates carried out on three different days, each containing three biological replicates. A transformant containing empty pRW50 was used as a negative control for background β-galactosidase activity.

2.2.17. Determination of minimum inhibitory concentration (MIC)

Overnight cultures were diluted to an OD_{650} of 0.05 in sterile distilled water, before being further diluted 1 in 20 in LB. A 96-well flat bottomed microtitre plate was prepared using the double dilution method (Andrews, 2001). Each well contained 50 µl diluted culture in a final volume of 100 µl per well with an appropriate concentration of antibiotic. A growth control was included, with LB and culture only. A sterility control was included, with LB only. The

plate was incubated for 18 hours at 37 °C. The MIC was recorded as the lowest concentration that prevented bacterial growth. *E. coli* strains NCTC 10418 and ATCC 25922 were used as controls. Results were only accepted if the MIC was within one double dilution of the expected MIC for these strains.

2.2.18. Growth curves

Overnight cultures were diluted to an OD_{650} of 0.05 in LB. These were incubated at 37 °C with 200 rpm shaking. Over the first 8 hours, samples were taken every 40 minutes and OD_{650} was measured. Once the OD_{650} was beyond 0.8, samples were diluted 1 in 10 with LB to account for inaccuracy of the spectrophotometer. After this, cultures were grown at 37 °C with 200 rpm shaking until they had been growing for 24 hours. A final OD_{650} measurement was taken.

2.2.19. Statistical analysis

Statistical significance of β-galactosidase activity was tested using a one-way analysis of variance (ANOVA) using a Geisser-Greenhouse correction to assume equal variability of differences. This was followed up with a post-hoc Tukey's HSD test with a 95 % confidence interval to allow for pairwise comparisons. An ANOVA was used rather than a t-test because experiments were grouped and therefore all means were compared. Statistical significance of growth curves was tested using a two-way ANOVA using a Geisser-Greenhouse correction to assume equal variability of differences. This was followed up with a two-stage step-up method of Benjamini, Kreiger and Yekutieli to control the false discovery rate. Pairwise comparisons were compared for each time point. Significance for each time point was defined as a q-value (adjusted p-value) < 0.05 and an overall statistical significance in growth was determined when over 50 % (7/14) time points had a significant q-value. Statistical significance of growth rate was tested using an unpaired two-tailed t-test with a 95 % confidence level with appropriate

pairwise comparisons. All statistical analysis was carried out using Graphpad Prism 9 and significance was defined as $p < 0.05$.

2.2.20. Bioinformatic analysis to locate putative MarA binding sites

Novel putative marboxes were located by scanning the *E. coli* K-12 MG1655 genome with a 15 bp marbox motif (5' – GCANNNNNNGCNAAA-3') using Colibri. Search parameters were filtered to identify sites up to 200 bp upstream of start codons, with only 1 mismatch and associated with "lipid", "lipo" or "LPS". Targets were manually sorted by discarding genes of unknown function. Of the remaining targets, only those directly involved in cell envelope biosynthesis, including outer membrane biosynthesis and cell wall biogenesis, were chosen for further experimental testing.

2.2.21. *In vitro* transcription assays

pSR plasmid containing a promoter of interest upstream of *oriT* were used for *in vitro* transcription. 335 ng pSR maxiprep was mixed with 1 x TNSC buffer, 100 µg/ml BSA, 200 µM ATP/GTP/CTP, 10 µM UTP and 4 µCi [α-^{32}P]-UTP. The reaction was made up to 11 µl with ddH_2O and incubated with 0 – 5 µM MarA at 37 ^{o}C for 10 minutes. RNAP core enzyme and σ^{70} were incubated at 37 ^{o}C for 5 minutes, and 4 µl reaction mix was added in timed intervals. The reaction was run for 10 minutes at 37 ^{o}C and terminated by addition of 20 µl STOP solution. Reactions were loaded onto a 6 % denaturing gel. The gel was calibrated using a G+A ladder or M13 T7 sequencing reactions. Denaturing PAGE was carried out at 60 W for approximately 1 hour in 1 x TBE running buffer. The gel was vacuum dried and exposed to a phosphorscreen overnight. The screen was scanned using a BioRad FX® phosphoimager.

2.2.22. Generation of 'G+A' ladder

The DNA sequence of interest was cloned into pSR and digested using AatII and HindIII. The fragment was radiolabelled at the HindIII end (as Section 2.2.12). 100 ng of this fragment was diluted in 8 µl dH_2O and mixed with 50 µl formic acid. This mixture was left at room temperature for 2.5 minutes. 200 µl 0.3 M sodium acetate, 1 µl 20 mg/ml glycogen and 700 µl ice-cold 100% ethanol was added. DNA was precipitated at -80 ºC for 15 minutes and centrifuged at 17,000 x g for 15 minutes at 4 ºC. The pellet was washed with 70 % ethanol and centrifuged for 17,000 x g at 4 ºC for 10 minutes. This was repeated two times. The pellet was dried in a vacuum and re-suspended in 1 M piperidine. The reaction was incubated at 90 ºC for 30 minutes and stopped by adding 1 µl glycogen, 10 µl 3 M sodium acetate, and 300 µl ice-cold 100 % ethanol. DNA was precipitated at -80 ºC for 15 minutes. DNA was centrifuged at 17,000 x g for 15 minutes and washed twice in 70 % ethanol. The pellet was dried under a vacuum and re-suspended in DNAse I blue.

2.2.23. Generation of M13 T7 sequencing reactions

M13 sequencing reactions were generated using the T7 sequencing kit supplied by USB. The template DNA was denatured by mixing 2 µg single-stranded template M13mp18 phage DNA with 24 µl ddH_2O and 8 µl 2 M NaOH. The mixture was left at room temperature for 10 minutes. 7 µl 3 M sodium acetate (pH 4.8), 4 µl ddH_2O and 120 µl ice-cold 100 % ethanol was added. The mixture was precipitated at -80 ºC for 15 minutes, then centrifuged at 17,000 x g for 30 minutes at 4 ºC. The pellet was washed with ice-cold 70 % ethanol and centrifuged at 17,000 x g for 10 minutes at 4 ºC. The pellet was dried under a vacuum and re-suspended in 10 µl ddH_2O. The primer was annealed to the DNA by adding 5-10 ρmol of undiluted universal primer stock and 2 µl annealing buffer, before vortexing. The mixture was incubated at 65 ºC, 37 ºC and room temperature for 5 minutes, 10 minutes and 5 minutes, respectively. 2.5 µl each

of “A/C/G/T Mix-short” was transferred into four tubes. 1 µl T7 polymerase stock was diluted by the addition of 4 µl T7 dilution buffer. 3 µl label mix “A”, 1 µl [α-^{32}P]-ATP and 2 µl diluted T7 DNA polymerase was added to the template mixture and incubated at room temperature for 5 minutes. During the last minute of incubation, the "A", "C", "G", and "T" reactions were incubated at 37 ºC. Termination of the reactions was achieved by transferring 4.5 µl reaction into each of the 4 tubes, mixing gently and incubating at 37 ºC for 5 minutes. The reactions were stopped by adding 8 µl STOP solution. Tubes could be used immediately or stored at -20 ºC. Reactions were used as calibrations for primer extensions. Before loading onto a 6 % denaturing gel, the tube was heated at 80 ºC for 2 minutes. 1-3 µl of each sample was loaded.

2.2.24. Primer extension assays

Primer extension reactions were carried out using RNA purified from *E. coli* JCB387 transformants containing the pRW50 plasmid with the promoter of interest. The experiment was carried out over 2 days.

Day 1: 0.5 µl 100 µM D49724 primer (anneals on pRW50 downstream of HindIII) was radiolabelled by adding 2 µl polynucleotide kinase buffer, 15.5 µl dH_2O, 1 µl [γ-^{32}P]-ATP and 1 µl T4 polynucleotide kinase. This was incubated for 30 minutes at 37 ºC, followed by 10 minutes at 68 ºC to inactivate the enzyme. 30 µg purified RNA was mixed with 1 µl radiolabelled D49724 primer and precipitated using 1/10 volume 3 M sodium acetate pH 7.0 and 2.5 volumes of ice-cold 100 % ethanol and incubated at -80 ºC for 30 minutes. The mixture was centrifuged at 17,000 x g for 20 minutes at 4 ºC. The pellet was washed with 750 µl ice-cold 70 % ethanol and centrifuged at 17,000 x g for 10 minutes at 4 ºC. The pellet was dried under a vacuum and re-suspended in 30 µl hybridisation buffer, before mixing and incubation at 50 ºC for 5 minutes. To anneal the primer, the solution was incubated at 75 ºC for 15 minutes,

then 50 °C for 3 hours. 75 µl ice-cold 100 % ethanol was added and the sample was incubated overnight at -80 °C.

Day 2: The annealed primer/RNA sample was centrifuged at 17,000 x g for 20 minutes at 4 °C. The pellet was washed by addition of 750 µl ice-cold 70 % ethanol and centrifuged at 17,000 x g for 10 minutes at 4 °C. The pellet was dried under a vacuum and re-suspended in 31 µl dH_2O. Primer extensions were carried out by adding 10 µl 5 x reverse transcriptase buffer, 1 µl 50 mM DTT, 5 µl 10 mM dNTPs (giving final concentration of 0.2 mM), 2.5 µl AMV reverse transcriptase and 0.6 µl RNasin®. The sample was incubated at 37 °C for 1 hour, followed by inactivation of the enzyme at 72 °C for 10 minutes. RNA was degraded by addition of 1 µl 10 mg/ml RNase A and incubated at 37 °C for 30 minutes. DNA was precipitated by the addition of 6.7 µl 3 M sodium acetate pH 4.8 and 125 µl ice-cold 100 % ethanol and incubation at -80 °C for 30 minutes. The sample was centrifuged at 17,000 x g for 20 minutes at 4 °C. The pellet was washed in 1 ml ice-cold 70 % ethanol and centrifuged at 17,000 x g for 10 minutes at 4 °C. The pellet was dried under a vacuum and re-suspended in 4 µl STOP solution. 1-3 µl was run on a 6 % denaturing gel with M13 sequencing reactions at 60 W for 2 hours.

2.2.25. Crystal violet assays

Membrane permeability was measured using a crystal violet assay described by Halder *et al*., 2015. Briefly, cell cultures were harvested at 4500 x g for 5 minutes at 4 °C. Cells were washed three times and re-suspended in 0.5 mM phosphate-buffered saline (PBS) (pH 7.4) containing 10 µg/ml crystal violet. This was incubated at 37 °C for 10 minutes and centrifuged at 13,400 x g for 15 minutes. The absorbance of the supernatant at OD_{590} was measured. The absorbance of PBS solution was used as a blank. The OD_{590} of PBS with 10 µg/ml crystal violet was

considered as 100 %. Percentage uptake of crystal violet was calculated using the following formula:

Dye uptake (%) = 100 x $\frac{OD590\ (sample)}{OD590(CV\ solution)}$

2.2.26. Membrane separation

Overnight cultures were diluted to an OD_{650} of 0.8 in LB. Samples were harvested at 11,300 x g for 10 minutes at 4 ºC using a JA 10.5 rotor. Pellets were re-suspended in 10 mM HEPES buffer and harvested at 4300 x g for 10 minutes at 4 ºC. Pellets were re-suspended in 3 ml 10 mM HEPES, 300 µl 10 x cOmplete™ Protease Inhibitor Cocktail, 100 µl DNase I buffer and 10 µl DNase I. Cells were lysed using 4 passes on a French pressure cell press at 1000 psi. Lysed cells were centrifuged at 4300 x g for 10 minutes at 4 ºC. 10 mM HEPES was added and samples were harvested at 75,600 x g for 60 minutes at 10 ºC using a JA 25.5 rotor. Pellets were re-suspended in 10 mM HEPES and re-harvested. Pellets were re-suspended in 20 % sucrose (in 10 mM HEPES). A sucrose gradient was prepared in a 14 ml ultracentrifuge tube. Briefly, 3.3 ml 73 % sucrose was added to the tube, followed with 6.7 ml 53 % sucrose. The sample re-suspended in 20 % sucrose was layered on top. The sucrose gradient was centrifuged at 141,000 x g for 16 hours at 4 ºC in a SW40 rotor with maximum acceleration and a deceleration of 5. Inner and outer membrane bands were removed by pipetting at sucrose interfaces and diluted to 30 ml in 10 mM HEPES. Separated membrane samples were harvested at 75,600 x g for 60 minutes at 10 ºC using a JA 25.5 rotor. The pellet was re-suspended in 10 mM HEPES and re-harvested. The pellet was re-suspended in 1 ml 10 mM HEPES. Membrane samples were stored at stored at -80 ºC.

2.2.27. SDS-PAGE

SDS-PAGE was used to check that the inner and outer membrane samples had distinct profiles, therefore confirming successful separation. 5 µl of membrane samples were mixed with 12.5 µl NUPAGE™ LDS sample buffer and 27.5 µl sterile water and boiled at 72 ºC for 10 minutes. Samples were mixed with 5 x SDS loading dye and loaded onto a Mini-PROTEAN TGX gel 4-15 % in 1 x Tris-Glycine SDS running buffer for 20 minutes at 200 V. Gels were treated with InstantBlue™ Coomassie stain for 16 hours then destained by washing with water three times for 15 minutes.

2.2.28. Lipid extraction

Overnight cultures were diluted to an OD_{650} of 0.05 in LB. These were grown at 37 ºC with 200 rpm shaking until OD_{650} was equal to 0.5. 1 ml of this culture (or 500 µl separated membrane sample) was added to a 2 ml Chromacol vial and harvested at 2880 x g for 15 minutes at 4 ºC. The pellet was re-suspended in 500 µl ice-cold methanol, 300 µl dH_2O and 1 ml chloroform. The vial was centrifuged at 2880 x g for 15 minutes at 4 ºC with the brakes off. The chloroform-rich bottom phase containing phospholipids was transferred to a fresh vial and dried under nitrogen. This was re-suspended in 1 ml 100 % acetonitrile. Lipid extractions was stored at -80 ºC.

2.2.29. Liquid chromatography/mass spectrometry (LC/MS)

LC/MS was performed using a Dionex UltiMate 3000 with a 2.5 µm, 3 mm x 150 mm BEH Amide XP column coupled to a Bruker amazon SL electrospray ion-trap spectrometer and a beta-RAM radio chromatography detector. The column had been stored at 30 ºC and the needle was cleaned with 10 % isopropanol. The column was equilibrated for 10 minutes with 95:5 (v/v) 100 % acetonitrile:10 mM ammonium acetate. 5 µl lipid extractions were injected onto

the LC/MS and separated on a stepwise gradient from 0-28 % ammonium acetate using a constant flow rate of 150 µl min^{-1} for 15 minutes. The negative ion ESI/MS and MS/MS were set as follows: capillary voltage 3500 V, end plate offset 500 V, 8 L min^{-1} drying gas at 300 ^{o}C, nebulizing gas pressure 15 psi. Qualitative and quantitative analyses were performed using Bruker Compass™ software. Compounds were identified by comparing their respective retention times and spectra (MS and MS–MS) to previous lipidomic studies and the LIPIDBLAST database (Kind *et al*., 2014).

2.2.30. Flexible recombineering using integration of *thyA* (FRUIT)

To introduce chromosomal point mutations, a novel recombineering technique, known as Flexible Recombineering Using Integration of *thyA* (FRUIT), was used (Stringer *et al*., 2012). This is shown in Figure 2.1.

Generation of Δ*thyA* JCB387: Genomic DNA from Δ*thyA* MG1655 F_3-*araC*-F_3-*thyA* was isolated. Primers JW472 and JW473 were used to amplify *thyA* flanking regions. The PCR product was purified using a Qiagen Gel Extraction kit. This was electroporated into JCB387 cells containing pACBSR, which had previously been grown in LB containing 0.2 % arabinose to induce expression of the λ Red genes, before being made electrocompetent. Following the electroporation, cells were recovered at 37 ^{o}C for one hour and plated onto M9 minimal medium containing 100 µg/ml thymine, 20 µg/ml trimethoprim and chloramphenicol. Colonies were confirmed using colony PCR with primers flanking the *thyA* site. Single colonies were inoculated into MyTaq™ Red mix with appropriate primers. PCR was carried out as Table 2.4. Colony PCR products were sequenced and successful Δ*thyA* recombinants were re-streaked onto the same medium.

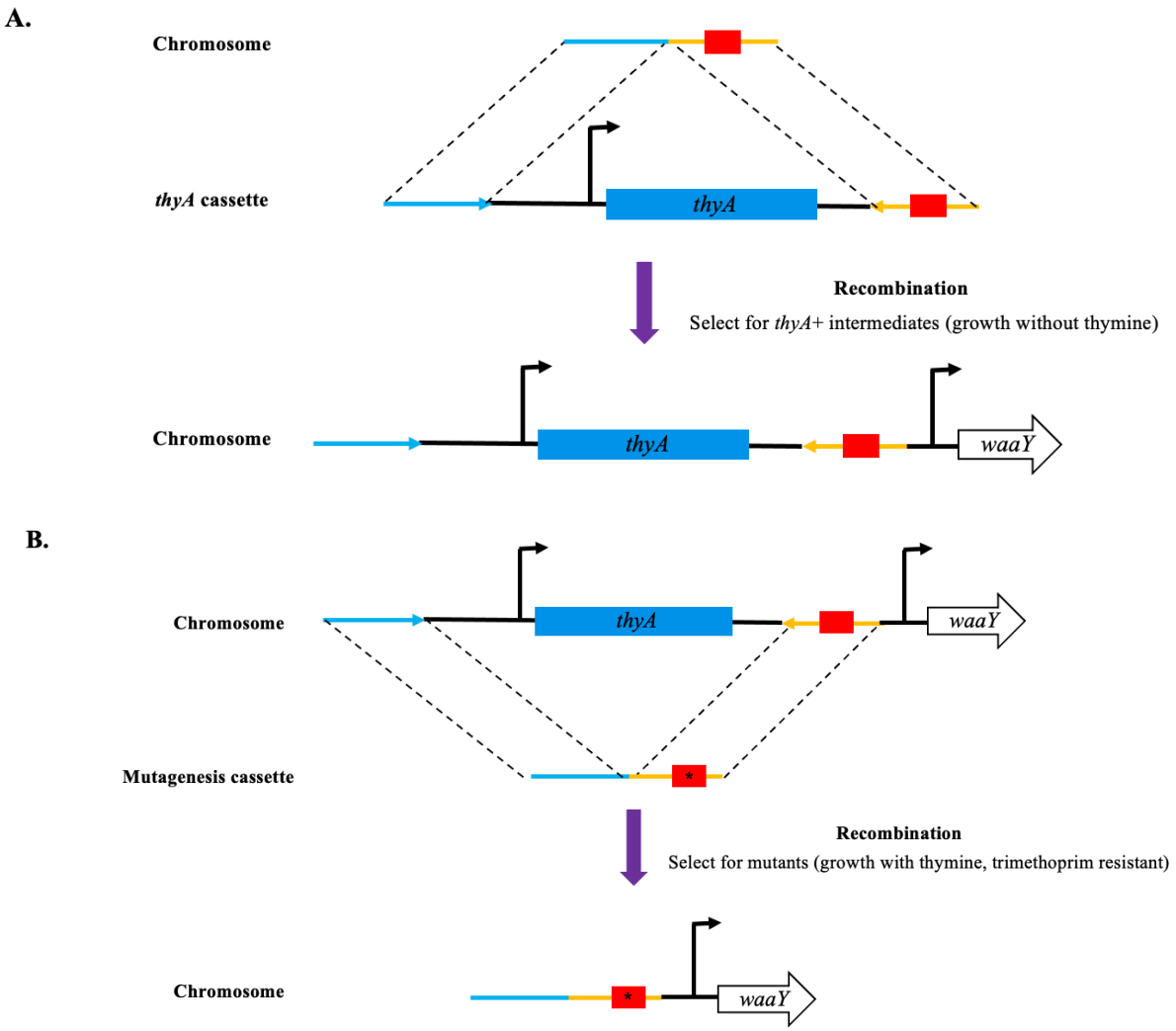

Figure 2.1. Flexible recombineering using integration of *thyA* (FRUIT).

A *thyA* cassette containing the *thyA* gene and a strong constitutive promoter was amplified from pAM001 using primers with 5′ regions that anneal to the desired region of recombination e.g. in the *waaY* promoter, as shown in this example. The marbox is shown in red. Recombinants were confirmed using colony PCR and sequencing. A. The *thyA* cassette was electroporated into Δt*hyA* cells containing pACBSR, grown with chloramphenicol, 100 µg/ml thymine, 20 µg/ml trimethoprim and 0.2 % arabinose to allow expression of λ Red genes. Recombinants were selected on M9 minimal medium containing chloramphenicol. B. A PCR product containing the desired point mutations (*) was electroporated into *thyA*+ intermediate cells containing pACBSR, grown with chloramphenicol and 0.2 % arabinose to allow expression of λ Red genes. Recombinants were selected on M9 minimal medium containing chloramphenicol, 100 µg/ml thymine and 20 µg/ml trimethoprim. Based on Stringer *et al.*, 2012.

Genome Editing: A *thyA* cassette, which contains a strong constitutive promoter, was amplified using primers with 80 bp 5′ sequence that matched the desired site of recombination ("Targeting Upstream" and "Targeting Downstream" primers). pAMD001 was used as a template for this, as described in Stringer et *al*., 2012. PCR products were purified using a Qiagen Gel Extraction kit. These were electroporated into Δ*thyA* JCB387 cells containing pACBSR, which had previously been grown in LB containing chloramphenicol, 100 µg/ml thymine and 0.2 % arabinose to induce expression of the λ Red genes, before being made electrocompetent. Following the electroporation, cells were recovered at 37 ºC for one hour, plated onto M9 minimal medium (lacking thymine) containing chloramphenicol, and grown at 37 ºC for 24 – 48 hours. Colonies were confirmed using colony PCR with primers flanking the expected site of *thyA* insertion. Colony PCR products were then sequenced and successful *thyA*+ intermediates were re-streaked onto the same medium. The desired chromosomal sequence, containing the point mutations, was ordered as a gene strand from Eurofins and further amplified using primers to amplify the entire fragment ("Mutagenesis Upstream" and "Mutagenesis Downstream" primers). PCR products were purified using a Qiagen Gel Extraction kit. These were electroporated into *thyA*+ intermediate cells containing pACBSR, which had previously been grown in LB containing chloramphenicol and 0.2 % arabinose to induce expression of the λ Red genes, before being made electrocompetent. Following the electroporation, cells were recovered at 37 ºC for one hour, plated onto M9 minimal medium containing 100 µg/ml thymine, 20 µg/ml trimethoprim and chloramphenicol, and grown at 37 ºC for 24 – 48 hours. Colonies were confirmed using colony PCR with primers flanking the expected site of mutagenesis. Colony PCR products were then sequenced, and successful mutants were re-streaked onto the same medium.

Chapter 3 – MarA Activation of *lpxC*

3.1 Introduction

The MarA regulon has been researched increasingly in recent years. Estimates suggest that the regulon comprises around 100 genes but only 32 experimentally confirmed targets are listed in Ecocyc (Griffith *et al.,* 2002; Barbosa and Levy, 2000). Recently, 33 novel MarA targets were identified in a ChIP-seq experiment (Sharma *et al*., 2017). Some of these have been proven experimentally to be regulated by MarA, including the *mlaFEDCB* operon (Sharma *et al*., 2017). Briefly, the *mlaFEDCB* operon encodes an ABC transport system that removes unwanted phospholipids from the outer leaflet of the OM (Malinverni *et al*., 2009). This is important because the barrier function of the Gram-negative cell envelope heavily relies on OM asymmetry (Kamio and Nikaido, 1976). Thus, it is hypothesised that upregulation of *mlaFEDCB* by MarA improves barrier function (Sharma *et al*., 2017). This also suggests that additional cell envelope factors may be regulated by MarA. In further ChIP experiments, *lpxC* was identified as a SoxS target in *E. coli* (Seo *et al*., 2015). Additionally, *lpxC* has been demonstrated to bind RamA, a MarA paralogue found in *K. pneumoniae* (De Majumdar *et al*., 2015). *lpxC* is an essential gene that encodes a protein involved in lipid A biosynthesis.

The cell envelope of Gram-negative bacteria is characterised by an IM and OM (Glauert and Thornley, 1969). Between these membranes is the periplasm, which contains the peptidoglycan cell wall (Figure 3.1). Unlike the IM, which is a phospholipid bilayer, the OM is highly asymmetric. The inner leaflet is a phospholipid layer but the outer leaflet is made up of lipopolysaccharide (LPS) (Kamio and Nikaido, 1976). LPS is composed of lipid A, a core oligosaccharide, and the O-antigen (Raetz and Dowhan, 1990). Lipid A, a hydrophobic glucosamine disaccharide, forms the outer leaflet of the OM. Lipid A is linked to a core oligosaccharide, which contains 3-deoxy-D-manno-octulosonic acid (KDO) residues,

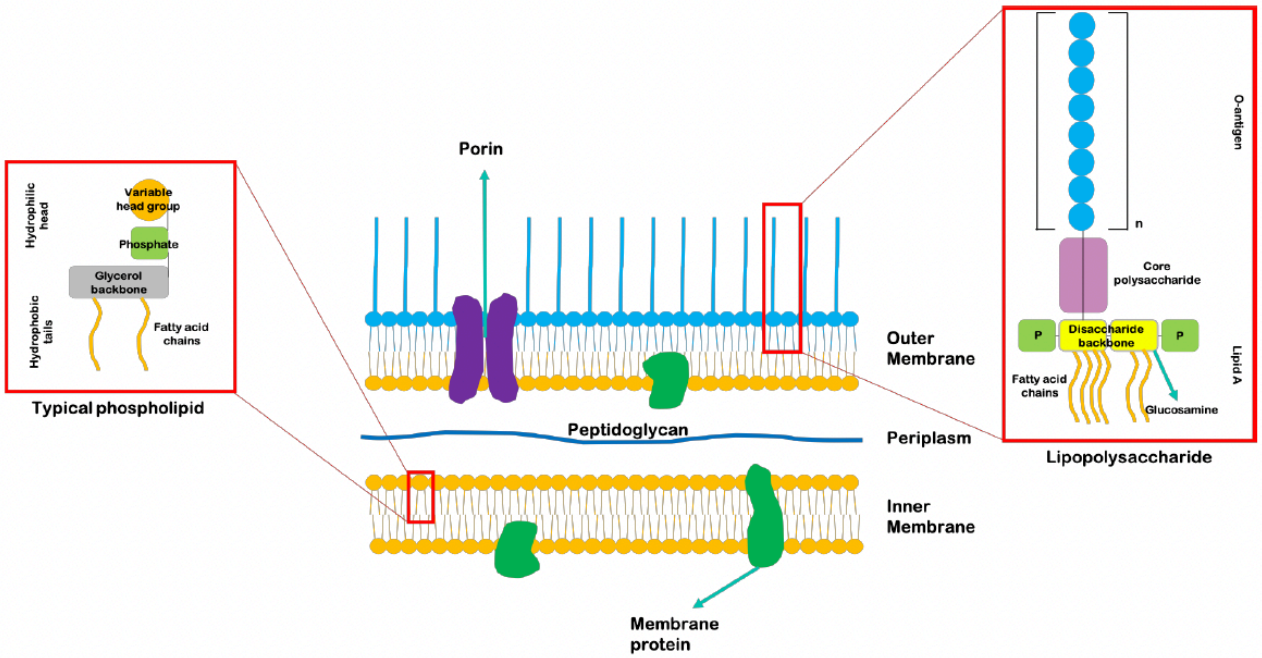

Figure 3.1. The Gram-negative cell envelope.

The IM is a phospholipid bilayer that surrounds the cytoplasm. These phospholipids are composed of a variable head group, a phosphate moiety, a glycerol backbone and hydrophobic fatty acid chains. The periplasm is found between the IM and OM and contains a peptidoglycan cell wall layer. The OM contains phospholipids on the inner leaflet and LPS on the outer leaflet. LPS is composed of O-antigen, a core polysaccharide and lipid A, which anchors it into the membrane. Membrane proteins and porins are important components found within the membranes.

heptoses, and hexoses. The O-antigen is attached to the core oligosaccharide and is composed of two to eight sugars.

Lipid A biosynthesis begins with a UDP-GlcNAc precursor (N-acetyl glucosamine linked to a nucleotide carrier) (Anderson, Bulawa and Raetz, 1985). In the cytoplasm, UDP-GlcNAc is acylated to produce UDP-3-O-(acyl)-GlcNAc by enzyme LpxA. This reaction is unfavourable, so the first committed step of lipid A biosynthesis is the deacetylation of UDP-3-O-(acyl)-GlcNAc to UDP-3-O-(acyl)-GlcN achieved by LpxC. Considering that LpxC catalyses the first committed step in lipid A biosynthesis, it is an important regulatory control point for the pathway (Sorensen *et al*., 1996). UDP-3-O-(acyl)-GlcN is acylated further and the nucleotide carrier is removed by LpxD and LpxH, respectively, to generate 2,3-diacylglucosamine-1-phosphate, or 'lipid X' (Kelly *et al*., 1993; Ray, Painter and Raetz, 1984; Babinski, Kanjiala and Raetz, 2002). Lipid X is added to UDP-2,3-diacylglucosamine, the product of the LpxD reaction, and the UDP carrier is released (Ray, Painter and Raetz, 1984). The resulting product is referred to as lipid A disaccharide, and this is inserted into the IM. LpxK phosphorylates lipid A disaccharide at the 4' position to become lipid IV_A (Ray and Raetz, 1987). Two KDO sugars of the core oligosaccharide are added to lipid IV_A by enzyme WaaA (Brozek *et al*., 1989). Further acylation events, catalysed by LpxL and LpxM, occur to produce KDO_2-Lipid A (Brozek and Raetz, 1990; Clementz, Bednarski and Raetz, 1996; Clementz, Zhou and Raetz, 1997). Figure 3.2 illustrates the lipid A biosynthetic pathway.

LPS provides the OM with a permeability barrier again small, hydrophobic molecules (Silhavy, Kahne and Walker, 2010). Compounds with a molecular weight (MW) of over 600 Da cannot penetrate the OM (O'Shea and Moser, 2008). This explains why many Gram-negative bacteria are intrinsically resistant to some antibiotics, such as vancomycin and daptomycin. Lipid A

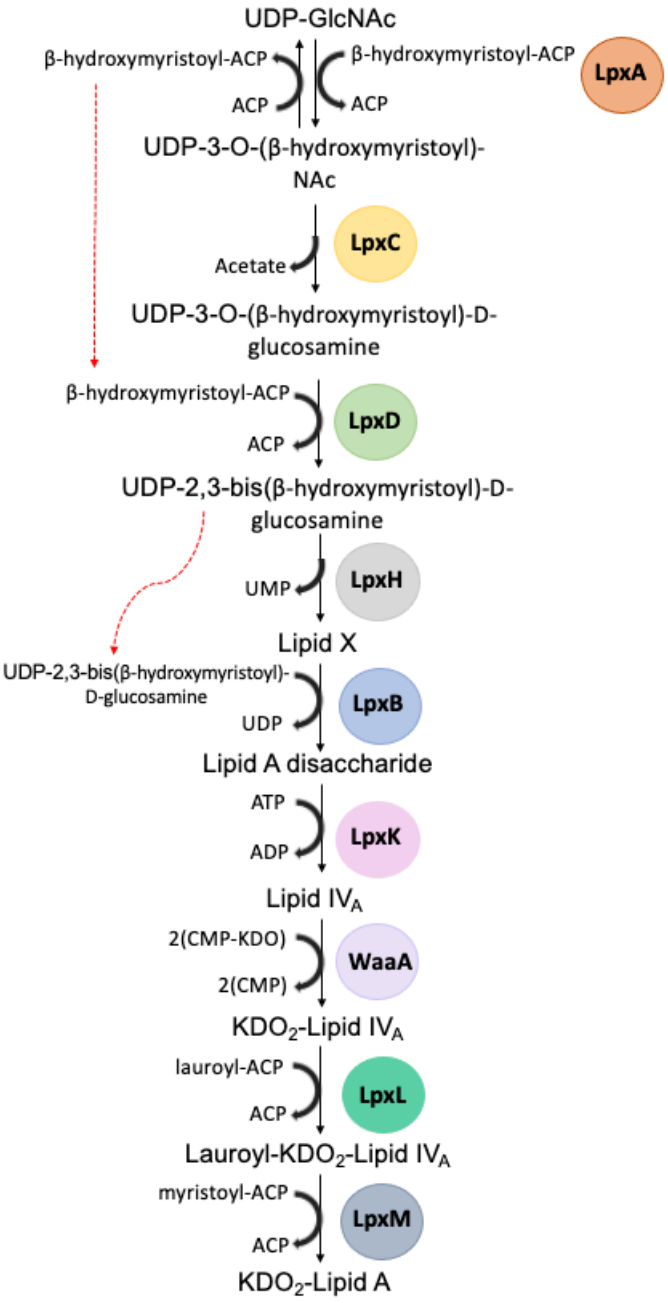

Figure 3.2. Lipid A biosynthesis (The Raetz pathway).

The UDP-GlcNAc precursor is used to make KDO_2-Lipid A through the Raetz pathway, which relies on enzymes LpxA, LpxC, LpxD, LpxH, LpxB, LpxK, WaaA, LpxL and LpxM, respectively. Straight black arrows demonstrate the reaction direction. Curved black arrows demonstrate additional substrates used in the reaction, including where they are used. Dotted red arrows demonstrate substrates that are re-used later in the pathway. Adapted from Emiola, George and Andrews, 2015.

biosynthesis is a promising target for new therapeutic agents. Inhibitors of LpxA and LpxD have been designed and are currently undergoing further research (Ryan *et al*., 2021; Ma *et al*., 2020). Multiple LpxC inhibitors have reached clinical trials but, so far, all have failed due to unexpected toxicity in mouse models (Cohen *et al*., 2019; Theruetzbacher *et al*., 2020).

In this chapter we show that MarA activates *lpxC* expression *in vitro* and *in vivo*. This requires binding to a marbox, in the forward orientation, overlapping the *lpxC* promoter -35 element. Hence, *lpxC* is controlled by a Class II MarA activated promoter (Martin *et al*., 1999). Prior to this work, regulation of this gene by MarA has not been shown in *E. coli*.

3.2. Regulation of *lpxC* by MarA

3.2.1. MarA binds to a marbox in the *lpxC* promoter

The DNA sequence upstream of *lpxC* is shown in Figure 3.3 (Panel A). The region has 2 promoters (P1*lpxC* and P2*lpxC*) (Beall and Lutkenhaus, 1987; Mendoza-Vargas *et al*., 2009). The putative marbox sequence overlaps the -10 element of P1*lpxC* and the -35 element of P2*lpxC*. A 123 bp DNA sequence, containing the marbox and all promoter elements, was prepared and referred to as *lpxC*.1 (Figure 3.3, Panel A). This DNA fragment was used in an EMSA with purified MarA. Briefly, DNA was radiolabelled with [γ-^{32}P]-ATP and incubated with increasing concentrations of MarA. The complexes were separated on a 6 % polyacrylamide gel. A DNA-protein complex was formed when MarA was added (Figure 3.3, Panel B). As the concentration of MarA increases, more MarA:DNA complexes form, and there is less free DNA. This indicates that MarA binds to the marbox within the *lpxC* regulatory region.

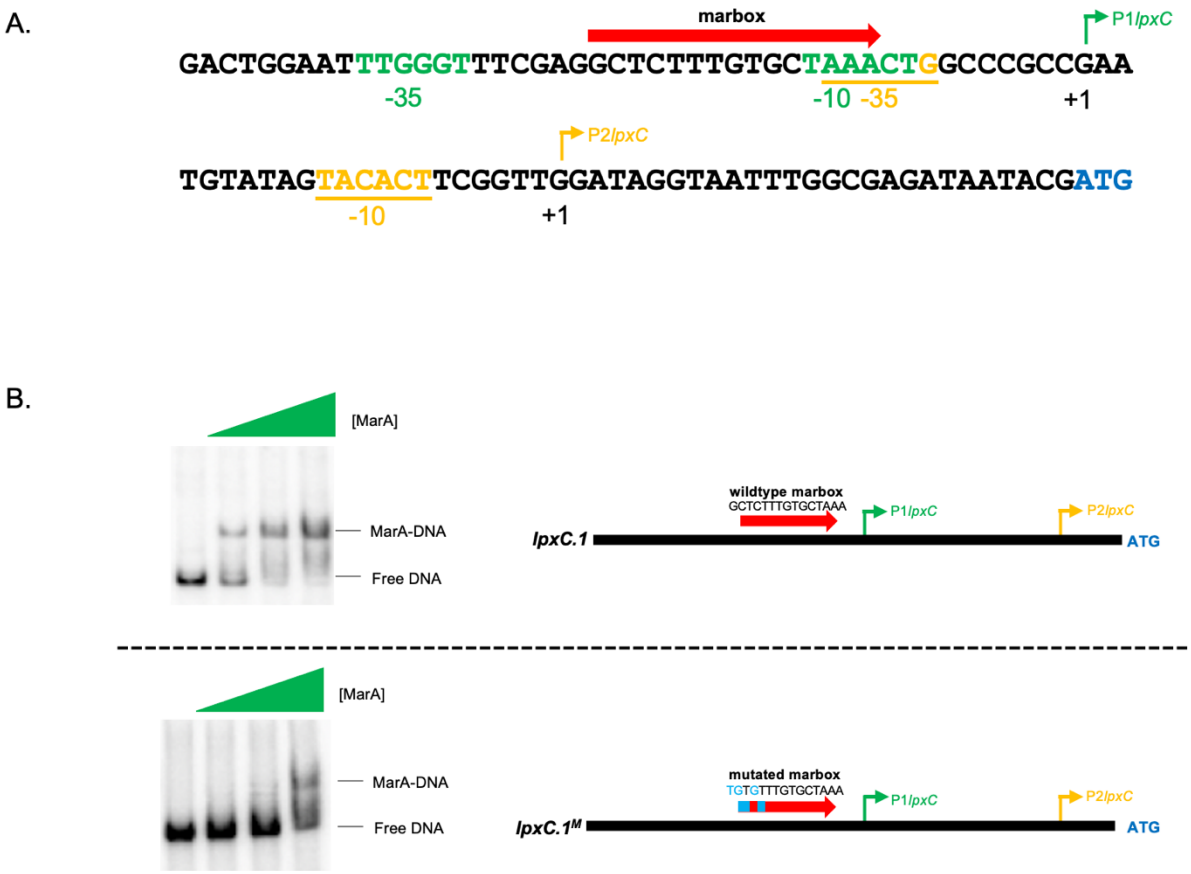

Figure 3.3. Binding of MarA to the marbox of P*lpxC*.

A. The P*lpxC* regulatory region. The promoter region contains two promoters, P1*lpxC* and P2*lpxC*, shown in green and yellow, respectively. The -10 and -35 elements of P1*lpxC* are shown in green. The -10 and -35 elements of P2*lpxC* are shown in yellow and underlined. Transcription start sites are labelled as +1. The *lpxC* start codon is shown in blue. B. Binding of MarA to the P*lpxC* marbox in an EMSA. Images of 6 % polyacrylamide gels used to separate MarA:DNA complexes are shown. The EMSA assay was carried out with the *lpxC*.1 promoter derivatives shown. Increasing concentrations of MarA (1 µM – 2 µM – 4 µM) are shown by green triangles. MarA:DNA complexes and free DNA are indicated.

To determine the importance of the marbox sequence of P*lpxC*, key residues were mutated. The GCA motif at positions 1-3 (as Figure 1.12) is highly conserved due to contacts with MarA amino acids R96 and T93 (Rhee *et al*., 1998). The marbox of P*lpxC* is already a suboptimal GCT at these positions (Figure 3.3, Panel A). To prevent MarA binding, mutations were made at positions 1 and 2 as well as the adjacent C at position 4 (Figure 3.3, Panel B). This *lpxC*.1^{M} derivative was used in an EMSA, as previously. Mutating this motif was sufficient to reduce binding of MarA substantially. MarA:DNA complexes only formed at the highest concentration of MarA (4 μM), in contrast to binding at the lowest concentration (1 μM) for the wildtype *lpxC*.1 derivative.

3.2.2. MarA activates *lpxC* expression *in vivo*

To understand how MarA affects the expression of *lpxC*, the *lpxC*.1 and *lpxC*.1^{M} fragments were cloned in reporter plasmid pRW50, containing promoterless *lacZ*. *E. coli* JCB387 was transformed with these pRW50 derivatives and β-galactosidase activity was measured. A significant increase in promoter activity was seen when *marA* was expressed (Figure 3.4). This suggests that MarA activates *lpxC*. A reduction in promoter activity was noted when the marbox was mutated, consistent with loss of binding demonstrated in Figure 3.3, Panel B (Figure 3.5).

3.2.3. MarA activates *lpxC* expression *in vitro*

In vitro transcription was used to further investigate activation of *lpxC* by MarA. The *lpxC*.1 and *lpxC*.1^{M} fragments were cloned into plasmid pSR, upstream of the phage-derived transcription terminator λoop. The RNAP holoenzyme was added to initiate transcription from P*lpxC* and transcripts were terminated at λoop. The RNAI transcript acts as an internal control for RNAP activity and gel loading. Increasing concentrations of MarA were added to generate

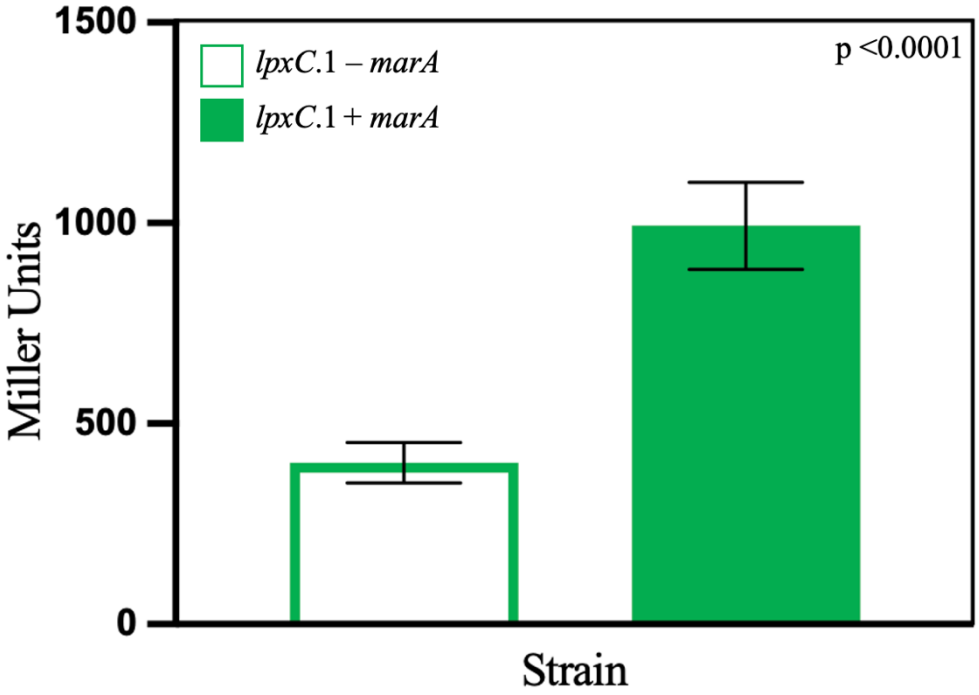

Figure 3.4 *In vivo* activation of the *lpxC* regulatory region by MarA.

Promoter activity was determined by assessing β-galactosidase activity in *E. coli* JCB387 cells transformed with pRW50 containing *lpxC*.1 (wildtype marbox). Cells containing empty pRW50 were used as the control. Promoter activity shown in Miller units is the mean of assays from 3 separate days, each day comprising of 3 biological replicates. MarA was provided on pJ203 with constitutive expression of *marA*. The mean activity and standard deviation is shown. A one-way ANOVA was calculated using the promoter activities, showing the analysis was significant ($p < 0.0001$, $F(2,24) = 54.39299$). A post-hoc Tukey's HSD test showed that all groups were significantly different from each other ($p < 0.05$ for each pair compared).

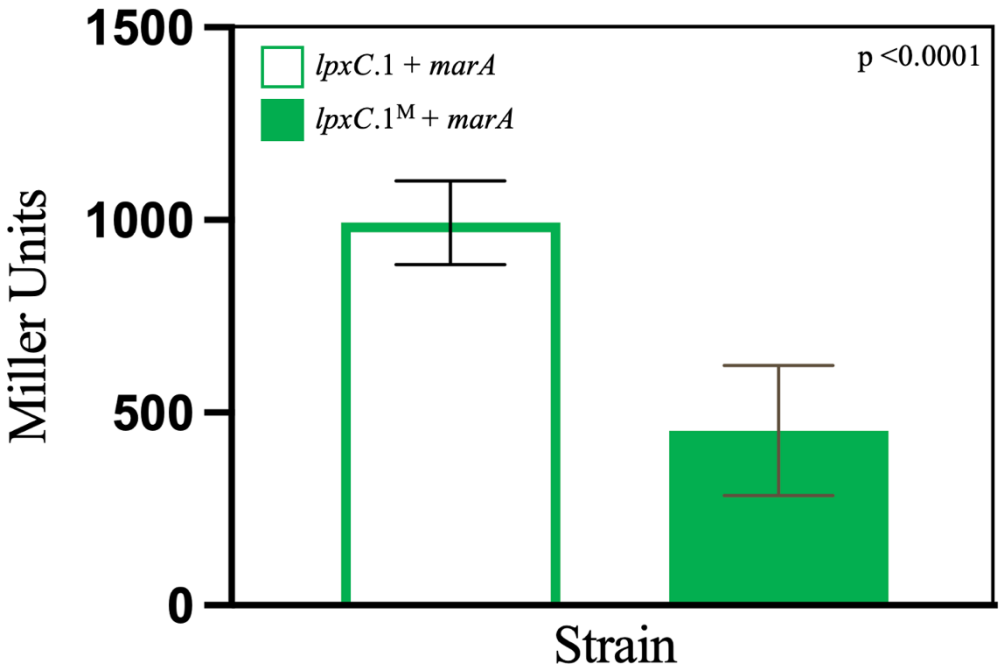

Figure 3.5. *In vivo* activation of the *lpxC* regulatory region by MarA requires the marbox. Promoter activity was determined by assessing β-galactosidase activity in *E. coli* JCB387 cells transformed with pRW50 containing either *lpxC*.1 (wildtype marbox) or *lpxC*.1^{M} (mutated marbox). Cells containing empty pRW50 were used as the control. Promoter activity shown in Miller units is the mean of assays from 3 separate days, each day comprising of 3 biological replicates. MarA was provided on pJ203 with constitutive expression of *marA*. A one-way ANOVA was calculated using the promoter activities, showing the analysis was significant ($p < 0.0001$, $F(2,24) = 45.06$). A post-hoc Tukey's HSD test showed that all groups were significantly different from each other ($p<0.05$ for each pair compared).

[α-^{32}P]-UTP labelled transcripts prior to analysis on a denaturing gel (Figure 3.6). An increase in the intensity of a 118 nt transcript corresponding to that from P2*lpxC* was seen when MarA was added. This suggests that MarA activates transcription of *lpxC* from P2*lpxC*. A decrease in the amount of a 140 nt transcript from P1*lpxC* was observed in parallel. This suggests that MarA represses transcription of *lpxC* from P1*lpxC*. When the marbox was mutated, no increase in the intensity of the band derived from P2*lpxC* was demonstrated, showing that activation no longer occurs. Repression of P1*lpxC* is still observed but greatly reduced.

3.3. Investigating the Repression of P1*lpxC* by MarA

Activation of *lpxC* by MarA *in vivo* is significant (Figure 3.4). However, *in vitro*, activation of P2*lpxC* is offset by repression of P1*lpxC* (Figure 3.6). There is no significant difference in the additive transcript levels, demonstrated by P1/RNAI and P2/RNAI ratios, as MarA is added. Hence, there is little change in overall *lpxC* transcription. We next aimed to understand the discrepancy between the observations noted *in vitro* and *in vivo*.

3.3.1. The transcripts from P1*lpxC* and P2*lpxC* are degraded at the same rate

First, we considered the possibility that the stability of the mRNA generated from each promoter might be different *in vivo* due to the presence of RNA processing factors. In particular, the transcript from P1*lpxC* could be degraded at a faster rate than the P2*lpxC* transcript. This might explain why there is activation of *lpxC in vivo* despite the small overall change in transcription demonstrated *in vitro*.

To characterise stability of the *lpxC* transcripts, primer extension assays were done in the presence and absence of rifampicin (Figure 3.7). Rifampicin inhibits RNAP activity to inhibit transcription elongation and thus, transcription is inhibited (Wehrli, 1983). After the addition

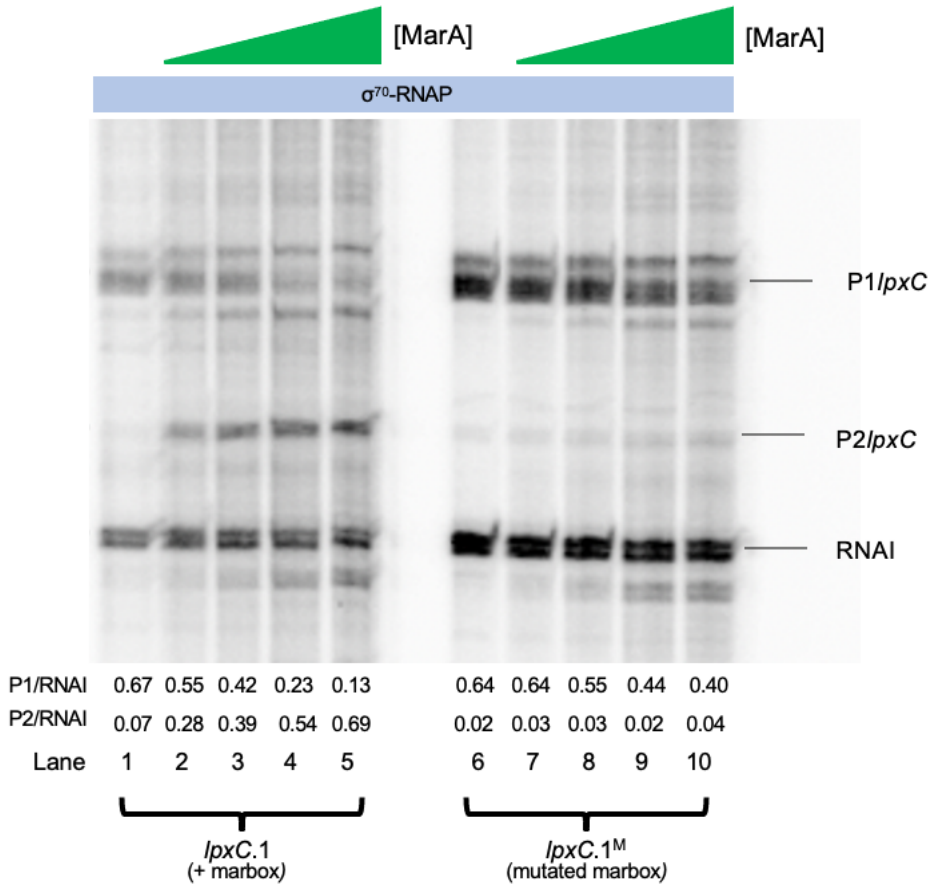

Figure 3.6. MarA activation of transcription from the P*lpxC* promoter.

Images of 6 % polyacrylamide gels used to separate transcripts generated *in vitro* using the *lpxC*.1 and *lpxC*.1^{M} derivatives, respectively. Assays were done with RNAP-σ^{70}. Increasing concentrations of MarA (1 μM – 2 μM – 4 μM – 5 μM) are shown by green triangles. Bands formed by transcripts originating from P1*lpxC*, P2*lpxC* and RNAI are indicated by solid lines. The ratio of transcript to P*lpxC*:RNAI is shown.

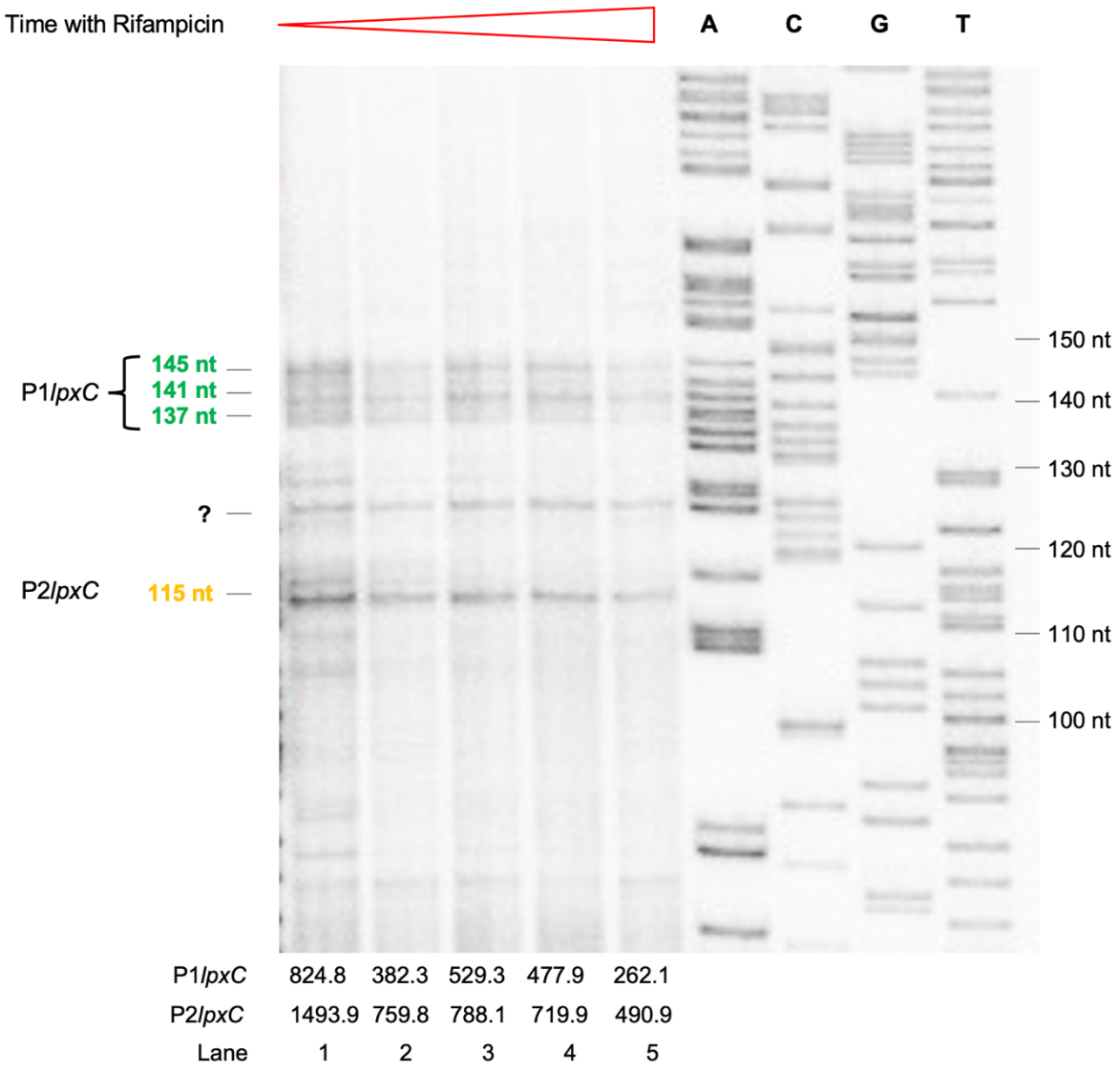

Figure 3.7. Analysis of *lpxC* transcript stability using primer extension and inhibition of transcription.

E. coli JCB387 transformants containing pRW50 with *lpxC.1* (wildtype marbox) and pJ203 with *marA* were incubated with rifampicin. RNA was isolated 0, 2.5, 5, 10 and 20 minutes after rifampicin addition (Lanes 1 – 5, respectively). RNA was used for a primer extension assay and run of a 6 % polyacrylamide gel. Transcripts from P1*lpxC* and P2*lpxC* were determined to be degraded at similar rates based on quantitative analysis of band intensities. The gel was calibrated using M13 T7 sequencing reactions. Note the presence of a new potential transcription start site (denoted "?"). Based on sequence analysis, it was determined that this is likely an artefact.

of rifampicin, degradation of existing transcripts can be measured over time. To monitor this degradation, we used primer extension, a technique to map the level and 5′ end of RNA transcripts. Briefly, a radiolabelled primer anneals to a region within the RNA and reverse transcriptase is used to synthesise complementary DNA (cDNA). The product is run on a gel to determine quantity and size. RNA was isolated from *E. coli* JCB387 containing the *lpxC*.1 fragment cloned into pRW50 at intervals between 0 and 20 minutes after rifampicin addition. A 115 bp product was observed that maps to the transcription start site (+1) at P2*lpxC* (Figure 3.7). There were 3 TSSs for P1*lpxC*, as demonstrated by 137, 141 and 145 bp products. There was an overall decrease in the amount of RNA present between 0 and 20 minutes, indicated by a decrease in band intensity. The final percentage decrease of band intensity, indicative of RNA stability, was 68.22% and 67.12%, respectively, for transcripts from P1*lpxC* and P2*lpxC*. Hence, there was no difference in degradation over this time course.

3.3.2. Termination of transcription from P1*lpxC* and P2*lpxC* occurs at the same rate

We next hypothesised that the longer 5′ UTR of mRNA transcribed from P1*lpxC* might be a better target for the termination factor Rho. Briefly, Rho binds the 5' end of mRNA, translocates along to the RNA-DNA hybrid and unwinds the duplex structure using helicase activity. To investigate the role of Rho, primer extension assays were done in the absence and presence of bicyclomycin, which inhibits Rho (Figure 3.8, Panel A). RNA was isolated from *E. coli* JCB387 containing the *lpxC*.1 and *lpxC*.1^{M} fragments. In the absence of bicyclomycin (Figure 3.8, Panel A, Lanes 1 - 4), MarA activated transcription from P2*lpxC* in a marbox dependent manner, demonstrated by an increase in the band intensity as RNA is increased. A similar result was obtained in the presence of bicyclomycin (Figure 3.8, Panel A, Lanes 5 – 8). There was also no significant difference in *lpxC* expression *in vivo* when bicyclomycin was added (Figure 3.8, Panel B). Hence, termination by Rho does not explain the discrepancy between our *in vitro*

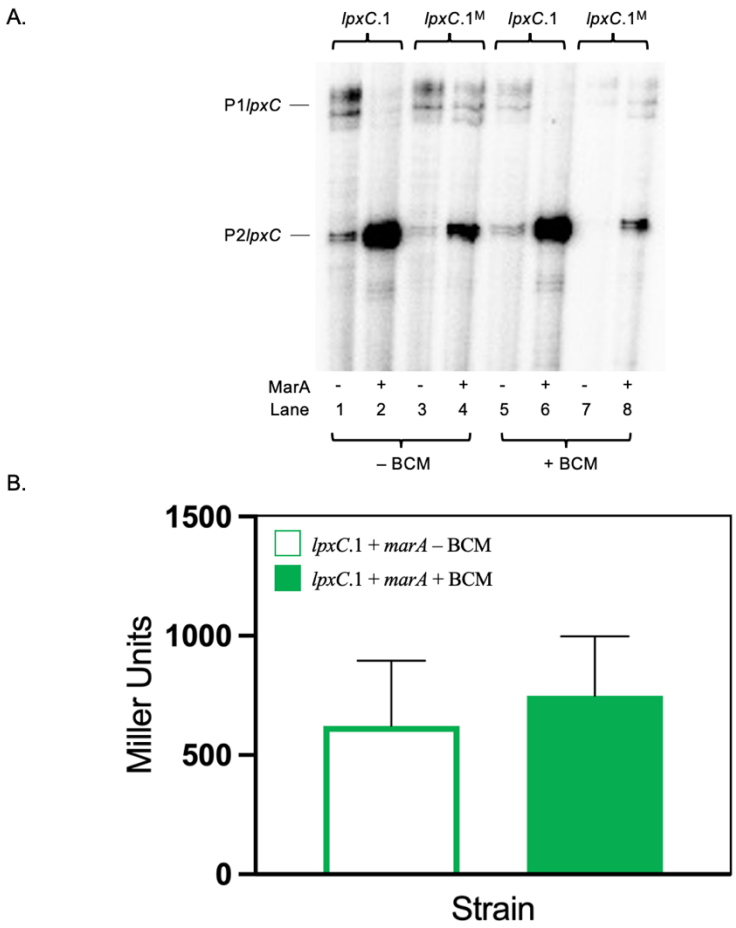

Figure 3.8. Understanding differences in Rho-dependent transcription termination of the *lpxC* transcripts.

A. *E. coli* JCB387 transformants containing pRW50 with *lpxC.1* (wildtype marbox) and pJ203 with *marA* were incubated with bicyclomycin. RNA was isolated from these cells and used for a primer extension assay and run of a 6 % polyacrylamide gel. There were no notable differences in promoter activity in the absence and presence of BCM. M13 T7 sequencing reactions were used to calibrate the gel (not shown). B. Promoter activity was determined by assessing β-galactosidase activity in *E. coli* JCB387 cells transformed with pRW50 containing either *lpxC*.1. Cells containing empty pRW50 were used as the control. Promoter activity shown in Miller units is the mean of assays from 3 separate days, each day comprising of 3 biological replicates. MarA was provided on pJ203 with constitutive expression of *marA*. A one-way ANOVA was calculated using the promoter activities, showing the analysis was non-significant ($p = 0.0547$, $F(1.003, 2.007) = 16.70$). A post-hoc Tukey's HSD test showed that addition of BCM was non-significant ($p > 0.05$ for each pair compared).

transcription and *lacZ* assays. We also note that *in vitro*, P2*lpxC* is activated to a far higher level than that observed for P1*lpxC* in the absence of MarA (Figure 3.8, Panel A, Lanes 1 and 2). This is consistent with previous *in vitro* transcription assays (Figure 3.6).

3.3.3. The small net change in overall transcription *in vitro* is due to promoter saturation

P2*lpxC* is a much more active promoter than P1*lpxC* (Figure 3.8, Panel A). To understand combined transcription from P1*lpxC* and P2*lpxC* further *in vitro*, transcription assays were repeated using decreasing concentrations of RNAP to prevent saturation of the promoters (Figure 3.9). This is likely to mimic the cellular environment more accurately, whereby RNAP is less readily available. Only the *lpxC*.1 derivative was used. Strong activation of P2*lpxC* is noted at all RNAP concentrations, highlighting the importance of MarA-mediated activation of *lpxC*. Conversely, as RNAP levels fall, transcription from P1*lpxC* is lost. Hence, *in vitro* transcription with lower levels of RNAP more faithfully match *in vivo* assays of promoter activity (Figure 5.9, Lanes 6 – 10). Thus, it is suggested that P1*lpxC* is a weak promoter meaning that transcription of P1*lpxC* is minimal and makes a small contribution to overall transcription.

3.4. Sodium salicylate, a natural inducer of the *mar* operon, causes activation of *lpxC* expression *in vivo*

MarA activation of P*lpxC* was further verified by measuring β-galactosidase activity with and without the addition of 5 mM sodium salicylate to the growth media (Figure 3.10). Salicylate induces MarA by binding to, and inhibiting, the MarR repressor. This results from a

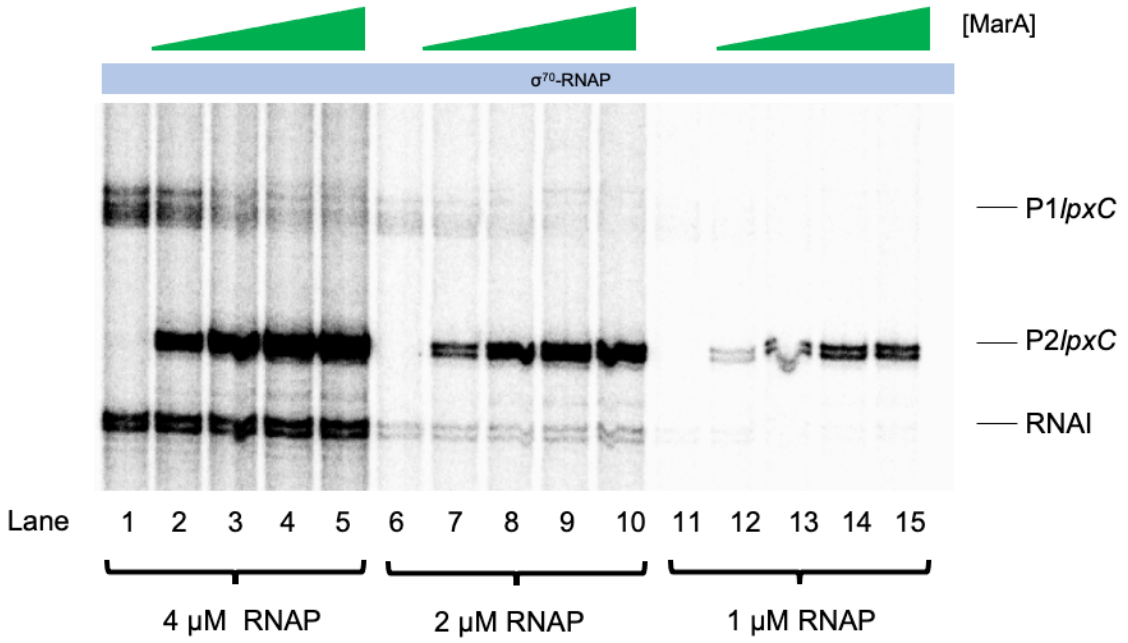

Figure 3.9. *In vitro* transcription assays with decreasing RNA polymerase concentrations to prevent promoter saturation.

Images of 6 % polyacrylamide gels used to separate transcripts generated *in vitro* using the *lpxC*.1 derivative and decreasing concentrations of RNAP-σ^{70} (4 μM – 2 μM – 1μM). Increasing concentrations of MarA (1 μM – 2 μM – 4 μM – 5 μM) are shown by green triangles. Bands formed by transcripts originating from P1*lpxC*, P2*lpxC* and RNAI are indicated by solid lines. Repression of P1*lpxC* is not seen at 1 μM RNAP-σ^{70}.

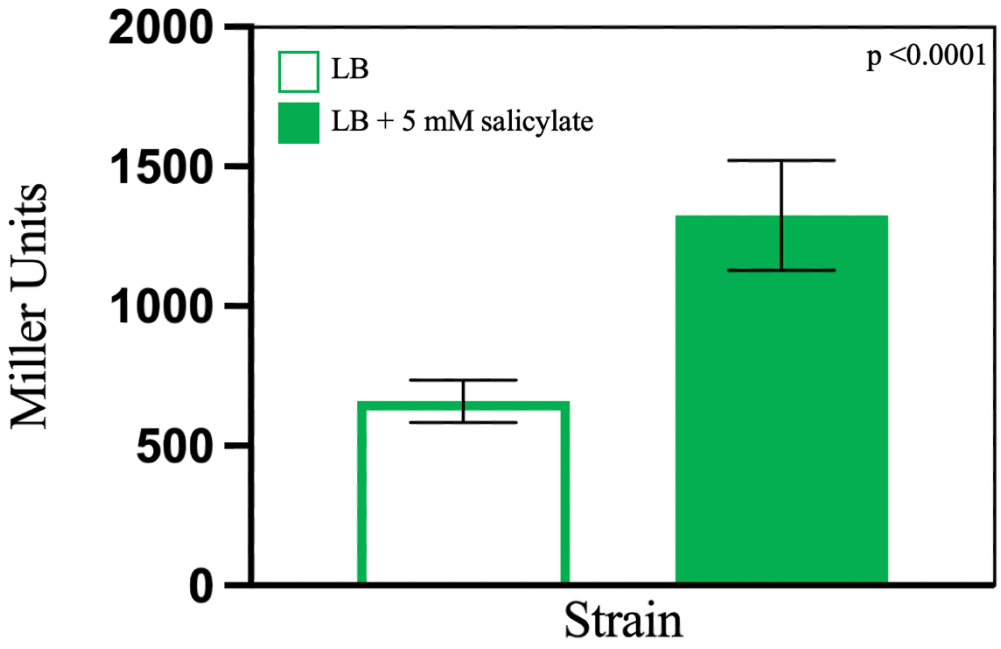

Figure 3.10. Effect of sodium salicylate on *in vivo* promoter activity from the *lpxC* regulatory region.

marA expression was induced by the addition of 5 mM sodium salicylate, a natural inducer of the *mar* operon. Promoter activity was determined by assessing β-galactosidase activity in *E. coli* JCB387 cells transformed with pRW50 containing *lpxC.1* (wildtype marbox), with and without the addition of 5 mM salicylate to LB media. Sodium salicylate was added to LB after overnight growth, and cells were grown to mid-log phase. Cells containing empty pRW50 were used as the control. Promoter activity shown in Miller units is the mean of assays from 3 separate days, each day comprising of 3 biological replicates. A one-way ANOVA was calculated using the promoter activities, showing the analysis was significant ($p < 0.0001$, $F(3, 32) = 333.3$). A post-hoc Tukey's HSD test showed that all groups were significantly different from each other, with the exception of the control in the absence and presence of 5 mM salicylate ($p<0.05$ for each pair compared; >0.9999 for the pairwise comparison between Control (LB) and Control (LB + 5 mM salicylate).

conformational change in MarR and de-repression of the *marRAB* operon (Alekshun and Levy, 1999). When salicylate was added to the media, there was an increase in promoter activity.

3.5. Discussion

LPS, the main constituent of the outer leaflet of the OM, serves as an effective barrier against antimicrobial agents (Snyder and McIntosh, 2000). Evidence suggests that lipid A and the core polysaccharide provide this barrier property, whereas the O-antigen does not affect membrane permeability (Schnaitman and Klena, 1993; Heinrichs, Yethon, Whitfield, 1998). Thus, changes in the structure of both core polysaccharide and lipid A could be a useful strategy in improving the barrier function of the OM. Previously, the gene *waaY*, associated with LPS core biosynthesis, was shown to be activated by SoxS and MarA (Lee *et al*., 2009). This causes modification of LPS. Considering that LPS biosynthesis is a complex process, it is likely that other genes encoding enzymes involved in this biosynthesis pathway are targeted by MarA.

LpxC-dependent deacetylation of UDP-3-O-(acyl)-GlcNAc to UDP-3-O-(acyl)-GlcN is the first committed step of lipid A biosynthesis. The aim of this chapter was to confirm *lpxC* as a novel MarA target. Previous work identified a putative soxbox upstream of *lpxC*, by ChIP-exo, and l*pxC* was noted to be activated by SoxS in RNA-seq (Seo *et al*., 2015). Activation of *lpxC* by RamA, an AraC family transcription factor related to MarA, found in some Gram-negative bacteria, was demonstrated in *K. pneumoniae* (De Majumdar *et al*., 2015). The data in this chapter shows that MarA binds to the marbox upstream of *lpxC* in *E. coli* and activates expression of the gene.

There are 2 promoters found within the *lpxC* regulatory region. The marbox overlaps with the -10 element of P1*lpxC* and the -35 element of P2*lpxC*. The *lpxC* marbox is in the forward

orientation. *In vitro* transcription assays showed that P2*lpxC* is activated by MarA and that P1*lpxC* is repressed simultaneously. Hence, P2*lpxC* is a Class II MarA-dependent promoter. In initial *in vitro* experiments, this suggested that the overall level of *lpxC* transcription did not change in the presence of MarA (Figure 3.6). Rather, addition of MarA caused a shift from use of P1*lpxC* to use of P2*lpxC.* Conversely, *in vivo*, overall levels of transcription from the *lpxC* regulatory region increased due to MarA (Figure 3.4). Furthermore, primer extension assays showed that P2*lpxC* was much more active than P1*lpxC* (Figure 3.8). *In vivo* it is likely that the concentration of RNAP is lower than that supplied in the *in vitro* assay due to many more promoters competing to bind RNAP. Thus, further *in vitro* assays were carried out with a lower concentration of RNAP (Figure 3.9). Transcription from P1*lpxC* was greatly reduced, whilst activation of P2*lpxC* by MarA remained. Overall, results suggest that MarA activates the expression of *lpxC* from P2*lpxC* and that this promoter is much more active than P1*lpxC*, which is repressed. Thus, MarA leads to high level activation of *lpxC* expression.

Considering the importance of LPS, lipid A biosynthesis is a logical target for antimicrobial activity. Inhibitors of LpxC, such as carbohydroxamido-oxazolidin, exhibit antibacterial activity against *E. coli* JB 1104 (Jackman *et al.,* 2000). It is thought that this compound coordinates the active site zinc ion on LpxC, which is required for catalytic activity (Jackman, Raetz and Fierke, 1999). More recently, several novel LpxC inhibitors have been identified (Clements *et al*., 2002; Chen *et al*., 1999; Dreger *et al.,* 2021; Zhou and Hong, 2021) Of most interest, a novel non-hydroxmate LpxC inhibitor was demonstrated to have *in vitro* and *in vivo* antibacterial activities against carbapenem-resistant Enterobacteriaceae in murine infection models (Fujita *et al*., 2021; Fujita *et al*., 2022).

In summary, this chapter has identified lipid A as a novel MarA target. The hypothesis is that MarA upregulates lipid A biosynthesis to improve the barrier function of the OM. Thus, less antibiotics agents can enter the cell via passive diffusion.

Chapter 4 – Elucidation of Novel MarA Targets

4.1. Introduction

As outlined previously, the outer leaflet of the OM is primarily LPS, composed of lipid A, a core oligosaccharide, and the O-antigen. The core oligosaccharide of LPS is an important linker between lipid A and the O-antigen on the surface. The core oligosaccharide is divided into two regions: the inner core and outer core (Holst, 1999). The inner core, which is well conserved within a genus or family, is composed of KDO and phosphorylated L-glycero-D-manno-heptose (Hep) residues (Holst and Brade, 1992). The outer core is typically composed of glucose (Glc) and Hep residues and is much more diverse than the inner core. For example, 5 known outer core structures have been demonstrated in *E. coli* (Whitfield *et al*., 1999). Core oligosaccharide assembly on KDO_2-lipid A occurs via sequential glycosyl transfer from sugar precursors, as shown in Figure 4.1. Enzymes required for biosynthesis of the inner core are encoded by the *waaDFC* operon (Yethon *et al*., 1998). The outer core biosynthetic process occurs via enzymes encoded by the *waaQ* operon (Pradel *et al*.,1992; Yethon *et al*., 2000). Biosynthesis begins with assembly of the inner core. The heptosyltransferases WaaC and WaaF transfer the first and second Hep residues, respectively, onto KDO_2-Lipid A (Chen and Coleman, 1993). WaaD encodes an L-glycero-D-manno-heptose-6-epimerase. This catalyses the conversion of D-glycero-D-manno-heptose to L-glycero-D-manno-heptose, the preferred substrate of WaaC and WaaF (Coleman, 1983). The kinase enzymes WaaP and WaaY add phosphate groups to the first and second Hep residues, respectively (Yethon *et al.,* 1998). The heptosyltransferase WaaQ adds a third Hep to the second Hep. These modifications must occur in a specific order with the enzymes WaaP, WaaQ and WaaY. Following this, biosynthesis of the outer core begins with the transfer of the first Glc residue to the second Hep residue by the glucosyltransferase enzyme WaaG (Yethon *et al*., 2000). Modification of the Glc residue is achieved by WaaB, which allows the transfer of a galactose (Gal) residue. Glucosyltransferases WaaO and WaaR add two more Glc residues (Yethon *et al*., 1998; Qian,

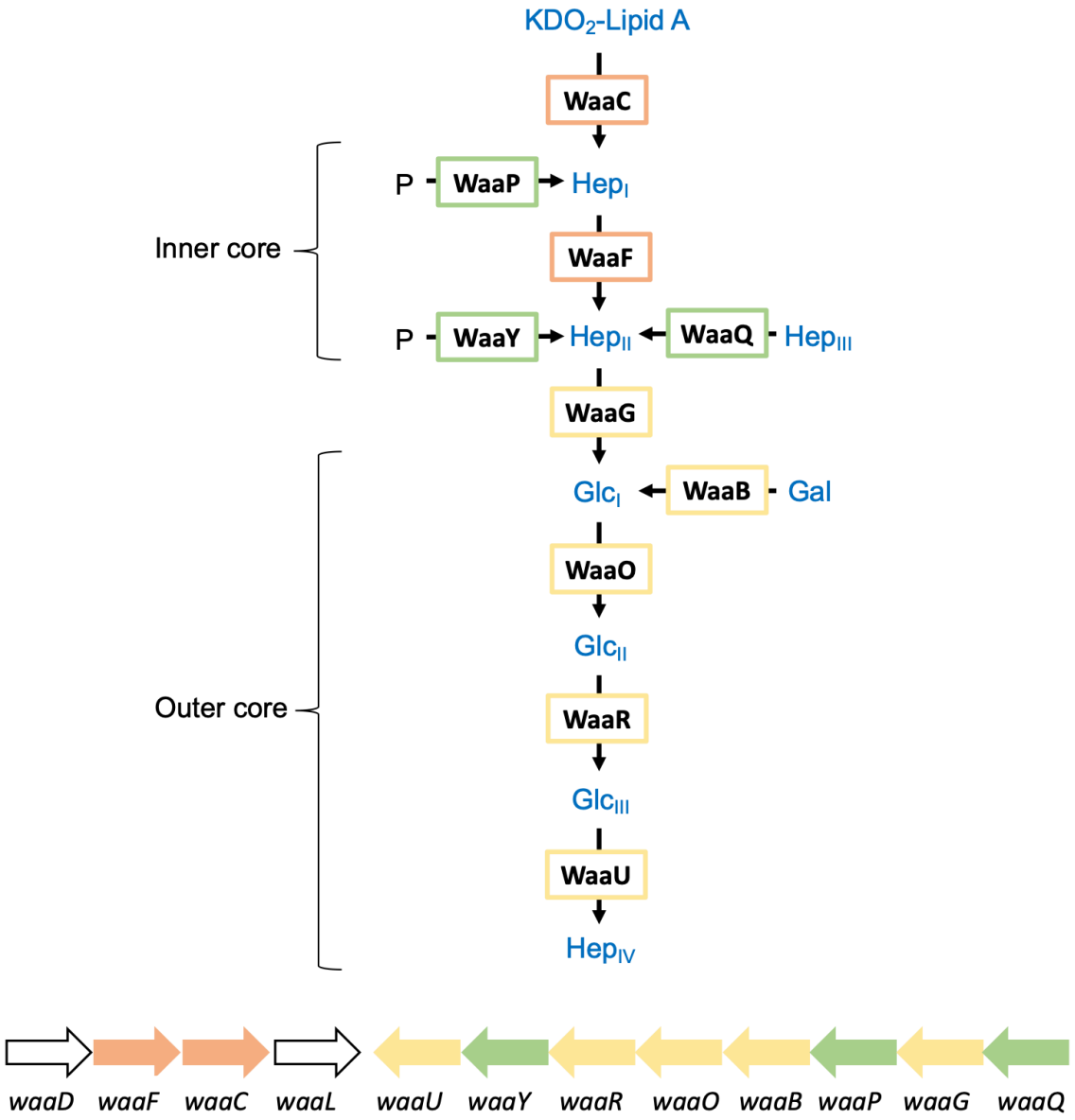

Figure 4.1. Structure and biosynthesis of LPS core oligosaccharide in *E. coli* K-12.

The organization of the *waa* locus, including the *waaDFC* operon, the *waaL* gene and the *waaQ* operon is shown. Gene sizes not to scale. Heptosyltransferase enzymes that construct the inner core and the genes encoding these enzymes are shown in orange. Enzymes involved in modification of the inner core and the genes encoding them are shown in green. Glycosyltransferase enzymes that construct the outer core and the genes encoding them are shown in yellow. The overall structure of core oligosaccharide is shown in blue. *waaL* is thought to be involved in ligation of the core oligosaccharide to the O-antigen (Klena, Ashford and Schnaitman, 1992). Adapted from Raetz and Whitfield, 2002.

Garrett and Raetz, 2014). Finally, WaaU transfers a fourth Hep residue to the outer core (Heinrichs, Yethon and Whitfield, 1998). This outer core structure is found in *E. coli* K-12 (Whitfield *et al*., 1999). Other outer core structures can be composed of alternate Glc and Gal residues. The core oligosaccharide is vital in the stability of the OM, as well as bacterial viability and biofilm formation (Yethon *et al*., 1998; Yethon et al., 2000; Loutet *et al*., 2006; Wang *et al*., 2015).

Peptidoglycan acts as an additional permeability barrier. Peptidoglycan, found within the periplasm of Gram-negative bacteria, is made up of alternating N-acetylglucosamine (GlcNAc) and N-acetyl muramic acid (MurNAc) sugars that form glycan chains (Figure 4.2) (Rogers *et al*., 1980). These glycan chains are cross-linked by chains of amino acids (Schleifer and Kandler, 1972). Peptidoglycan is a highly dynamic molecule due to constant remodelling (Holtje, 1998; Layec *et al*., 2008). This is achieved by enzymes capable of hydrolysing glycan chains or peptide cross-links (Shockman & Höltje, 1994). The endopeptidases, including PBP7 (PbpG), PBP4 (DacB) and MepA in *E. coli*, cleave within the peptide cross-links (Henderson *et al*., 1995; Kishida *et al*., 2006; Keck and Schwarz, 1979).

In Chapter 3, MarA was demonstrated to target lipid A biosynthesis through the activation of *lpxC*, a novel MarA target identified by ChIP experiments. Additionally, MarA activates transcription of the *mlaFEDCB* operon, which encodes a lipid trafficking ABC transport system to remove unwanted phospholipids from the outer leaflet of the OM (Sharma *et al*., 2017). Targeting the barrier of the cell to alter cell permeability is an excellent strategy to alter uptake of antimicrobial agents. In this chapter, we searched for other novel MarA target genes encoding functions associated with the cellular envelope.

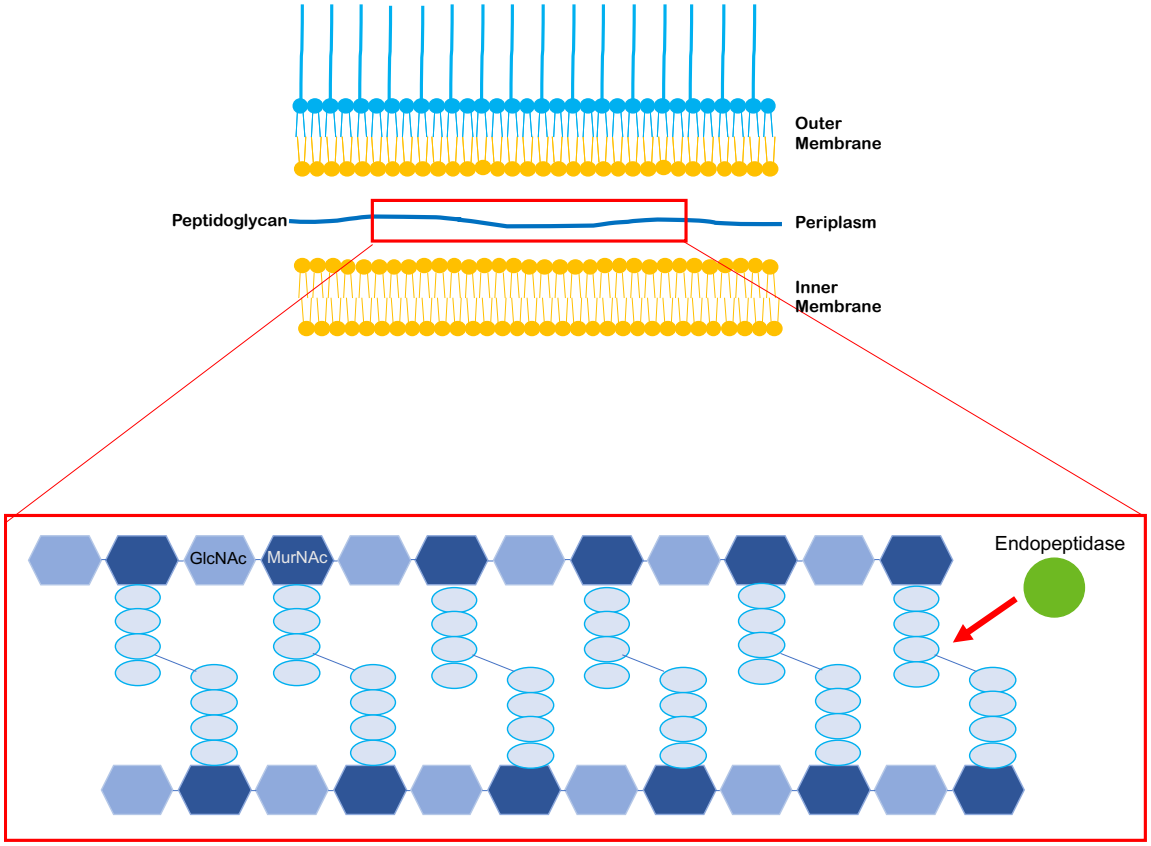

Figure 4.2. The structure of peptidoglycan.

Peptidoglycan, found within the periplasm, is composed of glycan chains. These are made up of alternating GlcNAc and MurNAc sugars (hexagons), which are linked by β-1→4 bonds. Chains of amino acids are attached to MurNAc sugars. This peptide stem is commonly made up of L-Ala, D-Glu, L-Lys and D-Ala. Adjacent stems are cross-linked, which commonly occurs between the carboxyl group of position 4 D-Ala and the amino group of position 3 L-Lys. The endopeptidase enzymes cleave these cross-links during peptidoglycan hydrolysis. Information from Rogers *et al.,* 1980.

Using a bioinformatic approach to search for novel MarA binding sites, putative marboxes were found in several promoters of genes associated with OM biosynthesis and cell wall biogenesis. Subsequently, MarA was shown to regulate the promoters of *lpxL* and *pbpG*, not previously identified as MarA targets. A SoxS target, *waaY*, appeared in the search and was demonstrated to be activated by MarA (Lee *et al.,* 2009). LpxL and WaaY are involved in lipid A biosynthesis and core oligosaccharide biosynthesis, respectively. PbpG is an endopeptidase involved in peptidoglycan biogenesis. SoxS and Rob regulation of these promoters, as well as *lpxC* from Chapter 3, was also investigated.

4.2. Identification and confirmation of novel putative marboxes in promoters of genes associated with the cell envelope

ChIP-seq previously identified many MarA targets in *E. coli*. However, this technique is prone to false negatives. Using the DNA-binding motif identified by ChIP, a bioinformatic approach was used to identify novel putative marboxes in the *E. coli* genome that may have been missed previously. Briefly, the *E. coli* genome was searched for marboxes with 1 mismatch to the sequence GCANNNNNNGCNAAA. Results were filtered to include only intergenic sites up to a maximum of 200 bp upstream of a start codon. 585 matches were identified. These are shown in Appendix 1. 255 (43.59%) of these targets were found in promoters of genes with unknown function and these were discounted. The remaining 330 targets were searched manually to identify target genes involved in cell envelope biology. Table 4.1 shows the chosen 15 targets, with the function of the genes, potential marbox sequence, and strand information shown.

Table 4.1. Putative marboxes found in promoters of genes associated with outer membrane biosynthesis and cell wall biosynthesis and degradation.

Bioinformatic analysis was used to identify novel putative marboxes throughout the *E. coli* genome. Parameters allowed up to 1 mismatch. Functions were limited to those associated with OM biosynthesis (O-antigen biosynthesis, colonic acid biosynthesis, LPS core biosynthesis, lipid A biosynthesis and Enterobacterial common antigen biosynthesis) and cell wall biogenesis (peptidoglycan synthesis, hydrolysis and degradation). Gene names are shown alongside the function of the encoded proteins. The marbox sequence is shown with the appropriate DNA strand and the location of the marbox relative to the TSS.

Gene	Function	Marbox sequence	Strand	bp
wbbK	**O-antigen biosynthesis** (putative glycosyltransferase) (Stevenson *et al*., 1994)	ggagtaccagcaaaa	-	-47
wzxC	**Colanic acid** (capsule) biosynthesis (Stevenson *et al*., 1996)	gctggcgcggcgaaa	-	-150
waaU (rfaK)	**LPS core biosynthesis** (glycosyltransferase) (Parker *et al*., 1992)	gcagaagaatcaaaa	-	-104
wcaD	**Colanic acid (capsule) biosynthesis** (Stevenson *et al*., 1996)	ggaagtgttgcaaaa	-	-167
wzc	**Colanic acid (capsule) biosynthesis** (Stevenson *et al*., 1996)	gcaaaagccgggaaa	-	-94
waaJ (rfaJ)	**LPS core biosynthesis** (glucosyltransferase) (Carstenius, Flock and Lindberg, 1990)	gcatagatatctaaaa	-	-103
waaA (kdtA)	**Lipid A biosynthesis** (Clementz and Raetz, 1991)	gcagatcagaccaa	+	-109
rffA	**Enterobacterial common antigen biosynthesis** (Meier-Dieter *et al.,* 1990)	gcaaacggcgctaaa	+	-146
waaD (rfaD)	**LPS core biosynthesis** (Pegues *et al*., 1990)	gaaggactagctaaaa	+	-149
waaY (rfaY)	**LPS core biosynthesis** (Parker *et al*., 1992)	gcacaaatgggcaat	-	-143
lpxL (waaM)	**Lipid A biosynthesis** (Brozek and Raetz, 1990)	gcaattatcgataa, ttacgctacatttgc, tttcgcccagtcttc	-	-174, -144, -93
amiC (ygdN)	**Degradation of peptidoglycan during cell division** (Uehara and Park, 2008)	gcgtctttcgctaaa	-	-78
pbpG (yohB)	**Cell wall hydrolysis** (Henderson, Templin and Young, 1995)	gcattgctggcgtaa	-	-157
dacB	**Cell wall hydrolysis** (Henderson, Templin and Young, 1995)	ggaccagaagcaaaa	+	-30
mepA	**Cell wall hydrolysis** (Henderson, Templin and Young, 1995)	gcaacgggcgcaaaa	-	-52

4.3. MarA binds putative marboxes in the promoter regions of *lpxL*, *waaY* and *pbpG*

To determine whether MarA bound to the 15 putative marboxes identified, DNA fragments for each target gene were generated by PCR. The DNA sequences are shown in Appendix 2. DNA binding was measured using an EMSA. DNA was radiolabelled with [γ ^{32}P]-ATP, incubated with increasing concentrations of MarA and separated on a 6 % polyacrylamide gel. Of the 15 putative marboxes found, 3 were demonstrated to bind MarA (Figure 4.3). The data indicate that MarA binds to DNA fragments *lpxL*.1, *waaY*.1 and *pbpG*.1. and therefore, the regulatory regions of P*lpxL*, P*waaY* and P*pbpG*.

4.4. The marbox sequence is important for transcriptional regulation of *lpxL*, *waaY* and *pbpG*

Within the *lpxL* regulatory region, 3 putative marboxes were identified. Each marbox was separately mutated and these promoter derivatives (*lpxL*.1^{M1}, *lpxL*.1^{M2} and *lpxL*.1^{M3}) were used in an EMSA, as described previously (Figure 4.4). Mutating marboxes 2 and 3 did not prevent MarA binding (Figure 4.4, Panel iii and Panel iv). Mutating marbox 1 was sufficient to prevent MarA binding (Figure 4.4, Panel ii). Hence, MarA binds to marbox 1. The putative marboxes in the regulatory regions of *waaY* and *pbpG* both match the consensus GCA sequence. To prevent MarA binding, mutations were made in these positions (Figure 4.5). These promoter derivatives (*waaY*.1^{M} and *pbpG*.1^{M}) were used in an EMSA. As expected, the mutations were sufficient to prevent binding of MarA in both cases, confirming correct identification of the marbox.

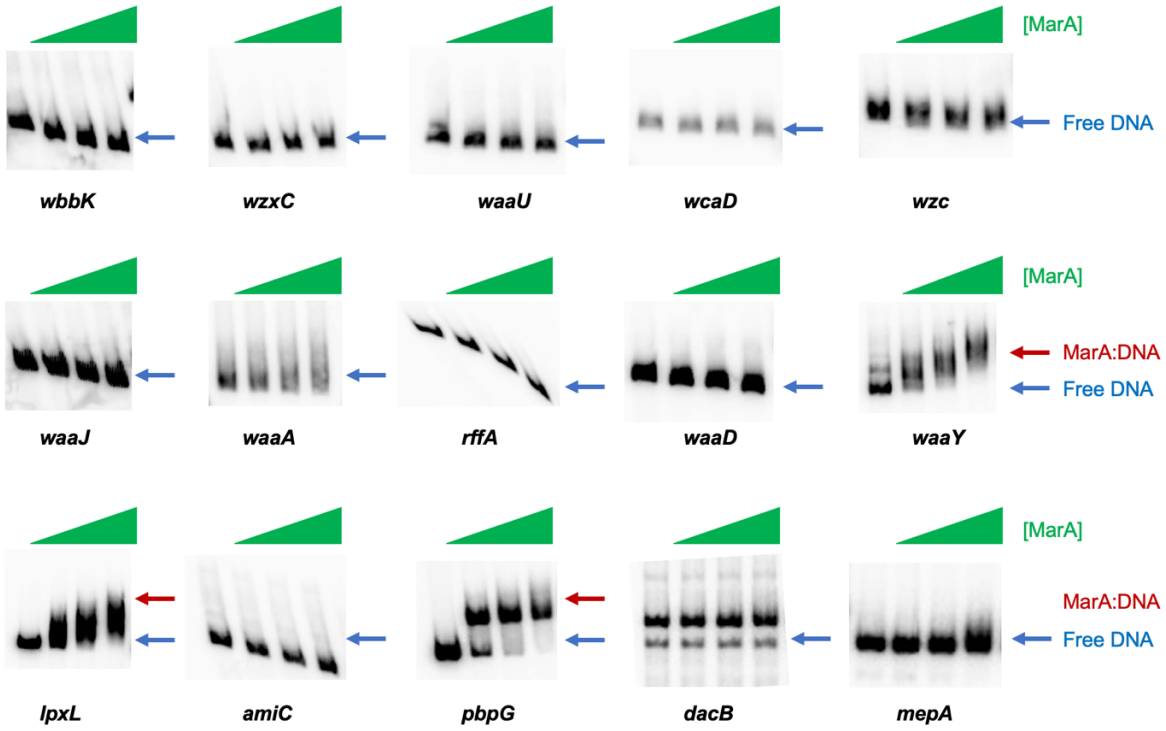

Figure 4.3. Images showing EMSAs to assess the binding of MarA to 15 marboxes found using bioinformatic analysis.

Images of 6 % polyacrylamide gels used to separate MarA:DNA complexes are shown. Increasing concentrations of MarA (1 µM – 2µM – 4µM) are shown by green triangles. MarA:DNA complexes and free DNA are indicated. Binding of MarA to the marbox is demonstrated by MarA-DNA and shown in red.

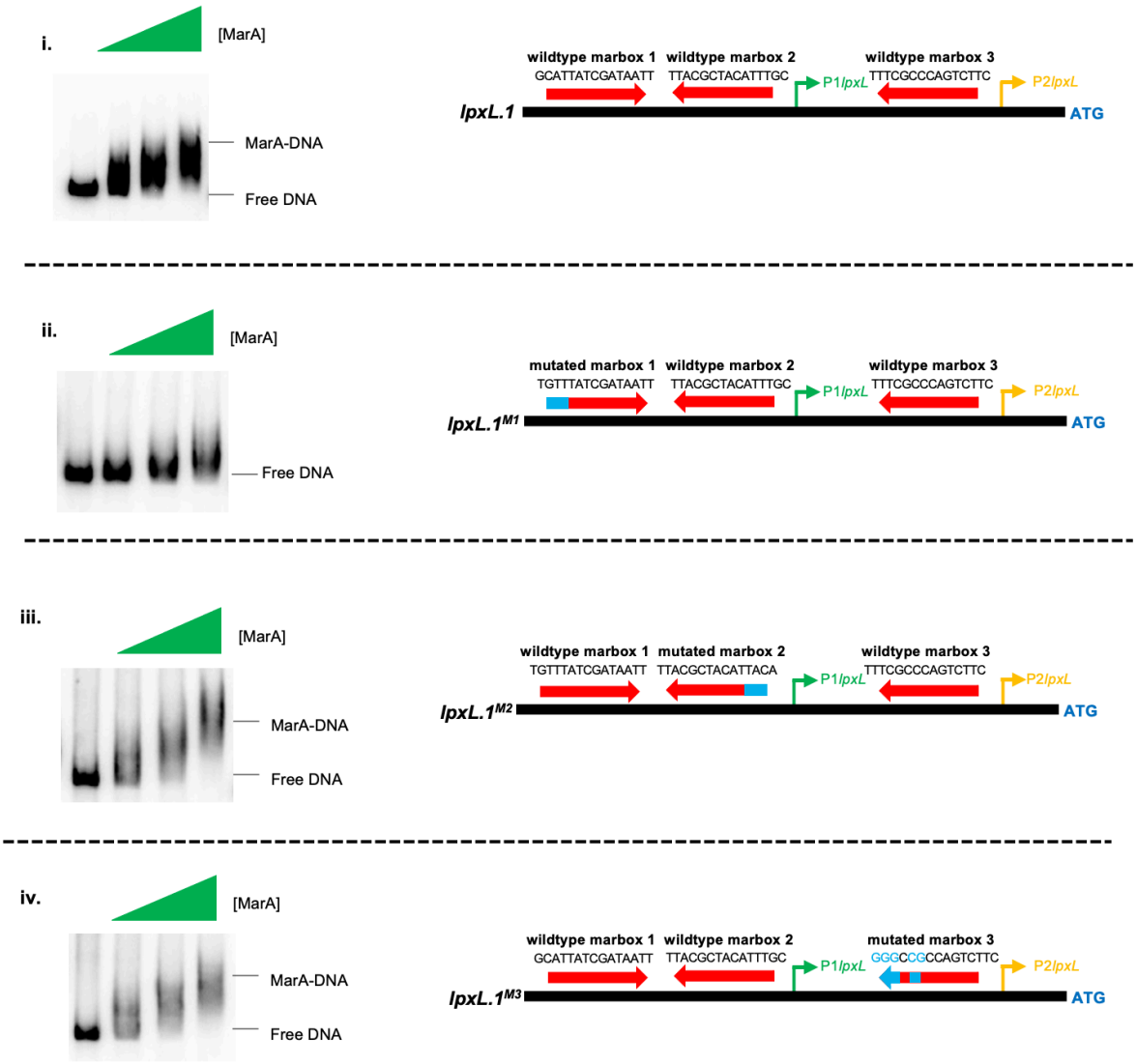

Figure 4.4. Determining the marbox of P*lpxL* that is bound by MarA *in vitro*.

An EMSA was carried out with the *lpxL*.1, *lpxL*.1^{M1}, *lpxL*.1^{M2} and *lpxL*.1^{M3} derivatives shown. Images of 6 % polyacrylamide gels used to separate MarA:DNA complexes are shown. Increasing concentrations of MarA (1 µM – 2µM – 4µM) are shown by green triangles. MarA:DNA complexes and free DNA are indicated. Binding of MarA occurs when no marboxes are mutated, as expected (i), When putative marbox 2 and putative marbox 3 are mutated, this binding still occurs (iii and iv). Only mutating putative marbox 1 prevents binding of MarA.

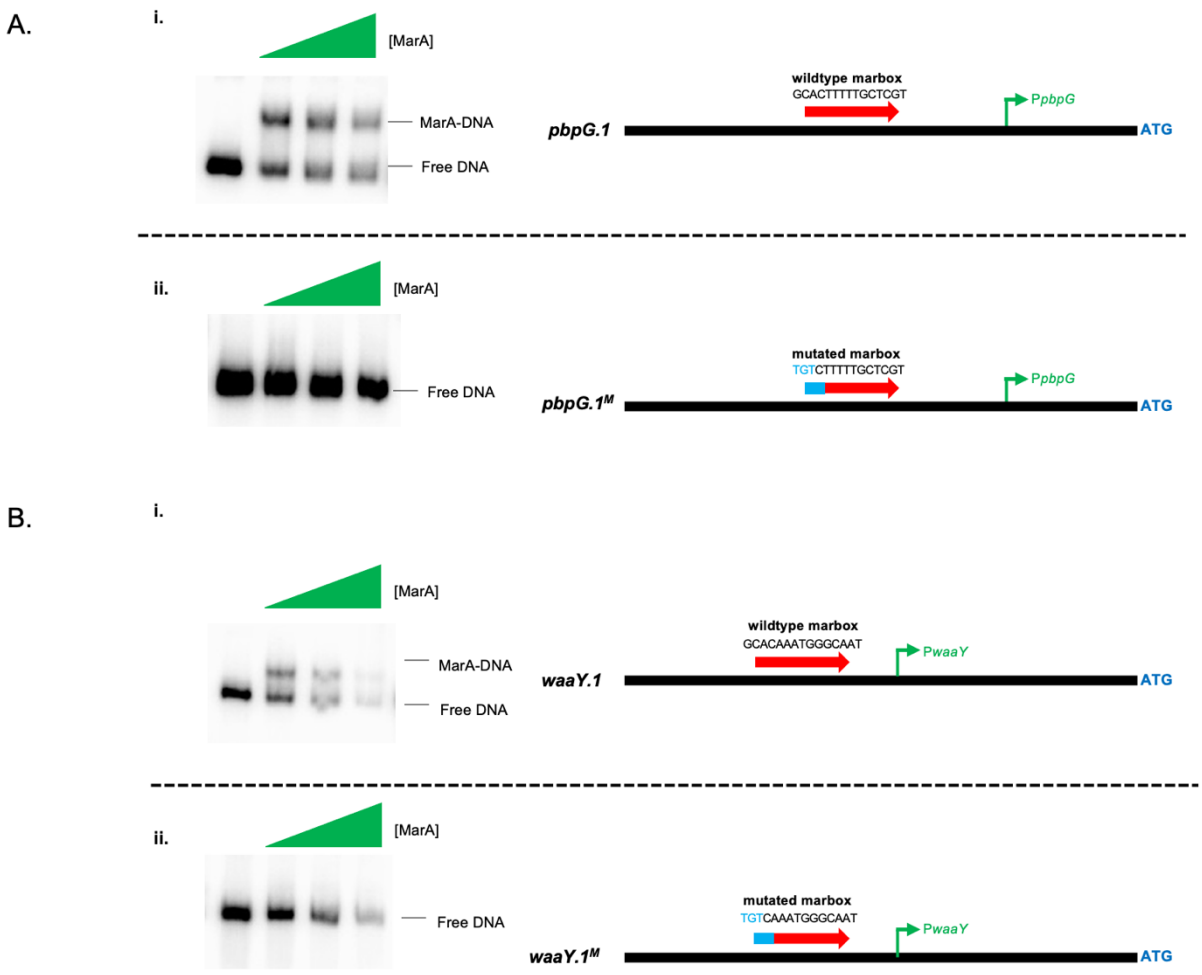

Figure 4.5. Binding of MarA to the P*pbpG* and P*waaY* promoter regions in an EMSA. Images of 6 % polyacrylamide gels used to separate MarA:DNA complexes are shown. A. The panels show experiments for EMSA assays done with i) the *pbpG*.1 promoter derivative with a wildtype marbox present, and ii) the *pbpG*.1^{M} derivative with a mutated marbox. B. The panels show experiments for EMSA assays done with i) the *waaY*.1 promoter derivative with a wildtype marbox present, and ii) the *waaY*.1^{M} derivative with a mutated marbox. Increasing concentrations of MarA (1 µM – 2µM – 4µM) are shown by green triangles. Specific binding of MarA is indicated by indicated by solid lines.

4.5. SoxS and Rob bind the marbox in the promoter regions of *lpxC*, *lpxL*, *waaY* and *pbpG*

To determine whether transcription factors related to MarA also bind the various marboxes, the EMSA assay was repeated using increasing concentrations of SoxS and Rob (Figure 4.6). The DNA sequences used were *lpxL*.1, *waaY*.1 and *pbpG*.1. The *lpxC*.1 fragment, previously shown to bound by MarA in Chapter 3, was also tested. SoxS and Rob bound the DNA in all cases, showing that the marboxes of P*lpxC*, P*lpxL*, P*waaY* and P*pbpG* are bound by MarA, SoxS and Rob in *E. coli*.

4.6. *In vivo* regulation of *lpxL*, *waaY* and *pbpG* by MarA and SoxS

To understand MarA regulation of the 15 targets, the promoter regions (Table 4.1, Appendix 2) were also cloned into reporter plasmid pRW50. *E. coli* JCB387 was transformed with these constructs and β-galactosidase activity was measured (Table 4.2). Significant changes in promoter activity were only noted for those promoters found to bind MarA *in vitro*: P*lpxL*, P*waaY* and P*pbpG*. Further *in vivo* assays were carried out to show these promoters were also regulated by SoxS and by the MarA-inducer sodium salicylate (Table 4.2 and Table 4.3, respectively).

4.6.1. MarA and SoxS activate *lpxL* and *waaY* expression *in vivo*

A significant increase in promoter activity was seen for *lpxL*.1 and *waaY*.1 when *marA* was expressed (Table 4.2). Likewise, when *soxS* was expressed, an increase in promoter activity was seen for these promoters. This suggests that both *lpxL* and *waaY* are activated by MarA and SoxS. MarA regulation of *lpxL* and *waaY* was further verified by measuring

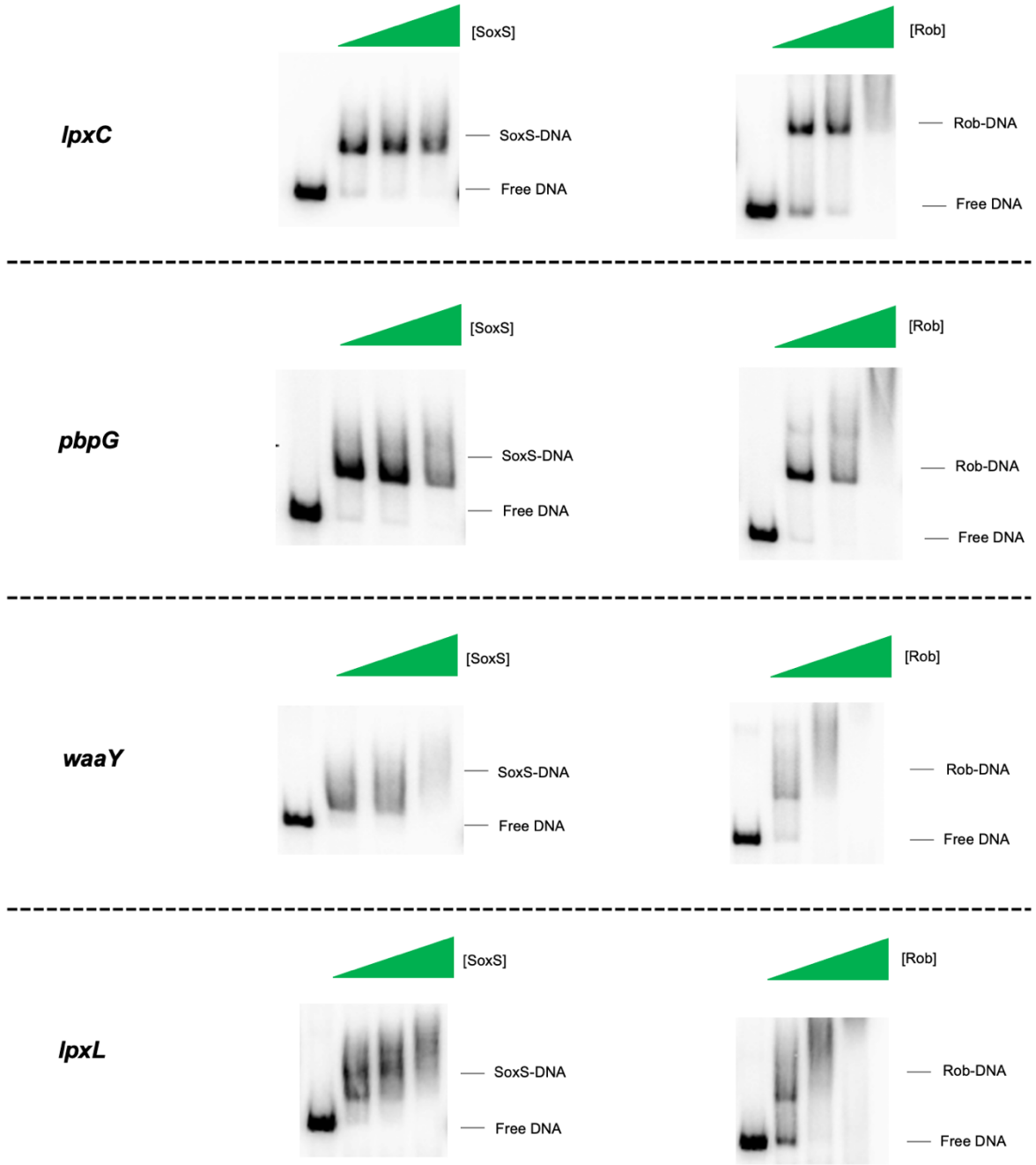

Figure 4.6. Binding of SoxS and Rob to P*lpxC*, P*pbpG*, P*waaY* and P*lpxL* regulatory regions.

Images of 6 % polyacrylamide gels used to separate Protein:DNA complexes are shown. The panels show experiments for EMSA assays done with the *lpxC*.1, *pbpG*.1, *waaY*.1 and *lpxL*.1 promoter derivatives. Increasing concentrations of SoxS (1 µM – 2 µM – 4 µM) and Rob (0.2 µM – 0.4 µM – 0.8 µM) are shown by green triangles. Specific binding of proteins is indicated by solid lines.

Table 4.2. β-galactosidase activity of pRW50/promoter derivatives of all promoter targets.

Promoter activity was determined by assessing β-galactosidase activity in *E. coli* JCB387 cells transformed with pRW50 containing all promoter derivatives. Cells containing empty pRW50 were used as the control. Promoter activity (3 d.p.) shown in Miller units is the mean of assays from 3 separate days, each day comprising of 3 biological replicates. Standard deviation (2 d.p.) is shown in brackets. Promoter derivatives shown to bind MarA an in EMSA are underlined. MarA was provided on pJ203 with constitutive expression of *marA*. A one-way ANOVA was calculated using the promoter activities, showing the analysis was significant ($p < 0.0001$, $F(1.566, 12.53) = 106.4$). A post-hoc Tukey's HSD test determined which groups were significantly different and these are denoted as "*" ($p<0.05$ for each pair compared). These promoter derivatives found to be regulated by MarA *in vivo* were further tested to determine whether they were also regulated by SoxS. SoxS was provided on pAM with constitutive expression of *soxS*. A one-way ANOVA was calculated using the promoter activities, showing the analysis was significant ($p < 0.0001$, $F(1.413, 11.31) = 35.44$). A post-hoc Tukey's HSD test showed that for each promoter, all groups were significantly different from each other ($p<0.05$ for each pair compared).

β-galactosidase Activity (Miller Units)				
Transcription factor	MarA		SoxS	
Promoter	- *marA*	+ *marA*	- *soxS*	+ *soxS*
P*lpxC*	402.662 (57.41)	964.908* (333.90)	42.542 (6.20)	878.990* (343.44)
P*wbbK*	59.811 (4.78)	51.439 (0.19)		
P*wzxC*	8.822 (1.71)	8.048 (1.19)		
P*waaU*	197.973 (44.71)	260.309 (89.67)		
P*wcaD*	5.812 (2.58)	7.013 (3.14)		
P*wzc*	5.579 (3.05)	7.697 (3.42)		
P*rfaJ*	34.192 (6.18)	47.174 (12.36)		
P*waaA*	113.624 (24.05)	110.315 (2.93)		
P*rffA*	12.942 (0.53)	14.718 (1.09)		
P*rfaD*	102.622 (14.14)	108.484 (12.86)		
P*waaY*	86.996 (12.92)	916.666* (169.51)	25.241 (7.21)	328.154* (188.37)
P*lpxL*	63.309 (4.94)	541.688* (34.64)	35.987 (12.63)	526.725* (204.07)
P*amiC*	89.703 (23.98)	77.723 (17.36)		
P*pbpG*	39.9742 (1.75)	28.5688* (4.13)	43.871(18.10)	24.638* (7.96)

Table 4.3. β-galactosidase activity of pRW50/promoter derivatives of P*lpxC*, P*rfaY*, P*lpxL* and P*pbpG* by 5 mM sodium salicylate.

Promoter expression was determined by assessing β-galactosidase activity in *E. coli* JCB387 cells transformed with pRW50 containing P*lpxC*, P*rfaY*, P*lpxL* and P*pbpG*. Cells containing empty pRW50 were used as the control. Promoter activity (3 d.p.) shown in Miller units is the mean of assays from 3 separate days, each day comprising of 3 biological replicates. Standard deviation (2 d.p.) is shown in brackets. Assays were carried out in the absence and presence of 5 mM sodium salicylate. A one-way ANOVA was calculated using the promoter activities, showing the analysis was significant ($p < 0.0001$, $F(9, 80) = 338.7$). A post-hoc Tukey's HSD test showed that for each promoter, all groups were significantly different from each other ($p < 0.05$ for each pair compared).

β-galactosidase Activity (Miller Units)		
Promoter	- *sal*	+ *sal*
P*lpxC*	659.322 (76.40)	1325.137 (196.88)
P*waaY*	69.739 (5.74)	414.652 (6.01)
P*lpxL*	78.809 (34.12)	323.677 (40.69)
P*pbpG*	95.816 (1.41)	49.871 (10.68)

β-galactosidase activity with and without the addition of 5 mM sodium salicylate to the growth media (Table 4.3). When salicylate was added to the media, it caused an increase in promoter activity of P*lpxL* and P*waaY*. This is consistent with promoter activity seen when *marA* is overexpressed (Table 4.2).

4.6.2. MarA and SoxS repress *pbpG* expression *in vivo*

A significant decrease in promoter activity was seen for *pbpG*.1 when either *marA* or *soxS* were overexpressed (Table 4.2). Further, a decrease in promoter activity was seen with the addition of sodium salicylate (Table 4.3). This suggests that *pbpG* is repressed by MarA and SoxS.

4.6.3. SoxS regulates *lpxC* expression *in vivo*

To determine whether SoxS regulates the expression of *lpxC*, shown to be activated by MarA in Chapter 3, β-galactosidase activity was measured in the absence and presence of SoxS. SoxS was demonstrated to activate *lpxC* expression (Table 4.2).

4.7. MarA, SoxS and Rob regulate the expression of *lpxC*, *lpxL*, *waaY* and *pbpG in vitro*

4.7.1. MarA, SoxS and Rob regulate *lpxL*, *waaY* and *pbpG* expression *in vitro*

In vitro transcription was used to further investigate the regulation of *lpxL*, *waaY* and *pbpG* by MarA, SoxS and Rob. The *lpxL*.1, *waaY*.1 and *pbpG*.1 promoter regions were cloned into the plasmid pSR, upstream of the phage-derived transcription terminator λoop. The assay proceeded as previously described. Increasing concentrations of MarA, SoxS or Rob were added. An increase in the intensity of a 218 nt transcript from P1*lpxL* was demonstrated when MarA and SoxS were added (Figure 4.7). Although only 1 TSS is listed in Ecocyc for the *lpxL*

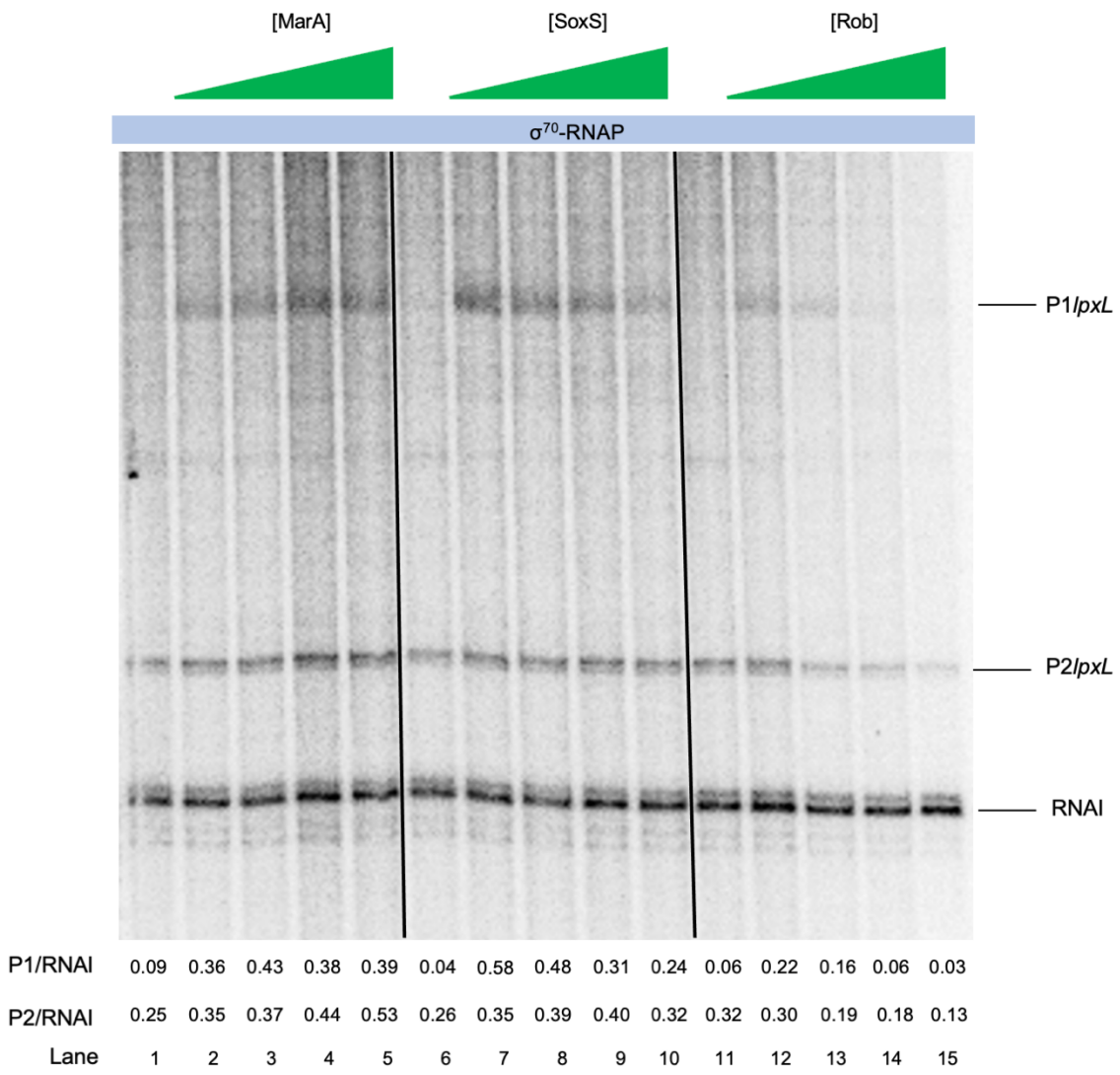

Figure 4.7. MarA, SoxS and Rob activation of transcription from the P*lpxL* promoter. Images of 8 % polyacrylamide gels used to separate transcripts generated *in vitro* using the *lpxL*.1 derivative. Assays were done with RNAP-σ^{70}. Increasing concentrations of MarA (1 µM – 2 µM – 4 µM – 5 µM), SoxS (0 µM – 1 µM – 2 µM – 4 µM) and Rob (0.2 µM – 0.4 µM – 0.8 µM – 1 µM) are shown by green triangles. Bands formed by transcripts originating from P1*lpxL*, P2*lpxL* and RNAI are indicated by solid lines. The ratio of transcript to P*lpxL*:RNAI is shown.

regulatory region, an additional transcript of 128 nt was seen that also increased in band intensity as MarA and SoxS were added. An increase in the amount of both transcripts was not induced by Rob (Figure 4.7). This suggests that MarA and SoxS activate transcription of *lpxL* but that Rob does not. An increase in the intensity of a 262 nt transcript from P*waaY* was demonstrated when MarA, SoxS or Rob was added (Figure 4.8). This suggests *waaY* is also activated by MarA, SoxS and Rob. A decrease in band intensity of a 162 nt transcript corresponding to that from P*pbpG* was demonstrated when MarA, SoxS or Rob were added (Figure 4.9). This demonstrates that *pbpG* is repressed by these transcription factors. This is especially noticeable with SoxS.

4.7.2. SoxS and Rob activate *lpxC* expression *in vitro*

MarA was previously shown to activate the expression of *lpxC in vitro* (Figure 3.6). To determine whether *lpxC* expression was also activated by SoxS and Rob, *in vitro* transcription was repeated with the addition of SoxS and Rob. (Figure 4.10). An increase in band intensity of the band derived from P2*lpxC* is noted with both SoxS and Rob. This suggests that *lpxC* is activated by SoxS and Rob. Activation by Rob is small and is more prevalent when the marbox is mutated (Lanes 16 – 20). This is consistent with the higher degeneracy of sequences bound by Rob compared with MarA and SoxS.

4.8. Conservation of marboxes differs throughout Enterobacteriaceae

To determine whether the genes found to be regulated by MarA here were likely to be clinically relevant in multiple antibiotic resistance in other enteric bacteria, the targets were analysed for conservation amongst a range of Enterobacteriaceae (Figure 4.11). Only strains encoding MarA with identical amino acid sequences of the DNA recognition helix were chosen. The

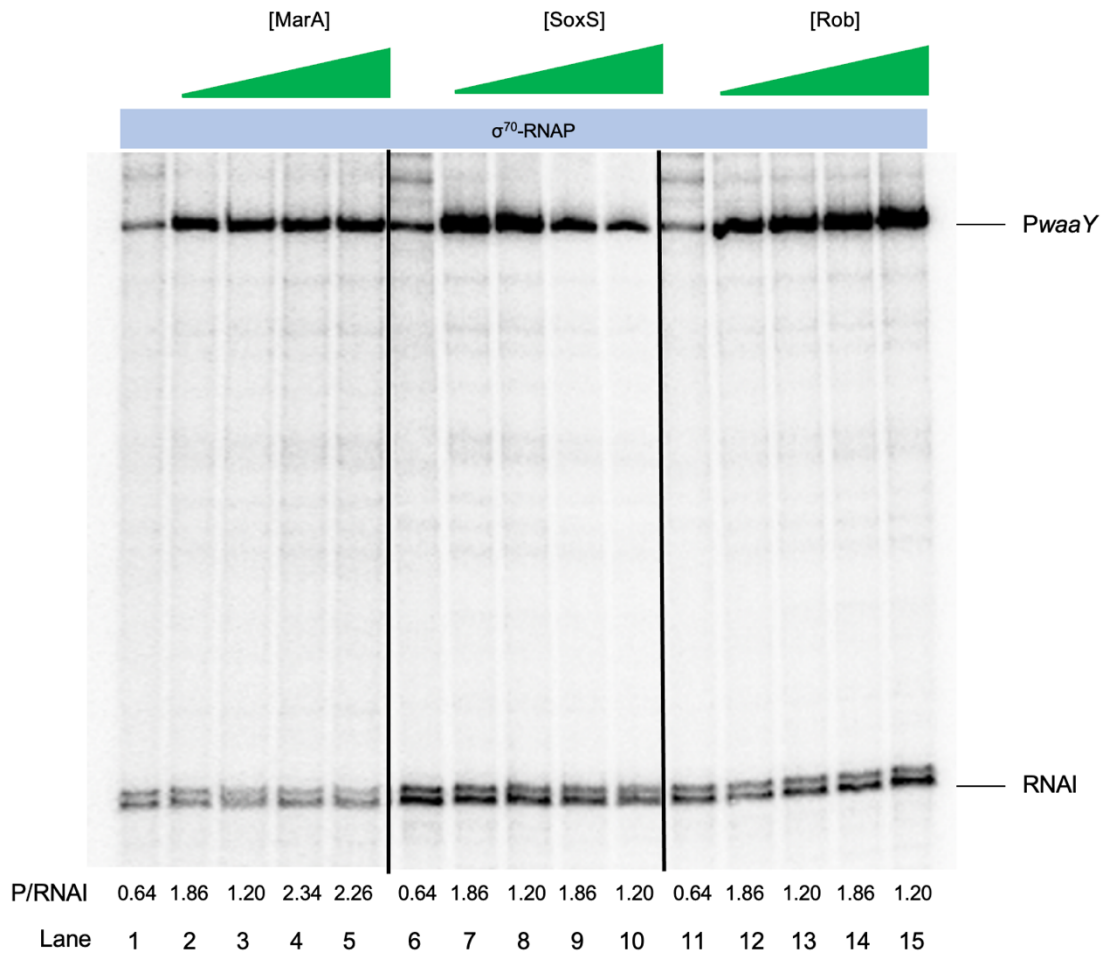

Figure 4.8. MarA, SoxS and Rob activation of transcription from the P*waaY* promoter. Images of 8 % polyacrylamide gels used to separate transcripts generated *in vitro* using the *waaY*.1 derivative. Assays were done with RNAP-σ^{70}. Increasing concentrations of MarA (1 µM – 2 µM – 4 µM – 5 µM), SoxS (1 µM – 2 µM – 4 µM – 5 µM) and Rob (0.2 µM – 0.4 µM – 0.8 µM – 1 µM) are shown by green triangles. Bands formed by transcripts originating from P*waaY* and RNAI are indicated by solid lines. The ratio of transcript to P*waaY*:RNAI is shown.

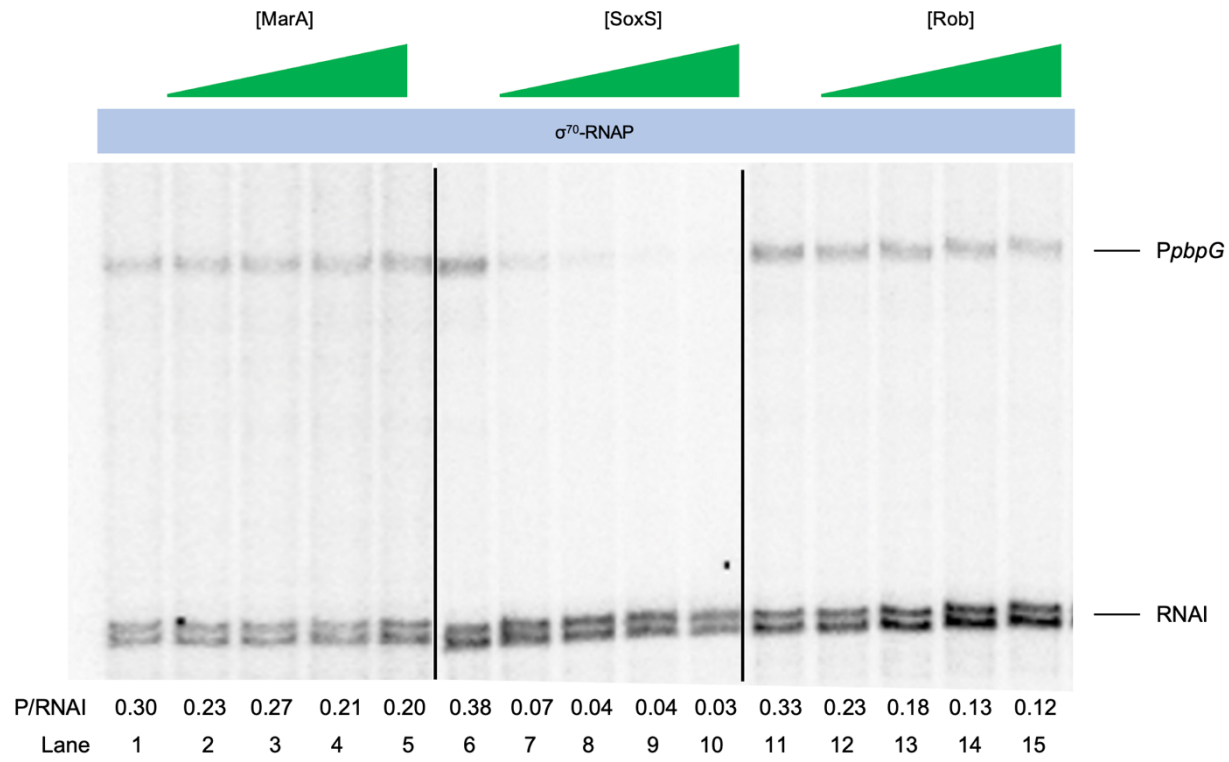

Figure 4.9. MarA, SoxS and Rob activation of transcription from the P*pbpG* promoter. Images of 8 % polyacrylamide gels used to separate transcripts generated *in vitro* using the *pbpG*.1 derivative. Assays were done with RNAP-σ70. Increasing concentrations of MarA (1 µM – 2 µM – 4 µM – 5 µM), SoxS (1 µM – 2 µM – 4 µM – 5 µM) and Rob (0.2 µM – 0.4 µM – 0.8 µM – 1 µM) are shown by green triangles. Bands formed by transcripts originating from P*pbpG* and RNAI are indicated by solid lines. The ratio of transcript to P*pbpG*:RNAI is shown.

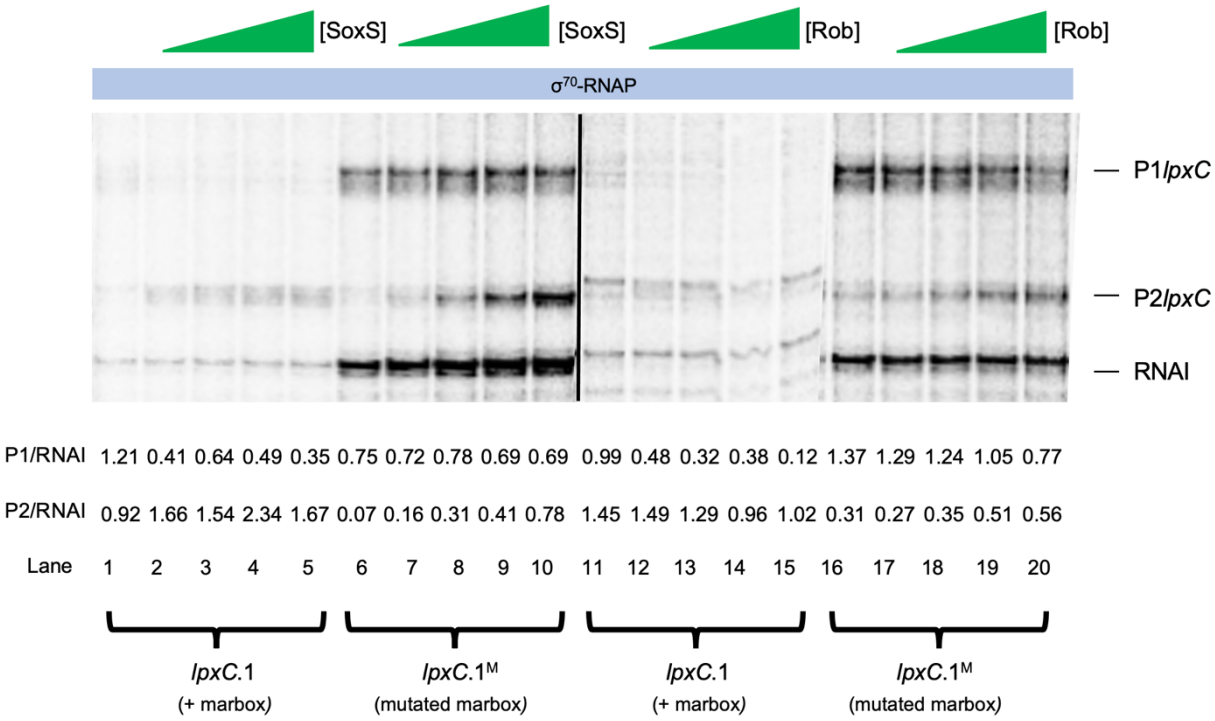

Figure 4.10. SoxS and Rob activation of transcription from the P*lpxC* promoter.

Images of 8 % polyacrylamide gels used to separate transcripts generated *in vitro* using the *lpxC*.1 and *lpxC*.1^{M} derivatives. Assays were done with RNAP-σ^{70}. Increasing concentrations of SoxS (1 µM – 2 µM – 4 µM – 5 µM) and Rob (0.2 µM – 0.4 µM – 0.8 µM – 1 µM) are shown by green triangles. Bands formed by transcripts originating from P1*lpxC*, P2*lpxC* and RNAI are indicated by solid lines. The ratio of transcript to P*lpxC*:RNAI is shown.

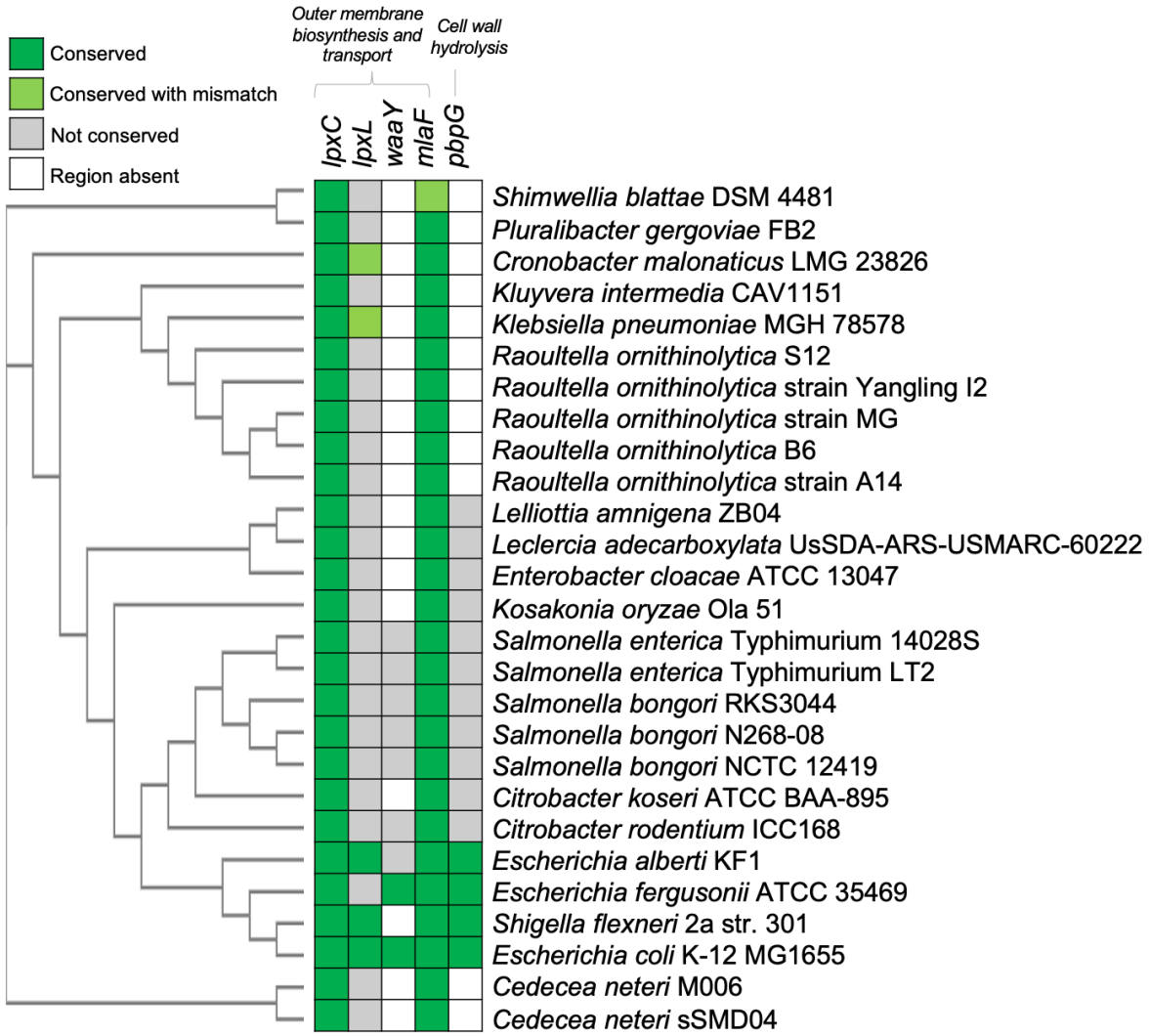

Figure 4.11. Phylogenetic analysis of marbox conservation in the promoters of *lpxC*, *lpxL*, *waaY*, the *mlaFEDCB* operon and *pbpG*.

The heatmap illustrates conservation of marboxes in promoters of interest, identified by ChIP-seq or bioinformatic analysis (x-axis) in the genomes of different enteric bacteria (y-axis). All strains contain MarA with identical DNA-recognition helices. Dark green indicates conservation of a marbox with a maximum of one mismatch, light green indicates a maximum of two mismatches, grey indicates the region is present but poorly conserved, and white indicates that the region was not identified in the genome. The phylogenetic tree demonstrates the evolutionary relationship between the organisms, determined based on the *polA* gene sequence.

marboxes upstream of *lpxC* and *mlaFEDCB* were found to be highly conserved. The MarA target sequence found in the regulatory regions of *lpxL*, *waaY* and *pbpG* were demonstrated to be poorly conserved throughout the Enterobacteriaceae. Conservation of the marboxes upstream of *pbpG* and *waaY* was only demonstrated in *Escherichia* and S*higella* species. The marbox upstream of *lpxL* was found to be conserved in *Escherichia*, *Shigella*, *Klebsiella* and *Cronobacter*.

4.9. Discussion

The aim of this chapter was to identify MarA targets bioinformatically, and experimentally determine if they were genuine. 15 putative marboxes were identified in the promoters of genes involved in the cellular envelope regulation. These included genes important for LPS biosynthesis, capsule biosynthesis, Enterobacterial common antigen (ECA) biosynthesis, and peptidoglycan hydrolysis. Experimental follow up work confirmed that 3 of these targets bound, and were regulated by, MarA: *lpxL*, *waaY* and *pbpG*. The presence of a marbox in these promoters was demonstrated to be poorly conserved throughout Enterobacteriaceae.

MarA targets found in separate ChIP studies were compared (Appendix 3) (Seo *et al.,* 2015; Sharma *et al*., 2017). A ChIP-exo by Seo *et al*. identified 25 SoxS targets in E. *coli* K-12 and ChIP-seq carried out by Sharma *et al*. identified 33 MarA targets in ETEC strain H10407. Only 4 of the targets were identified in both studies. Additionally, less than 30 % (15/54) targets from both ChIP experiments were flagged in the Colibri search used in this work. This highlights the limitations of *in vivo* ChIP techniques and sequence scanning in locating transcription factor binding sites. Moreover, it suggests that there could be other important MarA binding sites that have not yet been discovered. The question as to why the aforementioned studies found different sets of targets is unknown, although differences in *in*

vivo ChIP and *in vitro* analyses have previously been noted (Cho *et al*., 2008; Myers *et al*., 2013; Federowicz *et al*., 2014; Seo *et al*., 2014). It has been hypothesised that it could be due to competitive binding of other transcription factors to the binding site of interest. Hence, MarA or SoxS are blocked from binding (Seo *et al*., 2015). Furthermore, it is noted that SoxS and Rob often have preferential binding to known marboxes (Martin *et al*., 2002). Hence, a ChIP-seq with MarA may only identify marboxes with the highest affinity for MarA (Sharma *et al*., 2017).

There were 3 putative marboxes found in the *lpxL* regulatory region, within 200 bp of the start codon. By mutating each marbox, only the most upstream marbox, designated 'marbox 1' was shown to bind MarA. Further experimentation demonstrated that MarA causes activation of *lpxL* expression *in vitro* and *in vivo*. *lpxL* encodes an enzyme involved in lipid A biosynthesis. This is part of the same pathway involving LpxC, which we showed to be induced by MarA in Chapter 3. This is consistent was the overall hypothesis that MarA upregulates lipid A biosynthesis to decrease the permeability of the OM. Targeting more than one enzyme in the pathway is an excellent method to ensure upregulation of lipid A biosynthesis. Previous work found that RamA activated the expression of *lpxL*-2 in *K. pneumoniae* (De Majumdar *et al*., 2015). Interestingly, *K. pneumoniae* encodes two orthologues of LpxL (Mills *et al.,* 2017). Despite this, *lpxL* has not previously been identified as a target of MarA or SoxS in *E. coli* or other Gram-negative bacteria.

Another target identified by the bioinformatic marbox search was *waaY*. Further research into this gene demonstrated that it had previously been identified as a MarA and SoxS target and had been shown to be upregulated by both transcription factors (Lee *et al*., 2009). This was determined using reporter assays in the presence of *mar* and *sox* inducers sodium salicylate and

paraquat, respectively, demonstrating an increase in *waaY* promoter activity. Additionally, this promoter activation was abolished in Δ*marA* and Δ*soxRS* mutants. This chapter confirmed this work and demonstrated direct binding of MarA and SoxS to the *waaY* promoter, as well as direct binding by Rob. We also identified the marbox sequence by bioinformatic analysis and confirmed this by mutating key residues of the operator sequence. *waaY* encodes an enzyme involved in LPS core oligosaccharide biosynthesis. Previously, it was shown that deleting the *waaY* gene causes changes in the structure of LPS, as demonstrated by faster migration of LPS in SDS-PAGE compared to wildtype (Lee *et al*., 2009). WaaY is a kinase, and this change in LPS is likely due to changes in phosphorylation (Heinrichs, Yethon and Whitfield, 1998). It is hypothesised that this change in oligosaccharide structure alters the permeability of LPS.

The third target confirmed to bind MarA was *pbpG*, which encodes an endopeptidase involved in cell wall hydrolysis. Peptidoglycan biogenesis has not previously been noted to be MarA regulated. The data shown here confirm that MarA, SoxS and Rob repress *pbpG* expression. The hypothesis is that downregulation of endopeptidase activity causes a decrease in cross-link cleavage of peptidoglycan. Whilst peptidoglycan biosynthesis continues and hydrolysis decreases, it is likely that the peptidoglycan layer will stiffen or thicken. As peptidoglycan acts as an additional permeability barrier for bacteria, this would likely reduce passive diffusion of antimicrobial agents into the cytoplasm. Interestingly, *pbpG* repression was most notable with SoxS rather than the other AraC family transcription factors. SoxS is associated with the oxidative stress response. This suggests that perhaps *pbpG* downregulation is more important in survival of oxidative stress than antimicrobial attack.

Intriguingly, OxyR was found to activate *mepM*, encoding an alternative endopeptidase (Seo *et al*., 2015). It was hypothesised that this results in structural changes of peptidoglycan. OxyR

is a transcription factor associated with oxidative stress, much like SoxS (Zheng *et al*., 1998). Although OxyR was demonstrated to activate *mepM*, the promoter was not found to bind SoxS. It remains unclear why OxyR would cause upregulation of endopeptidase activity whereas SoxS appears to cause downregulation of endopeptidase activity.

In summary, this chapter has confirmed MarA activation of *waaY* and *lpxL*, genes associated with LPS biosynthesis. MarA repression of *pbpG*, involved in cell wall biogenesis, was also noted. It is hypothesised that MarA regulation of these genes leads to improved barrier function of the cell through the OM and the cell wall. This is illustrated in Figure 4.12. SoxS and Rob also regulate all investigated genes.

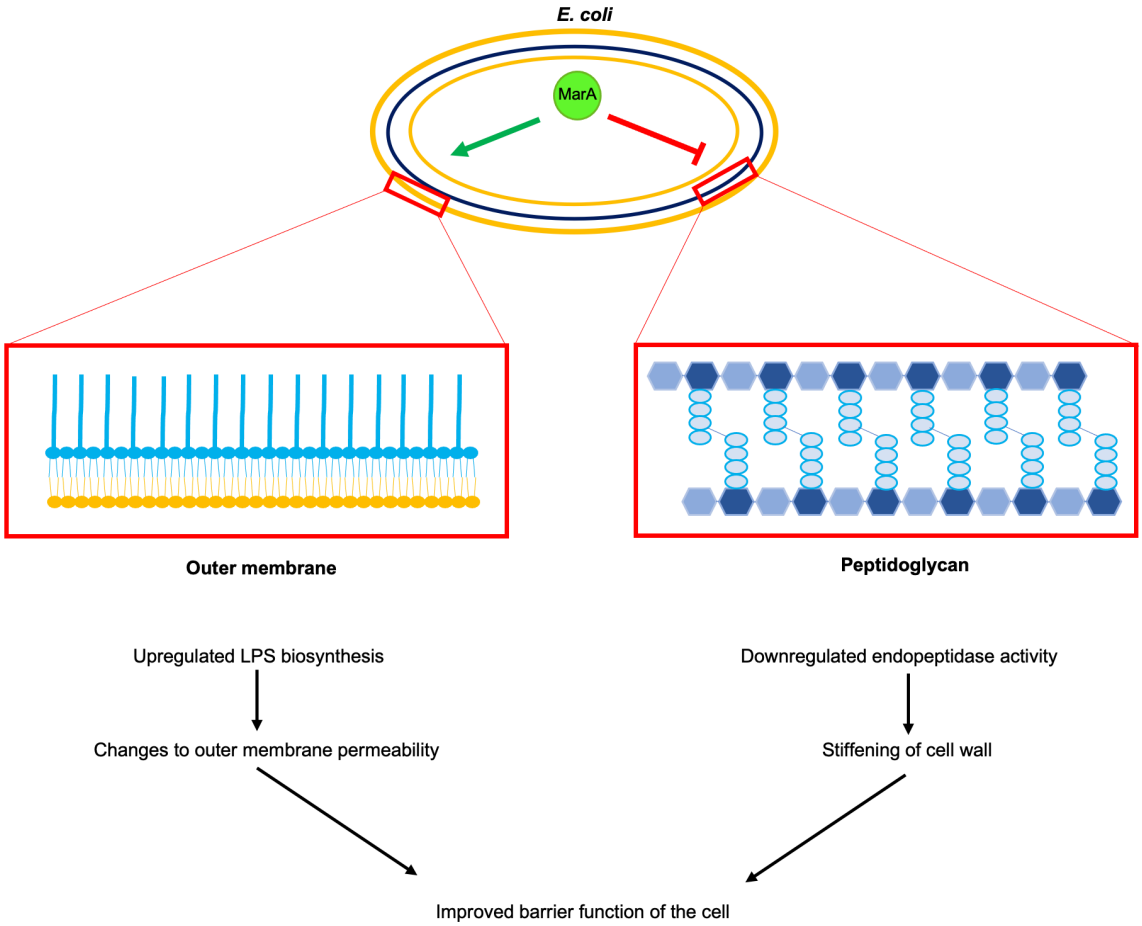

Figure 4.12. MarA targets the cell envelope of Gram-negative bacteria to improve the barrier function of the cell.

Data suggests that MarA targets OM biosynthesis and peptidoglycan hydrolysis to increase barrier function and allow less antibiotics into the cell by passive diffusion. MarA activates *lpxC*, *lpxL* and *waaY*, all of which encode LPS biosynthetic enzymes. This likely changes the structure of LPS, which forms the outer leaflet of the OM. Additionally, MarA represses *pbpG*, encoding an endopeptidase associated with cell wall hydrolysis. It is hypothesised that this downregulation in cleavage of the cross-links causes slight stiffening of the peptidoglycan macromolecule. This could act as an additional barrier against outside threats. Other AraC family transcription factors, SoxS and Rob, also regulate all promoters in the same way, suggesting that they are also important in oxidative stress.

Chapter 5 – Synergy between MarA Target Genes that Control Cell Envelope Biology

5.1. Introduction

MarA targets various genes involved in regulation of cell envelope composition. For example, Chapters 3 and 4 demonstrate that MarA regulates *lpxC*, *lpxL* and *waaY,* which are associated with OM biosynthesis, and *pbpG*, a peptidoglycan hydrolase. Additionally, MarA has previously been found to upregulate the *mlaFEDCB* operon to improve barrier function of the OM (Sharma *et al*., 2017).

The inner and outer membranes of bacteria are phospholipid bilayers that form a polar barrier that must be crossed to enter the cell (Vance and Vance, 1985). Phospholipids are composed of a variable head group, a phosphate group, a glycerol moiety and two fatty acid chains (Figure 5.1). The most common phospholipid head groups in *E. coli* include phosphatidylglycerol (PG) (20 %), phosphatidylethanolamine (PE) (75 %) and cardiolipin (CL) (5 %) (Raetz and Dowhan, 1990). In addition, the membranes can contain several less common lipids, including glycolipids, sphingolipids and hopanoids (Olsen and Jantzen, 2001; Sohlenkamp and Geiger, 2016). Whilst the IM is a symmetrical bilayer, the OM is not; the outer leaflet is made of LPS rather than phospholipids. This is important for OM barrier function. The exact composition of each membrane differs between species and can change in response to stress (Raetz and Dowhan, 1990).

The *mlaFEDCB* operon encodes the maintenance of lipid asymmetry (Mla) proteins (MlaA-F), which form an ABC transporter involved in phospholipid translocation between the IM and OM of Gram-negative bacteria (Figure 5.2) (Malinverni *et al*., 2009). MlaFEDB makes up the IM transporter and MlaC is the periplasmic protein. MlaA is an OM lipoprotein that can form complexes with porins OmpF and OmpC. Recent structural work suggests that the MlaFEDB transporter extracts and releases phospholipids from a central translocation cavity in MlaD (Chi

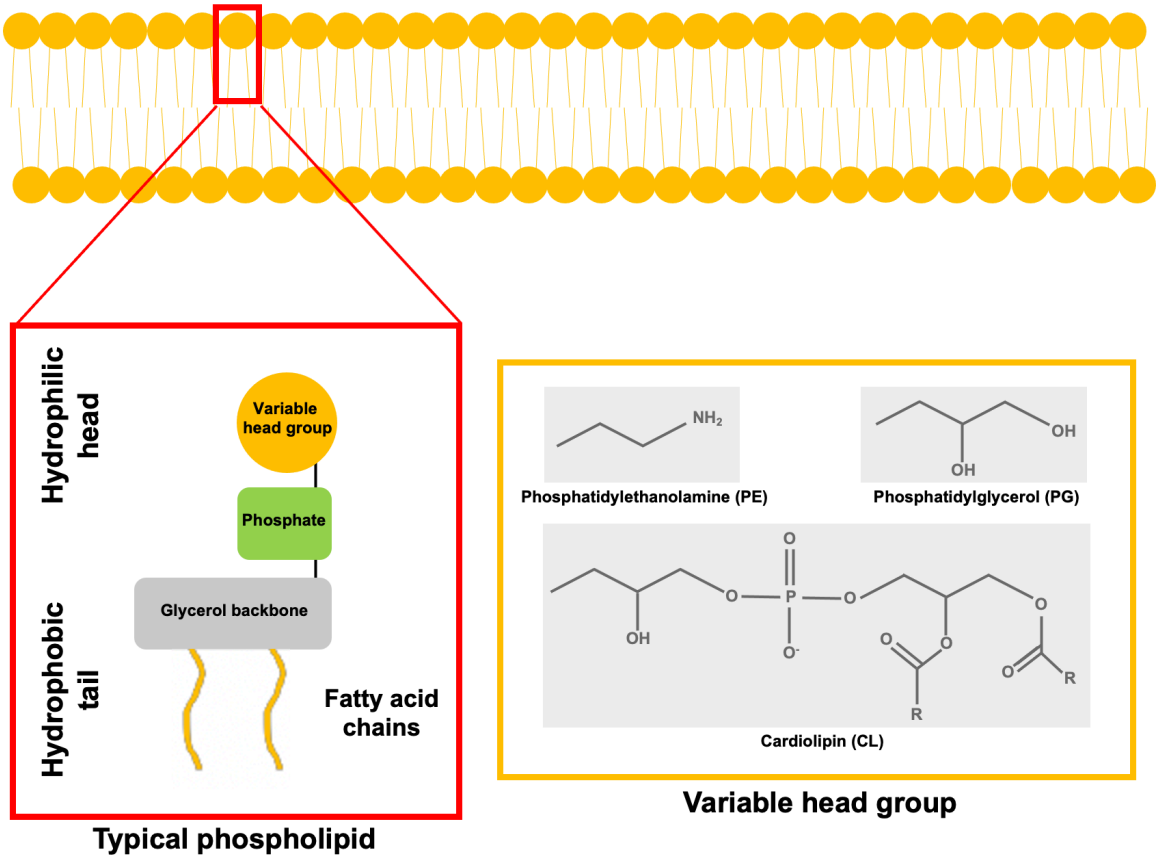

Figure 5.1. Typical phospholipid structure and variable head groups commonly found in *E. coli*.

A typical phospholipid is composed of 2 fatty acid chains, a glycerol backbone, a phosphate group and a variable head group. These phospholipids make up the inner and outer membrane of Gram-negative bacteria. The common phospholipids in *E. coli* include phosphatidylethanolamine, phosphatidylglycerol and cardiolipin. Head group structures are adapted from Aktas *et al*., 2014 and Berezhnoy *et al*., 2022. The R groups of cardiolipin are variable fatty acid chains to produce a diphosphatidylgycerol.

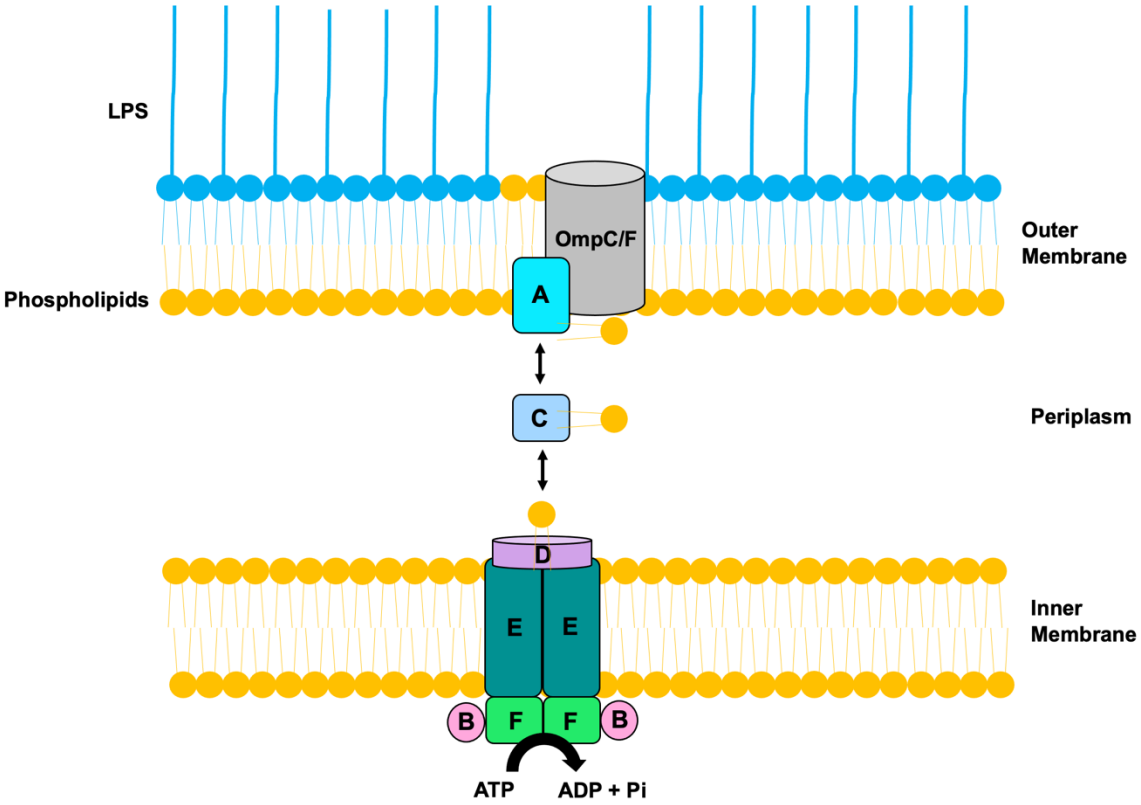

Figure 5.2. Translocation of phospholipids between the inner and outer membranes of Gram-negative bacteria via the Mla pathway.

The MlaFEDB complex is found in the IM. MlaC is a periplasmic protein. MlaA, bound to the OM porins OmpC and OmpF, is found in the OM. Adapted from Tang *et al*., 2020.

et al., 2020). Initial studies demonstrated that phospholipids moved in a retrograde direction from the OM to IM (Hughes *et al*., 2019; Tang *et al*., 2020). However, the Mla pathway may also be able to transport lipids in the anterograde direction from the IM to the OM (Chi *et al*., 2020). The precise mechanism of phospholipid transport by MlaFEDCB remains unclear. MarA activation of *mlaFEDCB* is hypothesised to decrease cell permeability and improve barrier function (Sharma *et al*., 2017).

Previous high throughput phenotyping experiments identified an inverse correlation between effects of *mlaE* and *pbpG* deletions (Nichols *et al*., 2011). This is intriguing because MarA inversely regulates these genes; *mlaFEDCB* is activated whilst *pbpG* is repressed. Hence, the aim of this chapter is to understand synergy between MarA target genes that control cell envelope biology and barrier function. Antibiotic susceptibility testing and growth measurements, with sub-lethal concentrations of doxycycline, were used to assess strains lacking different MarA regulated genes, or constitutively expressing MarA repressed *pbpG*. Significant growth defects were only noted when genetic changes were combined, consistent with MarA targets acting synergistically. Expression of *mlaFEDCB*, *pbpG* and *waaY* was uncoupled from MarA regulation by mutating chromosomal marboxes to similar effect. This chapter demonstrated that MarA targeting of multiple cell envelope genes is important in reducing cell permeability during response to antibiotics.

5.2. Role of the *mlaFEDCB* operon in antibiotic resistance

The MlaFEDCB ABC transport system is known to remove unwanted phospholipids from the outer leaflet of the OM. MarA activation of *mlaFEDCB* has been demonstrated to improve the barrier function of the OM (Sharma *et al*., 2017). To investigate this further, *mla* mutants were used in growth experiments and antibiotic susceptibility testing to determine the importance of

the operon in antibiotic resistance. Ampicillin, doxycycline, and tetracycline were chosen for these assays because they move into the cytoplasm by passive diffusion through the cell envelope and they represent different lipid solubilities (Livermore, 1990). Doxycycline, a synthetic member of the tetracycline family, is highly lipophilic and can cross multiple membranes to easily penetrate bacteria (Sagar, 2010). Tetracycline is 5-10 times less lipophilic than doxycycline (Sagar, 2010). Ampicillin demonstrates low lipid solubility and is largely hydrophilic (Liu, Leonas and Zhao, 2010). Thus, uptake of tetracycline antibiotics, especially doxycycline, is largely affected by cell barrier function. In contrast, passive diffusion of ampicillin relies more on porins OmpC and OmpF and less on the cell envelope.

5.2.1. Deleting the *mlaFEDCB* operon causes a change in susceptibility to doxycycline

A range of strains, including *E. coli* BW25113 Δ*mlaE*, were investigated for sensitivity to 3 different antibiotics (Table 5.1). This strain was obtained from the Keio collection (Baba *et al*., 2006), and therefore the parent strain BW25113 was used as a control. There was a four-fold reduction in the doxycycline MIC for Δ*mlaE* compared to wildtype cells. This suggests that deleting the MlaFEDCB ABC transport system allows more doxycycline into the cell, as was shown previously (Sharma *et al*., 2017). Only a two-fold reduction in the tetracycline MIC was noted, and the ranges of MICs overlapped, so this is not noted as significant. No difference in the susceptibility to ampicillin was noted between the control (BW25113) and Δ*mlaE*. This is consistent with the low lipid solubility of ampicillin compared to doxycycline.

5.2.2. Deleting the *mlaFEDCB* operon causes no change in growth rate in the presence of doxycycline

To understand the role of the MlaFEDCB transport system in antibiotic susceptibility further, growth rate of the *mlaE* mutant was compared to wildtype BW25113. Growth was measured

Table 5.1. Minimum inhibitory concentration of 3 antibiotics for BW25113, Δ*mlaE* and Δ*pbpG* and the same strains overexpressing *pbpG*.

96-well MIC assays were done for *E. coli* strains BW25113, BW25113 Δ*mlaE* and BW25113 Δ*pbpG*. *pbpG* was overexpressed on plasmid pJ203, and empty pJ203 was used as a control (results not shown). 3 antibiotics were chosen. MIC is shown as the minimum concentration of antibiotic required to inhibit growth of the strain. Numbers shown are range and modal value in brackets. Assays were done in triplicate and repeated on 3 separate days. Results were only accepted if they were in line with the control strains ATCC 25922 and NCTC 10418.

	Minimum inhibitory concentration (MIC) (µg/ml)		
Strain	**Ampicillin**	**Doxycycline**	**Tetracycline**
BW25113	4 - 8 (8)	4 (4)	1 (1)
BW25113 pJ203 + *pbpG*	4 - 8 (4)	2 - 4 (2)	0.5 - 1 (1)
Δ*mlaE*	8 - 16 (8)	1 (1)	0.5 - 1 (1)
Δ*mlaE* pJ203 + *pbpG*	4 - 16 (4)	1 - 2 (2)	0.25 - 0.5 (0.5)
Δ*pbpG*	8 - 16 (8)	2 - 4 (2)	1 (1)
Δ*pbpG* pJ203 + *pbpG*	8 (8)	2 - 4 (2)	1 - 2 (1)

in the presence of 1.0 µg/ml doxycycline, previously noted to be the MIC of Δ*mlaE* cells (Table 5.1). BW25113 and Δ*mlaE* were grown in LB media with or without 1.0 µg/ml doxycycline. Samples were taken every 40 minutes for 480 minutes, then left overnight and sampled again at 1440 minutes. An OD_{650} of each sample was taken to assess growth (Figure 5.3). The assay was performed in triplicate and repeated on 3 separate days to obtain a mean and standard deviation. The calculated growth rates (doubling time) are shown in Appendix 4. In the absence of doxycycline, both BW25113 and Δ*mlaE* strains had no significant difference in growth (Figure 5.3, Panel A). In the presence of doxycycline, growth of both strains was reduced, as expected due to the presence of the antibiotic (Figure 5.3, Panel B). No significant difference in growth rate was demonstrated between the strains. This result was unexpected considering that, in the antimicrobial susceptibility tests, Δ*mlaE* has a doxycycline MIC of 1.0 µg/ml. The results here demonstrate that there is no growth defect at 1 µg/ml doxycycline when the *mlaFEDCB* operon is deleted.

5.2.3. Deleting the *mlaFEDCB* operon causes no change in the overall lipid composition of the outer membrane

It was hypothesised that the MlaFEDCB transporter could target specific phospholipids for removal from the OM. To test this hypothesis, liquid chromatography/mass spectrometry (LC/MS) was used to determine which phospholipids were present in the total and OM fractions of BW25133 and Δ*mlaF* strains. As expected, PG and PE phospholipids, with the same fatty acid chain lengths, were identified in both strains (Appendix 5). Lipid amounts were quantified by calculating the area under the peak in the resulting chromatogram (Figure 5.4). It was demonstrated that there was no significant difference in the relative amount of PG and PE species between the control and Δ*mlaF*. The results here suggest that lipid trafficking by

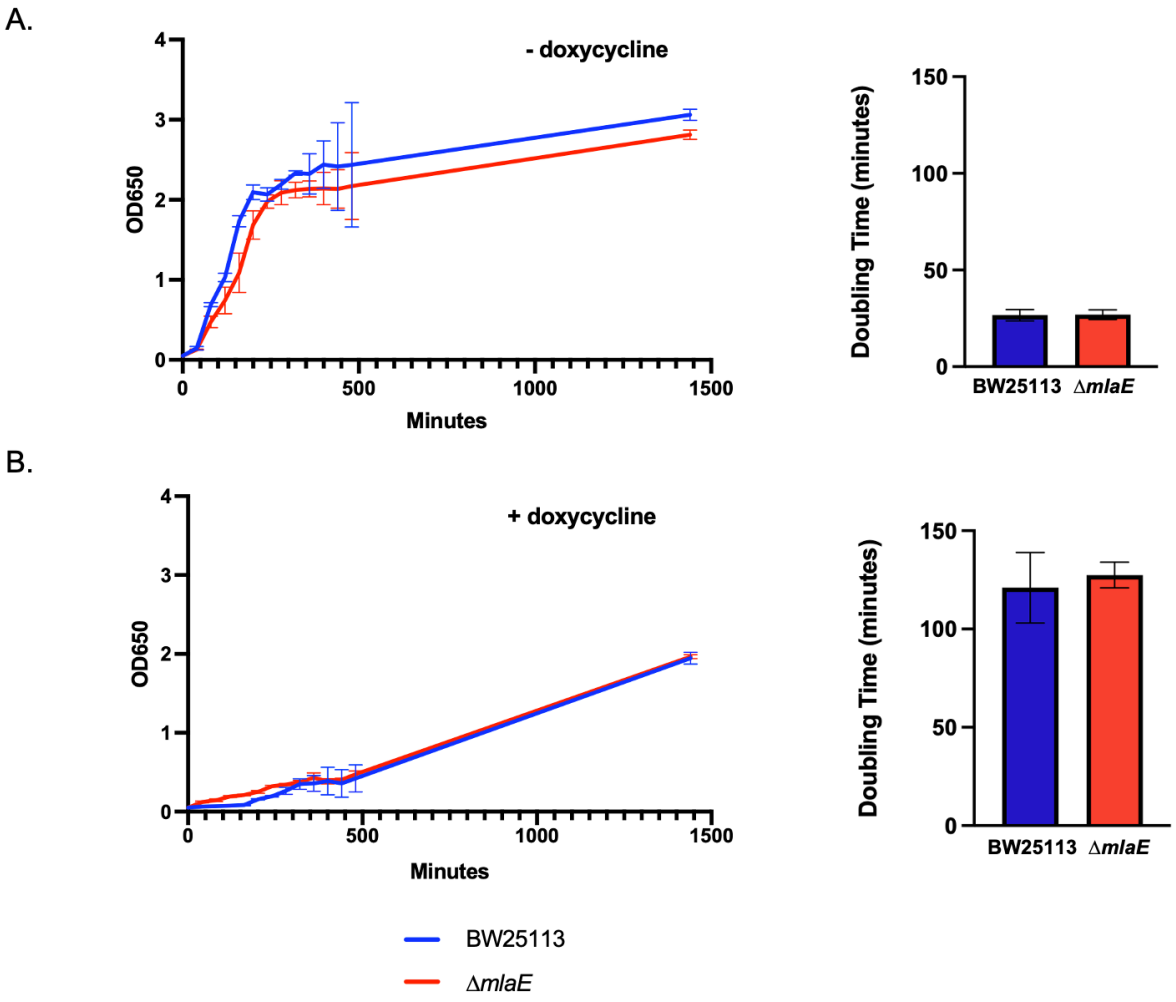

Figure 5.3. Growth of BW25113 and Δ*mlaE* in the absence and presence of 1.0 µg/ml doxycycline.

Growth was assessed using a standard growth curve assay in LB. Samples were taken every 40 minutes and OD_{650} was measured. Blue lines represent wildtype BW25113 and orange lines represent Δ*mlaE*. Assays were done in triplicate and repeated on 3 separate days. The mean and standard deviation are shown on the graphs. Graphpad Prism 9 was used for logistic growth analysis to determine growth rate. A 95 % confidence interval was used for interpolation. Doubling time (minutes) was calculated using the equation ln(2)/k, where k is the growth rate constant. A. Growth in the absence of doxycycline. B. Growth in the presence of 1.0 µg/ml doxycycline. A two-way ANOVA followed by the two-stage linear step-up procedure of Benjamini, Krieger and Yekutieli showed that there were no significant differences in growth curves between the strains in the absence or presence of doxycycline (Appendix 4). An unpaired two-tailed t-test was used to analysis the significance of growth rate.

the MlaFEDCB transport system does not lead to changes in the overall lipid composition of the OM.

5.3. Role of *pbpG* in antibiotic resistance

Peptidoglycan hydrolysis involves several enzymes, including PbpG. Chapter 4 demonstrated that MarA, SoxS and Rob repress *pbpG* expression. We hypothesised that downregulating peptidoglycan hydrolysis leads to stiffening of the cell wall to act as a barrier against antimicrobial threats. To investigate the role of *pbpG* further, *pbpG* mutants were subjected to growth experiments and antimicrobial susceptibility testing. Additionally, the same tests were carried out on strains that were made to constitutively express *pbpG* to uncouple *pbpG* expression from MarA regulation.

5.3.1. Deleting or overexpressing *pbpG* causes no change in antibiotic susceptibility

As previously, antibiotic susceptibility testing was done to investigate the role of *pbpG* in controlling sensitivity to 3 different antibiotics (Table 5.1). First, *pbpG* was expressed on plasmid pJ203. No differences in susceptibility to any antibiotics tested were noted between wildtype cells and wildtype cells overexpressing *pbpG* (BW25113 pJ203 + *pbpG*). Second, *pbpG* was deleted and no difference compared to wildtype cells was demonstrated. This data suggests that *pbpG* does not impact antibiotic susceptibility alone. However, it should be noted that this does not necessarily mean that *pbpG* has no involvement in antibiotic susceptibility in combination with other factors. Furthermore, differences due to PbpG could be below the level detectable in this assay.

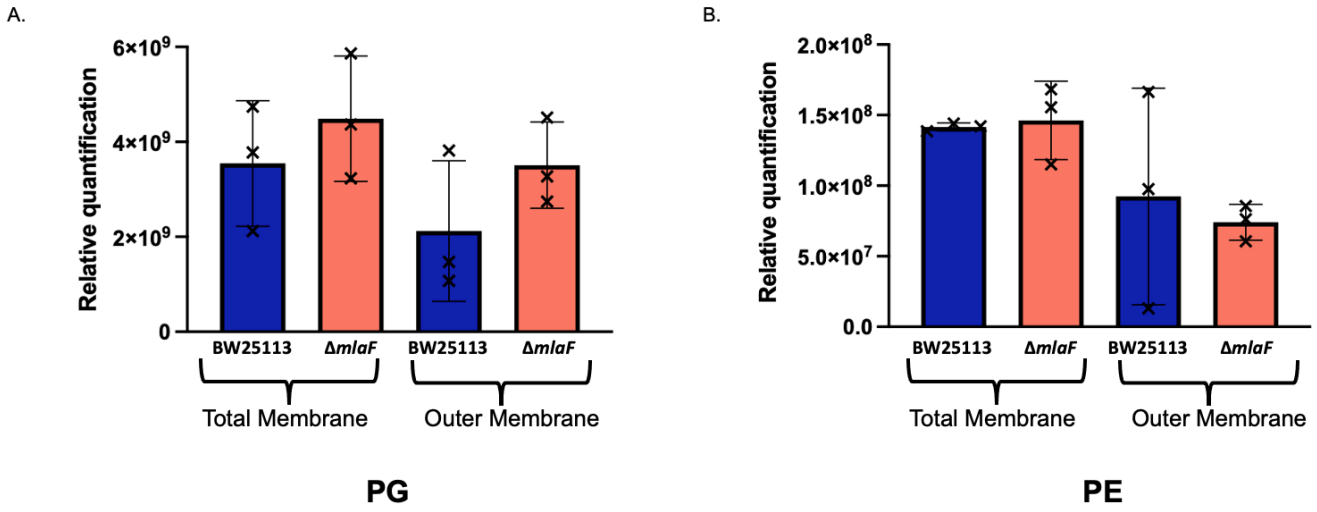

Figure 5.4. Relative quantification of major phospholipids PG and PE in total membrane and outer membrane fractions extracted of BW25113 and Δ*mlaF*.

LC/MS was carried out on total membrane fractions extracted by a modified Folch lipid extraction method (Folch *et al*., 1957). Membrane fractions were further separated by sucrose density gradient centrifugation. LC/MS was carried out on OM fractions. Relative quantification of lipids was calculated as the peak area. The mean activity, individual data points and standard deviation are shown, as the mean of assays from 3 separate days. A. Relative quantification of PG in total and OM fractions of BW25113 and Δ*mlaF*. B. Relative quantification of PE in total and OM fractions of BW25113 and Δ*mlaF*. Results were found to be insignificant, as demonstrated by a one-way ANOVA.

5.3.2. Deleting or overexpressing *pbpG* causes a small change in growth rate

To investigate the role of *pbpG* in antibiotic susceptibility further, *pbpG* mutants and wildtype cells artificially overexpressing *pbpG* were subjected to growth experiments in the presence of 1.0 μg/ml doxycycline, which was noted as sub-lethal for these strains (Figure 5.5). Growth experiments were done as previously described. The calculated growth rates (doubling time) are shown in Appendix 6.. In the absence of doxycycline, overexpressing *pbpG* in wildtype cells (pink line) causes a significant reduction in growth compared to wildtype cells (blue line) (Figure 5.5, Panel A). Deleting *pbpG* (grey line) also causes a significant reduction in growth compared to wildtype cells. In the presence of doxycycline, deleting and overexpressing *pbpG* increased growth rate (Figure 5.5, Panel B). For cells overexpressing *pbpG,* this increase was not statistically significant. However, *pbpG* deletion allowed cells to grow significantly faster compared to wildtype cells. At the end of the experiment all cells reached the same OD_{650}. These data suggest that small changes in peptidoglycan hydrolysis are deleterious in normal conditions but can enhance growth during exposure to antimicrobial agents.

5.4. Combining cell wall and outer membrane defects changes antibiotic susceptibility

5.4.1. Deleting the *mlaFEDCB* operon and overexpressing *pbpG* simultaneously causes a significant reduction in growth rate

Considering that MarA activates *mlaFEDCB* and represses *pbpG*, we hypothesised that deleting the *mlaFEDCB* operon whilst constitutively expressing *pbpG* would increase antibiotic sensitivity. Growth and antimicrobial susceptibility were investigated in an Δ*mlaE* deletion strain that expressed *pbpG* from a plasmid. As previously described, growth was

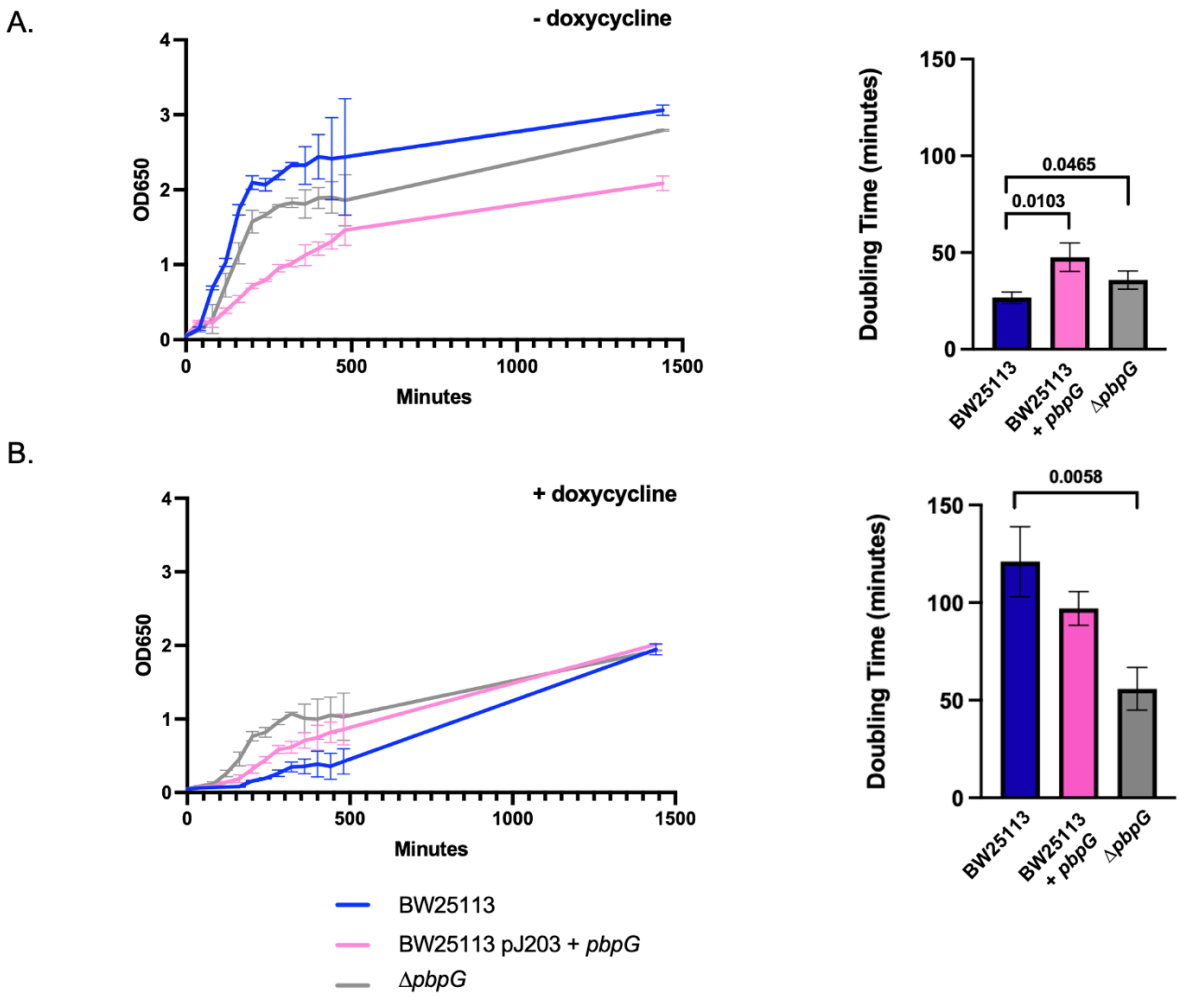

Figure 5.5. Growth of BW25113, BW25113 overexpressing *pbpG* and Δ*pbpG* in the absence and presence of 1.0 µg/ml doxycycline.

Growth was assessed using a standard growth curve assay in LB. Samples were taken every 40 minutes and OD_{650} was measured. Blue lines represent wildtype BW25113, pink lines represent BW25113 pJ203 + *pbpG*, and grey lines represent Δ*pbpG*. Assays were done in triplicate and repeated on 3 separate days. The mean and standard deviation are shown on the graphs. Graphpad Prism 9 was used for logistic growth analysis to determine growth rate. A 95 % confidence interval was used for interpolation. Doubling time (minutes) was calculated using the equation ln(2)/k, where k is the growth rate constant. A. Growth in the absence of doxycycline. B. Growth in the presence of 1.0 µg/ml doxycycline. A two-way ANOVA followed by the two-stage linear step-up procedure of Benjamini, Krieger and Yekutieli showed that there was a significant difference in growth between BW25113 and Δ*pbpG*, but no significant difference in growth between BW25113 and BW25113 pJ203 + *pbpG* (Appendix 4). An unpaired two-tailed t-test was used to analysis the significance of growth rate.

analysed by measuring OD_{650} over 1440 minutes. The Δ*mlaE* strain was measured, as before, and this was compared to Δ*mlaE* artificially overexpressing *pbpG* (Figure 5.6). This was done to combine defects in the *mlaFEDCB* operon and *pbpG* (hereafter referred to as Δ*mlaE* + *pbpG*). The calculated growth rates (doubling time) are shown in Appendix 6. In the absence of doxycycline, growth of the Δ*mlaE* + *pbpG* strain is significantly reduced compared to the Δ*mlaE* control. This suggests that combining these changes can cause growth defects (Figure 5.6, Panel A). In the presence of doxycycline, the same trend is seen (Figure 5.6, Panel B). Interestingly, at the end of the experiment (1440 minutes), growth rate increases in the absence of doxycycline (OD_{650} = 1.97 at 1440 minutes). Conversely, in the presence of doxycycline, growth rate remains low throughout the experiment (OD_{650} = 0.44 at 1440 minutes). Essentially, in the presence of doxycycline, growth of the Δ*mlaE* + *pbpG* strain is negligible (that is, these cells are barely viable). This implies that changes in the cell envelope are very important for uptake of doxycycline and that combining defects in *mlaFEDCB* and *pbpG* lead to significantly reduced cell permeability.

5.4.2. Deleting the *mlaFEDCB* operon and overexpressing *pbpG* simultaneously causes no change in antibiotic susceptibility

No large changes in MICs were noted for any of the antibiotics tested between Δ*mlaE* and Δ*mlaE* + pbpG (Table 5.1).

5.5. Combining cell wall and outer membrane defects result in decreased cell permeability

Considering that targeting *mlaFEDCB* and *pbpG* simultaneously causes significant changes in

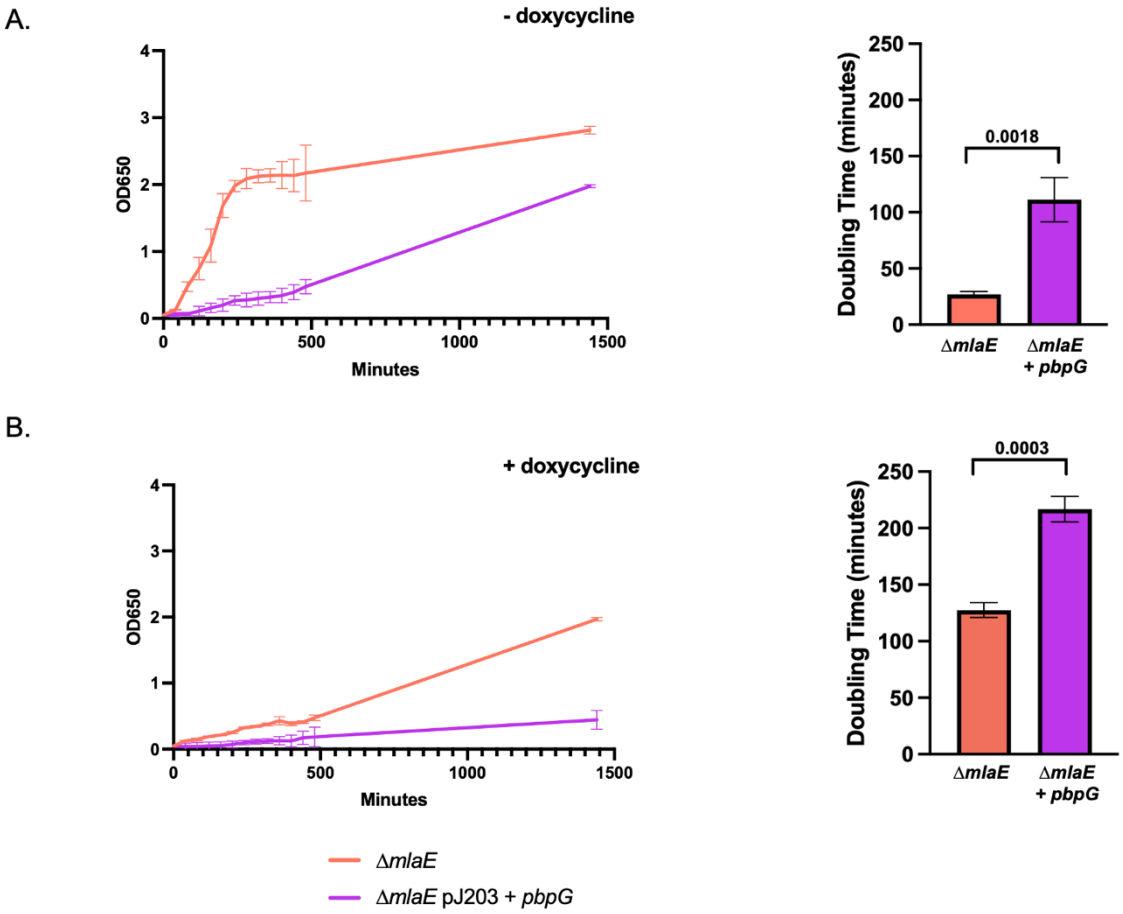

Figure 5.6. Growth of Δ*mlaE* and Δ*mlaE* overexpressing *pbpG* in the absence and presence of 1.0 µg/ml doxycycline.

Growth was assessed using a standard growth curve assay in LB. Samples were taken every 40 minutes and OD_{650} was measured. Orange lines represent Δ*mlaE* and purple lines represent Δ*mlaE* with pJ203 + *pbpG*. Assays were done in triplicate and repeated on 3 separate days. The mean and standard deviation are shown on the graphs. Graphpad Prism 9 was used for logistic growth analysis to determine growth rate. A 95 % confidence interval was used for interpolation. Doubling time (minutes) was calculated using the equation ln(2)/k, where k is the growth rate constant. A. Growth in the absence of doxycycline. B. Growth in the presence of 1.0 µg/ml doxycycline. A two-way ANOVA followed by the two-stage linear step-up procedure of Benjamini, Krieger and Yekutieli showed that there was a significant difference in growth between Δ*mlaE* and Δ*mlaE* + *pbpG* (Appendix 4). An unpaired two-tailed t-test was used to analysis the significance of growth rate.

cell growth (Figure 5.6), it was hypothesised that this is due to changes in cell permeability. Cell permeability of BW23115 and several mutants was calculated using a modified crystal violet assay, as described by Halder *et al*., 2015. A significant increase in crystal violet uptake was demonstrated when *mlaE* was deleted, *pbpG* was overexpressed in a wildtype background and particularly when *pbpG* was overexpressed in the Δ*mlaE* background (Figure 5.7). This is consistent with the overall hypothesis that MarA regulation of genes involved in the cell envelope, including *mlaFEDCB* and *pbpG,* contributes to the multiple antibiotic resistance phenotype by improving the barrier function of the cell.

5.6. Mutating multiple marboxes in the regulatory regions of cell envelope genes simultaneously changes antibiotic susceptibility

In Chapters 3 and 4, MarA, SoxS and Rob were shown to activate the expression of LPS biosynthesis genes (*lpxC*, *lpxL* and *waaY*) and the repress the expression of peptidoglycan biosynthesis gene *pbpG*. To investigate the extent to which regulation of these genes contributes to the multiple antibiotic resistance phenotype, a series of chromosomal mutations were prepared to prevent MarA binding *in vivo*. Point mutations were made in marboxes of the regulatory regions of *waaY*, *pbpG* and the *mlaFEDCB* operon. This was done using a technique known as Flexible Recombineering using Integration of *thyA* (FRUIT), as described in Stringer *et al*., 2012. Briefly, a *thyA* cassette flanked by regions complementary to the desired recombination site was electroporated into a Δ*thyA* strain. This strain contained the pACBSR plasmid, which encodes λ Red genes required for homologous recombination into the chromosome. Recombinants, known as *thyA*+ intermediates, were selected on M9 minimal media lacking thymine. A DNA fragment containing the desired point mutations was used to

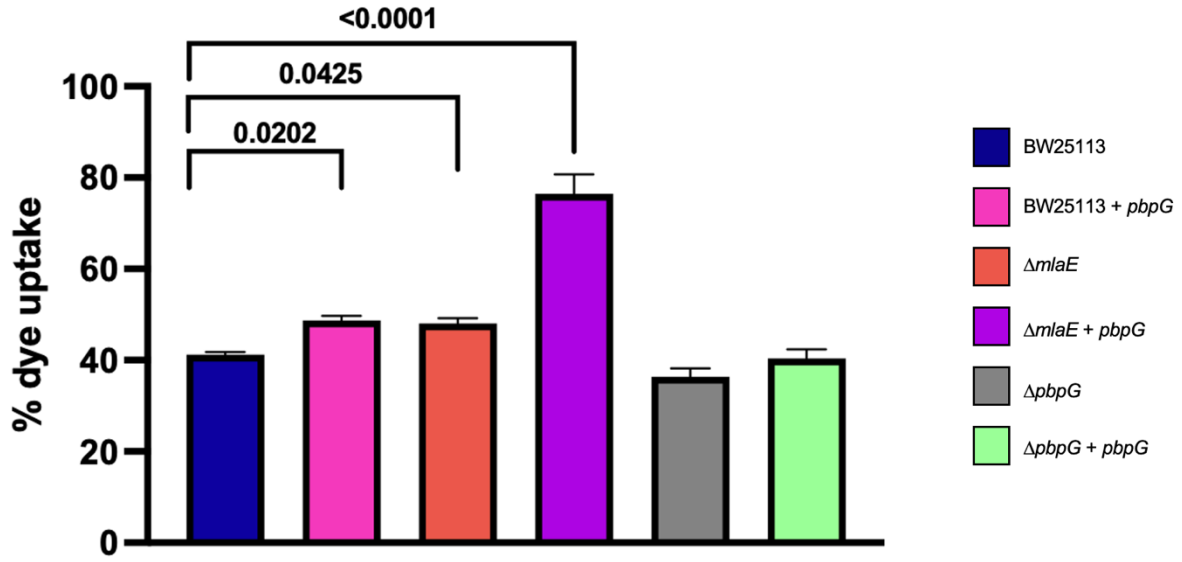

Figure 5.7. Membrane permeability of BW25113, Δ*mlaE* and Δ*pbpG* strains demonstrated by percentage uptake of crystal violet dye.

Uptake of 10 µg/ml crystal violet was measured at OD_{590} and percentage dye uptake was calculated as in Devi *et al*., 2010. Results shown is the mean of assays from 3 separate days. PbpG was provided on pJ203 with constitutive expression of *pbpG*. A one-way ANOVA was calculated using the promoter activities, showing the analysis was significant ($p < 0.0001$, $F(5,12) = 133.5$). A post-hoc Tukey's HSD test showed that there were significant pairwise differences between the control (BW25113) and BW25113 + *pbpG*, Δ*mlaE* or Δ*mlaE* + *pbpG*. p values are shown on the graph.

replace the *thyA* cassette and recombinants were selected on M9 minimal media containing 100 μg/ml thymine. Point mutations were confirmed by colony PCR and sequencing. In all cases, the point mutations made to each marbox to prevent MarA binding were of positions 1-3 from GCA (*waaY* and *pbpG*) or CCA (*mlaFEDCB*) to TGT. Several strains were prepared with marbox mutations in one, two or three marboxes simultaneously (Appendix 7).

5.6.1. Point mutations were unsuccessful in the regulatory regions of essential genes *lpxC* and *lpxL*

Attempts were made to make point mutations to the regulatory regions of *lpxC* and *lpxL* (Appendix 8). However, this was unsuccessful, likely because these are essential genes and insertion of the *thyA* cassette requires disruption of the promoter region. To bypass this issue, further attempts were made to enable constitutive expression of these genes whilst mutations were being prepared. Firstly, a strong constitutive promoter was incorporated into the *thyA* cassette to allow expression of *lpxC* or *lpxL* even when the promoter was disrupted (Appendix 8, Panel A). Secondly, a plasmid was prepared that contained *lpxC* and *lpxL* under control of a strong constitutive promoter (Appendix 8, Panel B). *E. coli* JCB387 was transformed with the plasmid and FRUIT was carried out. Unfortunately, neither of these techniques worked and mutations were unable to be introduced in the regulatory regions of *lpxC* or *lpxL*.

5.6.2. Mutating a single marbox causes no change in growth rate in the presence of doxycycline

To understand the extent to which MarA regulation of *waaY*, *mlaFEDCB* and *pbpG* contribute to the antibiotic resistance phenotype, growth of mutants was measured in the presence of doxycycline. *E. coli* JCB387 Δ*thyA* strains with mutations in the marboxes upstream of *waaY*, *pbpG* or *mlaFEDCB* (*waaY* M*, *pbpG* M* or *mlaF* M*, respectively) were subjected to growth

experiments in the presence of 1.0 μg/ml doxycycline. Plasmid pJ203 was used to provide *marA* and experiments were also done with only basal levels of *marA*, which is likely low due to repression of *marRAB* by MarR (Alekshun and Levy, 1999). Growth experiments were done as previously described using the strains *E. coli* JCB387 Δ*thyA*, *waaY* M*, *pbpG* M* and *mlaF* M* (Figure 5.8). The calculated growth rate (doubling time) is shown in Appendix 9. In the absence and presence of doxycycline, there was no significant difference in growth between the control strain (green line) and the mutant strains (blue lines) (Figure 5.8). The results suggest that preventing MarA regulation of *waaY*, *pbpG* or *mlaFEDCB* independently has no impact on the multiple antibiotic resistance phenotype.

5.6.3. Mutating a single marbox causes no change in antibiotic susceptibility

To determine whether MarA regulation of *waaY*, *mlaFEDCB* and *pbpG* is important for resistance to different antibiotics, these mutants were also tested for sensitivity to various antibiotics (Table 5.2). *marA* was expressed on pJ203. There was found to be no significant difference in the susceptibility to kanamycin, tetracycline or doxycycline when a single marbox was mutated (*waaY* M*, *pbpG* M*, *mlaF* M*) compared to the control (Δ*thyA*). This data suggests that MarA regulation of the cell envelope genes *waaY*, *mlaFEDCB* or *pbpG* independently do not contribute highly to the multiple antibiotic resistance phenotype.

5.6.4. Mutating multiple marboxes simultaneously causes a significant change in growth rate in the presence of doxycycline

To further investigate the role of cell envelope genes *waaY*, *mlaFEDCB* and *pbpG* in MarA-associated antimicrobial resistance, growth experiments were carried out as previously with mutants containing point mutations in multiple marboxes (Figure 5.9). These mutants contained mutations in the marboxes upstream of *waaY* and *mlaF* (*waaY* M* *mlaF* M*), *pbpG*

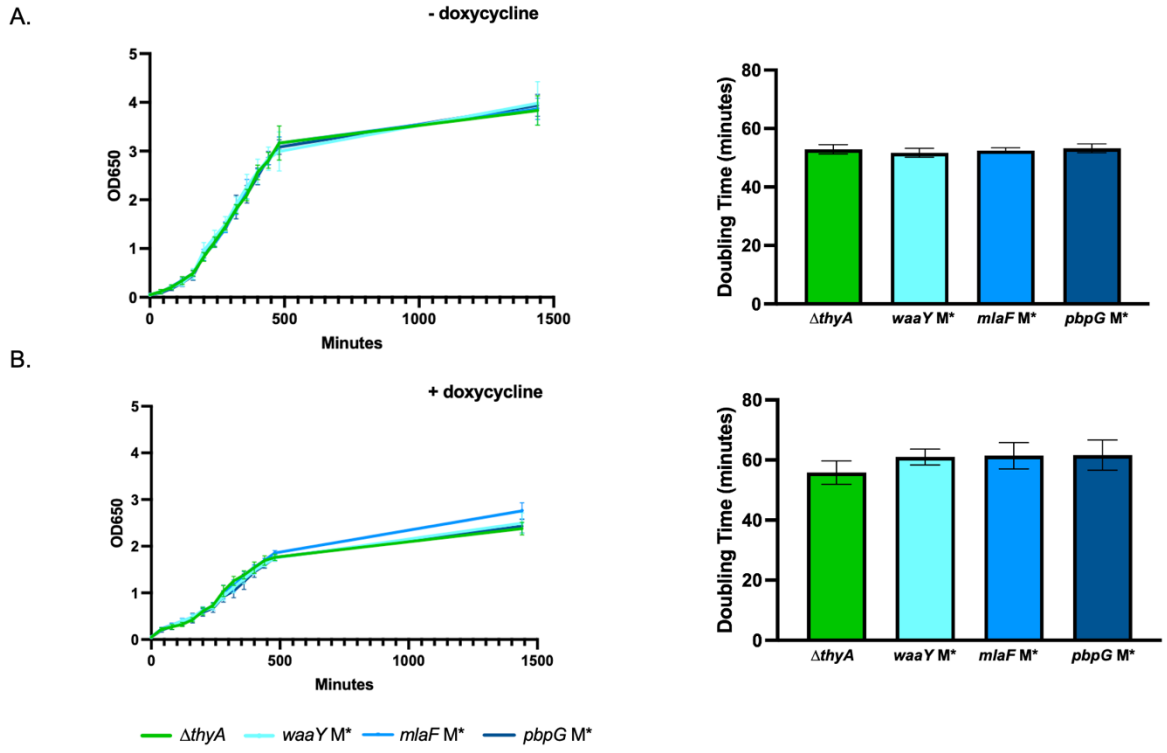

Figure 5.8. Growth of Δ*thyA* JCB387 and a range of Δ*thyA* JCB387 strains with marbox mutations in the *waaY*, *mlaF* and *pbpG* promoters in the presence of MarA and the absence and presence of 1.0 µg/ml doxycycline.

Growth was assessed using a standard growth curve in LB. Samples were taken every 40 minutes and OD_{650} was measured. Green lines represent Δ*thyA* JCB387 and blue lines represent strains with marbox mutations in a single marbox (*waaY*, *mlaF* and *pbpG*, respectively). In all cases, *marA* was overexpressed on plasmid pJ203, and empty pJ203 was used as a control (results not shown). Assays were done in triplicate and repeated on 3 separate days. The mean and standard deviation are shown on the graphs. A. Growth in absence of doxycycline. B. Growth in the presence of 1.0 µg/ml doxycycline. A two-way ANOVA followed by the two-stage linear step-up procedure of Benjamini, Krieger and Yekutieli showed that there was no significant difference in growth between Δ*thyA* JCB387 and the mutant strains (Appendix 10).

Table 5.2. Minimum inhibitory concentration of 3 antibiotics for Δ*thyA* JCB387 and derivatives with point mutations in the regulatory regions of *waaY*, *mlaF* and *pbpG*.

96-well MIC assays were done for *E. coli* strains Δ*thyA* JCB387 containing point mutations in the marboxes upstream of *waaY*, *mlaF* and *pbpG*. In all cases, *marA* was overexpressed on plasmid pJ203, and empty pJ203 was used as a control (results not shown). 3 antibiotics were chosen. MIC is shown as the minimum concentration of antibiotic required to inhibit growth of the strain. Numbers shown are range and modal value in brackets. Assays were done in triplicate and repeated on 3 separate days. Results were only accepted if they were in line with the control strains ATCC 25922 and NCTC 10418.

	Minimum inhibitory concentration (MIC) (µg/ml)		
Strain	**Doxycycline**	**Kanamycin**	**Tetracycline**
Δ*thyA* JCB	8 – 32	2 – 16	4 – 16
Δ*thyA* JCB *waaY* M*	8 – 16 (8)	8 – 16 (8)	8 – 16 (8)
Δ*thyA* JCB *mlaF* M*	8 – 16 (8)	8 – 16 (16)	4 – 8 (4)
Δ*thyA* JCB *pbpG* M*	16	16	8
Δ*thyA* JCB *pbpG* M* *mlaF* M*	1 – 2 (2)	2	2
Δ*thyA* JCB *waaY* M* *mlaF* M*	1 – 4	1 – 2 (1)	1 – 2 (2)
Δ*thyA* JCB *pbpG* M* *waaY* M* *mlaF* M*	8 – 16 (16)	8 – 64	4 – 16

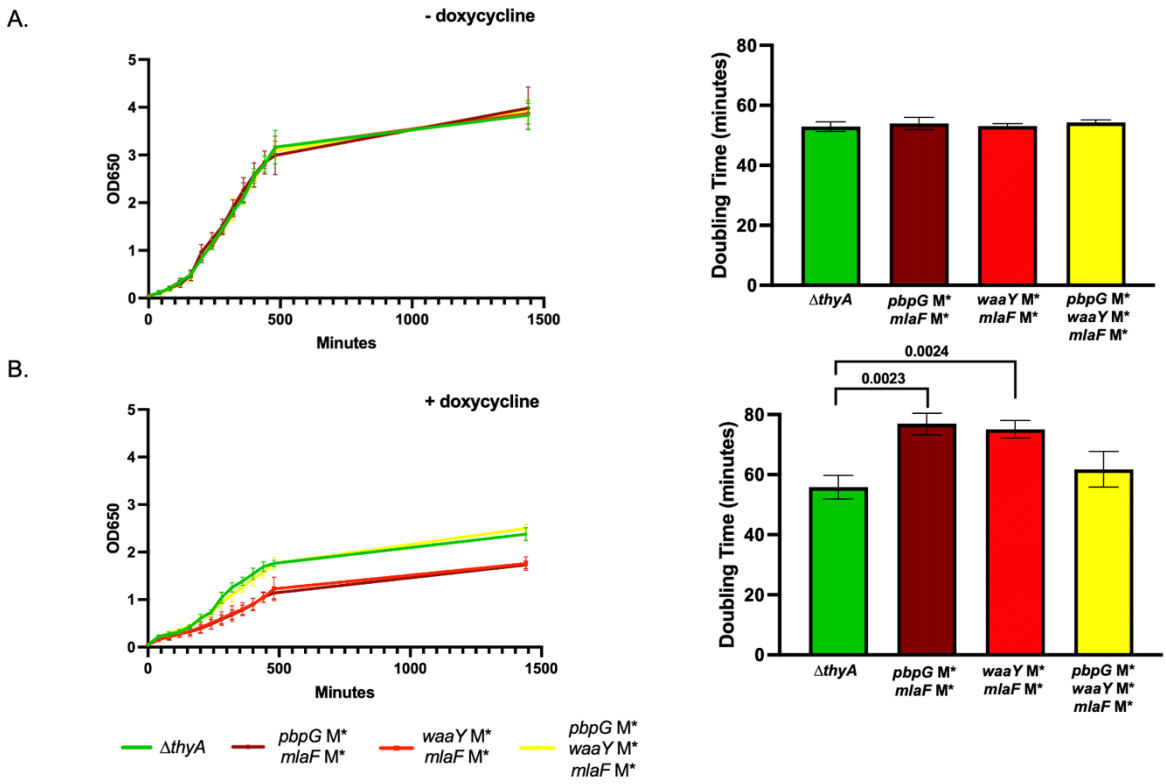

Figure 5.9. Growth of Δ*thyA* JCB387 and a range of Δ*thyA* JCB387 strains with marbox mutations in the *waaY*, *mlaF* and *pbpG* promoters in the presence of MarA and the absence and presence of 1.0 µg/ml doxycycline.

Growth was assessed using a standard growth curve in LB. Samples were taken every 40 minutes and OD650 was measured. Green lines represent Δ*thyA* JCB387, blue lines represent strains with marbox mutations in a single marbox (*waaY*, *mlaF* and *pbpG*, respectively), red lines represent strains with marbox mutations in two marboxes (*pbpG* and *mlaF* promoters, and *waaY* and *mlaF* promoters, respectively) and yellow lines represent a strain with marbox mutations in three marboxes (*pbpG*, *waaY* and *mlaF* promoters). In all cases, *marA* was overexpressed on plasmid pJ203, and empty pJ203 was used as a control (results not shown). Assays were done in triplicate and repeated on 3 separate days. The mean and standard deviation are shown on the graphs. A. Growth in absence of doxycycline. B. Growth in the presence of 1.0 µg/ml doxycycline. A two-way ANOVA followed by the two-stage linear step-up procedure of Benjamini, Krieger and Yekutieli showed that there was a significant difference in growth between Δ*thyA* JCB387 and both strains containing two marbox mutations (Appendix 10).

and *mlaF* (*pbpG* M* *mlaF* M*) or *waaY*, *mlaF* and *pbpG* (*pbpG* M* *waaY* M* *mlaF* M*). *marA* was overexpressed in these strains on pJ203. In the absence of doxycycline, there was no significant difference in growth between the control strain (green line) and the mutant strains (red lines and yellow line) (Figure 5.9, Panel A). In the presence of doxycycline, mutants containing 2 marbox mutations (*waaY* M* *mlaF* M* and *pbpG* M* *mlaF* M*, red lines) had significantly reduced growth compared with the control (Figure 5.9, Panel B). The doubling time of these strains was significantly higher than the control (Appendix 10). The growth rate of these strains was significantly reduced even when *marA* was not constitutively expressed, relying on basal levels of *marA* (Appendix 10). Conversely, growth of the mutant containing 3 marbox mutations (*pbpG* M* *waaY* M* *mlaF* M*) showed no significant difference compared to the control. The results suggest that targeting multiple cell envelope genes simultaneously can decrease the susceptibility to doxycycline, likely due to reduced diffusion of this antibiotic through the permeability barrier. The reason for no observed change in the growth rate of the mutant with mutations in 3 marbox remains unknown.

5.6.5. Mutating multiple marboxes simultaneously causes a significant change in antibiotic susceptibility

To determine whether targeting more than one cell envelope gene simultaneously causes changes in susceptibility to various antibiotics, susceptibility testing was carried out on mutants containing mutations in more than 1 marbox (Table 5.2). *marA* was expressed on pJ203. The MIC for doxycycline was decreased up to 16-fold for *pbpG* M* *mlaF* M* and up to 8-fold for *waaY* M* *mlaF* M* compared to the control (Δ*thyA*). The MICs for kanamycin and tetracycline were decreased up to 8-fold for both mutants containing mutations in 2 marboxes compared to the control. The MICs for doxycycline, kanamycin and tetracycline in the mutant containing mutations in 3 marboxes were demonstrated to show no difference compared to the control.

5.7. Discussion

The aim of this chapter was to understand synergy between different MarA targets. The data show that deleting *mlaFEDCB* caused no change in growth with sub-lethal concentrations of doxycycline (Figure 5.3). Additionally, deleting and/or overexpressing *pbpG* caused significant but small changes in growth with the same doxycycline concentration (Figure 5.5). When the defects were combined, growth rate was significantly reduced even in the absence of doxycycline, although it did eventually reach a final OD_{650} similar to the wildtype (Figure 5.6). This is logical as remodelling of the cell envelope is vital for cells to divide (Holtje, 1998). In the presence of sub-lethal doxycycline concentrations, growth was further reduced and remained low even at the end of the time course, showing that growth with doxycycline was negligible. Cell permeability was analysed using crystal violet uptake assays. Constitutive expression of *pbpG* or deletion of *mlaE* caused small but significant increases in permeability (Figure 5.7). When combined, *pbpG* expression and *mlaE* deletion caused a much larger permeability increase. This suggests these cell envelope defects allow doxycycline to easily enter the cell and lead to cell death. Hence, MarA regulation of these genes directly targets cell permeability.

Hydrophobic crystal violet dye poorly penetrates the outer membrane (Gustafsson, Nordstöm, and Normark, 1973; Vaara and Vaara, 1981). Interestingly, crystal violet is effectively able to penetrate cells with impaired membranes; thus, it can be used to detect altered membrane permeability (Halder *et al*., 2015). However, it should be noted that there are limitations of this technique. Firstly, crystal violet that enters the cells through permeable membranes does not necessarily remain in the cell during the assay. It could be removed using efflux pumps, thereby skewing the results of dye uptake. Additionally, it is possible that the crystal violet stain could bind to the cell envelope: crystal violet is positively charged and therefore binds to negatively

charged molecules, such as the biofilm matrix. Despite the limitations, previous studies have demonstrated that results of the crystal violet uptake assay have been consistent with other membrane permeability assays, including measurement of the fluorescent probe 1-*N*-phenylnaphthylamine (Halder *et al*., 2015; Sharma *et al*., 2017).

Considering that *mlaFEDCB* is involved in lipid trafficking we investigated whether the lipids of the OM were different in strains lacking the operon. Deleting *mlaFEDCB* caused no changes in the lipid composition of total fraction and OM fractions (Figure 5.4). Major phospholipids PG and PE were found in both strains (wildtype BW25113 and Δ*mlaF*). The third common phospholipid of *E. coli*, cardiolipin, was not detected in the membrane samples. The reason for the absence of this lipid is unknown but suggested to be due to it only accounting for 5 % of total membrane lipids. There was no difference in the relative quantity of PG and PE between wildtype and Δ*mlaF* in total and OM fractions. It should be noted that relative quantification suggested more PG was present than PE, which disagrees with the expected 4:1 ratio of PE:PG (Raetz and Dowhan, 1990). Additionally, the standard deviation is large. Hence, we must emphasise that this should not be taken as exact measurements of phospholipid concentration and is only a comparison of peak area between strains. It is likely that lipid transport by MlaFEDCB, and resulting changes in cell permeability, is not caused by movement of specific phospholipids.

Chapters 3 and 4 demonstrated that MarA regulates *lpxC*, *lpxL*, *waaY* and *pbpG*. In this chapter, we aimed to uncouple regulation of these genes to determine the importance of these genes in the multiple antibiotic resistance phenotype. The marboxes of the regulatory regions of these genes, confirmed in Chapters 3 and 4, and that of the *mlaFEDCB* operon, were targeted by point mutations to prevent MarA binding. This was successful for *waaY*, *pbpG* and

mlaFEDCB. Antibiotic susceptibility testing and growth kinetics were used to measure antibiotic susceptibility of the strains. Significant changes in antibiotic susceptibility and growth rate with 1.0 µg/ml doxycycline were only demonstrated when multiple marboxes were mutated simultaneously (Table 5.2, Figure 5.8). Hence, changes in cell permeability are synergistic and targeting multiple genes simultaneously results in large changes in barrier function. Interestingly, changes in antibiotic susceptibility were noted for strains with mutations in 2 marboxes (*waaY* M* *mlaF* M* and *pbpG* M* *mlaF* M*) but not for the strain with mutations in 3 marboxes (*pbpG* M* *waaY* M* *mlaF* M*). A strain with mutations in 2 marboxes upstream of *waaY* and *pbpG* was not tested. Perhaps this combination of mutations prevents a change in antibiotic susceptibility, accounting for the unusual result observed with *pbpG* M* *waaY* M* *mlaF* M*, but this seems unlikely. The reason for this atypical result remains unknown.

The synergy between LPS biosynthesis and peptidoglycan biogenesis must be regulated. However, how this occurs would require further research. Interestingly, recent work has demonstrated a direct interaction between committed enzymes for the peptidoglycan and LPS synthetic pathways in *P. aeruginosa* (Hummels *et al*., 2023). The peptidoglycan biosynthesis enzyme MurA interacts specifically with LpxC. This suggests a high level of coordination between bacterial cell wall and outer membrane biosynthesis. This interaction was not noted in *E. coli* but it is likely there is coordination of the biosynthetic processes in Enterobacteriaceae. This could explain how regulation of genes of this pathway results in a synergistic change in cell permeability.

In summary, this chapter has shown that changes in the cell envelope due to MarA regulation is a synergistic effect. Changes in *mlaFEDCB* and *pbpG* expression cause small changes in

antibiotic susceptibility unless defects are combined. Additionally, combinatorial effects are also demonstrated when MarA is prevented from binding to the marboxes of upstream of *mlaFEDCB*, *pbpG* and *waaY*. It is hypothesised that MarA targets these promoters to allow increased survival with antibiotics by targeting both the OM and peptidoglycan layers simultaneously. The resulting decrease in permeability is due to simultaneous changes in LPS biosynthesis, increased lipid trafficking, and stiffening of the peptidoglycan layer.

Chapter 6 – Final Conclusions

Gene regulation is tightly controlled in response to external signals, allowing bacteria to adapt to growth in a range of conditions. Transcriptional initiation is a common regulatory target (Browning and Busby, 2016). Transcriptional regulators bind specific sequences upstream of genes to regulate their expression. Antimicrobial agents can induce expression of transcription factors that, in turn, improve fitness of bacterial under antibiotic threat (Tavio *et al*., 2010).

Here, we have investigated the role of MarA, the activator of multiple antibiotic resistance, in regulating key cell envelope genes. The MarA regulon remains a topic of interest and further work to elucidate the MarA regulon continues. A ChIP-seq experiment identified a putative marbox in the regulatory region upstream of *lpxC*, an essential gene involved in lipid A biosynthesis (Seo *et al*., 2015). We demonstrated that MarA functions by binding to a marbox upstream of *lpxC*, activating transcription from P2*lpxC* in a σ^{70}-dependent manner. Interestingly, *in vitro* MarA was found to repress P1*lpxC*. Further work found that P1*lpxC* is weak and that it makes a minimal contribution to overall transcription of *lpxC*.

We further hypothesised that MarA could target other genes involved in cell envelope biogenesis. The DNA-binding motif obtained from previous ChIP-seq experiments (GCANNNNNNGCNAAA) was used to identify novel putative marboxes in the *E. coli* genome (Sharma *et al*., 2017). 15 potential targets, involved in OM biosynthesis, peptidoglycan biosynthesis and capsule biosynthesis were flagged. MarA bound 3 of these targets: *waaY*, *lpxL* and *pbpG*. *waaY*, involved in LPS core biosynthesis, and *lpxL*, involved in lipid A biosynthesis, are activated by MarA. Activation of *lpxC*, *lpxL* and *waaY* suggests that MarA causes upregulation of LPS biosynthesis. LPS is found on the OM as an external barrier against antibiotic attack (Silhavy, Kahne and Walker, 2010). It is suggested that MarA improves the barrier function of the OM to reduce uptake of antimicrobial agents, contributing towards the

multiple antibiotic resistance phenotype. Interestingly, MarA was demonstrated to repress *pbpG* expression from P*pbpG in vitro* and *in vivo*. PbpG is an endopeptidase involved in the cleavage of cross-links within peptidoglycan (Henderson *et al*., 1995). We hypothesise that downregulation of *pbpG* results in a reduction of cross-link cleavage leading to stiffening or thickening of the cell wall. Peptidoglycan acts as an additional barrier; thus, MarA can decrease cell permeability by targeting the OM and cell wall.

SoxS and Rob are transcription factors that are highly connected to MarA (Li and Demple, 1994; Kwon *et al*., 2000). These transcription factors respond to distinct stimuli but have overlapping regulons. In clinical isolates, MarA, SoxS and Rob are increasingly implicated in multidrug resistance (Pérez *et al*., 2012; Majewski *et al*., 2020; Goodarzi *et al*., 2021; Albarri *et al*., 2022). The genes found to be regulated by MarA throughout this work (*lpxC*, *lpxL*, *waaY* and *pbpG*) were also demonstrated to be regulated by SoxS and Rob.

Finally, this work examined the importance of MarA regulation of cell envelope genes in antibiotic susceptibility. Previous work found that MarA activates the *mlaFEDCB* operon, encoding a lipid trafficking system, to improve the cell barrier (Sharma *et al*., 2017). Thus, we decided to include the marbox upstream of *mlaFEDCB* in further studies. This work demonstrated that mutating marboxes to uncouple MarA regulation from *waaY*, *mlaFEDCB* and *pbpG* causes a change in antibiotic susceptibility when more than one is targeted simultaneously. Additionally, a significant reduction in growth was demonstrated when *mlaFEDCB* was deleted and *pbpG* was overexpressed in both the absence and presence of a sub-lethal dose of doxycycline.

This work demonstrates the role of MarA in regulating genes associated with cell envelope biology. MarA targets OM biosynthesis by upregulating genes involved in LPS biosynthesis (*lpxC*, *lpxL* and *waaY*) whilst also activating the *mlaFEDCB* operon, resulting in increased lipid trafficking. Simultaneously, MarA targets cell wall biogenesis by repressing *pbpG*. This likely downregulates peptidoglycan hydrolysis and causes stiffening of the peptidoglycan barrier. Regulation of cell envelope genes acts synergistically to decrease permeability by improving barrier function of the OM and cell wall, illustrated in Figure 6.1.

Future work could aim to understand the synergy of cell envelope biosynthesis. This work clearly demonstrates a link between the regulation of genes involved in OM and peptidoglycan biosynthesis, which we have defined as a synergistic effect. However, how this synergy works remains poorly understood. The extent to which MarA regulation of the cell envelope genes investigated here is involved in clinical tolerance and resistance should be further examined. Additionally, further work in this area could aim to understand the exact differences in LPS and peptidoglycan structure due to MarA regulation of *lpxC*, *lpxL*, *waaY* and *pbpG*. Furthermore, it is likely that there are additional cell envelope genes regulated by MarA. The bioinformatic approach could be repeated to locate marboxes with more than one mismatch. Considering that Rob binds less stringent sequences, and is increasingly implicated in multidrug resistance, this could find novel binding sites (Taliaferro *et al.,* 2012). Finding novel MarA targets in cell envelope genes will lead to further understanding of how the cell envelope contributes to multidrug resistance.

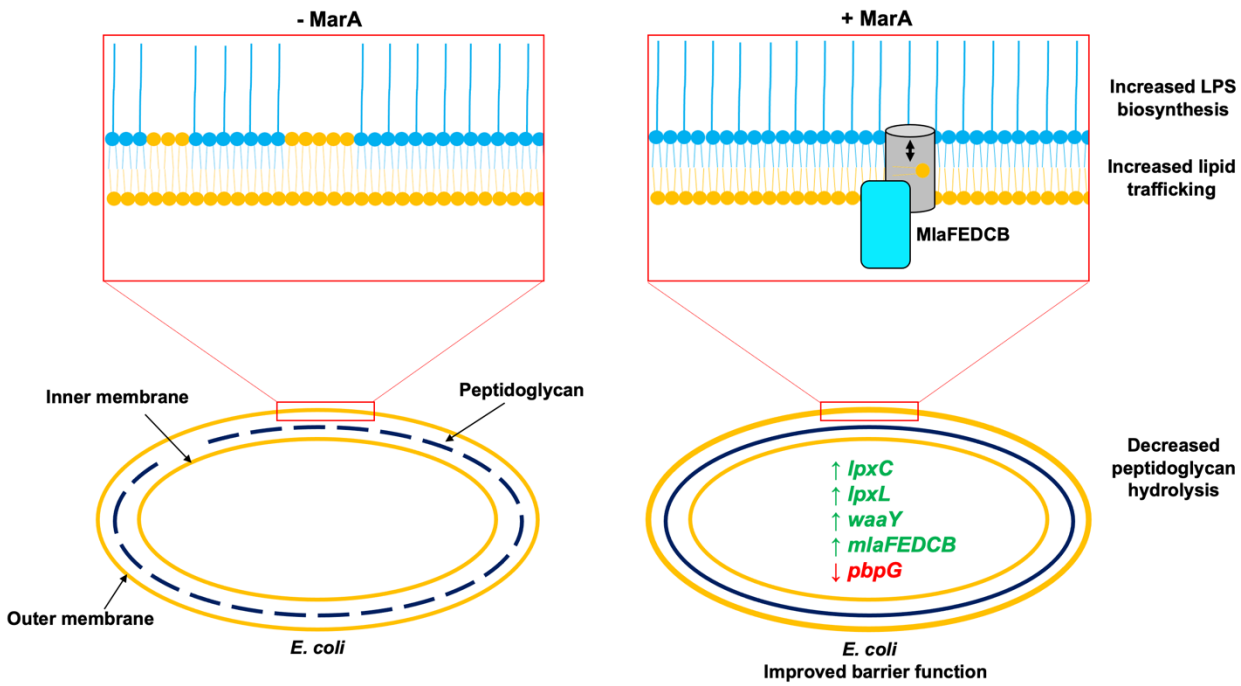

Figure 6.1. MarA improves barrier function of the cell envelope.

MarA activates *lpxC*, *lpxL* and *waaY* to upregulate LPS biosynthesis. MarA activates *mlaFEDCB* to increase lipid trafficking between leaflets of the OM. Repression of *pbpG* by MarA is hypothesised to downregulate peptidoglycan hydrolysis and result in stiffening or thickening of the peptidoglycan layer. Synergistic regulation of these genes contributes to the *mar* phenotype by improving barrier function.

Appendices

Appendix 1. MarA targets identified by a bioinformatic marbox search.

The *E. coli* genome was searched for marboxes with up to 1 mismatch to the sequence GCANNNNNNGCNAAA using Colibri. Results were filtered to include only sites up to 200 bp upstream of a start codon. Gene name and function are shown alongside strand information and location and sequence of the putative MarA binding sequence.

Gene	Gene function	Strand	bp from start codon of gene	Putative marbox sequence
dnaJ	Chaperone with DnaK; DNA chain elongation; stress-related DNA biosynthesis, responsive to heat shock	+	-154	gcaaacaacgcgaaa
caiE	Stimulates carnitine racemase activity of CaiD and CaiB activity	-	-157	gcaccaccagcgaaa
yadB	Function unknown	-	-119	gcatcgactgcaaaa
map	Methionine aminopeptidase	-	-107	gcacgtttggcgaaa
yafC	Function unknown	-	-15	gcaacaggagcaaaa
ybcI	Function unknown	-	-178	gcaaacgctgcaaaa
ybdK	Function unknown	-	-135	gcaaaagtagccaaa
ybeT	Function unknown	-	-142	gcagaaagcgcaaaa
ybgO	Function unknown	-	-14	gcagtggaggcgaaa
ybhE	Function unknown	+	-66	gcattcaccgccaaa
ybjC	Function unknown	+	-84	gcattaattgctaaa
artJ	Periplasmic binding protein of Arg transport system	-	-46	gcagacacggccaaa
serS	Serine hydroxamate resistance; seryl-tRNA synthetase	-	-161	gcaagattggcgaaa
solA	Homology with sarcosine oxidases, but stronger activity with methyltryptophan than with sarcosine	-	-174	gcaggaatcgccaaa

yceP	Function unknown	-	-194	gcaggaatcgccaaa
ycgZ	Function unknown	+	-106	gcaggaatcgccaaa
yciS	Function unknown	+	-87	gcaggaatcgccaaa
marC	Multiple antibiotic resistance protein	-	-88	gcaggaatcgccaaa
ydhD	Function unknown	-	-192	gcaggaatcgccaaa
ynhG	Function unknown	-	-181	gcaggaatcgccaaa
ruvB	Branch migration of Holliday structures; lexA regulon	-	-85	gcaggaatcgccaaa
cpsG	Phosphomannomutase isozyme; colanic acid biosynthesis synthesis	-	-92	gcaggaatcgccaaa
folX	Dihydroneopterin triphosphate epimerase	+	-105	gcaggaatcgccaaa
accD	Acetyl-CoA carboxylase beta-carboxyltransferase subunit	-	-173	gcaggaatcgccaaa
dedA	Temporary designation for genes in pdxB and folC operons; unknown function	-	-187	gcaggaatcgccaaa
guaB	IMP dehydrogenase	-	-92	gcaggaatcgccaaa
rpsP	30S ribosomal subunit protein S16	-	-101	gcaggaatcgccaaa
yqaE	Function unknown	-	-80	gcaggaatcgccaaa
ygbD	Function unknown	+	-14	gcaggaatcgccaaa
mutS	Methyl-directed mismatch repair	+	-165	gcaggaatcgccaaa
ygdQ	Function unknown	+	-200	gcaggaatcgccaaa
pgk	Phosphoglycerate kinase	-	-32	gcaggaatcgccaaa
hybF	Regulatory gene	-	-15	gcaggaatcgccaaa
yheO	Function unknown	-	-187	gcaggaatcgccaaa
arsB	Resistance to arsenate, arsenite, and antimonite	+	-173	gcaggaatcgccaaa

xylB	Xylulokinase	-	-179	gcaggaatcgccaaa
rpoZ	RNA polymerase, omega subunit	+	-113	gcaggaatcgccaaa
yigC	Function unknown	+	-139	gcaggaatcgccaaa
sgaE	Putative sugar isomerase	+	-71	gcaggaatcgccaaa
yjiD	Function unknown	+	-32	gcaggaatcgccaaa
thrL	Regulatory leader petide for thrABC operon	+	-37	gcacagacagataaa
thrA	Aspartokinase I-homoserine dehydrogenase I	+	-184	gcacagacagataaa
thrC	Threonine synthase	+	-79	gaactacctgcaaa
yaaA	Function unknown	-	-45	tcatttttgctaaa
lytB	Penicillin tolerance and stringent response effects	-	-120	gcgtgatccgcgaaa
carA	Carbamoylphosphate synthase (glutamine-hydrolysing) light subunit	+	-175	gcactggaggcgtaa
thiP	Homolog to Salmonella thiamine and thiamine pyrophosphate ABC transporter	-	-192	gcatgagccacaaaa
leuB	Beta-Isopropylmalate dehydrogenase	-	-62	gcagaagtcgaaaaa
leuL	leu operon leader peptide	-	-127	gcacaattagctaaa
fruR	Regulatory gene for fru operon, other catabolite-regulated genes	+	-135	gctttttttgcgaaa
murE	D-alanyl:D-alanine adding enzyme	+	-182	gccggacatgccaaa
ftsA	Cell division, septation	+	-135	gcagcaggcgcaaac
mutT	AT to GC transversions	+	-161	gcactggcggcgcaa
yacC	Function unknown	-	-145	gcaggcgaaacaaaa
yadE	Function unknown	+	-121	gcaccaacaacaaaa

htrE	Sequence homology with pilin protein PapC	-	-109	gcgaattctgcaaaa
yadR	Function unknown	+	-127	gcaactggcgcgaag
yadT	Function unknown	-	-58	gctgttgccgctaaa
yaeH	Function unknown	-	-59	gcgggccaggccaaa
ldcC	Lysine decarboxylase	+	-104	gcgtaattcgcaaaa
yaeJ	Function unknown	+	-134	gaacaactggcgaaa
cutE	Copper sensitivity	+	-79	gcatcgaaagcacaa
yafB	Function unknown	+	-103	gccagaatcgcaaaa
yafD	Function unknown	+	-148	ccataatgagcaaaa
dnaO	DNA polymerase III epsilon-subunit; streptomycin, azaserine resistant; 3' to 5' proofreading, lexA regulon	+	-181	gtagccagcgctaaa
aspY	Aspartate tRNA1 triplicated gene	+	-86	gcaaacgattcaaaa
yafE	Function unknown	+	-128	gcaaaagaagccaga
lpcA	Phosphoheptose isomerase, T-phage resistance	+	-110	gcacttcaggtcaaa
dinP	Enhances mutatgenesis	+	-125	gccgctggtgcaaaa
ykgG	Function unknown	+	-129	tcaatggcggcaaaa
hetA	Choline dehydrogenase	-	-108	gcattggtcgcgaga
yahE	Function unknown	+	-109	gcaactcaggcaata
yahK	Function unknown	+	-43	tcaggcgttgccaaa
aroL	Shikimate kinase II	+	-196	tagtcgtggctaaa
brnO	Mutants are valine and o-methylthreonine resistant, glycylvaline sensitive; transport system I for Ile, Leu, and Val	+	-101	gtatttcccgctaaa

queA	S-Adenosylmethionine:tRNA ribosyltransferase- isomerase	+	-130	gcgagatgggctaaa
yajD	Function unknown	+	-177	gcagaaagtggaaaa
yhaD	Function unknown	+	-109	gtaaaagcagcgaaa
thiI	Thiamin biosynthesis; also 4-thiouridine generation in tRNAs	+	-145	gcaaataacgcgcaa
cyoC	Cytochrome o oxidase subunit III	-	-61	gcagaaatcgaaaaa
amtB	Putative ammonia transporter	+	-16	gcaacaggaacgaaa
ffs	4.5S rRNA; mammalian counterpart, SRP, includes 4.5S RNA; cotranslational integration of proteins into membrane	+	-105	gcataatctggaaaa
ylaC	Function unknown	-	-190	gcagttgtcacaaaa
dnaX	Subunit of DNA polymerase III holoenzyme; DNA elongation factor III; tau and gamma subunits	+	-169	gcattaccagctaca
adk	Adenylate kinase; pleiotropic effects on glycerol-3-phosphate acyltransferase activity	+	-129	gcactttccgcaaat
yhaO	Function unknown	+	-180	gcagcgcggcccaaa
yhaT	Function unknown	+	-47	gcatcggtcgctaag
ybbL	Function unknown	+	-121	ccataatcagcaaaa
ylbH	Function unknown	+	-155	gcagaagaagaaaaa
ybbO	Function unknown	+	-32	tcaggaaaagcgaaa
ylhA	Function unknown	-	-176	gcacgacgcgcaaat
ybbF	Function unknown	-	-57	ccaggacgtgccaaa
ppiB	Rotamase; peptidylprolyl-cis-trans-isomerase B	-	-15	gaacaggatgcaaaa
ybcJ	Function unknown	-	-130	gaagacgcggctaaa

sfmD	Salmonella fimbriae gene homolog	+	-106	gcagggaaagctgaa
argU	Arginine tRNA4	+	-130	gccgctatagcgaaa
argU	Arginine tRNA4	+	-78	gcaaccagatcaaaa
ybcL	Function unknown	+	-60	gcataatgagataaa
ybcM	Function unknown	+	-180	gcatgtcctcctaaa
Rus	Resolvase; resolves Holliday structures	+	-80	gctggatatgcaaaa
ylcG	Function unknown	+	-187	gcattgagtgccaca
ylcG	Function unknown	+	-147	ggataatctgcaaaa
rzoD	Homolog to lambda Rz1 lipoprotein in prophage DLP12	+	-34	gcgctcgatgcaaaa
ybcW	Function unknown	+	-15	gcatggagcgacaaa
tfaD	Phage lambda tail fiber gene homolog in prophage DLP12	+	-22	gcataagcagcgcaa
pheP	Phenylalanine-specific permease	+	-53	gcactaaatgttaaa
fepA	Outer membrane component of ferribactin transport system	-	-32	gcaattcgtggcaaa
fes	Enterochelin esterase	+	-119	gcaatcaatgaaaaa
ybdA	Function unknown	+	-53	gcatgtgcagcctaa
fepP	Ferrienterobactin permease, membrane-bound subunit	-	-179	gaatactgcgcgaaa
ahpC	Alkyl hydroperoxide reductase small subunit	+	-58	gccgaatcggcaaaa
citD	Putative citrate lyase acyl carrier protein	-	-84	gcattatttgcagaa
citC	Putative acetate:SH-citrate lyase ligase	-	-141	ggatgtatagcgaaa
dcuC	C4-dicarboxylate carrier, anaerobic; W3110 has an IS5 insertion	-	-90	gcattcatcgccaat

dacA	D-alanine carboxypeptidase IA; penicillin-binding protein; deletion suppresses ftsK mutant block	-	-193	gcaacgtttgcaaac
glnU	Glutamine tRNA1	-	-108	gcgggagtggcgaaa
nagD	Function unknown, expressed as part of nag operon	-	-66	gcatttgctggaaaa
kdpD	Sensor kinase for K+-kdp system	-	-142	cacgcgtggcgaaa
sucD	Succinyl-CoA synthetase alpha-subunit	+	-17	gcagtggaggggaaa
nadA	Quinolinate synthetase, A protein	+	-138	gcacattaggcgtaa
moaB	MPT synthesis; chlorate resistance protein B	+	-35	acattggcggctaaa
ybhQ	Function unknown	+	-169	gcaccttgaacgaaa
ybhP	Function unknown	-	-17	gcaaagacaggaaaa
ybhS	Function unknown	-	-88	gcacagtcggctaac
ybiJ	Function unknown	-	-153	gccgctacggcgaaa
ybiF	Function unknown	-	-110	gcattttagtcaaaa
ybiK	Function unknown	+	-36	gcaaaagtggcgaac
yliH	Function unknown	+	-66	gcattttgctcaaaa
dacC	Penicillin-binding protein 6	+	-175	gcaacagctggcaaa
ybjH	Function unknown	-	-43	gcataattcgcggaa
ybjH	Function unknown	-	-77	gcacgcccggcaaca
ybjI	Function unknown	-	-65	gctattgtcgcgaaa
ybjK	Function unknown	+	-162	acaggcctggcaaaa
ybjM	Function unknown	+	-84	gcatggaatgcgaag
ybjL	Function unknown	-	-196	gcattccatgctaat

ybjM	Function unknown	+	-50	gccacactggcgaaa
grxA	Glutaredoxin 1	-	-86	gcaattaatgcaaca
ybjS	Function unknown	-	-61	gcatcatgggggaaa
cydD	ATP-binding cassette membrane transporter; bd-type oxidase	-	-170	gcacttgatgcggaa
ftsK	Cell division and growth, septation; NA-binding membrane protein; homology with B. subtilis SpoIIIE protein; filamentous growth mutants, suppressed by dacA deletion;	+	-131	ggaacaggtgcaaaa
ycaJ	Function unknown	+	-98	gaaatcccagcaaaa
ycaR	Function unknown	+	-83	gcaccggctgggaaa
ycbC	Function unknown	-	-164	gcaatatcatcaaaa
mukE	Involved in chromosome partioning, null mutants die above 30C and produce some anucleate cells at permissive temperatures	+	-82	gactgccagcgaaa
ycbL	Function unknown	+	-130	gcaatattcgcaaag
aspC	Aspartate aminotransferase	-	-111	tcacgtcttgcaaaa
ycbO	Function unknown	-	-116	ccagttcacgccaaa
ycbS	Function unknown	+	-111	ccaaaggggccaaa
ycbV	Function unknown	+	-170	gcaaagtcagcaaga
ymbA	Function unknown	+	-108	gcaaccggtgctgaa
fabA	Beta-hydroxydecanoylthioester dehydrase	-	-144	gcaagcatcgcaaca
mgsA	Methylglyoxal synthase	-	-126	gcagtgggcggaaaa
yccW	Function unknown	-	-65	ccaaagggcgcgaaa
hyaD	Processing of HyaA and HyaB	+	-34	acaaatttggcaaaa

torT	TorRT system	+	-75	gcactttaggtgaaa
ycdB	Function unknown	+	-191	gaactgctggcaaaa
phoB	Member of pho regulon, P starvation induced	+	-83	gcaataaatgcgaga
ycdY	Function unknown	+	-53	gcaccgattgcggaa
csgB	Curlin nucleator protein, homology with major curlin, CsgA	+	-87	gcagcgttaacaaaa
mdoG	Periplasmic oligosaccharide synthesis	+	-168	gcacggaaagtgaaa
mdoH	Membrane glycosyltransferase	+	-150	gcacggtgcgctata
yceA	Function unknown	+	-146	gaagactgggcgaaa
yceA	Function unknown	+	-95	gcaaatgtagcgtaa
pyrC	Dihydro-orotase	-	-180	gaagcaatggcgaaa
pyrC	Dihydro-orotase	-	-191	gcagccagggcgaag
grxB	Glutaredoxin 2	-	-27	gaactgacagccaaa
yceH	Function unknown	+	-106	gaaggctatgcgaaa
flgM	Anti-sigma F factor (FliA); regulator of FlhD	-	-39	gcaacacatgataaa
flgA	Flagellar synthesis; flagellar regulon member	-	-90	ggaataaacgcaaaa
flgH	Flagellar synthesis, basal body L-ring protein	+	-83	tcagatgctgcaaaa
flgJ	Flagellar synthesis; flagellar regulon member	+	-51	gcaatcaatgcaaag
flgK	Flagellar synthesis; flagellar regulon member; hook-associated protein I	+	-112	acaaggtgagcaaaa
yceD	Function unknown	+	-88	gcaatgtgtgcgaat
yceD	Function unknown	+	-77	gaattattggcaaaa

tmk	Deoxythymidine kinase	+	-127	gcgcatccggcaaaa
holB	DNA polymerase III, delta'-subunit	+	-107	gcagcacaagataaa
ycfJ	Function unknown	+	-37	gcatgattggcataa
ycfD	Function unknown	-	-100	gcattctgcgccgaa
phoQ	In Salmonella two-component regulatory system with phoP	-	-184	gcaataatggcaaag
ymgD	Function unknown	-	-33	gcaattctgggtaaa
ymgD	Function unknown	-	-177	gcagtaacagaaaaa
ycgI	Function unknown; pseudogene	+	-71	gcactgcgtgtaaaa
dadA	D-amino acid dehydrogenase subunit	+	-157	gcaggagatactaaa
ycgC	Function unknown	-	-28	gcgttagccgcaaaa
ychB	Function unknown	-	-136	gccagaatggcaaaa
hemA	Neomycin sensitivity; hemin biosynthesis; glutamyl tRNA dehydrogenase	+	-101	gcaattactccaaaa
ychO	Function unknown	+	-55	gcaaaaagcggcaaa
rssA	Two-component response regulator, affecting sigma S-dependent proteins	+	-124	gcaacataggctata
ychJ	Function unknown	-	-87	gcaatcgtagccaca
galU	Glucose-1-P uridylyltransferase (UDP-glucose pyrophosphorylase)	+	-176	gcattacctgctaat
hns	DNA-binding protein, histone-like; diverse mutant phenotypes affecting transcription, transposition, inversion, cryptic-gene expression; involved in chromosome organization	-	-199	tcacgtgctgcgaaa
ychG	Function unknown	-	-168	gctgctccggctaaa
ychE	Function unknown	+	-150	gcatgttttgcacaa

oppB	Oligopeptide transport	+	-92	gcactaatggcaata
yciU	Function unknown	-	-190	gcaatcgacgataaa
kch	Homology to potassium channel proteins	-	-169	gcatattcaggaaaa
yciK	Function unknown	-	-65	gcataaagccccaaa
ribA	Riboflavin biosynthesis; GTP-cyclohydrolase II	-	-43	gcaaaataagccaat
ycjJ	Function unknown	-	-74	gcttcccttgctaaa
ycjL	Function unknown	+	-41	gcagtaatggcgata
ordL	Putative oxidoreductase	+	-81	gcaacggtcgcgaca
pspF	Transcriptional sigma 54-dependent activator of psp	-	-189	gcaaagcgagaaaaa
pspC	Positive regulatory gene, cooperatively with PspB	+	-86	gctgatgaagcaaaa
pspE	Expressed in response to stress as part of psp operon, but also transcribed independently	+	-64	gcaaaaattgttaaa
ycjO	Function unknown	+	-176	gcagtaggggataaa
ycjQ	Function unknown	+	-44	gcgtgaagggctaaa
yciX	Function unknown	+	-190	gcaaccctggcaata
ydaF	Function unknown	-	-43	gcagaagtcgctata
rzpR	Defective homolog to lambda Rz gene in prophage Rac	+	-46	gcataccgggcgata
rzoR	Homolog to lambda Rz1 lipoprotein in prophage Rac	+	-34	gcgctcgatgcaaaa
lomR	Defective lom gene in Rac prophage, interrupted by IS5Y	+	-128	ggaatgtcggcaaaa
pad	Phenylacetic acid degradation	+	-106	gcactggcggtaaaa
paaH	Phenylacetic acid degradation	+	-43	gcgttcctggctaaa

ydcP	Function unknown	+	-48	gcgcttgtggctaaa
yncJ	Function unknown	-	-123	gaatgcaatgcaaaa
ydcR	Function unknown	+	-157	gcatcatgcgacaaa
yncB	Function unknown	+	-182	gctttgcgggcaaaa
ydcD	Function unknown	+	-91	gcatgtattgaaaaa
narY	Cryptic NR II, beta-subunit	-	-17	gtacaggaggcgaaa
narZ	Cryptic NR II, alpha-subunit	-	-101	ggaagttcagccaaa
yddG	Function unknown	-	-59	gcatgacacgacaaa
yddG	Function unknown	-	-80	gcaagagagacaaaa
yneA	Function unknown	+	-69	gcatcgccagcaaat
yneE	Function unknown	-	-108	gcagcgcctgctaat
marC	Multiple antibiotic resistance protein	-	-129	ccacgttttgctaaa
marR	Repressor of mar operon	+	-66	gcaactaatgtgaaa
dcp	Dipeptidyl carboxypeptidase II	-	-98	gcacgggatgcttaa
dgsA	Affects function of phosphotransferase system enzyme IIA/IIB, anaerobic growth on glucosamine; binds NagC promoters; regulates manX; makes large colonies	-	-132	gaaatttcagcgaaa
ynfL	Function unknown	-	-104	gaaatccttgctaaa
ydgF	Function unknown	-	-131	gcagcactggcgcaa
ydgG	Function unknown	+	-27	gcaaaggaagaaaaa
fumC	Fumarase C, aerobic; member of soxRS regulon	-	-108	gcacgaaagaccaaa
Gst	Glutathione S-transferase	+	-120	gcagccgtagcgtaa

slyA	Transcriptional regulator that activates crytpic hemolysin gene hlyE	-	-51	gcacactattctaaa
slyA	Transcriptional regulator that activates crytpic hemolysin gene hlyE	-	-121	gcaatttctgaaaaa
ydhF	Function unknown	-	-110	gcaaattacgcgcaa
purr	Purine repressor	+	-180	tcaagatcggccaaa
ribC	Riboflavin synthase alpha-chain	-	-167	gaatgggcagcaaaa
ydhS	Function unknown	+	-194	gaagttgtcgccaaa
ydhY	Function unknown	-	-18	gaagaggatgcgaaa
ydiI	Function unknown	-	-182	ggacatgaagcgaaa
aroD	3-Dehydroquinate dehydratase	+	-172	gcagcaggcgcaaca
aroD	3-Dehydroquinate dehydratase	+	-16	gcagaaagggtaaaa
ydiF	Function unknown	+	-197	gcaaatctcggtaaa
nlpC	Lipoprotein	-	-168	gctcacgccgccaaa
ihfA	Integration Host Factor (IHF), alpha subunit; host infection, mutant phage lambda; site-specific recombination; sequence-specific DNA-binding transcriptional activator	-	-67	gctaccgtcgccaaa
pheM	pheST operon regulatory leader peptide	-	-137	gcagctctggcataa
pheM	pheST operon regulatory leader peptide	-	-185	gcagtattcgacaaa
ydjM	Function unknown	+	-180	gaactcaccgcaaaa
cedA	Modulates cell division, affects inhibition after overreplication of chromosome in dnaAcos mutants	-	-38	gctaaatcggctaaa
chbG	Member of chb operon, function unknown	-	-67	gaaatggctgccaaa
astA	Putative arginine succinyltransferase	-	-176	gccgggcaagcgaaa

xthA	Exonuclease III	+	-145	gcagcgcgcaccaaa
xthA	Exonuclease III	+	-62	gtaagcaacgcgaaa
ynjD	Function unknown	+	-198	gcagtatatgccaac
ynjD	Function unknown	+	-47	gcgttagtcgcaaaa
ydjG	Function unknown	-	-120	gcacgctttgccaat
ydjL	Function unknown	-	-36	gccatctaagcaaaa
yeaE	Function unknown	-	-72	gcattttgtgcataa
yeaF	Function unknown	-	-161	gccagtaacgctaaa
yeaU	Function unknown	+	-179	gccacggcggcaaaa
yoaA	Function unknown	-	-97	gcaaagactgccaca
sdaA	L-Serine deaminase	+	-137	gcaatattagttaaa
yoaD	Function unknown	+	-186	ccaaataccgcgaaa
yobG	Function unknown	-	-119	gcaatatgcgctgaa
yobE	Function unknown	-	-162	gcacagcttgaaaaa
yebR	Function unknown	-	-79	ccatgacgtgccaaa
hole	DNA polymerase III, theta-subunit	+	-152	gcagttgaagccata
yebG	Function unknown	-	-105	gcagtataaacgaaa
yebK	Function unknown	+	-200	gcaaagtgcggcaaa
znuA	High-affinity ABC transport system for zinc	-	-78	gcggcgttggccaaa
ruvC	RuvC endonuclease; resolves Holliday structures; not SOS regulated	-	-199	gcagacagcgcggaa
bisZ	Responsible for background activity of biotin sulfoxide reductase in bisC mutants	-	-104	ccagcatgagcgaaa

cutC	Copper sensitivity	-	-90	tcaccgatggcaaaa
cheY	Response regulator CheY for chemotactic signal transduction; flagellar regulon member	-	-60	gcaaatgttggcaaa
glyW	Glycine tRNA3	-	-54	gcactgattgccaga
cyst	Cysteine tRNA		-185	gcactgattgccaga
yecF	Function unknown	+	-185	acaatacgggcaaaa
fliK	Hook filament junction; controls hook length	+	-77	gcactgcttgcagaa
fliQ	Flagellar synthesis; flagellar regulon member	+	-14	gctagagaggcaaaa
vsr	Repairs mismatches; minimizes effects of C methylation	-	-70	gccgcggtggcaaaa
yedV	Function unknown	-	-94	gcaggctccgcgcaa
yedV	Function unknown	-	-190	ccagagctggcgaaa
yedY	Function unknown	+	-116	gcagttaatgcataa
yeeO	Function unknown	-	-127	tcagatatagcaaaa
Cbl	Cys regulon member; perhaps an accessory regulatory circuit within the cys regulon	-	-182	gcacaggcagtgaaa
sbcB	Suppresses recB recC mutations; exonuclease I	+	-89	ccactcgctgccaaa
Gmm	Guanosine di-P mannose mannosyl hydrolase	-	-133	gcacgccgcgcaaac
yegI	Function unknown	-	-175	tcaaagttagcaaaa
yegK	Function unknown	-	-30	gctggaagcgccaaa
yegO	Function unknown	+	-48	gcattgtggaccaaa
yegP	Function unknown	+	-125	gcatggtcagcaaac

ogrK	Positive regulator of P2 growth (insertion of P2 ogr gene)	-	-33	gcaccatcaacaaaa
yegV	Function unknown	+	-38	acagcgctggcgaaa
yegX	Function unknown	-	-160	gtacaggaggcaaaa
yehQ	Function unknown	+	-180	gcatcaggtgaaaaa
yehY	Function unknown	-	-66	ggactggatgccaaa
dld	D-lactate dehydrogenase; vinylglycolate resistance, FAD enzyme	+	-159	gaaaatggtgcaaaa
mglA	Methyl-galactoside transport and galactose taxis; cytoplasmic membrane protein	-	-149	gcaccaactggaaaa
yeiE	Function unknown	-	-169	gcactcagggctaac
fruA	Fructosephosphotransferase enzyme II	-	-14	gcaggagaggcataa
fruB	Fructosephosphotransferase enzyme III	-	-193	ggaaaaatggcaaaa
narP	Regulatory protein for nitrate/nitrite response	+	-172	gaagctgatgcaaaa
narP	Regulatory protein for nitrate/nitrite response	+	-142	gaagctgatgcaaaa
ccmF	Required for synthesis of c-type cytochromes; similarity with NrfE	-	-104	gaagtgctggcgaaa
ccmC	ABC transporter, heme binding	-	-104	gcaggcaccgcgaca
napH	Ferredoxin homolog	-	-117	gcggtaagtgcgaaa
napF	Ferredoxin homolog	-	-194	gaaatgtgagcaaaa
yfaQ	Function unknown	-	-118	gcgcttctcgcaaaa
ubiG	Reaction: 1-octaprenyl-3-methyl-5-hydroxy-6-methoxy-1,4-benzoquinone to ubiquinone 8	+	-86	gcagtttgaggtaaa

nrdA	Ribonucleoside diphosphate reductase subunit B1; class I enzyme, aerobic, physiologically active	+	-113	gcagtgaatcccaaa
glpQ	Glycerol-3-phosphate diesterase, periplasmic	-	-18	gcaacggaggctaat
pmrD	Confers polymyxin B resistance	-	-125	gcaacgtcagcaata
yfbB	Function unknown	-	-144	tcatcgtccgcaaaa
elaA	Unspecified	-	-143	gcaggttaagcaata
elaD	Unspecified	+	-144	gcaacccgcgctaca
nuoK	NADH dehydrogenase I subunit	-	-185	ccaatcagtgctaaa
nuooJ	NADH dehydrogenase I subunit	-	-86	gcaatcgacggcaaa
nuoE	NADH dehydrogenase I subunit	-	-105	gcatttgcagcaaat
yfbQ	Function unknown	+	-28	gcgataacagcaaaa
ackA	Acetate kinase; mutants fluoroacetate resistant	+	-158	gaaaattacgcaaaa
Pta	Phosphotransacetylase	+	-188	gcacgtttcggcaaa
yfcE	Function unknown	-	-79	gcactttcggcgaag
ubiX	Sequence homologous to ubiX of S. typhimurium, which codes for 3-octaprenyl 4-hydroxybenzoate carboxy-lyase	-	-57	gcaactcccgccgaa
yfcQ	Function unknown	-	-65	gcaagcggggcgcaa
argW	Arginine tRNA5	+	-123	gcagaacgtgcggaa
yfdT	Function unknown	+	-35	gcagtaatgccaaaa
yfdY	Function unknown	-	-84	gcaaaaattgccaga
ypdC	Function unknown	+	-137	acaaaatacgcgaaa

Glk	Glucokinase	-	-143	gcaattggtgctgaa
yfeO	Function unknown	+	-46	gcaagctgggcaaac
Glk	Glucokinase	-	-168	gcccagcttgcaaaa
alaX	Alanine tRNA 2; tandemly duplicated alaW	-	-86	gcatggcatgcaaga
xapB	Xanthosine transport protein, NupG-like	-	-36	gcgggtgaggccaaa
xapB	Xanthosine transport protein, NupG-like	-	-82	gctttctgcgcaaaa
ypeB	Function unknown	-	-151	gaactgggcgcgaaa
ypeB	Function unknown	-	-198	gcagcttaagccaga
zipA	Essential gene, affects cell division and growth; septal ring structural protein	-	-142	gaaaaaacagcaaaa
ptsH	Phosphohistidinoprotein-hexose phosphotransferase	+	-76	acaatacaggctaaa
yfeV	Function unknown	+	-153	gcagagcaagcggaa
yfeV	Function unknown	+	-72	gccgcagaagctaaa
yffN	Function unknown	+	-144	gcttctggagcaaaa
yffO	Function unknown	+	-59	tcaattcttgcgaaa
eutT	Cobalamin adenosyl transferase; Salmonella homolog	-	-133	gccacgaaggccaaa
eutQ	Protein of unknown function in eut operon; Salmonella homolog	-	-28	gcatctctcaccaaa
hyfI	Putative hydrogenase 4 component I	+	-193	gcagccgttgcgaac
hyfI	Putative hydrogenase 4 component I	+	-152	gcactggctgctgaa
yfgC	Function unknown	+	-173	gcaattgtatcgaaa
Ppx	Exopolyphosphatase	+	-75	gcaatcgccgcaaag
yfgI	Function unknown	+	-55	gcgtattcagccaaa

yfgJ	Function unknown	-	-55	gcacatcaagaaaaa
hisS	Histidyl-tRNA synthetase	-	-66	gcatggctcccgaaa
sseA	Enhances serine sensitivity (inhibits homoserine deHase) on lactate; rhodanese-like protein	+	-90	gctcagacagccaaa
yfhP	Function unknown	-	-147	gcactgaaggttaaa
purl	Phosphoribosylformylglycinamide synthetase	-	-129	gcacgcgttgctaat
pdxJ	Codon overlap with recO; complex operon	-	-54	gcagtttatgcctaa
rseC	Deletion does not affect sigma E activity	-	-121	gcaccggacgcagaa
rpoE	RNA polymerase, sigma E-subunit, high-temperature transcription (heat shock and oxidative stress)	-	-138	gcatgacaaacaaaa
yfiK	Function unknown	+	-169	gcgaagctcgcaaaa
pheL	pheA gene regulatory leader peptide	+	-154	gcaacatcggtgaaa
tyrA	Chorismate mutase T-prephenate dehydrogenase, bifunctional; TyrR regulon	-	-93	gcattagctgggaaa
yfiR	Function unknown	+	-32	gcatttcgagcgaag
ffh	4.5S-RNP protein; RNP has mammalian protein-targeting counterpart: SRP	-	-189	gcgagcagagcaaaaa
yfjI	Function unknown	+	-49	gccatatttgctaaa
nrdI	Part of nrdHIEF operon; function unknown	+	-27	gcatccagcgccaca
nrdF	Nonessential ribonucleoside-diP reductase 2, subunit beta, class I, function unknown	+	-101	gcaagggtatcaaaa
proW	High-affinity transport for glycine, betaine, and proline; see also proL	+	-151	gcagtcgatgcacaa

emrB	Hydrophobic, inner membrane-spanning domains; multidrug resistance pump family	+	-90	gcaccgcgcgtgaaa
alaS	Alanyl-tRNA synthetase 1B (ligase)	-	-156	ggagatttggcgaaa
hycF	Hydrogenase 3 subunit	-	-41	gcattgagcgtaaaa
ygbK	Function unknown	+	-152	gccgatacagccaaa
Pcm	L-Isoaspartyl protein carboxyl methyltransferase; repair of isoaspartyl residues	-	-57	gcatagcgcgcaaga
ygbP	Function unknown	-	-98	ccaggccgggcgaaa
ygcI	Function unknown	-	-200	gcggttaaagcgaaa
ygcK	Function unknown	-	-94	gcacatcatcctaaa
ygcQ	Function unknown	-	-53	gcagaaaaagctcaa
ygcR	Function unknown	-	-55	gcaccagaaactaaa
ygcF	Function unknown	-	-46	gcaggatctgcaata
eno	Enolase	-	-138	gcaggctttgtgaaa
sdaC	Regulator of L-SD2; putative serine transporter	+	-49	gctgaactggctaaa
xni	Exonuclease IX, a 3'-5' exonuclease acting preferentially on single-stranded DNA, probable excision repair function	+	-80	ccaagtaccgcgaaa
ygdD	Function unknown	-	-111	gcagaactgggtaaa
metZ	Initiator methionine tRNAf1; triplicate gene	+	-124	gcaaattttgcacaa
argA	N-acetylglutamate synthase; growth on acetylornithine;	+	-173	gaaactttagcgaaa
argA	N-acetylglutamate synthase; growth on acetylornithine;	+	-64	gcaccctgcgaaaaa

recB	Recombination and repair; RecBCD enzyme (exonuclease V) subunit	-	-185	gctgacgccgcaaaa
recC	Recombination and repair; RecBCD enzyme (exonuclease V) subunit	-	-59	gcagagaaggcgaga
ptsP	PEP-protein phosphotransferase	-	-67	ggaaaatacgccaaa
kduD	2-deoxy-D-gluconate 3-dehydrogenase	-	-94	gcatggtcggtgaaa
ygeG	Function unknown	+	-105	gcaatgcaagcttaa
ygeT	Function unknown	+	-65	gccgctgacgccaaa
ygeY	Function unknown	+	-131	gcactgaaggcgaca
ygeZ	Function unknown	+	-142	gcacctaacgaaaaa
fldB	Flavodoxin	+	-43	acactagccgcaaaa
ygfE	Function unknown	+	-165	gcattcgtcgtcaaa
cmtA	Similar to mannitol phosphotransferase enzymes	-	-72	gcatcatcagaaaaa
yqgC	Function unknown	+	-102	gaaagttcggcgaaa
sprT	Regulator of bolA gene in stationary phase	+	-150	gtaaactgcgcgaaa
pheV	Phenylalanine tRNA	+	-97	gcaatatcggcaaag
glcB	Malate synthase G	-	-30	gcgaaataagcgaaa
glcB	Malate synthase G	-	-39	gcggtgttggcgaaa
glcB	Malate synthase G	-	-63	gcgcaggtcgcgaaa
hybO	Hydrogenase 2 [Ni, Fe], small subunit	-	-49	gcgattgaggcaaaa
yqhH	Function unknown	+	-90	gcagattgaggcaaa
ygiS	Function unknown	-	-93	ggagtgtgagccaaa
mdaB	Modulator of drug activity	+	-96	gctaaattcgcaaaa

mdaB	Modulator of drug activity	+	-75	gcacattttgctaat
tolC	Specific tolerance to ColE1; affects chromosome segregation; OM porin	+	-100	gcacgtaacgccaac
ygiE	Function unknown	-	-135	gccgctaccgcaaaa
ygiC	Function unknown	+	-131	gcaatggcaccaaaac
yiC	Function unknown	+	-77	gaatctgttgccaaa
ygiM	Function unknown	+	-165	gtattttgcgccaaa
ygiH	Function unknown	+	-72	ccacttccggcgaaa
rpsU	*rpsU*: 30S ribosomal subunit protein S21	+	-86	gcaattgcagtaaaa
aer	*aer*: Flavoprotein, mediates positive aerotactic responses; signal transducer	-	-15	gcacaggacgcgaac
ygjG	*ygjG*: Function unknown	+	-148	gcaatccctgcaata
ebgA	*ebgA*: Cryptic beta-galactoside utilization	+	-197	gcacgacccgttaaa
uxaA	Altronate hydrolase galacturonate	-	-148	gcattctgtgccaga
exuR	Negative regulatory gene for exu regulon (exu, uxu, uxa)	+	-68	gcgagtagagctaaa
exuR	Negative regulatory gene for exu regulon (exu, uxu, uxa)	+	-59	gctaaactcgcaaaa
yqjA	Function unknown	+	-86	gcagaacataccaaa
yqjB	Function unknown	+	-149	acatgctcggcaaaa
yqjD	Function unknown	+	-77	gcaggaagagctgaaa
yhaK	Function unknown	+	-187	gccgccgccgcaaaa
tdcE	Pyruvate formate-lyase/ketobutyrate formate-lyase	-	-48	gcagaatttgcataa
yhaD	Function unknown	-	-129	gaaaaactggcgaaa
yhaV	Function unknown	+	-102	gaacaacccgcaaaa

yraL	Function unknown	-	-147	ccacaaccggcgaaa
yhbU	Function unknown	+	-69	gcaaggttaactaaa
metY	Initiator methionine tRNAf2	-	-193	gcaggagaaggcaaa
yhbY	Function unknown	+	-21	ccaacgtaagcaaaa
ispB	Octaprenyl diphosphate synthase	+	-188	gaatattacgcaaaa
ispB	Octaprenyl diphosphate synthase	+	-30	gtaatcggggcgaaa
yhbH	Function unknown	+	-166	gaaaacccagcgaaa
yhbJ	Function unknown	+	-198	gcagaccaaactaaa
yhcC	Function unknown	-	-165	acaagataagcaaaa
gltB	Glutamate synthase, large subunit	+	-200	gaattttgcgctaaa
yhcA	Function unknown	+	-73	gcaaacagtgcataa
nanT	Sialic acid transport	-	-133	gcagttgatgcaaga
sspA	Stress response protein	-	-169	gcaaaatctggtaaa
sspA	Stress response protein	-	-178	acaatggtcgcaaaa
yhcO	Function unknown	-	-32	gaactcgccgcgaaa
cafA	Cell division and growth, overexpression forms minicells and chains with long axial structures	-	-25	gcactgcgtgagaaa
yhdG	Function unknown	+	-66	tcatctcgtgcaaaa
yhdG	Function unknown	+	-57	gcaaaaaatgcgtaa
yhdU	Function unknown	+	-176	gaagaactggcgaaa
yhdZ	Function unknown	+	-69	gcatgtcgcgctata
smf	Gene of unknown function divergent to fms gene	-	-39	gcaaagattgctaag

smf	Gene of unknown function divergent to fms gene	-	-151	gtaacacttgcaaaa
rpsE	30S ribosomal subunit protein S5	-	-155	gcagctgtgggtaaa
rpsQ	30S ribosomal subunit protein S17	-	-194	gtaatgaaagcaaaa
gspK	General secretory pathway genes of unknown function	+	-101	gcagactcagcaata
rpsL	30S ribosomal subunit protein S12	-	-30	gaagcaaaagctaaa
yheV	Function unknown	-	-195	gcacagcgagcgcaa
yheR	Function unknown	-	-52	gcaatggtagcccaa
crp	cAMP receptor protein	+	-190	gaaagctatgctaaa
nirB	Nitrite reductase [NAD(P)H] subunit	+	-15	gaaatcgaggcaaaa
nirD	Nitrite reductase [NAD(P)H] subunit	+	-81	gcagatggtgccaga
cysG	Uroporphyrinogen III methyltransferase; transcribed from nirB operon and cysG promoters	+	-194	gcaaccacagcgaag
yhfR	Function unknown	+	-141	gcgtgcgcggcgaaa
Gph	Phosphoglycolate phosphatase activity, in dam operon	-	-123	acaacattggcgaaa
bioH	Blocked prior to pimeloyl CoA formation	-	-70	gcatagccagcataa
glpR	Repressor of glp operon	-	-41	gctcaatgcgcgaaa
glpG	Gene of glp regulon	-	-169	gcaatagcagcaaag
glgX	Glycogen debranching enzyme	-	-166	gcaaatggcgtgaaa
yhhY	Function unknown	+	-85	acacttttgcaaaa
yhhA	Function unknown	+	-96	gcaaccccagctaag
ugpQ	Glycerophosphoryl diester phosphodiesterase; cytosolic	-	-54	gcatctggcggaaaa

livG	High-affinity branched-chain amino acid transport system; membrane (transport)	-	-42	gcaactgaagctgaa
yhhK	Function unknown	+	-191	gcacaaagggcggaa
yhiH	Function unknown	-	-192	ccagttcacgccaaa
pitA	Low-affinity Pi transport	+	-64	gcccgcgccgcgaaa
yhiR	Function unknown	+	-198	gcagtcctggttaaa
prlC	Oligopeptidase A; opdA in Salmonella	-	-121	gccgccgccgcgaaa
yhjG	Function unknown	-	-132	gcattcgccgcacaa
yhQ	Function unknown	-	-59	gcagagtttgcgcaa
dppD	Uptake of dipeptides	-	-137	gcagttcgcgcaaag
dspA	Cold shock protein CS7.4; similar to Y-box DNA binding proteins of eukaryotes; transcription factor	+	-194	gcatcacccgccaat
yiaO	Function unknown	+	-148	tcaggggtggcaaaa
sgbU	Putative hexulose-6-phosphate isomerase	+	-73	gcaggcgcggcaaat
sgbU	Putative hexulose-6-phosphate isomerase	+	-64	gcaaatccggcgcaa
yiaU	Function unknown	+	-158	gcaaataacgccaca
yibA	Function unknown	+	-95	gctaaagatgcaaaa
yibG	Function unknown	+	-48	gcaaggtacgccaga
yibS	Function unknown	+	-52	gctcaaaaagctaaa
grxC	Glutaredoxin 3	-	-182	gctgggctggcgaaa
kdtA	3-deoxy-D-manno-octulosonate-lipid A transferase	+	-109	gcagatcagaccaaa
yicC	Function unknown	+	-51	gcatcgatggctata

recG	Branch migration of Holliday junctions, junction-specific DNA helicase (see ruvABC)	+	-110	gcgaaagtcgcaaaa
yicI	Function unknown	-	-132	gcgattatcgctaaa
yicM	Function unknown	-	-39	gtaaaagttgcaaaa
uhpT	Fosfomycin sensitivity; sugar P transport system; transport protein for hexose P's	-	-118	tcatatccggcaaaa
ibpA	Chaperone, heat-inducible protein of HSP20 family	-	-164	ccataaactgcaaaa
yidQ	Function unknown	+	-117	gcacgaaacgttaaa
bglF	BglG kinase; transport	-	-92	gcaaaacctgaaaaa
bglF	Positive regulatory gene, RNA-binding protein; regulated by phosphorylation	-	-79	gcattcgcaggcaaa
pstB	High-affinity P-specific transport; cytoplasmic ATP-binding protein	-	-22	gcacgatgaggaaaa
yieN	Function unknown	-	-42	gcaatttacgcagaa
ilvL	ilvG operon leader peptide	+	-15	gcaagaaaagacaaa
ilvM	Acetohydroxy acid synthase II (AHAS-II); acetolactate synthase II (ALS-II); valine insensitive; small subunit	+	-169	gcatccatggccaac
ppiC	Peptidylprolyl-cis-trans isomerase C	-	-51	gcggatcatgctaaa
argX	Arginine tRNA3	+	-108	gaataagcagcaaaa
hemY	Member of uro (hemC) operon	-	-71	acaacggaagctaaa
cyaA	Adenylate cyclase	+	-19	gcaaatcaggcgata
yigJ	Function unknown	+	-179	tcaccgccagcgaaa
yigM	Function unknown	+	-106	gcattatctgcgtaa
tatD	Involved in membrane translocation of periplasmic proteins that preserves folded structures and bound ligands	+	-56	gcagaaagcgaaaaa

mobA	MPT guanine dinucleotide synthesis; chlorate resistance	-	-166	ccagtttctgcaaaa
spf	Spot 42 RNA	+	-67	gcaacaactgaaaaa
yihM	Function unknown	+	-75	gcaatattgtccaaa
yshA	Function unknown	-	-130	tcaaccaacgcaaaa
yihS	Function unknown	-	-40	gaaatgatggctaaa
yihX	Function unknown	+	-168	gcccgctgcgctaaa
fdoH	Formate dehydrogenase-O subunit, Fe-S	-	-126	gaaggcgtagctaaa
yiiM	Function unknown	+	-190	gccagagcagcgaaa
fpr	Ferredoxin NADP+ reductase; anaerobic	-	-27	gcaagtcaatcaaaa
cytR	Regulatory gene for deo, udp, and cdd; mutants show improved growth on uridine	-	-78	gcgctatctgctaaa
yijF	Function unknown	-	-200	gcaatctctgcaata
gldA	Glycerol dehydrogenase, NAD+ dependent	-	-101	gcaacaaatgctcaa
pflD	Putative pyruvate formate lyase II	+	-94	ccattatgagcaaaa
birA	Biotin-[acetyl-CoA carboxylase] holoenzyme synthetase, and repressor	+	-143	gaagacaatgcaaaa
rplL	*rplL*: 50S ribosomal subunit protein L7/L12	+	-93	gtacgcgatgcgaaa
thiG	Thiamin-thiazole moiety synthesis	-	-71	gcagtgggcgcaaca
purH	Phosphoribosylaminoimidazolecarboxamide formyltransferase	-	-106	acaatgcgggcgaaa
iclR	Isocitrate lyase	-	-136	gcatctgtggtaaaa
yjbF	Function unknown	+	-79	gcatctgtggctaga
dgkA	Diglyceride kinase	+	-131	gcaaggatagcagaa

yjcB	Function unknown	-	-90	gcaagccccgcgata
yjcC	Function unknown	+	-110	tcaaatcaggcaaaa
nrfA	Formate-dependent nitrite reduction; tetraheme cytochrome c552	+	-31	gcaacaatggcgcaa
nrfB	Formate-dependent nitrite reduction; pentaheme cytochrome c formate-dependent	+	-30	gcaaggggcggaaaa
nrfC	Formate-dependent nitrite reduction; nonheme FE-S protein, probably transmembrane formate-dependent	+	-132	gcatccacagcaaga
alsK	Allose kinase	-	-145	gcaacttacgaaaaa
phnJ	Carbon-phosphorus lyase complex subunit (phosphonate utilization cryptic in K-12)	-	-17	gcaacaggagcagaa
phnH	Carbon-phosphorus lyase complex subunit (phosphonate utilization cryptic in K-12)	-	-65	gcacgccaggccgaa
phnD	Phosphonate transporter subunit, periplasmic (cryptic in K-12)	-	-48	gaagagaacgcgaaa
basR	BasRS two-component regulatory system homologous with OmpR-EnvZ family	-	-141	gaactgcctgcaaaa
adiA	Arginine decarboxylase, inducible by acid; homology with CadA, SpeC, SpeF	-	-187	tcagtatcagccaaa
dcuA	C4-dicarboxylate transporter, anaerobic	-	-159	gcttacaaagcaaaa
fxsA	Suppresses F exclusion of phage T7	+	-75	acaatataagctaaa
mutL	Methyl-directed mismatch repair	+	-188	gcaacaacagcgaag
yjfK	Function unknown	+	-179	gcacagttggagaaa
yjfK	Function unknown	+	-43	gccagcctcgctaaa
ygiM	Function unknown	+	-114	gcattaagcgaaaaaa
sgaA	Putative pentitol phosphotransferase enzyme IIA	+	-140	acattgcgggcgaaa

sgaE	Putative sugar isomerase	+	-38	gcgcgcatggcgaaa
ytfA	Function unknown	+	-104	gcacccggggagaaa
ytfE	Function unknown	-	-152	gcaaaaccagaaaaa
ytfE	Function unknown	-	-161	gcggtcagagcaaaa
treR	Repressor	-	-123	gcatctatggcgata
yigF	Function unknown	-	-122	gcaaatactgtgaaa
valS	Valyl-tRNA synthetase	-	-175	gcagccggcgcgata
fecB	Citrate-dependent iron transport, periplasmic protein	-	-167	gcattcggtgtgaaa
fecR	Regulatory gene mediating induction by iron	-	-168	gctggacgggctaaa
sgcR	Putative sgc cluster trasncriptional regulator	-	-106	gcagctggggcgcaa
fimD	Export and assembly of type 1 fimbrial outer membrane protein	+	-103	gcacttacccccaaa
fimG	Fimbrin type 1 minor component; pilus length; perhaps inhibits polymerization in 18340 pilus assembly	+	-190	gaatgagcagcaaaa
iadA	Isoaspartyl dipeptidase	-	-102	gaagtgaatgccaaa
yjiS	Function unknown	+	-135	acagatgaggctaaa
dnaC	DNA biosynthesis; sliding clamp subunit, required for high processivity; DNA polymerase III beta-subunit	-	-129	gcagtggcaacaaaa
bglJ	Mutation bglJ4 activates silent bgl operon, allowing arbutin and salicin transport and utilization	+	-117	gcactcatagaaaaa
rsmC	16S rRNA m5C967 SAM-dependent methyltransferase	-	-76	gcaaatatagcaaat
rimI	Modification of 30S ribosomal subunit protein S18; acetylation of N-terminal alanine	+	-176	gcaactgacgccaga

rimI	Modification of 30S ribosomal subunit protein S18; acetylation of N-terminal alanine	+	-138	gcagtcactgcaaca
Smp	Transcribed divergently from serB, overlapping promoter; membrane protein	-	-163	gcagacccggccata
radA	Sensitivity to gamma and UV radiation	+	-151	ccatgccaagccaaa
Slt	Lytic transglycosylase, major autolysin FK-506-BP-like lysis protein for phiX174; metal ion-regulated peptidyl-prolyl	+	-115	gcagtaaaagtaaaa
gpmB	Putative phosphoglycerate mutase	+	-158	gcaacggatgcaata
gpmB	Putative phosphoglycerate mutase	+	-20	gcagtatacggaaaa
rob	OriC-binding protein, binds to right border of oriC	-	-75	gctaaaacagcaaaaa
wbbK	**O-antigen biosynthesis (putative glycosyltransferase)**	-	-47	ggagtaccagcaaaa
wzxC	**Colanic acid (capsule) biosynthesis**	-	-150	gctggcgcggcgaaa
waaU (rfaK)	**LPS core biosynthesis (glycosyltransferase)**	-	-104	gcagaagaatcaaaa
wcaD	**Colanic acid (capsule) biosynthesis**	-	-167	ggaagtgttgcaaaa
wzc	**Colanic acid (capsule) biosynthesis**	-	-94	gcaaaagccgggaaa
waaJ (rfaJ)	**LPS core biosynthesis (glucosyltransferase)**	-	-103	gcatagatatctaaaa
waaA (kdtA)	**Lipid A biosynthesis**	+	-109	gcagatcagaccaa
rffA	**Enterobacterial common antigen biosynthesis**	+	-146	gcaaacggcgctaaa
waaD (rfaD)	**LPS core biosynthesis**	+	-149	gaaggactagctaaaa
waaY (rfaY)	**LPS core biosynthesis**	-	-143	gcacaaatgggcaat

lpxL (waaM)	**Lipid A biosynthesis**	-	-174, -144, -93	gcaattatcgataa, ttacgctacatttgc, tttcgcccagtcttc
amiC (ygdN)	**Degradation of peptidoglycan during cell division**	-	-78	gcgtctttcgctaaa
pbpG (yohB)	**Cell wall hydrolysis**	-	-157	gcattgctggcgtaa
dacB	**Cell wall hydrolysis**	+	-30	ggaccagaagcaaaa
mepA	**Cell wall hydrolysis**	-	-52	gcaacgggcgcaaaa

Appendix 2. Promoter fragments generated by PCR.

The regulatory regions of genes found to contain putative marboxes were amplified. Putative marboxes are shown in underlined in red. Promoter elements, as found on Ecocyc, are shown in green and yellow with the TSS (+1) capitalised. The start codon is capitalised. Primer sequences anneal to the sequence shown in bold.

Gene	Promoter Sequence (-200bp or -400bp from TSS*)
wbbK	cgcacgttggaatcttcagctgttgta**attggccagagggtttggttg**ggtgagaatgtgacggttttgcctggaacaattattg gtaatggagtcgtagtcgGcgccaattctgttgttagaggttctattcccgaaaatactgtcattgcggagtaccagcaaaaat cataaagaaata**caatcatgagaccaaattATG**
wzxC	atggagaacgacaaagtggtgacccaggcgacgcagaacgatccgcgcgtcaccaaagtggggaactttctgcgccgtac ctcgctggatgaattgccgcagtttatcaatgtgctgaccgggggggatgtcgattgtcggtccacgtccgcacgcagta**gcgc ataacgaacagtatcg**acagctcattgaaggctacatgctgcgccataaggtgaaaccgGgcattaccggctgggcgcag attaacggctggcgcggcgaaaccgacacgctggagaaaatggaaaaacgcgtcgagttcgaccttgagtacatccgcgaa tggagcgtctggttcgatatcaaaatcgttttcctgacggtgttcaaaggtt**tcgttaacaaagcggcatattgatATG**
waaU (rfaK)	ttagtcttggttattgctcatgccatactattgcctttgctgcaattcaaatcgcatattcacttaagtatgcgcggattatttgttctgg tcttgatttaacgggtagctgttctcgtttctatgatgagaataaaaatcccatgccctcggaattaagtagggatttattcaaaatat tgccatttttttcgttttatgcatgataatgtaaaAgatattaatatttataatttatcagat**gatacagcta**tttctt**acg**atgtaattcc atttattaaacttcaagAcatcagtgcagaagaatcaaaagatatgacaagaaaaaaaatgcaatatagaacttcaaccgattct tatgctaattaatcatcctgaaa**ctaaaataatatggtataaaaATG**
wcaD	gcc**ggtgattgccacccatag**cgatgcggcgcgggaagtgttgcaaaaatccggcggtaaaaccgtcagcgaagaagag gtgctgcaactggtgcagttaagcaaaccggaaatcgcgcaggcgatatttggtaccacgctggctgagttcagccaacgca gccgcgccgcctacagtggacaaca**gatgctggaggagtATG**
wzc	gaaaagcgccatatcgaacgcttatgcgagatggcaccggagatgcgcggcaaagtg**atgctgtttggtcactggg**ataac gaatgtgaaatccccgatccgtatcgcaaaagccgggaaacgtttgcagcggtgtacacattacttgaacggtctgcccgcca gtgggcgcaggcattgaa**cgcagagcaggtataagaATG**
waaJ (rfaJ)	tggaggcaaaaaatgcttcgccatggaagaatacggcgttgctgaaaccgaacaata**gcaatcaattaagatatagcg**caa aacatatgcttaaaaagcatagatatctaaaaggatttagcaactatctttttattttattgaaaagataaagcattaaaactgggaa actataaagtaat**gatataagggtagcattGTG**
waaA (kdtA)	tcgataatgtcagtacggcctatgtagatttgaaaatg**gggccgagtttcaatgaatc**gcataaaaatacaaaaaaaatgaag atgtagcggcagatcagaccaaactgaagctatttaagtcaaaaacgggaaaagtaatggtaagccacagctaaatacatag aatccccagcAcat**ccataagtcagctatttactATG**
rffA	gacagatgcgcgaattggcctgctggct**ggacgcggtgcaggtg**tgagctgatgcaaacggcgctaaactgggcgtatgct cgcggtaaaacaacttgcgggtggcgacccaaatgggcaacaccgccgcgcttaaacgatacatacaaagtggtgcgaat gtagaaagcaccgcgtact**ggttatacaggtgatcacATG**
waaD (rfaD)	cggaatattgatactaaa**gcactattcacatgcaaaac**caacatccgccatgaaggactagctaaaacccaaactagtttgtt gcaattagcatccttgcacctctatgTaaagggctgaaggattcggatgtgatggtatgattacagacattcgtgtctgagatt gtctctgactc**catAttcgaaggttacagttATG**
waaY (rfaY)	aataccctgatcaggatgttatgaatgtcttactgaaagggatgacattatttttgcctcgtgagtacaatacaatttatacaattaaa agtgaattaaaagacaaaacacatcaaaactataaaaagctgattacagaaagtactcttcttattcattatacaggt**gcaactaa accgtgg**cacaaatgggcaatttatccatcggtaaaatactataaaatagctttAgaaaattccccctggaaagatgactctcca cgagatgcgaaatcaattattgaatttaaaaaaagatataaacatcttttagtgcaacatcattatatctcaggaattatagcagga gtctgttatctttgccgaaaatattaccgtaaataa**catttaactggtttattATG**
lpxL (waaM)	(yceA)**CATggtgtacggttcctgc**gagatgggaaagTaaaaatccgcggcatgatatagcaattatcgataattaacat ccacacatttttacgctacatttgcgcAttaaaaattatttgttatttacaagcgcggcaatttcgcccagtcttcagccacaaatttt ggttgcgggcgaaaaaatgcgacaatacatacaattgcccgaata**ggttgaaaaacaggattgatATG**

amiC (ygdN)	agtgtatttttattctgttttttcgca**gggtgcaagtgtaaattttatgcgagagcgac**ttttttatcagtaatgccgtgaatataaa aagaatgtttaccgtttattagatgacagattatgcgtctttcgctaaagttccgGtcaaattagtcgtttacttgttacacagctta gatttcttttgct**cgggagaggcATG**
pbpG (yohB)	tggggctacggttatcgtttgttctagaaagttctttgacgttgcattgct**ggcgtaaatgtcagcaatgca**gcatttcctcacga ttctccttgacgatcgcactttttgctcgttatgatggcgtcGctagcctcagtaaatccttactccggcggtgcgcaacccgtg cgcgtgaacca**ctatctgaatgctcatcATG**
dacB	agctgcgtggtattcggcgttttctttcaggtcgccatgctcacgcgcttccgcgatagcagcaatgatttcaggacggcgcaca gatttcagaaaatccagctcttcgcgtaatttttcagcgccgcgtaaggtcatcggaatagcttgcatttgttata**cctcttgaata ttcctgatgggg**caagtcttcacccaccccggctgttcggcctgcccggcataactcctcaccg**ggaccagaagcaaaa**aaa taccgacccgggtacaagtcccaggtcagctacaattcacAttttgatagtcattttaccctgaagttcccgaagggtcatcgttt actttatagggcgttgcgccgtagtatgacggctcgattcca**ggttgttagcgcgagattATG**
mepA	**gcattaccgtgccgggtcgtac**cattaaccgctttggcgaagaagttgagatgatcaccaaaggccgtcacgatccctgtgtc gggatccgcgcagtgccgatcgcagaagcgatgctggcgatcgttttaatggatcacctgttacg**gcaacgggcgcaaaa**tg ccgatgtgaagact**gatattccacgctggtaaaaaATG**

Appendix 3. A comparison of MarA and SoxS targets identified by and Sharma *et al.*, 2017 and Seo *et al.*, 2015, respectively.

Seo *et al.*, 2015 identified 25 SoxS targets in *E. coli* K-12 using ChIP-Exo. Sharma *et al.,* 2017 identified 33 MarA targets in ETEC strain H10407 using ChIP-Seq. Only 4 genes were identified in both experiments. Underlined genes are those that had not previously been identified as targets prior to the investigation. * denotes that they were also found in the bioinformatic search used in this study.

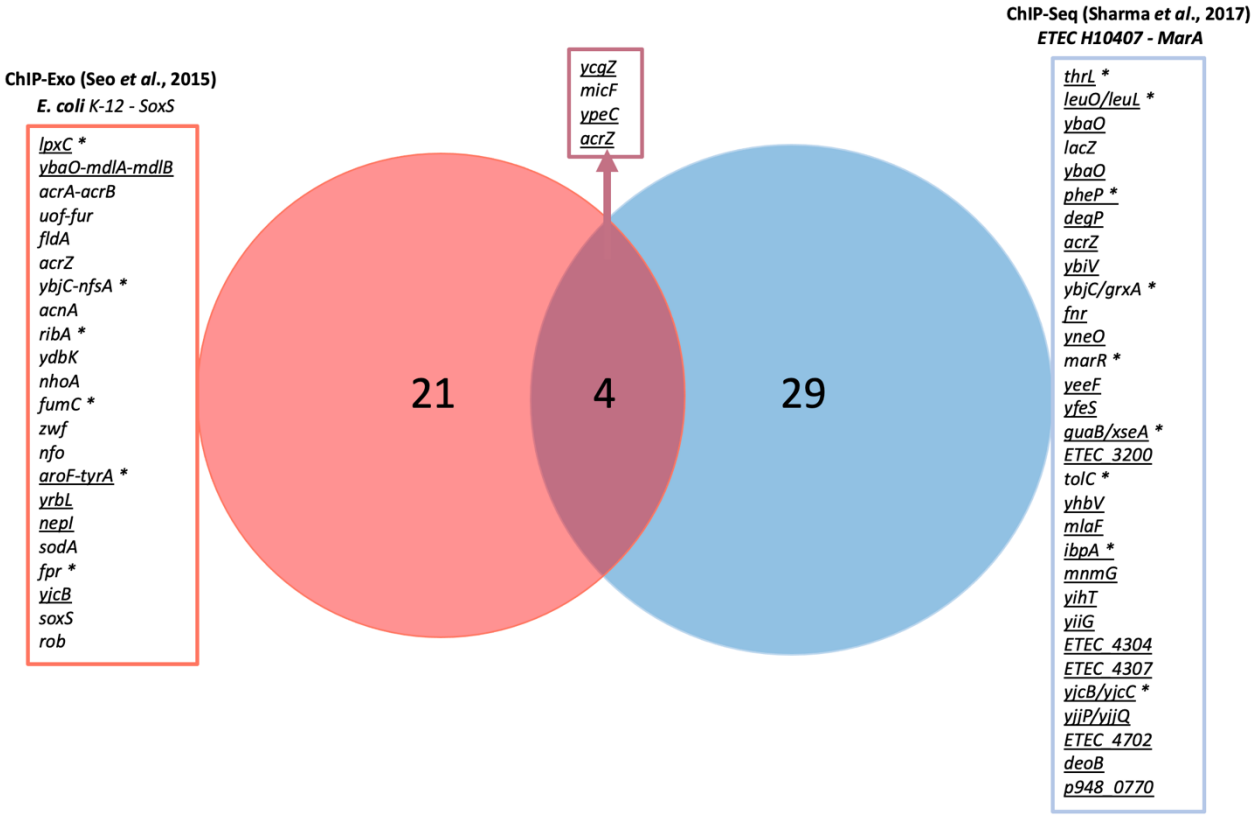

Appendix 4. Statistical significance of growth of BW25113, Δ*mlaE*, Δ*pbpG* and strains expressing *pbpG* on pJ203.

Significance determined by a two-way ANOVA followed by the post-hoc two-stage linear step-up procedure of Benjamini, Krieger and Yekutieli. Pairwise comparisons for strains of interest were compared for each time point and the q-value (p-value adjusted to correct for multiple comparisons by controlling the False Discovery Rate) is presented. Statistical significance is determined as a q-value < 0.05 (underlined). A cut-off of 50 % (7/14) was used to determine overall statistical significance e.g. when ≥ 50 % q-values were significant, pairwise comparisons were noted as significant (noted as "*").

	Q value							
Pairwise comparison	BW25113 / Δ*mlaE* Doxycycline		BW25113 / Δ*pbpG* Doxycycline		BW2115 / BW2115 pJ203 + *pbpG* Doxycycline		Δ*mlaE* / Δ*mlaE* pJ203 + *pbpG* Doxycycline	
Time (minutes)	- (6/14)	+ (5/14)	- (8/14) *	+ (7/14) *	- (11/14) *	+ (6/14)	- (11/14) *	+ (9/14) *
0	-	-	-	-	-	-	-	-
40	0.2750	0.1794	0.2708	0.2230	0.0140	0.4088	0.0615	0.9295
80	0.0284	0.0666	0.0554	0.1988	0.0063	0.1988	0.0095	0.0717
120	0.0593	0.0008	0.0486	0.0165	0.0010	0.0035	0.0109	0.0371
160	0.0328	0.0043	0.0116	0.0344	0.0002	0.0625	0.0164	0.0462
200	0.0289	0.0026	0.0101	0.0025	0.0012	0.0186	0.0019	0.0013
240	0.1045	0.0005	0.0052	0.0015	0.0012	0.0029	<0.0001	0.0015
280	0.1882	0.0369	0.0053	<0.0001	0.0001	0.0014	0.0004	0.0026
320	0.0382	0.1242	0.0019	0.0006	0.0001	0.0035	0.0136	0.0008
360	0.2510	0.1287	0.0741	0.0083	0.0093	0.0083	0.0003	0.0046
400	0.1888	>0.9999	0.0741	0.0835	0.0195	0.0961	0.0024	0.0719
440	0.5778	0.7535	0.4142	0.1316	0.1726	0.1316	0.0196	0.1352
480	0.8986	0.7735	0.7803	0.1948	0.5216	0.1948	0.1443	0.2006
1440	0.0067	0.6918	0.0141	0.6918	0.0002	0.5061	0.0006	0.0041

Appendix 5. Spectra of total membrane extracts from BW25113 and Δ*mlaF*.

A. Total ion chromatogram of intact mass of total membrane extracts from BW25113, Δ*marA*, Δ*mlaF* and Δ*mlaF* pBR322 + *mlaF* (- or + marbox). Negative ionization mode only. Peaks corresponding to PG and PE head groups are labelled. Note that the chromatogram for the OM shows the same peaks. B. Diacyl PG species and their acyl chains found in BW25113 and Δ*mlaF*. C. Diacyl PE species and their acyl chains found in BW25113 and Δ*mlaF*. Spectra show m/z of diacyl chains. Further analysis using Bruker software showed fragmentation patterns within each diacyl chain. LIPIDBLAST was used to identify acyl chain lengths using m/z values. BW25133 is shown in blue. Δ*mlaF* is shown in orange. All diacyl chains are found in both strains. Results shown are from replicate 1 but the same fragmentation pattern was demonstrated in all replicates.

A.

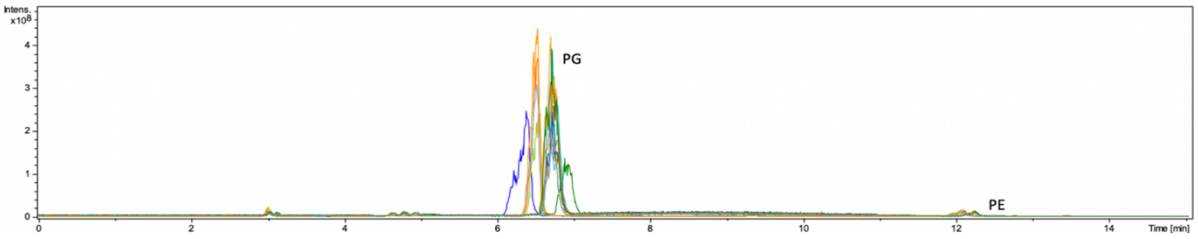

B.

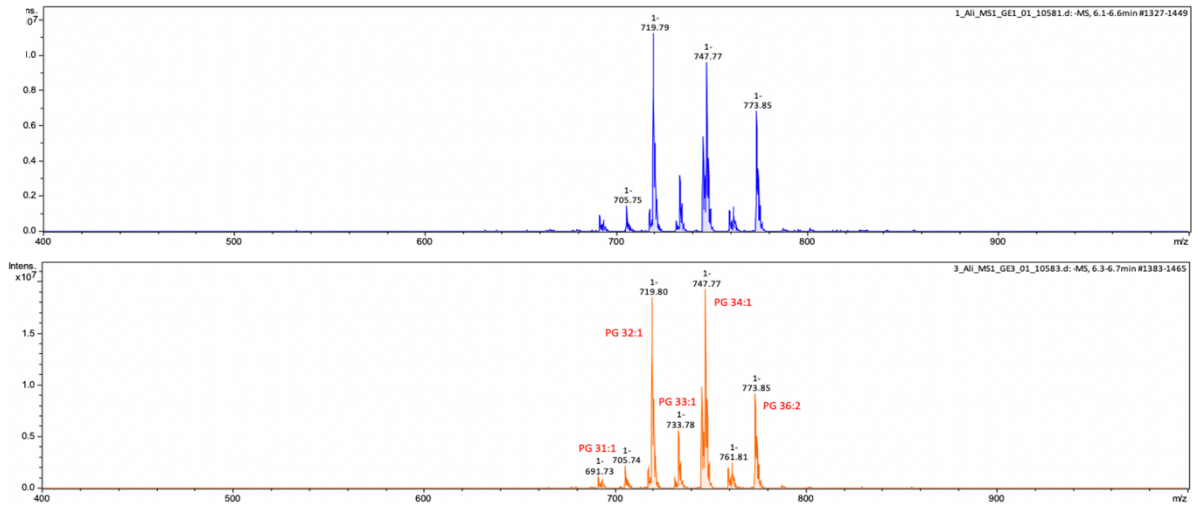

C.

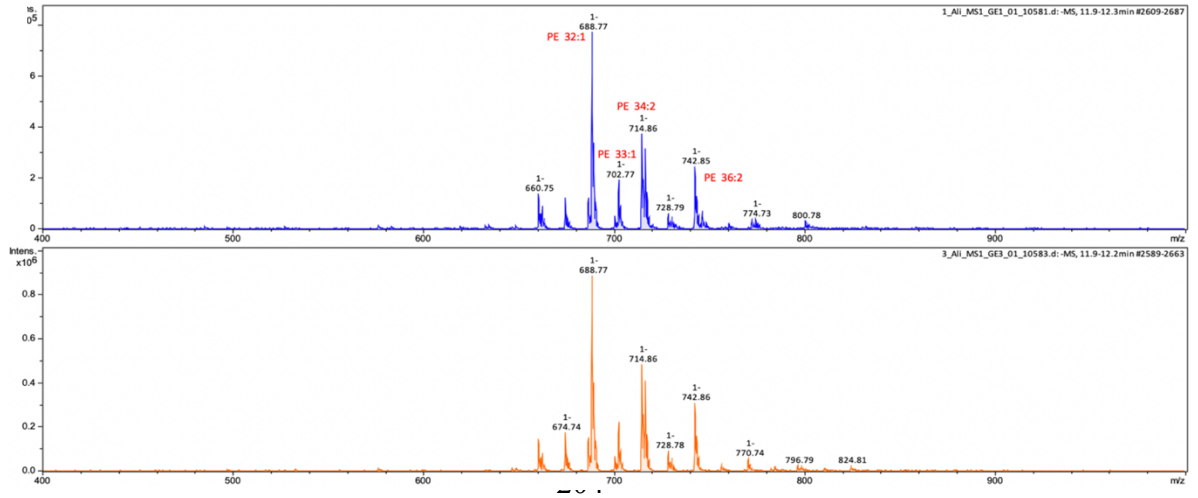

Appendix 6. Logistic growth of BW25113, Δ*mlaE* and Δ*pbpG*, and each of these strains containing pJ203 -/+ *pbpG*.

Logistic growth of BW25113, Δ*mlaE* and Δ*pbpG*, and each of these strains containing pJ203 -/+ *pbpG*. Logistic growth analysis was used to analyse growth rates of a range of Δ*thyA* strains with various mutations in the absence and presence of 1.0 µg/ml doxycycline. A 95 % confidence interval was used for interpolation. K value (growth rate constant, min^{-1}) and R^2 (coefficient of determination) were calculated on Graphpad Prism 9 using the above parameters. Doubling time was calculated using the equation ln(2)/k. (Kacena *et al*., 1999; Allen and Waclaw, 2019). Specific growth rate was calculated by multiplying the growth rate constant (k) by 60 to convert units to hours.

	- Doxycycline				+ Doxycycline			
Strain	K value	Doubling time (mins)	Specific growth rate (h^{-1})	R^2	K value	Doubling time (mins)	Specific growth rate (h^{-1})	R^2
BW25113	0.026	26.648	1.574	0.920	0.006	121.020	0.349	0.989
BW25113 pJ203 - *pbpG*	0.025	27.880	1.493	0.911	0.010	89.683	0.586	0.803
BW25113 pJ203 + *pbpG*	0.015	46.469	0.915	0.895	0.007	97.044	0.431	0.955
Δ*mlaE*	0.026	26.978	1.551	0.923	0.005	127.488	0.327	0.962
Δ*mlaE* pJ203 - *pbpG*	0.024	29.132	1.434	0.918	0.006	121.366	0.343	0.991
Δ*mlaE* pJ203 + *pbpG*	0.006	118.019	0.361	0.959	0.003	216.756	0.192	0.984
Δ*pbpG*	0.020	35.773	1.177	0.936	0.013	55.852	0.764	0.828
Δ*pbpG* pJ203 - *pbpG*	0.028	30.701	1.365	0.899	0.013	56.048	0.759	0.897
Δ*pbpG* pJ203 + *pbpG*	0.024	28.910	1.458	0.940	0.011	72.180	0.639	0.907

Appendix 7. Point mutations in the marboxes of the regulatory regions of *waaY*, *pbpG* and *mlaFEDCB*.

Point mutations were made in the chromosome to prevent MarA binding to the regulatory regions of *waaF*, *pbpG* and *mlaF*. 6 mutations were successfully prepared – *waaY* M*, *pbpG* M*, *mlaF* M*, *pbpG* M* *mlaF* M*, *waaY* M* *mlaF* M* and *pbpG* M* *waaY* M* *mlaF* M*. The location of genes on the chromosome is not accurate.

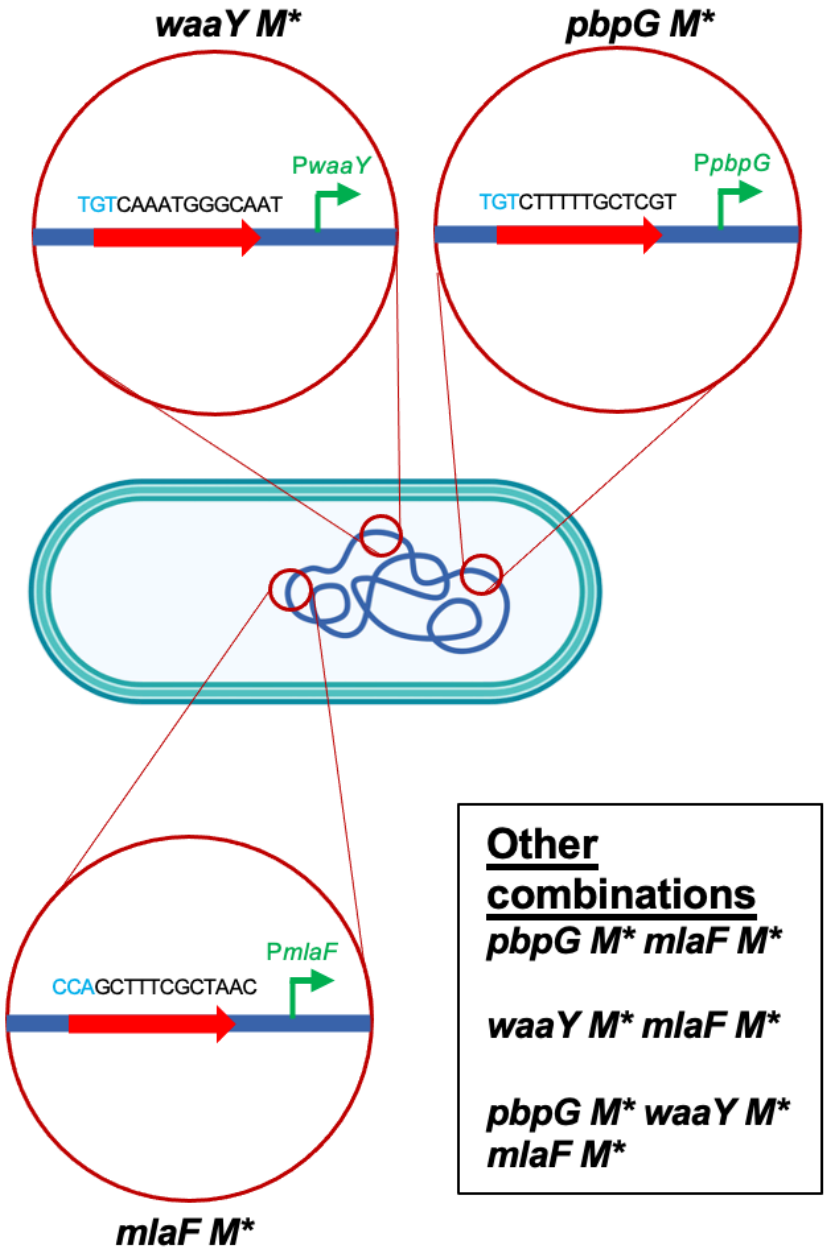

Appendix 8. Attempts to mutate the marboxes upstream of essential genes *lpxC* and *lpxL*.

A. A constitutive promoter was incorporated into the *thyA* cassette used in FRUIT. This was electroporated into Δ*thyA* cells containing pACBSR with λ Red genes B. *E. coli* JCB387 Δ*thyA* was transformed with a plasmid expressing *lpxC* and *lpxL* under control of a strong constitutive promoter. FRUIT was carried out as shown in Figure 2.1. Both methods were unsuccessful. No recombinants were found on M9 minimal media plates lacking thymine.

A.

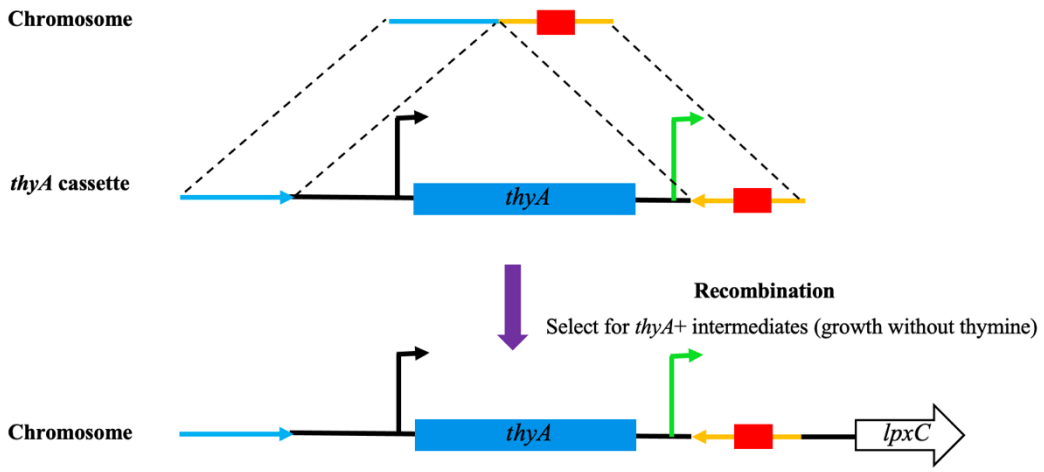

B.

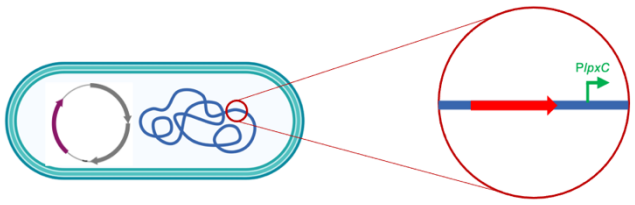

Appendix 9. Logistic growth of Δ*thyA* and strains containing mutations in specific regulatory regions to prevent MarA binding with pJ203 -/+ *marA*.

Logistic growth analysis was used to analyse growth rates of a range of Δ*thyA* strains with various mutations in the absence and presence of 1.0 µg/ml doxycycline. A 95 % confidence interval was used for interpolation. K value (growth rate constant, min^{-1}) and R^2 (coefficient of determination) were calculated on Graphpad Prism 9 using the above parameters. Doubling time was calculated using the equation ln(2)/k (Kacena *et al*., 1999; Allen and Waclaw, 2019). Specific growth rate was calculated by multiplying the growth rate constant (k) by 60 to convert units to hours.

	- Doxycycline				+ Doxycycline			
Strain	K value	Doubling time (mins)	Specific growth rate (h^{-1})	R^2	K value	Doubling time (mins)	Specific growth rate (h^{-1})	R^2
Δ*thyA*	0.014	50.329	0.826	0.964	0.008	88.423	0.471	0.949
Δ*thyA* pJ203 - *marA*	0.014	49.978	0.832	0.967	0.008	86.858	0.479	0.956
Δ*thyA* pJ203 + *marA*	0.013	52.904	0.787	0.980	0.012	55.811	0.748	0.962
rfaY M*	0.014	50.316	0.827	0.960	0.008	86.737	0.480	0.945
rfaY M* pJ203 - *marA*	0.014	50.104	0.830	0.964	0.008	86.194	0.483	0.942
rfaY M* pJ203 + *marA*	0.013	51.680	0.805	0.969	0.011	61.003	0.683	0.942
mlaF M*	0.014	49.962	0.832	0.966	0.009	81.315	0.512	0.960
mlaF M* pJ203 - *marA*	0.014	50.048	0.831	0.965	0.008	81.905	0.508	0.969
mlaF M* pJ203 + *marA*	0.013	52.508	0.792	0.981	0.011	61.339	0.680	0.945
pbpG M*	0.014	49.256	0.844	0.965	0.008	82.792	0.503	0.940
pbpG M* pJ203 - *marA*	0.014	49.256	0.844	0.966	0.008	82.814	0.502	0.942
pbpG M* pJ203 + *marA*	0.013	53.226	0.782	0.976	0.011	61.641	0.678	0.951
pbpG M* *mlaF* M*	0.014	50.172	0.829	0.962	0.007	104.077	0.400	0.962
pbpG M* *mlaF* M* pJ203 - *marA*	0.014	49.558	0.839	0.961	0.007	102.497	0.406	0.964
pbpG M* *mlaF* M* pJ203 + *marA*	0.013	53.962	0.771	0.976	0.009	76.950	0.541	0.973
rfaY M* *mlaF* M*	0.014	49.714	0.837	0.959	0.007	101.649	0.410	0.893
Δ*thyA rfaY* M* *mlaF* M* pJ203 - *marA*	0.014	50.080	0.831	0.960	0.007	101.578	0.410	0.957
rfaY M* *mlaF* M* pJ203 + *marA*	0.013	53.082	0.784	0.980	0.009	75.087	0.554	0.958
pbpG M* *mlaF* M* *rfaY* M*	0.014	50.598	0.822	0.960	0.009	78.923	0.527	0.970
pbpG M* *mlaF* M* *rfaY* M* pJ203 - *marA*	0.014	50.564	0.823	0.959	0.009	79.164	0.525	0.974
pbpG M* *mlaF* M* *rfaY* M* pJ203 + *marA*	0.013	54.275	0.766	0.974	0.011	61.778	0.677	0.949

Appendix 10. Statistical significance of growth of Δ*thyA* JCB387 and a range of Δ*thyA* JCB387 strains with marbox mutations in the *waaY*, *mlaF* and *pbpG* promoters.

Significance determined by a two-way ANOVA followed by the post-hoc two-stage linear step-up procedure of Benjamini, Krieger and Yekutieli. Pairwise comparisons for strains of interest were compared for each time point and the q-value (p-value adjusted to correct for multiple comparisons by controlling the False Discovery Rate) is presented. Statistical significance is determined as a q-value < 0.05 (underlined). A cut-off of 50 % (7/14) was used to determine overall statistical significance e.g. when ≥ 50 % q-values were significant, pairwise comparisons were noted as significant (noted as "*").

	Q value											
Pairwise comparison	Δ*thyA* / *rfaY* M* Doxy		Δ*thyA* / *mlaF* M* Doxy		Δ*thyA* / *pbpG* M* Doxy		Δ*thyA* / *pbpG* M* *mlaF* M* Doxy		Δ*thyA* / *rfaY* M* *mlaF* M* Doxy		Δ*thyA* / *pbpG* M* *rfaY* M* *mlaF* M* Doxy	
Time (minutes)	- (0/14)	+ (6/14)	- (0/14)	+ (4/14)	- (0/14)	+ (3/14)	- (0/14)	+ (11/14) *	- (0/14)	+ (10/14) *	- (0/14)	+ (4/14)
0	-	-	-	-	-	-	-	-	-	-	-	-
40	>0.9999	0.5469	0.9408	0.4371	0.4701	0.2219	0.7273	0.0289	0.4701	0.0095	0.4701	0.6470
80	0.9731	0.1249	0.9214	0.1249	0.8054	0.5848	0.9214	0.1031	0.9536	0.0889	0.9536	0.3008
120	0.8675	0.0091	0.9648	0.0121	0.8675	0.1019	0.8675	0.0646	0.8675	0.0636	0.8675	0.0127
160	0.9396	0.0402	0.9396	0.0723	0.9396	0.3247	0.9396	0.0088	0.9396	0.0655	0.9396	0.1998
200	0.6120	0.4876	0.7408	0.4290	0.7408	0.4221	0.7993	0.0002	0.7408	0.0020	>0.9999	0.4407
240	0.4751	0.1961	0.7459	0.3623	0.9712	0.1131	0.8526	0.0003	0.8526	0.0010	0.8529	0.1131
280	0.5373	0.0455	0.8368	0.4748	0.3411	0.0523	0.2841	<0.0001	0.1170	<0.0001	0.9730	0.1893
320	0.8345	0.0119	0.8345	0.0491	0.8345	0.0016	>0.9999	<0.0001	0.8345	<0.0001	>0.9999	0.0096
360	0.5388	0.0445	0.5388	0.4656	>0.9999	0.0375	>0.9999	<0.0001	0.9432	<0.0001	>0.9999	0.0363
400	0.9163	0.1786	0.9077	0.4758	0.7160	0.1112	0.7160	<0.0001	0.7283	<0.0001	0.5243	0.112
440	>0.9999	0.0245	>0.9999	0.3082	>0.9999	0.0144	>0.9999	<0.0001	>0.9999	<0.0001	>0.9999	0.0167
480	0.7939	0.3408	>0.9999	0.0030	0.7939	0.3930	0.8773	<0.0001	0.9454	0.0001	0.8421	0.3930
1440	0.8015	0.0911	0.8967	<0.0001	0.8015	0.1808	0.3611	<0.0001	0.8015	<0.0001	0.3539	0.0192

References

Adedeji, W.A. (2016) "The Treasure Called Antibiotics." Ann Ib Postgrad Med **14**(2): 56-57.

Adhya, S. (2001) "Repression Mechanism." eLS **1**:1-8.

Aktas, M., Danne, L., Möller, P. and Narberhaus, F. (2014) "Membrane lipids in *Agrobacterium tumefaciens*: biosynthetic pathways and importance for pathogenesis." Front Plant Sci **5**: 109.

Albarri, O., AlMatar, M., Meral, M. and Köksal, F. (2022) "Overexpression of efflux pumps AcrAB and OqxAB contributes to ciprofloxacin resistance in clinical isolates of *K. pneumoniae.*" Curr Protein Pept Sci. **23**(5): 356-368.

Alekshun, M. N. and Levy, S. B. (1997) "Regulation of chromosomally mediated multiple antibiotic resistance: the *mar* regulon." Antimicrobial Agents and chemotherapy **41**(10): 2067-2075.

Anderson, M. S., Bulawa, C. E. and Raetz, C. R. (1985) "The biosynthesis of Gram-negative endotoxin. Formation of lipid A precursors from UDP-GlcNAc in extracts of *Escherichia coli*." J Biol Chem **260**(29): 15536-41.

Andrews, J. M. (2001) "Determination of minimum inhibitory concentrations." J Antimicrob Chemother **48**:5-16.

Andrey, R., Chenyu, L., Richard, H. E. and Terence, R. S. (2006) "Abortive Initiation and Productive Initiation by RNA Polymerase Involve DNA Scrunching." Science **314**(5802): 1139.

Annik, P. and Uwe, S. (2005) "Impact of Global Transcriptional Regulation by ArcA, ArcB, Cra, Crp, Cya, Fnr, and Mlc on Glucose Catabolism in *Escherichia coli.*" Journal of Bacteriology **187**(9): 3171-3179.

Ariza, R. R., Cohen, S. P., Bachhawat, N., Levy, S. B. and Demple, B. (1994) "Repressor mutations in the *marRAB* operon that activate oxidative stress genes and multiple antibiotic resistance in *Escherichia coli*." Journal of Bacteriology **176**(1): 143-148.

Arnaud-Barbe, N., Cheynet-Sauvion, V., Oriol, G., Mandrand, B. and Mallet, F. (1998) "Transcription of RNA templates by T7 RNA polymerase." Nucleic acids research **26**(15): 3550-3554.

Astrid, P., Margarita, P., Jesús, A., Cristina, L., Francisco Javier, M., María, T., Antonio, R., Iñigo, L. and Germán, B. (2012) "Effect of Transcriptional Activators SoxS, RobA, and RamA on Expression of Multidrug Efflux Pump AcrAB-TolC in *Enterobacter cloacae*." Antimicrobial Agents and Chemotherapy **56**(12): 6256-6266.

Babinski, K. J., Kanjilal, S. J. and Raetz, C. R. (2002) "Accumulation of the lipid A precursor UDP-2,3-diacylglucosamine in an *Escherichia coli* mutant lacking the *lpxH* gene." J Biol Chem **277**(29): 25947–56.

Bae, B., Feklistov, A., Lass-Napiorkowska, A., Landick, R. and Darst, S. A. (2015) "Structure of a bacterial RNA polymerase holoenzyme open promoter complex." eLife **4**: e08504.

Balaban, N.Q., Gerdes, K., Lewis, K. and McKinney, J.D. (2013) "A problem of persistence: still more questions than answers?" Nat Rev Microbiol **11**(8); 587-91,

Bar-Nahum, G., Epshtein, V., Ruckenstein, A. E., Rafikov, R., Mustaev, A. and Nudler, E. (2005) "A Ratchet Mechanism of Transcription Elongation and Its Control." Cell **120**(2): 183-193.

Barker, M. M., Gaal, T., Josaitis, C. A. and Gourse, R. L. (2001) "Mechanism of regulation of transcription initiation by ppGpp. I. Effects of ppGpp on transcription initiation *in vivo* and *in vitro*." Journal of Molecular Biology **305**(4): 673-688.

Barne, K. A., Bown, J. A., Busby, S. J. and Minchin, S. D. (1997) "Region 2.5 of the *Escherichia coli* RNA polymerase sigma^{70} subunit is responsible for the recognition of the 'extended-10' motif at promoters." The EMBO journal **16**(13): 4034-4040.

Beall, B. and Lutkenhaus, J. (1987) "Sequence analysis, transcriptional organization, and insertional mutagenesis of the *envA* gene of *Escherichia coli*." J Bacteriol **169**(12): 5408-15.

Beatriz, C., Minhao, L., Jonathan, R., Andrey, S., Bing, L., King, K., Peter, S., Robert, W., Konstantin, S., Ernesto, C., Steve, M., Siva, R. W. and Geiduschek, E. P. (2010) "T7 Phage Protein Gp2 Inhibits the Escherichia Coli RNA Polymerase by Antagonizing Stable DNA Strand Separation Near the Transcription Start Site." PNAS **107**(5): 2247-2252.

Benoff, B., Yang, H., Lawson, C. L., Parkinson, G., Liu, J., Blatter, E., Ebright, Y. W., Berman, H. M. and Ebright, R. H. (2002) "Structural Basis of Transcription Activation: The CAP-alpha CTD-DNA Complex." Science **297**(5586): 1562-1566.

Berezhnoy, N. V., Cazenave-Gassiot, A., Gao, L., Foo, J. C., Ji, S., Regina, V. R., Yap, P. K. P., Wenk, M. R., Kjelleberg, S., Seviour, T. W. and Hinks, J. (2022) "Transient Complexity of *E. coli* Lipidome Is Explained by Fatty Acyl Synthesis and Cyclopropanation." Metabolites **12**(9): 784.

Bhavin, S. P. and Hatfield, G. W. (1996) "Transcriptional Activation by Protein-Induced DNA Bending: Evidence for a DNA Structural Transmission Model." PNAS **93**(3): 1173-1177.

Bhunia, A. K. (2018) "*Escherichia coli*." in Foodborne Microbial Pathogens. New York, NY: Springer.

Blair, J. M. A., La Ragione, R. M., Woodward, M. J. and Piddock, L. J. V. (2009) "Periplasmic adaptor protein AcrA has a distinct role in the antibiotic resistance and virulence of *Salmonella enterica* serovar Typhimurium." Journal of Antimicrobial Chemotherapy **64**(5): 965-972.

Blair, J. M. A., Richmond, G. E. and Piddock, L. J. V. (2014) "Multidrug efflux pumps in Gram-negative bacteria and their role in antibiotic resistance." Future Microbiology **9**(10): 1165-1177.

Blatter, E. E., Ross, W., Tang, H., Gourse, R. L. and Ebright, R. H. (1994) "Domain organization of RNA polymerase α subunit: C-terminal 85 amino acids constitute a domain capable of dimerization and DNA binding." Cell 78(5): 889-896.

Borukhov, S., Lee, J. and Laptenko, O. (2005) "Bacterial transcription elongation factors: new insights into molecular mechanism of action." Molecular Microbiology **55**(5): 1315-1324.

Bougdour, A., Lelong, C. and Geiselmann, J. (2004) "Crl, a low temperature-induced protein in *Escherichia coli* that binds directly to the stationary phase sigma subunit of RNA polymerase." The Journal of Biological Chemistry **279**(19): 19540-50.

Boyaci, H., Chen, J., Jansen, R., Darst, S. A. and Campbell, E. A. (2019) "Structures of an RNA polymerase promoter melting intermediate elucidate DNA unwinding." Nature **565**(7739): 382-385.

Brauner, A., Fridman, O., Gefen, O. and Balaban, N.Q. (2016) "Distinguishing between resistance, tolerance and persistence to antibiotic treatment." Nat Rev Microbiol **14**(5): 320-30

Brenner, S., Jacob, F. and Meselson, M. (1961) "An unstable intermediate carrying information from genes to ribosomes for protein synthesis." Nature **190**: 576-581.

Brian, B., Elizabeth, D., Daniel, B., Elizabeth, A. C., Sivaramesh, W. and Seth, A. D. (2013) "Phage T7 Gp2 inhibition of *Escherichia coli* RNA polymerase involves misappropriation of σ^{70} domain 1.1." PNAS **110**(49): 19772-19777.

Brian, P. H., Joel, Q., Samuel, L.-G., Younggyu, K., Helen, M. B., Eddy, A., Richard, H. E. and Catherine, L. L. (2009) "Three-Dimensional EM Structure of an Intact Activator-Dependent Transcription Initiation Complex." PNAS **106**(47): 19830-19835.

Briat, J.-F., Bollag, G., Kearney, C. A., Molineux, I. and Chamberlin, M. J. (1987) "Tau factor from *Escherichia coli* mediates accurate and efficient termination of transcription at the bacteriophage T3 early termination site *in vitro*." Journal of Molecular Biology **198**(1): 43-49.

Browning, D. F. and Busby, S. J. W. (2004) "The regulation of bacterial transcription initiation." Nature Reviews Microbiology **2**(1): 57-65.

Browning, D. F. and Busby, S. J. W. (2016) "Local and global regulation of transcription initiation in bacteria." Nature Reviews Microbiology **14**(10): 638-650.

Brozek, K. A., Hosaka, K., Robertson, A. D. and Raetz, C. R. (1989) "Biosynthesis of lipopolysaccharide in *Escherichia coli*. Cytoplasmic enzymes that attach 3-deoxy-D-manno-octulosonic acid to lipid A." J Biol Chem **264**(12): 6956-66.

Brozek, K. A. and Raetz, C. R. (1990) "Biosynthesis of lipid A in *Escherichia coli*. Acyl carrier protein-dependent incorporation of laurate and myristate" J Biol Chem **265**(26): 15410-7.

Buck, M., Gallegos, M. a.-T., Studholme, D. J., Guo, Y. and Gralla, J. D. (2000a) "The Bacterial Enhancer-Dependent ς54(ςN) Transcription Factor." Journal of Bacteriology **182**(15): 4129-4136.

Buck, M., van Heel, M., Finn, R. D., Gowen, B. and Orlova, E. V. (2000b) "*Escherichia coli* RNA polymerase core and holoenzyme structures." The EMBO Journal **19**(24): 6833-6844.

Buckley, A. M., Webber, M. A., Cooles, S., Randall, L. P., La Ragione, R. M., Woodward, M. J. and Piddock, L. J. V. (2006) "The AcrAB–TolC efflux system of *Salmonella enterica* serovar Typhimurium plays a role in pathogenesis." Cellular Microbiology **8**(5): 847-856.

Burgess, R. R., Travers, A. A., Dunn, J. J. and Bautz, E. K. (1969) "Factor stimulating transcription by RNA polymerase." Nature **221**(5175): 43-46.

Burns, C. M., Richardson, L. V. and Richardson, J. P. (1998) "Combinatorial effects of NusA and NusG on transcription elongation and Rho-dependent termination in Escherichia coli" Journal of Molecular Biology **278**(2): 307.

Busby, S. and Ebright, R. H. (1999) "Transcription activation by catabolite activator protein (CAP)." Journal of Molecular Biology **293**(2): 199-213.

Campbell, E. A., Muzzin, O., Chlenov, M., Sun, J. L., Olson, C. A., Weinman, O., Trester-Zedlitz, M. L. and Darst, S. A. (2002) 'Structure of the Bacterial RNA Polymerase Promoter Specificity σ Subunit." Molecular Cell **9**(3): 527-539.

Carmen, M., Manuel, M. and Carmen, P. (2002) "SoxRS Down-Regulation of rob Transcription." Journal of Bacteriology **184**(17): 4733-4738.

Carstenius, P., Flock, J. and Lindberg, A. (1990) 'Nucleotide sequence of r*fal* and r*faJ* genes encoding lipopolysaccharide glycosyl transferases from S*almonella typhimurium*." Nucleic Acids Research **18**(20): 6128.

Cases, I., de Lorenzo, V. and Ouzounis, C.A. (2003) "Transcription regulation and environmental adaptation in bacteria." Trends Microbiol **11**(6): 248-253.

Chaudhuri, R.R. and Henderson, I.R. (2012) "The evolution of the Escherichia coli phylogeny." Infect Genet Evol **12**(2): 214-26.

Chen, H., Tang, H. and Ebright, R. H. (2003) "Functional interaction between RNA polymerase alpha subunit C-terminal domain and sigma^{70} in UP-element- and activator-dependent transcription." Molecular Cell **11**(6): 1621.

Chen, J., Chiu, C., Gopalkrishnan, S., Chen, A. Y., Olinares, P. D. B., Saecker, R. M., Winkelman, J. T., Maloney, M. F., Chait, B. T., Ross, W., Gourse, R. L., Campbell, E. A. and Darst, S. A. (2020) "Stepwise Promoter Melting by Bacterial RNA Polymerase." Molecular Cell **78**(2): 275-288.

Chen, L. and Coleman, W. G. (1993) "Cloning and characterization of the *Escherichia coli* K-12 *rfa*-2 (*rfaC*) gene, a gene required for lipopolysaccharide inner core synthesis." J Bacteriol **175**(9): 2534-40.

Chen, M. H., Steiner, M. G., de Laszlo, S. E., Patchett, A. A., Anderson, M. S., Hyland, S. A., Onishi, H. R., Silver, L. L. and Raetz, C. R. (1999) "Carbohydroxamido-oxazolidines: antibacterial agents that target lipid A biosynthesis." Bioorg Med Chem Lett **9**(3): 313-8.

Chetri, S., Das, B. J., Bhowmik, D., Chanda, D. D., Chakravarty, A. and Bhattacharjee, A. (2020) "Transcriptional response of *mar, sox* and *rob* regulon against concentration gradient carbapenem stress within *Escherichia coli* isolated from hospital acquired infection." BMC Research Notes **13**(1): 168.

Chetri, S., Singha, M., Bhowmik, D., Nath, K., Chanda, D. D., Chakravarty, A. and Bhattacharjee, A. (2019) "Transcriptional response of OmpC and OmpF in *Escherichia coli* against differential gradient of carbapenem stress." BMC Research Notes **12**(1): 138.

Chi, X., Fan, Q., Zhang, Y., Liang, K., Wan, L., Zhou, Q. and Li, Y. (2020) "Structural mechanism of phospholipids translocation by MlaFEDB complex." Cell Res **30**(12): 1127-1135.

Cho, B.K., Barrett, C.L., Knight, E.M., Park, Y.S. and Palsson, B. (2008) "Genome-scale reconstruction of the Lrp regulatory network in Escherichia coli." Proc Natl Acad Sci U S A **105**(49): 19462-7.

Cho, B.K., Kim, D., Knight, E. M., Zengler, K. and Palsson, B. O. (2014) 'Genome-scale reconstruction of the sigma factor network in *Escherichia coli*: topology and functional states." BMC biology **12**(1): 4.

Choi, J. and Groisman, E. A. (2020) "Salmonella expresses foreign genes during infection by degrading their silencer." PNAS **117**(14): 8074-8082.

Chuc, N. T. K. and Tomson, G. (1999) "“Doi moi” and private pharmacies: a case study on dispensing and financial issues in Hanoi, Vietnam." European Journal of Clinical Pharmacology **55**(4): 325-332.

Clements, J. M., Coignard, F., Johnson, I., Chandler, S., Palan, S., Waller, A., Wijkmans, J. and Hunter, M. G. (2002) "Antibacterial activities and characterization of novel inhibitors of LpxC." Antimicrob Agents Chemother **46**(6): 1793-9.

Clementz, T., Bednarski, J. J. and Raetz, C. R. (1996) "Function of the *htrB* high temperature requirement gene of *Escherichia coli* in the acylation of lipid A: HtrB catalyzed incorporation of laurate." J Biol Chem, **271**(20): 12095–102.

Clementz, T. and Raetz, C. R. (1991) "A gene coding for 3-deoxy-D-manno-octulosonic-acid transferase in *Escherichia coli*. Identification, mapping, cloning, and sequencing." J Biol Chem **266**(15): 9687-96.

Clementz, T., Zhou, Z. and Raetz, C. R. (1997) "Function of the *Escherichia coli msbB* gene, a multicopy suppressor of *htrB* knockouts, in the acylation of lipid A. Acylation by MsbB follows laurate incorporation by HtrB." J Biol Chem **272**(16): 10353–60.

Cobb, M. (2017) "60 years ago, Francis Crick changed the logic of biology." PLoS biology **15**(9): e2003243.

Cohen, F., Aggen, J. B., Andrews, L. D., Assar, Z., Boggs, J., Choi, T., Dozzo, P., Easterday, A. N., Haglund, C. M., Hildebrandt, D. J., Holt, M. C., Joly, K., Jubb, A., Kamal, Z., Kane, T. R., Konradi, A. W., Krause, K. M., Linsell, M. S., Machajewski, T. D., Miroshnikova, O., Moser, H. E., Nieto, V., Phan, T., Plato, C., Serio, A. W., Seroogy, J., Shakhmin, A., Stein, A. J., Sun, A. D., Sviridov, S., Wang, Z., Wlasichuk, K., Yang, W., Zhou, X., Zhu, H. and Cirz, R. T. (2019) "Optimization of LpxC Inhibitors for Antibacterial Activity and Cardiovascular Safety." ChemMedChem **14**(16): 1560-1572.

Cohen, S. P., Hächler, H. and Levy, S. B. (1993) "Genetic and functional analysis of the multiple antibiotic resistance (*mar*) locus in *Escherichia coli*." Journal of Bacteriology **175**(5): 1484-1492.

Cohen, S. P., McMurray, L. M., Hooper, D. C., Wolfson, J. S. and Levy, S. B. (1989) "Cross-Resistance to Fluoroquinolones in MultipleAntibiotic-Resistant (Mar) Escherichia coli Selected by Tetracycline or Chloramphenicol: Decreased Drug Accumulation Associated with Membrane Changes in Addition to OmpF Reduction." Antimicrobial Agents and Chemotherapy **33**(8): 1318-1325.

Coleman, W. G. (1983) "The *rfaD* gene codes for ADP-L-glycero-D-mannoheptose-6-epimerase. An enzyme required for lipopolysaccharide core biosynthesis." J Biol Chem **258**(3): 1985-90.

Colland, F., Kolb, A., Hengge-Aronis, R. and Barth, M. (2000) "σ factor selectivity of *Escherichia coli* RNA polymerase: role for CRP, IHF and Lrp transcription factors." The EMBO Journal **19**(12): 3028-3037.

Connell, S.R., Tracz, D.M., Nierhaus, K.H. and Taylor, D.E. (2003) "Ribosomal protection proteins and their mechanism of tetracycline resistance." Antimicrob Agents Chemother **47**(12): 3675-81.

Cox, G. and Wright, G.D. (2013) "Intrinsic antibiotic resistance: mechanisms, origins, challenges and solutions." Int J Med Microbiol **303**(6-7): 287-92.

Crick, F. (1958) "On protein synthesis." Symp Soc Exp Biol. **12**: 138-163.

Dalebroux, Z. D. and Swanson, M. S. (2012) "ppGpp: magic beyond RNA polymerase." Nature Reviews Microbiology **10**(3): 203-212.

Dangi, B., Gronenborn, A. M., Rosner, J. L. and Martin, R. G. (2004) "Versatility of the carboxy-terminal domain of the α subunit of RNA polymerase in transcriptional activation: use of the DNA contact site as a protein contact site for MarA." Molecular Microbiology **54**(1): 45-59.

Dangi, B., Pelupessey, P., Martin, R. G., Rosner, J. L., Louis, J. M. and Gronenborn, A. M. (2001) "Structure and dynamics of MarA-DNA complexes: an NMR investigation." J Mol Biol. **314**(1): 113-27.

Darst, S. A., Kubalek, E. W. and Kornberg, R. D. (1989) "Three-dimensional structure of *Escherichia coli* RNA polymerase holoenzyme determined by electron crystallography." Nature **340**(6236): 730-732.

De Majumdar, S., Yu, J., Fookes, M., McAteer, S. P., Llobet, E., Finn, S., Spence, S., Monahan, A., Monaghan, A., Kissenpfennig, A., Ingram, R. J., Bengoechea, J., Gally, D. L., Fanning, S., Elborn, J. S. and Schneiders, T. (2015) "Elucidation of the RamA regulon in *Klebsiella pneumoniae* reveals a role in LPS regulation." PLoS Pathogens **11**(1): e1004627.

Deborah, J. E., Vito, R. and Laura, J. V. P. (2004) "Expression of *acrB, acrF, acrD, marA*, and *soxS* in *Salmonella enterica* Serovar Typhimurium: Role in Multiple Antibiotic Resistance." Antimicrobial Agents and Chemotherapy **48**(4): 1145-1150.

deHaseth (2003) "Probing the role of region 2 of Escherichia coli σ 70 in nucleation and maintenance of the single-stranded DNA bubble in RNA polymerase–promoter open complexes." Methods Enzymol **370**: 553-567.

deHaseth, P. L., Zupancic, M. L. and Record, M. T. (1998) "RNA Polymerase-Promoter Interactions: The Comings and Goings of RNA Polymerase." Journal of Bacteriology **180**(12): 3019-3025.

Delihas, N. and Forst, S. (2001) "MicF: An Antisense RNA Gene Involved in Response of *Escherichia coli* to Global Stress Factors." J Mol Bio **313**(1):1-12.

Dönhöfer, A., Franckenberg, S., Wickles, S., Berninghausen, O., Beckmann, R. and Wilson, D.N. (2012) "Structural basis for TetM-mediated tetracycline resistance." Proc Natl Acad Sci U S A **109**(42): 16900-5.

Dorman, C. J. and Dillon, S. C. (2010) "Bacterial nucleoid-associated proteins, nucleoid structure and gene expression." Nature Reviews Microbiology **8**(3): 185-195.

Dove, S. L., Darst, S. A. and Hochschild, A. (2003) "Region 4 of σ as a target for transcription regulation." Molecular Microbiology **48**(4): 863-874.

Doxycycline. Available at: http://*www.drugbank.ca* (Accessed: 24th May 2022).

Dreger, A., Hoff, K., Agoglitta, O., Hotop, S. K., Brönstrup, M., Heisig, P., Kirchmair, J. and Holl, R. (2021) "Antibacterial activity of xylose-derived LpxC inhibitors - Synthesis, biological evaluation and molecular docking studies." Bioorg Chem **107**: 104603.

Duval, V. and Lister, I. M. (2013) "MarA, SoxS and Rob of Escherichia coli – Global Regulators of Multidrug Resistance, Virulence and Stress Response." International Journal of Biotechnology for Wellness Industries, **2**(3): 101-124.

Ebright, R. H. (1993) "Transcription activation at Class I CAP-dependent promoters." Molecular Microbiology **8**(5): 797-802.

Egan, S. M. (2002) "Growing Repertoire of AraC/XylS Activators." Journal of bacteriology **184**(20): 5529-5532.

Emiola, A., George, J. and Andrews, S. S. (2014) "A Complete Pathway Model for Lipid A Biosynthesis in *Escherichia coli*." PLoS One **10**(4): e0121216.

Escobar-Páramo, P., Le Menac'h, A., Le Gall, T., Amorin, C., Gouriou, S., Picard, B., Skurnik, D. and Denamur, E. (2006) "Identification of forces shaping the commensal Escherichia coli genetic structure by comparing animal and human isolates." Environ Microbiol **8**(11): 1975-84.

Estrem, S. T., Gaal, T., Ross, W. and Gourse, R. L. (1998) "Identification of an UP element consensus sequence for bacterial promoters." PNAS **95**(17): 9761-9766.

Etienne, G., Axel, C., Dominique, K. and Elisabeth, C.D. (2000) "Evidence for Active Efflux as the Primary Mechanism of Resistance to Ciprofloxacin in *Salmonella enterica* Serovar Typhimurium." Antimicrobial Agents and Chemotherapy **44**(5): 1223-1228.

EUCAST (2023) Breakpoint tables for interpretation of MICs and zone diameters available: [accessed 1st April 2023].

Fawcett, W. P. and Wolf, R. E. (1995) "Genetic definition of the *Escherichia coli zwf* "soxbox," the DNA binding site for SoxS-mediated induction of glucose 6-phosphate dehydrogenase in response to superoxide." J Bacteriol **177**(7): 1742-50.

Federowicz, S., Kim, D., Ebrahim, A., Lerman, J., Nagarajan, H., Cho, B.K., Zengler, K. and Palsson, B. (2014) "Determining the control circuitry of redox metabolism at the genome-scale." PLoS Genet **10**(4): e1004264.

Feklistov, A. and Darst, Seth A. (2011) "Structural Basis for Promoter −10 Element Recognition by the Bacterial RNA Polymerase σ Subunit." Cell **147**(6): 1257-1269.

Feklístov, A., Sharon, B. D., Darst, S. A. and Gross, C. A. (2014) "Bacterial Sigma Factors: A Historical, Structural, and Genomic Perspective." Annual Review of Microbiology **68**(1): 357-376.

Feng, Y., Zhang, Y. and Ebright, R. H. (2016) "Structural basis of transcription activation." Science **352**(6291): 1330-1333.

Folch, J., Lees, M. and Sloane, S. G. H. (1957) "A simple method for the isolation and purification of total lipides from animal tissues." The Journal of Biological Chemistry **226**(1): 497.

Friedman, D. I. (1988) "Integration host factor: A protein for all reasons." Cell **55**:545:554.

Fujita, K., Takata, I., Yoshida, I., Honma, Y., Okumura, H., Otake, K., Takashima, H. and Sugiyama, H. (2022) "Pharmacodynamic target assessment and prediction of clinically effective dosing regimen of TP0586532, a novel non-hydroxamate LpxC inhibitor, using a murine lung infection model." J Infect Chemother **28**(5): 635-642.

Fujita, K., Takata, I., Yoshida, I., Okumura, H., Otake, K., Takashima, H. and Sugiyama, H. (2021) 'TP0586532, a non-hydroxamate LpxC inhibitor, has *in vitro* and *in vivo* antibacterial activities against Enterobacteriaceae." J Antibiot **75**(2): 98-107.

Gaal, T., Bartlett, M. S., Ross, W., Turnbough, C. L., Jr. and Gourse, R. L. (1997) 'Transcription Regulation by Initiating NTP Concentration: rRNA Synthesis in Bacteria" Science **278**(5346): 2092-2097.

Garavaglia, M., Rossi, E. and Landini, P. (2012) "The Pyrimidine Nucleotide Biosynthetic Pathway Modulates Production of Biofilm Determinants in *Escherichia coli*." PloS one **7**(2): e31252.

Gentry, D. R. and Burgess, R. R. (1989) "*rpoZ*, encoding the omega subunit of *Escherichia coli* RNA polymerase, is in the same operon as *spoT*." Journal of Bacteriology **171**(3): 1271-1277.

George, A. M., Hall, R. M. and Stokes, H. W. (1995) "Multidrug resistance in *Klebsiella pneumoniae*: a novel gene, *ramA*, confers a multidrug resistance phenotype in *Escherichia coli*." Microbiology **141**(8): 1909-1920.

Gillette, W. K., Martin, R. G. and Rosner, J. L. (2000) "Probing the *Escherichia coli* transcriptional activator MarA using alanine-scanning mutagenesis: residues important for DNA binding and activation." Journal of Molecular Biology **299**(5): 1245-1255.

Glauert, A. M. and Thornley, M. J. (1969) "The topography of the bacterial cell wall." Annu Rev Microbiol **23**: 159-98.

Gnatt, A. L., Cramer, P., Fu, J., Bushnell, D. A. and Kornberg, R. D. (2001) "Structural Basis of Transcription: An RNA Polymerase II Elongation Complex at 3.3 A Resolution." Science **292**(5523): 1876-1882.

Goodarzi, R., Arabestani, M., Alikhani, M. Y., Keramat, F. and Asghari, B. (2021) "Emergence of tigecycline-resistant *Klebsiella pneumoniae* ST11 clone in patients without exposure to tigecycline." J Infect Dev Ctries **15**(11): 1677-1684.

Gourse, R. L., Ross, W. and Gaal, T. (2000) "UPs and downs in bacterial transcription initiation: the role of the alpha subunit of RNA polymerase in promoter recognition." Molecular Microbiology **37**(4): 687-695.

Grainger, D. C., Belyaeva, T. A., Lee, D. J., Hyde, E. I. and Busby, S. J. W. (2003) "Binding of the *Escherichia coli* MelR protein to the *melAB* promoter: orientation of MelR subunits and investigation of MelR–DNA contacts." Molecular Microbiology **48**(2): 335-348.

Greenblatt, J. and Schleif, R. (1971) "Arabinose C Protein: Regulation of the Arabinose Operon *in vitro."* Nature: New Biology **233**(40): 166-170.

Griffith, K. L., Fitzpatrick, M. M., Keen, r. E. F. and Wolf, J. R. E. (2009) "Two functions of the C-terminal domain of Escherichia coli Rob: mediating "sequestration-dispersal" as a novel off-on switch for regulating Rob's activity as a transcription activator and preventing degradation of Rob by Lon protease." Journal of Molecular Biology **388**(3): 415-430.

Griffith, K. L., Shah, I. M. and E. Wolf, R. (2004) "Proteolytic degradation of *Escherichia coli* transcription activators SoxS and MarA as the mechanism for reversing the induction of the superoxide (SoxRS) and multiple antibiotic resistance (Mar) regulons." Molecular Microbiology **51**(6): 1801-1816.

Gruber, T. M. and Gross, C. A. (2003) "Multiple sigma subunits and the partitioning of bacterial transcription space." Annual Review of Microbiology **57**: 441-466.

Gunnelius, L., Hakkila, K., Kurkela, J., Wada, H., Tyystjärvi, E. and Tyystjärvi, T. (2014) "The omega subunit of the RNA polymerase core directs transcription efficiency in cyanobacteria." Nucleic Acids Research **42**(7): 4606-4614.

Gustafsson, P., Nordström, K. and Normark, S. (1973) "Outer penetration barrier of Escherichia coli K-12: kinetics of the uptake of gentian violet by wild type and envelope mutants." J Bacteriol **16**(2):893-900.

Halder, S., Yadav, K. K., Sarkar, R., Mukherjee, S., Saha, P., Haldar, S., Karmakar, S. and Sen, T. (2015) "Alteration of Zeta potential and membrane permeability in bacteria: a study with cationic agents." Springerplus **4**: 672.

Hampsey, M. (2001) 'Omega meets its match." Trends in Genetics **17**(4): 190-191.

Hampton, T. (2013) "Report Reveals Scope of US Antibiotic Resistance Threat." JAMA **310**(16): 1661-1663.

Hart, C. M. and Roberts, J. W. (1994) "Deletion Analysis of the Lambda tR1 Termination Region: Effect of Sequences near the Transcript Release Sites, and the Minimum Length of Rho-dependent Transcripts." Journal of Molecular Biology **237**(3): 255-265.

Hashimoto, Y., Kurushima, J., Nomura, T., Tanimoto, K., Tamai, K., Yanagisawa, H., Shirabe, K., Ike, Y. and Tomita, H. (2018) "Dissemination and genetic analysis of the stealthy vanB gene clusters of *Enterococcus faecium* clinical isolates in Japan." BMC Microbiology **18**(1): 213.

Hassan, K.A., Elbourne, L.D., Li, L., Gamage, H.K., Liu, Q., Jackson, S.M., Sharples, D., Kolstø, A.B., Henderson, P.J. and Paulsen, I.T. (2015) "An ace up their sleeve: a transcriptomic approach exposes the AceI efflux protein of Acinetobacter baumannii and reveals the drug efflux potential hidden in many microbial pathogens." Front Microbiol **6:** 333.

Hein, P. P. and Landick, R. (2010) "The bridge helix coordinates movements of modules in RNA polymerase." BMC Biology **8**(1): 141.

Heinrichs, D. E., Yethon, J. A., Amor, P. A. and Whitfield, C. (1998) "The assembly system for the outer core portion of R1- and R4-type lipopolysaccharides of Escherichia coli. The R1 core-specific beta-glucosyltransferase provides a novel attachment site for O-polysaccharides." J Biol Chem **273**(45): 29497-505.

Heinrichs, D. E., Yethon, J. A. and Whitfield, C. (1998) "Molecular basis for structural diversity in the core regions of the lipopolysaccharides of *Escherichia coli* and *Salmonella enterica*." Mol Microbiol **30**(2): 221-32.

Helen, W. B., George, H. T., John, S. B., John, E. E., David, G., Louis, B. R., Michael, S., Brad, S. and John, B. (2009) "Bad Bugs, No Drugs: No ESKAPE! An Update from the Infectious Diseases Society of America." Clinical Infectious Diseases **48**(1): 1-12.

Helmann, J. D. and Chamberlin, M. J. (1988) "Structure and Function of Bacterial Sigma Factors." Annual Review of Biochemistry **57**(1): 839-872.

Henderson, T. A., Templin, M. and Young, K. D. (1995) "Identification and cloning of the gene encoding penicillin-binding protein 7 of *Escherichia coli*." J Bacteriol **177**(8): 2074-9.

Hermansson, M., Uphoff, A., Käkelä, R. and Somerharju, P. (2005) "Automated quantitative analysis of complex lipidomes by liquid chromatography/mass spectrometry." Analytical Chem **77**(7): 2166-75.

Hidalgo, E., Leautaud, V. and Demple, B. (1998) "The redox-regulated SoxR protein acts from a single DNA site as a repressor and an allosteric activator." The EMBO Journal **17**(9): 2629-2636.

Holmes, R. K. and Jobling, M. G. (1996) "Chapter 5: Genetics." in Baron, S. (ed.) Medical Microbiology. Galveston (TX): University of Texas Medical Branch at Galveston.

Holst, O. and Brade, H. (1992) "Chemical structure of the core region of lipopolysaccharides" in Morrison, D.C. and Ryan, J.L. (eds.) Bacterial Endotoxic Lipopolysaccharides. Boca Raton: CRC Press: 135-169.

Howard, V. J., Belyaeva, T. A., Busby, S. J. W. and Hyde, E. I. (2002) "DNA binding of the transcription activator protein MelR from Escherichia coli and its C-terminal domain." Nucleic Acids Res **30**(12):2692:700.

Hughes, G. W., Hall, S. C. L., Laxton, C. S., Sridhar, P., Mahadi, A. H., Hatton, C., Piggot, T. J., Wotherspoon, P. J., Leney, A. C., Ward, D. G., Jamshad, M., Spana, V., Cadby, I. T., Harding, C., Isom, G. L., Bryant, J. A., Parr, R. J., Yakub, Y., Jeeves, M., Huber, D., Henderson, I. R., Clifton, L. A., Lovering, A. L. and Knowles, T. J. (2019) "Evidence for phospholipid export from the bacterial inner membrane by the Mla ABC transport system." Nat Microbiol **4**(10): 1692-1705.

Hummel, J., Segu, S., Li, Y., Irgang, S., Jueppner, J. and Giavalisco, P. (2011) "Ultra performance liquid chromatography and high resolution mass spectrometry for the analysis of plant lipids." Front Plant Sci **2**: 54.

Höltje, J. V. (1998) "Growth of the stress-bearing and shape-maintaining murein sacculus of *Escherichia coli*." Microbiol Mol Biol Rev **62**(1): 181-203.

Igarashi, K., Fujita, N. and Ishihama, A. (1991) "Identification of a subunit assembly domain in the alpha subunit of *Escherichia coli* RNA polymerase." Journal of Molecular Biology **218**(1): 1-6.

Iyer, S. C., Casas-Pastor, D., Kraus, D., Mann, P., Schirner, K., Glatter, T., Fritz, G. and Ringgaard, S. (2020) 'Transcriptional regulation by σ factor phosphorylation in bacteria." Nature Microbiology **5**(3): 395-406.

Jackman, J. E., Fierke, C. A., Tumey, L. N., Pirrung, M., Uchiyama, T., Tahir, S. H., Hindsgaul, O. and Raetz, C. R. (2000) "Antibacterial agents that target lipid A biosynthesis in Gram-negative bacteria. Inhibition of diverse UDP-3-O-(r-3-hydroxymyristoyl)-n-acetylglucosamine deacetylases by substrate analogs containing zinc binding motifs." J Biol Chem **275**(15): 11002-9.

Jackman, J. E., Raetz, C. R. and Fierke, C. A. (1999) "UDP-3-O-(R-3-hydroxymyristoyl)-N-acetylglucosamine deacetylase of Escherichia coli is a zinc metalloenzyme." Biochemistry **38**(6): 1902-11.

Jair, K. W., Yu, X., Skarstad, K., Thöny, B., Fujita, N., Ishihama, A. and Wolf, R. E. (1996) "Transcriptional activation of promoters of the superoxide and multiple antibiotic resistance regulons by Rob, a binding protein of the Escherichia coli origin of chromosomal replication." J Bacteriol. **178**(9): 2507-13.

James, R. J., Abby, G., Alan, J. L. and Thomas, A. R. (2003) "Extraintestinal Pathogenic *Escherichia coli* as a Cause of Invasive Nonurinary Infections." Journal of Clinical Microbiology **41**(12): 5798-5802.

Jeon, Y. H., Yamazaki, T., Otomo, T., Ishihama, A. and Kyogoku, Y. (1997) "Flexible linker in the RNA polymerase alpha subunit facilitates the independent motion of the C-terminal activator contact domain." Journal of Molecular Biology **267**(4): 953-962.

Jeong, K.-C., Baumler, D. J. and Kaspar, C. W. (2006) "*dps* expression in *Escherichia coli* O157:H7 requires an extended − 10 region and is affected by the cAMP receptor protein." BBA - Gene Structure and Expression **1759**(1): 51-59.

Jishage, M. and Ishihama, A. (1998) "A stationary phase protein in *Escherichia coli* with binding activity to the major sigma subunit of RNA polymerase." PNAS **95**(9): 4953.

John, H. T. and George, A. J. (2002) "Mechanism of Plasmid-Mediated Quinolone Resistance." PNAS **99**(8): 5638-5642.

Jovanović, N., Jovanović, J., Stefan-Mikić, S., Kulauzov, M., Aleksic-Dordević, M. and Cvjetković, D. (2008) "Mechanisms of bacterial resistance to antibiotics." Medicinski Pregled **61**(1): 9.

Kacena, M. A., Merrell, G. A., Manfredi, B., Smith, E. E., Klaus, D. M. and Todd, P. (1999) 'Bacterial growth in space flight: logistic growth curve parameters for *Escherichia coli* and *Bacillus subtilis*." Appl Microbiol Biotechnol. **51**(2): 229-34.

Kamio, Y. and Nikaido, H. (1976) "Outer membrane of *Salmonella typhimurium*: accessibility of phospholipid head groups to phospholipase c and cyanogen bromide activated dextran in the external medium." Biochemistry **15**(12): 2561-70.

Kapanidis, A. N., Margeat, E., Ho, S. O., Kortkhonjia, E., Weiss, S. and Ebright, R. H. (2006) "Initial Transcription by RNA Polymerase Proceeds Through a DNA-Scrunching Mechanism." Science **314**(5802): 1144-1147.

Kaper, J. B., Nataro, J. P. and Mobley, H. L. (2004) "Pathogenic *Escherichia coli*." Nature Reviews Microbiology **2**: 123-140.

Karen, J. H., Hiroshi, N. and Michio, M. (1981) "Mutants of *Escherichia coli* That Are Resistant to Certain Beta-Lactam Compounds Lack the *ompF* Porin." Antimicrobial Agents and Chemotherapy **20**(4): 549-552.

Kassavetis, G. A. and Chamberlin, M. J. (1981) "Pausing and termination of transcription within the early region of bacteriophage T7 DNA *in vitro*." Journal of Biological Chemistry **256**(6): 2777.

Kate, L. H., Lindsey, C. F., Cristen, M. M., Irina, S., Si, W., Munish, C., Emily, F. R., Lauren, B., Joseph, E. K. and Record, M. T. (2017) "Mechanism of transcription initiation and promoter escape by *E. coli* RNA polymerase." PNAS Plus **114**(15): e3032-e3040.

Keck, W. and Schwarz, U. (1979) "*Escherichia coli* murein-DD-endopeptidase insensitive to beta-lactam antibiotics." J Bacteriol **139**(3): 770-4.

Keeney, D., Ruzin, A., McAleese, F., Murphy, E. and Bradford, P. A. (2008) "MarA-mediated overexpression of the AcrAB efflux pump results in decreased susceptibility to tigecycline in Escherichia coli." Journal of Antimicrobial Chemotherapy **61**(1): 46-53.

Kelly, T. M., Stachula, S. A., Raetz, C. R. and Anderson, M. S. (1993) 'The *firA* gene of *Escherichia coli* encodes UDP-3-O-(R-3-hydroxymyristoyl)-glucosamine N-acyltransferase. The third step of endotoxin biosynthesis." J Biol Chem **268**(26): 19866-74.

Keseler, I. M., Mackie, A., Santos-Zavaleta, A., Billington, R., Bonavides-Martínez, C., Caspi, R., Fulcher, C., Gama-Castro, S., Kothari, A., Krummenacker, M., Latendresse, M., Muñiz-Rascado, L., Ong, Q., Paley, S., Peralta-Gil, M., Subhraveti, P., Velázquez-Ramírez, D. A., Weaver, D., Collado-Vides, J., Paulsen, I. and Karp, P. D. (2017) "The EcoCyc database: reflecting new knowledge about *Escherichia coli* K-12." Nucleic Acids Research **45**(1): 543-550.

Kettles, R. A., Tschowri, N., Lyons, K. J., Sharma, P., Hengge, R., Webber, M. A. and Grainger, D. C. (2019) "The *Escherichia coli* MarA protein regulates the *ycgZ-ymgABC* operon to inhibit biofilm formation." Mol Microbiol **112**(5): 1609-1625.

Kimberly, A. W. and Robert, O. (2002) "Factors Affecting Start Site Selection at the *Escherichia coli* *fis* Promoter." Journal of Bacteriology 184(17): 4783-4791.

Kind, T., Liu, K. H., Lee, D. Y., DeFelice, B., Meissen, J. K. and Fiehn, O. (2013) "LipidBlast *in silico* tandem mass spectrometry database for lipid identification." Nat Methods **10**(8): 755-8.

Kishida, H., Unzai, S., Roper, D. I., Lloyd, A., Park, S. Y. and Tame, J. R. (2006) "Crystal structure of penicillin binding protein 4 (*dacB*) from *Escherichia coli*, both in the native form and covalently linked to various antibiotics." Biochemistry **45**(3): 783-92.

Klena, J. D., Ashford, R. S. and Schnaitman, C. A. (1992) "Role of *Escherichia coli* K-12 *rfa* genes and the *rfp* gene of *Shigella dysenteriae* 1 in generation of lipopolysaccharide core heterogeneity and attachment of O-antigen." J Bacteriol **174**(22): 7297-307.

Klug, A. and Rhodes, D. (1981) "Sequence-dependent helical periodicity of DNA." Nature **292**(5821): 378-380.

Kojima, I., Kasuga, K., Kobayashi, M., Fukasawa, A., Mizuno, S., Arisawa, A. and Akagawa, H. (2002) "The *rpoZ* Gene, Encoding the RNA Polymerase Omega Subunit, Is Required for Antibiotic Production and Morphological Differentiation in *Streptomyces kasugaensis*." Journal of Bacteriology **185**(1): 386.

Kolb, A., Busby, S., Buc, H., Garges, S. and Adhya, S. (1993) "Transcriptional regulation by cAMP and its receptor protein." Annu Rev Biochem **62**: 749-95.

Kolb, A., Kotlarz, D., Kusano, S. and Ishihama, A. (1995) "Selectivity of the *Escherichia coli* RNA polymerase $E\sigma^{38}$ for overlapping promoters and ability to support CRP activation." Nucleic Acids Research **23**(819-826).

Korzheva, N., Mustaev, A., Kozlov, M., Malhotra, A., Nikiforov, V., Goldfarb, A. and Darst, S. A. (2000) "A Structural Model of Transcription Elongation." Science **289**(5479): 619-625.

Kutkowska, J., Turska-Szewczuk, A., Kucharczyk, M., Kucharczyk, H., Zalewska, J. and Urbanik-Sypniewska, T. (2019) "Methicillin-resistant *Staphylococcus aureus* and glycopeptide-resistant enterococci in fecal samples of birds from South-Eastern Poland." BMC Veterinary Research **15**(1): 1-472.

Kwon, H. J., Bennik, M. H. J., Demple, B. and Ellenberger, T. (2000) "Crystal structure of the *Escherichia coli* Rob transcription factor in complex with DNA." Nature Structural Biology **7**(5): 424-430.

Körner, H., Sofia, H. J. and Zumft, W. G. (2003) "Phylogeny of the bacterial superfamily of Crp-Fnr transcription regulators: exploiting the metabolic spectrum by controlling alternative gene programs." FEMS Microbiology Reviews **27**(5): 559-592.

Lal, A., Krishna, S. and Seshasayee, A. S. N. (2018) "Regulation of Global Transcription in *Escherichia coli* by Rsd and 6S RNA." G3 **8**(6): 2079-2089.

Lamberti, L. M., Bourgeois, A. L., Fischer Walker, C. L., Black, R. E. and Sack, D. (2014) "Estimating Diarrheal Illness and Deaths Attributable to Shigellae and Enterotoxigenic *Escherichia coli* among Older Children, Adolescents, and Adults in South Asia and Africa." PLoS Neglected Tropical Diseases **8**(2): e2705.

Landis, L., Xu, J. and Johnson, R. C. (2000) "The cAMP receptor protein CRP can function as an osmoregulator of transcription in *Escherichia coli*." Genes & Development **14**(3): 389.

Lang, B., Blot, N., Bouffartigues, E., Buckle, M., Geertz, M., Gualerzi, C. O., Mavathur, R., Muskhelishvili, G., Pon, C. L., Rimsky, S., Stella, S., Babu, M. M. and Travers, A. (2007) "High-

affinity DNA binding sites for H-NS provide a molecular basis for selective silencing within proteobacterial genomes." Nucleic Acids Research **35**(18): 6330-6337.

Lange, R. and Hengge-Aronis, R. (1994) "The cellular concentration of the sigma S subunit of RNA polymerase in *Escherichia coli* is controlled at the levels of transcription, translation, and protein stability." Genes & development **8**(13): 1600-1612.

Laura, J. V. P., David, G. W., Karl, G., Lilian, P. and Deborah, J. G. (2000) "Evidence for an Efflux Pump Mediating Multiple Antibiotic Resistance in *Salmonella enterica* Serovar Typhimurium." Antimicrobial Agents and Chemotherapy **44**(11): 3118-3121.

Laura, M. M. and Stuart, B. L. (2010) "Evidence that Regulatory Protein MarA of *Escherichia coli* Represses rob by Steric Hindrance." Journal of Bacteriology **192**(15): 3977-3982.

Laura, T., Oleg, V. T. and Pieter, L. d. (2002) "Interaction of RNA Polymerase with Forked DNA: Evidence for Two Kinetically Significant Intermediates on the Pathway to the Final Complex." PNAS **99**(6): 3493-3498.

Lawson, C. L., Swigon, D., Murakami, K. S., Darst, S. A., Berman, H. M. and Ebright, R. H. (2004) "Catabolite activator protein: DNA binding and transcription activation" Current Opinion in Structural Biology 14(1): 10-20.

Layec, S., Decaris, B. and Leblond-Bourget, N. (2008) "Diversity of Firmicutes peptidoglycan hydrolases and specificities of those involved in daughter cell separation." Res Microbiol **159**(7-8): 507-15.

Levin, J. R., Krummel, B. and Chamberlin, M. J. (1987) "Isolation and properties of transcribing ternary complexes of *Escherichia coli* RNA polymerase positioned at a single template base." Journal of Molecular Biology **196**(1): 85-100.

Levin-Reisman, I., Brauner, A., Ronin, I. and Balaban, N.Q. (2019) "Epistasis between antibiotic tolerance, persistence, and resistance mutations." Proc Natl Acad Sci U S A **116**(29): 14734-14739.

Lewis, M. (1996) "Response: DNA Looping and Lac Repressor-CAP Interaction." Science **274**(5294): 1931-1932.

Li, B., Sun, J.Y., Han, L.Z., Huang, X.H., Fu, Q. and Ni, Y.X. (2010) "Phylogenetic groups and pathogenicity island markers in fecal Escherichia coli isolates from asymptomatic humans in China." Appl Environ Microbiol **76**(19): 6698-700.

Li, J., Horwitz, R., McCracken, S. and Greenblatt, J. (1992) "NusG, a new *Escherichia coli* elongation factor involved in transcriptional antitermination by the N protein of phage lambda." Journal of Biological Chemistry **267**(9): 6012.

Li, Z. and Demple, B. (1994) "SoxS, an activator of superoxide stress genes in *Escherichia coli*. Purification and interaction with DNA." Journal of Biological Chemistry **269**(28): 18371.

Li, Z. T., Sun, Y. C., Mao, X. J. and Wang, Y. P. (2002) "cAMP receptor protein (CRP) downregulates Klebsiella pneumoniae *nif* promoters in *Escherichia coli*." Chinese Science Bulletin **47**(19):1622-1628.

Liu, H., Leonas, K.K. and Zhao, Y. (2010) " Antimicrobial Properties and Release Profile of Ampicillin from Electrospun Poly(ε-caprolactone) Nanofiber Yarns." Journal of Engineered Fibers and Fabrics **5**(4): 10-19.

Liu, Y.Y. B. S., Wang, Y. P., Walsh, T. R. P., Yi, L.X. B. S., Zhang, R. P., Spencer, J. P., Doi, Y. M. D., Tian, G. P., Dong, B. B. S., Huang, X. P., Yu, L.-F. B. S., Gu, D. P., Ren, H. B. S., Chen, X. M. S., Lv, L. M. S., He, D. M. S., Zhou, H. P., Liang, Z. P., Liu, J.-H. P. and Shen, J. P. (2016) "Emergence of plasmid-mediated colistin resistance mechanism MCR-1 in animals and human beings in China: a microbiological and molecular biological study." Lancet Infectious Diseases **16**(2): 161-168.

Livermore, D.M. (2003) "Bacterial resistance: origins, epidemiology, and impact." Clin Infect Dis **36**(Suppl 1): S11-23.

Lodge, J., Fear, J., Busby, S., Gunasekaran, P. and Kamini, N. R. (1992) "Broad host range plasmids carrying the *Escherichia coli* lactose and galactose operons." FEMS Microbiology Letters **95**(2): 271-276.

Lon, M. C., George, D. G. and Christopher, V. R. (2012) "Transcriptional Cross Talk within the mar-*sox-rob* Regulon in *Escherichia coli* Is Limited to the *rob* and *marRAB* Operons." Journal of Bacteriology 194(18): 4867-4875.

Loutet, S. A., Flannagan, R. S., Kooi, C., Sokol, P. A. and Valvano, M. A. (2006) "A complete lipopolysaccharide inner core oligosaccharide is required for resistance of *Burkholderia cenocepacia* to antimicrobial peptides and bacterial survival *in vivo*." J Bacteriol **188**(6): 2073-80.

Ma, X., Prathapam, R., Wartchow, C., Chie-Leon, B., Ho, C. M., De Vicente, J., Han, W., Li, M., Lu, Y., Ramurthy, S., Shia, S., Steffek, M. and Uehara, T. (2020) " Structural and Biological Basis of Small Molecule Inhibition of Escherichia coli LpxD Acyltransferase Essential for Lipopolysaccharide Biosynthesis." ACS Infect Dis **6**(6): 1480-1489.

Madan Babu, M. and Teichmann, S. A. (2003) "Functional determinants of transcription factors in *Escherichia coli*: protein families and binding sites." Trends in Genetics **19**(2): 75-79.

Maeda, H., Fujita, N. and Ishihama, A. (2000) "Competition among seven *Escherichia coli* sigma subunits: relative binding affinities to the core RNA polymerase." Nucleic Acids Research **28**(18): 3497-3503.

Majewski, P., Gutowska, A., Sacha, P., Schneiders, T., Talalaj, M., Majewska, P., Zebrowska, A., Ojdana, D., Wieczorek, P., Hauschild, T., Kowalczuk, O., Niklinski, J., Radziwon, P. and Tryniszewska, E. (2020) "Expression of AraC/XylS stress response regulators in two distinct carbapenem-resistant *Enterobacter cloacae* ST89 biotypes." The Journal of Antimicrobial Chemotherapy **75**(5): 1146-1150.

Malinen, A. M., Bakermans, J., Aalto-Setälä, E., Blessing, M., Bauer, D. L. V., Parilova, O., Belogurov, G. A., Dulin, D. and Kapanidis, A. N. (2022) "Real-Time Single-Molecule Studies of RNA Polymerase–Promoter Open Complex Formation Reveal Substantial Heterogeneity Along the Promoter-Opening Pathway." Journal of Molecular Biology **434**.

Malinverni, J. C. and Silhavy, T. J. (2009) "An ABC transport system that maintains lipid asymmetry in the Gram-negative outer membrane." *PNAS,* **106**(19): 8009-14.

Mark, J. M. and Thomas, J. S. (2005) "Starvation for Different Nutrients in *Escherichia coli* Results in Differential Modulation of RpoS Levels and Stability." Journal of Bacteriology **187**(2): 434-442.

Marshall, N.J. and Piddock, L.J. (1997) "Antibacterial efflux systems." Microbiologia **13**(3): 285-300.

Martin, R. G., Jair, K. W., R. E. Wolf, J. and Rosner, J. L. (1996) "Autoactivation of the *marRAB* multiple antibiotic resistance operon by the MarA transcriptional activator in *Escherichia coli*." Journal of *Bacteriology* **178**(8): 2216-2223.

Martin, R. G., Nyantakyi, P. S. and Rosner, J. L. (1995) "Regulation of the multiple antibiotic resistance (mar) regulon by *marORA* sequences in *Escherichia coli*." Journal of Bacteriology **177**(14): 4176-4178.

Martin, R. G. and Rosner, J. L. (1997) "Fis, an accessorial factor for transcriptional activation of the *mar* (multiple antibiotic resistance) promoter of *Escherichia coli* in the presence of the activator MarA, SoxS, or Rob." Journal of Bacteriology **179**(23): 7410-7419.

Martínez-Antonio, A. and Collado-Vides, J. (2003) "Identifying global regulators in transcriptional regulatory networks in bacteria." Current Opinion in Microbiology **6**(5): 482-489.

Martucci, N., Lamberti, A., Vitagliano, L., Cantiello, P., Ruggiero, I., Arcari, P. and Masullo, M. (2012) "The magic spot ppGpp influences in vitro the molecular and functional properties of the elongation factor 1α from the archaeon *Sulfolobus solfataricus*." Extremophiles **16**(5): 743-749.

Mathew, R. and Chatterji, D. (2006) "The evolving story of the omega subunit of bacterial RNA polymerase." Trends in Microbiology **14**(10): 450-455.

McDermott, P. F., McMurry, L. M., Podglajen, I., Dzink-Fox, J. L., Schneiders, T., Draper, M. P. and Levy, S. B. (2008) "The *marC* Gene of *Escherichia coli* Is Not Involved in Multiple Antibiotic Resistance." Antimicrobial agents and chemotherapy **52**(1): 382-383.

Meier-Dieter, U., Starman, R., Barr, K., Mayer, H. and Rick, P. D. (1990) "Biosynthesis of enterobacterial common antigen in *Escherichia coli*. Biochemical characterization of Tn10 insertion mutants defective in enterobacterial common antigen synthesis." J Biol Chem **265**(23): 13490-7.

Mekler, V., Kortkhonjia, E., Mukhopadhyay, J., Knight, J., Revyakin, A., Kapanidis, A. N., Niu, W., Ebright, Y. W., Levy, R. and Ebright, R. H. (2002) "Structural Organization of Bacterial RNA Polymerase Holoenzyme and the RNA Polymerase-Promoter Open Complex." Cell **108**(5): 599-614.

Méndez-Moreno, E., Caporal-Hernandez, L., Mendez-Pfeiffer, P.A., Enciso-Martinez, Y., De la Rosa López, R., Valencia, D., Arenas-Hernández, M.M.P., Ballesteros-Monrreal, M.G. and Barrios-Villa, E. (2022) "Characterization of Diarreaghenic." Antibiotics (Basel) **11**(7).

Mendoza-Vargas, A., Olvera, L., Olvera, M., Grande, R., Vega-Alvarado, L., Taboada, B., Jimenez-Jacinto, V., Salgado, H., Juárez, K., Contreras-Moreira, B., Huerta, A. M., Collado-Vides, J. and Morett, E. (2009) "Genome-wide identification of transcription start sites, promoters and transcription factor binding sites in *E. coli*." PLoS One **4**(10): e7526.

Merrick, M. J. (1993) "'In a class of its own - the RNA polymerase sigma factor σ^{54} (σ)." Molecular Microbiology **10**(5): 903-909.

Michelle, C. S., Sonia, K. M.-L., Kimberly, M. C. and Lynn, Z. (2011) "Expression of Multidrug Efflux Pump Genes *acrAB-tolC*, *mdfA*, and *norE* in *Escherichia coli* Clinical Isolates as a Function of Fluoroquinolone and Multidrug Resistance." Antimicrobial Agents and Chemotherapy **55**(2): 921-924.

Miller, P. F. and Sulavik, M. C. (1996) "Overlaps and parallels in the regulation of intrinsic multiple-antibiotic resistance in *Escherichia coli*." Molecular Microbiology **21**(3): 441-448.

Mills, G., Dumigan, A., Kidd, T., Hobley, L. and Bengoechea, J. A. (2017) "Identification and Characterization of Two *Klebsiella pneumoniae*." Infect Immun **85**(9): e00068-17.

Molodstov, V., Wang, C., Firlar, E., Kaelber, J.T. and Ebirght, R.H. (2022) "Structural basis of Rho-dependent transcription termination." bioRxiv **doi**: https://doi.org/10.1101/2022.08.29.505764.

Munita, J. M. and Arias, C. A. (2016) "Mechanisms of antibiotic resistance." Microbiology spectrum **4**(2): 10.

Murakami, K. S. (2013) "X-ray crystal structure of *Escherichia coli* RNA polymerase σ^{70} holoenzyme." The Journal of biological chemistry **288**(13): 9126-9134.

Murakami, K. S. and Darst, S. A. (2003) "Bacterial RNA polymerases: the wholo story." Current Opinion in Structural *Biology* 13(1): 31-39.

Murakami, K. S., Masuda, S., Campbell, E. A., Muzzin, O. and Darst, S. A. (2002) "Structural Basis of Transcription Initiation: An RNA Polymerase Holoenzyme-DNA Complex." Science **296**(5571): 1285-1290.

Munita, J.M. and Arias, C.A. (2016) 'Mechanisms of Antibiotic Resistance." Microbiol Spectr **4**(2).

Myers, K.S., Yan, H., Ong, I.M., Chung, D., Liang, K., Tran, F., Keleş, S., Landick, R. and Kiley, P.J. (2013) "Genome-scale analysis of escherichia coli FNR reveals complex features of transcription factor binding."PLoS Genet **9**(6): e1003565.

Navarre, W. W., Porwollik, S., Wang, Y., McClelland, M., Rosen, H., Libby, S. J. and Fang, F. C. (2006) "Selective Silencing of Foreign DNA with Low GC Content by the H-NS Protein in *Salmonella*." Science **313**(5784): 236-238.

Neuberger, A., Du, D. and Luisi, B.F. (2018) "Structure and mechanism of bacterial tripartite efflux pumps." Res Microbiol **169**(7-8): 401-41.

Nichols, R. J., Sen, S., Choo, Y. J., Beltrao, P., Zietek, M., Chaba, R., Lee, S., Kazmierczak, K. M., Lee, K. J., Wong, A., Shales, M., Lovett, S., Winkler, M. E., Krogan, N. J., Typas, A. and Gross, C. A. (2011) "Phenotypic landscape of a bacterial cell." Cell **144**(1): 143-56.

Nikaido, E., Giraud, E., Baucheron, S., Yamasaki, S., Wiedemann, A., Okamoto, K., Takagi, T., Yamaguchi, A., Cloeckaert, A. and Nishino, K. (2012) "Effects of indole on drug resistance and virulence of *Salmonella enterica* serovar Typhimurium revealed by genome-wide analyses." Gut pathogens 4(1): 5.

Nikaido, E., Shirosaka, I., Yamaguchi, A. and Nishino, K. (2011) "Regulation of the AcrAB multidrug efflux pump in *Salmonella enterica* serovar Typhimurium in response to indole and paraquat." Microbiology **157**(3): 648-655.

Nikaido, H. (1992) "Porins and specific channels of bacterial outer membranes." *Molecular Microbiology,* 6(4): 435-442.

Nikaido, H. (1994) "Prevention of drug access to bacterial targets: permeability barriers and active efflux." Science **264**(5157): 382-8.

Nikaido, H. and Pagès, J.M. (2012) "Broad-specificity efflux pumps and their role in multidrug resistance of Gram-negative bacteria." FEMS Microbiol Rev **36**(2): 340-63.

Nikaido, H. and Vaara, M. (1985) "Molecular basis of bacterial outer membrane permeability." Microbiological reviews **49**(1): 1-32.

Niland, P., Hühne, R. and Müller-Hill, B. (1996) "How AraC Interacts Specifically with its Target DNAs." Journal of Molecular Biology **264**(4): 667-674.

O'Neill, J. (2014) "Antimicrobial Resistance: Tackling a crisis for the health and wealth of nations." The Review on Antimicrobial Resistance.

O'Shea, R. and Moser, H. E. (2008) "Physicochemical properties of antibacterial compounds: implications for drug discovery." J Med Chem **51**(10): 2871-8.

Okusu, H., Ma, D. and Nikaido, H. (1996) "AcrAB efflux pump plays a major role in the antibiotic resistance phenotype of *Escherichia coli* multiple-antibiotic-resistance (Mar) mutants." Journal of Bacteriology **178**(1): 306-308.

Olsen, I. and Jantzen, E. (2001) "Sphingolipids in Bacteria and Fungi." *Anaerobe* **7**(2): 103-112.

Pan, X., Cen, Y., Kuang, M., Li, B., Qin, R. and Zhou, H. (2020) "Artesunate interrupts the self-transcriptional activation of MarA to inhibit RND family pumps of *Escherichia coli*." Int J Med Microbiol **310**(8): 151465.

Park, J.-S., Marr, M. T. and Roberts, J. W. (2002) "*E. coli* Transcription Repair Coupling Factor (Mfd Protein) Rescues Arrested Complexes by Promoting Forward Translocation." Cell **109**(6): 757-767.

Parker, C. T., Kloser, A. W., Schnaitman, C. A., Stein, M. A., Gottesman, S. and Gibson, B. W. (1992) "Role of the *rfaG* and *rfaP* genes in determining the lipopolysaccharide core structure and cell surface properties of *Escherichia coli* K-12." J Bacteriol **174**(8): 2525-38.

Pegues, J. C., Chen, L. S., Gordon, A. W., Ding, L. and Coleman, W. G. (1990) "Cloning, expression, and characterization of the *Escherichia coli* K-12 *rfaD* gene." J Bacteriol **172**(8): 4652-60.

Piddock, L. J. V. (2006) 'Multidrug-resistance efflux pumps? Not just for resistance." Nature Reviews Microbiology **4**(8): 629-636.

Pokharel, P., Dhakal, S. and Dozois, C.M. (2023) "The Diversity of Escherichia coli Pathotypes and Vaccination Strategies against This Versatile Bacterial Pathogen" Microorganisms **11**(2).

Pradel, E., Parker, C. T. and Schnaitman, C. A. (1992) "Structures of the *rfaB, rfaI, rfaJ*, and *rfaS* genes of *Escherichia coli* K-12 and their roles in assembly of the lipopolysaccharide core." J Bacteriol 174(14): 4736-45.

Pratt, L. A. and Silhavy, T. J. (1998) "Crl stimulates RpoS activity during stationary phase." Molecular Microbiology **29**(5): 1225-1236.

Pérez-Rueda, E. and Collado-Vides, J. (2000) "The repertoire of DNA-binding transcriptional regulators in *Escherichia coli* K-12." Nucleic acids research **28**(8): 1838-1847.

Qian, J., Garrett, T. A. and Raetz, C. R. (2014) "*In vitro* assembly of the outer core of the lipopolysaccharide from *Escherichia coli* K-12 and *Salmonella typhimurium*." Biochemistry **53**(8): 1250-62.

Raetz, C. R. and Dowhan, W. (1990) "Biosynthesis and function of phospholipids in *Escherichia coli*." J Biol Chem **265**(3): 1235-8.

Raetz, C. R. and Whitfield, C. (2002) "Lipopolysaccharide Endotoxins." Annual Review of Biochemistry **71**: 635-700.

Rahman, M., Rubayat Husan, M., Takahiro, O. and Kazuyuki, S. (2006) "Effect of *rpoS* Gene Knockout on the Metabolism of *Escherichia coli* During Exponential Growth Phase and Early Stationary Phase

Based on Gene Expressions, Enzyme Activities and Intracellular Metabolite Concentrations." Biotechnology and Bioengineering **94**(3): 585-595.

Randall, C.P., Mariner, K.R., Chopra, I. and O'Neill, A.J. (2013) "The target of daptomycin is absent from Escherichia coli and other gram-negative pathogens." Antimicrob Agents Chemother **57**(1): 637-9.

Randall, L. P. and Woodward, M. J. (2002) "The multiple antibiotic resistance (*mar*) locus and its significance." Research in veterinary science **72**(2): 87-93.

Rao, L., Ross, W., Appleman, J. A., Gaal, T., Leirmo, S., Schlax, P. J., Record, M. T. and Gourse, R. L. (1994) "Factor independent activation of *rrnB* P1. An "extended" promoter with an upstream element that dramatically increases promoter strength." J Mol Biol **235**(5): 1421-35.

Ray, B. L., Painter, G. and Raetz, C. R. (1984) "The biosynthesis of Gram-negative endotoxin. Formation of lipid A disaccharides from monosaccharide precursors in extracts of *Escherichia coli*." J Biol Chem **259**(8): 4852-9.

Renaud, C., Jacqueline, C., Claude, B., Jean-Marie, P. and Anne, D.-R. (2004) 'RamA Is an Alternate Activator of the Multidrug Resistance Cascade in *Enterobacter aerogenes*." Antimicrobial Agents and Chemotherapy **48**(7): 2518-2523.

Ricci, V. and Piddock, L. J. V. (2009) "Ciprofloxacin selects for multidrug resistance in *Salmonella enterica* serovar Typhimurium mediated by at least two different pathways." Journal of Antimicrobial Chemotherapy **63**(5): 909-916.

Roberts, J. W. (1969) "Termination Factor for RNA Synthesis." Nature **224**(5225): 1168-1174.

Robison, K., McGuire, A. M. and Church, G. M. (1998) "A Comprehensive Library of DNA-binding Site Matrices for 55 Proteins Applied to the Complete *Escherichia coli* K-12 Genome." Journal of Molecular Biology 284(2): 241-254.

Rodloff, A., Bauer, T., Ewig, S., Kujath, P. and Müller, E. (2008) "Susceptible, intermediate, and resistant - the intensity of antibiotic action." Dtsch Arztebl Int **105**(39): 657-62.

Rogers, H. J., Perkins, H. R. and Ward, J. B. (1980) Microbial cell walls and membranes. London: Chapman and Hall.

Rosenblum, R., Khan, E., Gonzalez, G., Hasan, R. and Schneiders, T. (2011) "Genetic regulation of the *ramA* locus and its expression in clinical isolates of *Klebsiella pneumoniae*." International Journal of Antimicrobial Agents **38**(1): 39-45.

Rosner, J. L., Dangi, B., Gronenborn, A. M. and Martin, R. G. (2002) "Posttranscriptional Activation of the Transcriptional Activator Rob by Dipyridyl in *Escherichia coli*." Journal of Bacteriology **184**(5): 1407-1416.

Rosner, J. L. and Slonczewski, J. L. (1994) "Dual regulation of *inaA* by the multiple antibiotic resistance (*mar*) and superoxide (*soxRS*) stress response systems of *Escherichia coli*." Journal of Bacteriology **176**(20): 6262-6269.

Ross, W., Gosink, K. K., Salomon, J., Igarashi, K., Zou, C., Ishihama, A., Severinov, K. and Gourse, R. L. (1993) "A third recognition element in bacterial promoters: DNA binding by the alpha subunit of RNA polymerase." Science **262**(5138): 1407-1413.

Ross, W., Vrentas, Catherine E., Sanchez-Vazquez, P., Gaal, T. and Gourse, Richard L. (2013) 'The Magic Spot: A ppGpp Binding Site on *E. coli* RNA Polymerase Responsible for Regulation of Transcription Initiation." Molecular Cell **50**(3): 420-429.

Ryan, M. D., Parkes, A. L., Corbett, D., Dickie, A. P., Southey, M., Andersen, O. A., Stein, D. B., Barbeau, O. R., Sanzone, A., Thommes, P., Barker, J., Cain, R., Compper, C., Dejob, M., Dorali, A., Etheridge, D., Evans, S., Faulkner, A., Gadouleau, E., Gorman, T., Haase, D., Holbrow-Wilshaw, M., Krulle, T., Li, X., Lumley, C., Mertins, B., Napier, S., Odedra, R., Papadopoulos, K., Roumpelakis, V., Spear, K., Trimby, E., Williams, J., Zahn, M., Keefe, A. D., Zhang, Y., Soutter, H. T., Centrella, P. A., Clark, M. A., Cuozzo, J. W., Dumelin, C. E., Deng, B., Hunt, A., Sigel, E. A., Troast, D. M. and DeJonge, B. L. M. (2021) " Discovery of Novel UDP-N-Acetylglucosamine Acyltransferase (LpxA) Inhibitors with Activity against *Pseudomonas aeruginosa*." J Med Chem **64**(19): 14377-14425.

Said, N., Krupp, F., Anedchenko, E., Santos, K. F., Dybkov, O., Huang, Y.-H., Lee, C.-T., Loll, B., Behrmann, E., Bürger, J., Mielke, T., Loerke, J., Urlaub, H., Spahn, C. M. T., Weber, G. and Wahl, M. C. (2017) "Structural basis for λN-dependent processive transcription antitermination." Nature Microbiology **2**(7): 17062.

Sagar, J. (2010) "Doxycycline in Clinical Medicine." Clinical Medicine Insights: Therapeutics **2**: 133-136.

Sangkee, R., Robert, G. M., Judah, L. R. and David, R. D. (1998) 'A Novel DNA-Binding Motif in MarA: The First Structure for an AraC Family Transcriptional Activator" *Proceedings of the National Academy of Sciences of the United States of America,* 95(18): 10413-10418.

Schleifer, K. H. and Kandler, O. (1972) "Peptidoglycan types of bacterial cell walls and their taxonomic implications." Bacteriol Rev **36**(4): 407-77.

Schmidt, M. C. and Chamberlin, M. J. (1987) '*nusA* protein of *Escherichia coli* is an efficient transcription terminator factor for certain termination sites." Journal of Molecular Biology **195**: 809-818.

Schnaitman, C. A. and Klena, J. D. (1993) "Genetics of lipopolysaccharide biosynthesis in enteric bacteria." Microbiology Rev. **57**: 655-682.

Schultz, S. C., Shields, G. C. and Steitz, T. A. (1991) "Crystal structure of a CAP-DNA complex: the DNA is bent by 90 degrees." Science **253**(5023): 1001-1007.

Scott, S., Busby, S. and Beacham, I. (1995) "Transcriptional co-activation at the *ansB* promoters: involvement of the activating regions of CRP and FNR when bound in tandem." Molecular Microbiology **18**(3): 521-531.

Seo, S.W., Kim, D., Latif, H., O'Brien, E.J., Szubin, R. and Palsson, B.O. (2014) "Deciphering Fur transcriptional regulatory network highlights its complex role beyond iron metabolism in Escherichia coli." Nat Commun **5**: 4910.

Seo, S. W., Kim, D., Szubin, R. and Palsson, B. O. (2015) "Genome-wide Reconstruction of OxyR and SoxRS Transcriptional Regulatory Networks under Oxidative Stress in *Escherichia coli* K-12 MG1655." Cell Rep **12**(8): 1289-99.

Seoane, A. S. and Levy, S. B. (1995) "Identification of new genes regulated by the *marRAB* operon in *Escherichia coli*." Journal of Bacteriology **177**(3): 530-535.

Shanmugakani, R. K., Fujiya, Y., Akeda, Y., Hamaguchi, S., Hamada, S. and Tomono, K. (2020) "Rapid multiplex detection of the resistance genes *mecA, vanA* and *vanB* from Gram-positive cocci-

positive blood cultures using a PCR-dipstick technique." Journal of medical microbiology **69**(2): 249-255.

Shaw, D. J., Rice, D. W. and Guest, J. R. (1983) "Homology between CAP and Fnr, a regulator of anaerobic respiration in *Escherichia coli*." Journal of Molecular Biology **166**(2): 241-247.

Sheetal, U., Svetlana, R. M., Ramesh, S. H. and Narendra, J. (2011) 'Cyclic AMP Receptor Protein Regulates *cspE*, an Early Cold-Inducible Gene, in *Escherichia coli*." Journal of Bacteriology **193**(22): 6142-6151.

Shimada, T., Ogasawara, H. and Ishihama, A. (2018) "Single-target regulators form a minor group of transcription factors in *Escherichia coli* K-12." Nucleic Acids Res **46**(8): 3921-3936.

Shimada, T., Ogasawara, H., Kobayashi, I., Kobayashi, N. and Ishihama, A. (2021) "Single-Target Regulators Constitute the Minority Group of Transcription Factors in" Front Microbiol **12**: 697803.

Shockman, G. D. and Holtje, J. V. (1994) "Microbial peptidoglycan (murein) hydrolases" in Ghuysen, J.M. and Hakenbeck, R. (eds.) Bacterial Cell Wall. Amsterdam: Elsevier: 131-166.

Silhavy, T. J., Kahne, D. and Walker, S. (2010) "The bacterial cell envelope." Cold Spring Harb Perspect Biol **2**(5).

Singh, S. S., Typas, A., Hengge, R. and Grainger, D. C. (2011) "*Escherichia coli* σ^{70} senses sequence and conformation of the promoter spacer region." Nucleic Acids Research **39**(12): 5109-5118.

Snyder, D. S. and McIntosh, T. J. (2000) "The lipopolysaccharide barrier: correlation of antibiotic susceptibility with antibiotic permeability and fluorescent probe binding kinetics." Biochemistry **39**(38): 11777-87.

Sohlenkamp, C. and Geiger, O. (2016) "Bacterial membrane lipids: diversity in structures and pathways." FEMS Microbiology Reviews **40**(1): 133-159.

Soisson, S. M., MacDougall-Shackleton, B., Schleif, R. and Wolberger, C. (1997) "Structural Basis for Ligand-Regulated Oligomerization of AraC." Science **276**(5311): 421-425.

Sonia, K. M.-L., Lauren Becnel, B., David, S. and Lynn, Z. (2009) "Mechanisms Accounting for Fluoroquinolone Resistance in *Escherichia coli* Clinical Isolates." Antimicrobial Agents and Chemotherapy **53**(1): 235-241.

Sorensen, P. G., Lutkenhaus, J., Young, K., Eveland, S. S., Anderson, M. S. and Raetz, C. R. (1996) "Regulation of UDP-3-O-[R-3-hydroxymyristoyl-N-acetylglucosamine deacetylase in *Escherichia coli*. The second enzymatic step of lipid a biosynthesis." J Biol Chem **271**(42): 25898-905.

Steitz, T. A. (1998) "A mechanism for all polymerases." Nature **391**(6664): 231-232.

Stevenson, G., Andrianopoulos, K., Hobbs, M. and Reeves, P. R. (1996) "Organization of the *Escherichia coli* K-12 gene cluster responsible for production of the extracellular polysaccharide colanic acid." J Bacteriol **178**(16): 4885-93.

Stevenson, G., Neal, B., Liu, D., Hobbs, M., Packer, N. H., Batley, M., Redmond, J. W., Lindquist, L. and Reeves, P. (1994) "Structure of the O-antigen of *Escherichia coli* K-12 and the sequence of its *rfb* gene cluster." J Bacteriol **176**(13): 4144-56.

Strauß, M., Vitiello, C., Schweimer, K., Gottesman, M., Rösch, P. and Knauer, S. H. (2016) "Transcription is regulated by NusA:NusG interaction." Nucleic Acids Research **44**(12): 5971-5982.

Stringer, A. M., Singh, N., Yermakova, A., Petrone, B. L., Amarasinghe, J. J., Reyes-Diaz, L., Mantis, N. J. and Wade, J. T. (2012) "FRUIT, a scar-free system for targeted chromosomal mutagenesis, epitope tagging, and promoter replacement in *Escherichia coli* and *Salmonella enterica*" PLoS One **7**(9): e44841.

Stuger, R., Woldringh, C. L., van der Weijden, C. C., Vischer, N. O., Bakker, B. M., van Spanning, R. J., Snoep, J. L. and Westerhoff, H. V. (2002) "DNA supercoiling by gyrase is linked to nucleoid compaction." Mol Biol Rep **29**(2): 79-82.

Sun, J., Deng, Z. and Yan, A. (2014) "Bacterial multidrug efflux pumps: Mechanisms, physiology and pharmacological exploitations." Biochemical and Biophysical Research Communications **453**(2): 254-267.

Swint-Kruse, L. and Matthews, K. S. (2009) "Allostery in the LacI/GalR family: variations on a theme." Current Opinion in Microbiology **12**(2): 129-137.

Tahar van der, S., Laurence, Z., Angela van, D., Donald, L. G., Riny, J. and Jaap, T. v. D. (2004) "*Salmonella enterica* Serovar Typhimurium RamA, Intracellular Oxidative Stress Response, and Bacterial Virulence." Infection and Immunity **72**(2): 996-1003.

Taliaferro, L. P., Keen, E. F., Sanchez-Alberola, N. and Wolf, R. E. (2012) "Transcription Activation by *Escherichia coli* Rob at Class II Promoters: Protein-Protein Interactions between Rob's N-Terminal Domain and the σ^{70} Subunit of RNA Polymerase." Journal of Molecular Biology **419**(3-4): 139-157.

Tamara A. Belyaeva , J. A. B., Nobuyuki Fujita , Akira Ishihama , Stephen J. W. Busby, Belyaeve, T. A., Bown, J. A., Fujita, N., Ishihama, A. and Busby, S. J. W. (1996) "Location of the C-Terminal Domain of the RNA Polymerase α Subunit in Different Open Complexes at the E*scherichia coli* Galactose Operon Regulatory Region." Nucleic Acids Research **12**: 2243-2251.

Tang, X., Chang, S., Qiao, W., Luo, Q., Chen, Y., Jia, Z., Coleman, J., Zhang, K., Wang, T., Zhang, Z., Zhang, C., Zhu, X., Wei, X., Dong, C., Zhang, X. and Dong, H. (2021) "Structural insights into outer membrane asymmetry maintenance in Gram-negative bacteria by MlaFEDB." Nat Struct Mol Biol **28**(1): 81-91.

Tavío, M. M., Aquili, V. D., Poveda, J. B., Antunes, N. T., Sánchez-Céspedes, J. and Vila, J. (2010) "Quorum-sensing regulator *sdiA* and *marA* overexpression is involved in *in vitro*-selected multidrug resistance of *Escherichia coli*." The Journal of antimicrobial chemotherapy **65**(6): 1178-1186.

Thamarai, S. and Stuart, B. L. (2006) "MarA-mediated Transcriptional Repression of the *rob* Promoter." Journal of Biological Chemistry **281**(15): 10049.

Thamarai, S., Teresa, M. B., Laura, M. M. and Stuart, B. L. (2004) "The *Escherichia coli* Transcriptional Regulator MarA Directly Represses Transcription of *purA* and hdeA." Journal of Biological Chemistry **279**(10): 9037.

Theuretzbacher, U., Outterson, K., Engel, A. and Karlén, A. (2020) "The global preclinical antibacterial pipeline." Nat Rev Microbiol **18**(5): 275-285.

Thota, S. S. and Chubiz, L. M. (2019) "Multidrug Resistance Regulators MarA, SoxS, Rob, and RamA Repress Flagellar Gene Expression and Motility in *Salmonella enterica* Serovar Typhimurium." J *Bacteriol* **201**(23).

Timo, B., Anne, B., Stephen, J. W. B. and Jeffrey, G. (2002) 'Transcription Activation by FNR: Evidence for a Functional Activating Region 2." Journal of Bacteriology **184**(21): 5855-5861.

Tollerson, R. and Ibba, M. (2020) "Translational regulation of environmental adaptation in bacteria." J Biol Chem **295**(30): 10434-10445.

Touchon, M., Hoede, C., Tenaillon, O., Barbe, V., Baeriswyl, S., Bidet, P., Bingen, E., Bonacorsi, S., Bouchier, C., Bouvet, O., Calteau, A., Chiapello, H., Clermont, O., Cruveiller, S., Danchin, A., Diard, M., Dossat, C., Karoui, M.E., Frapy, E., Garry, L., Ghigo, J.M., Gilles, A.M., Johnson, J., Le Bouguénec, C., Lescat, M., Mangenot, S., Martinez-Jéhanne, V., Matic, I., Nassif, X., Oztas, S., Petit, M.A., Pichon, C., Rouy, Z., Ruf, C.S., Schneider, D., Tourret, J., Vacherie, B., Vallenet, D., Médigue, C., Rocha, E.P. and Denamur, E. (2009) "Organised genome dynamics in the Escherichia coli species results in highly diverse adaptive paths." PLoS Genet **5**(1): e1000344.

Tschowri, N., Busse, S. and Hengge, R. (2009) "The BLUF-EAL protein YcgF acts as a direct anti-repressor in a blue-light response of *Escherichia coli*." Genes & development **23**(4): 522-534.

Tuomanen, E., Durack, D.T. and Tomasz, A. (1986) "Antibiotic tolerance among clinical isolates of bacteria." Antimicrob Agents Chemother **30**(4): 521-7.

Typas, A. and Hengge, R. (2006) 'Role of the spacer between the -35 and -10 regions in σ^s promoter selectivity in *Escherichia coli*" Molecular Microbiology **59**(3): 1037-1051.

Ubukata, K., Nonoguchi, R., Matsuhashi, M. and Konno, M. (1989) "Expression and inducibility in Staphylococcus aureus of the mecA gene, which encodes a methicillin-resistant S. aureus-specific penicillin-binding protein." J Bacteriol **171**(5): 2882-5.

Uehara, T. and Park, J. T. (2008) "Growth of *Escherichia coli*: significance of peptidoglycan degradation during elongation and septation." J Bacteriol **190**(11): 3914-22.

Ukah, U. V., Glass, M., Avery, B., Daignault, D., Mulvey, M. R., Reid-Smith, R. J., Parmley, E. J., Portt, A., Boerlin, P. and Manges, A. R. (2018) "Risk factors for acquisition of multidrug-resistant Escherichia coli and development of community-acquired urinary tract infections." Epidemiology and Infection **146**(1): 46-57.

Vaara, M. and Vaara, T. (1981) "Outer membrane permeability barrier disruption by polymyxin in polymyxin-susceptible and -resistant Salmonella typhimurium." Antimicrob Agents Chemother **19**(4): 578-83

Vance, D.E. and Vance, J.E. (1996) Biochemistry of lipids, lipoproteins, and membranes.

Velasco, J. M. S., Valderama, M. T. G., Margulieux, K. R., Diones, P. C. S., Reyes, A. M. B., Leonardia, S. G., Liao, C. P., Chua, D. A., Navarro, F. C. S., Ruekit, S., Fernandez, S., Macareo, L. R., Crawford, J. M. and Swierczewski, B. E. (2020) "First report of the mcr-1 colistin resistance gene identified in two *Escherichia coli* isolates from clinical samples, Philippines, 2018." Journal of Global Antimicrobial Resistance **21**: 291-293.

Ventola, C. L. (2015) "The antibiotic resistance crisis: part 1: causes and threats." P&T :a peer-reviewed journal for formulary management **40**(4): 277-283.

Vicente, M., Chater, K. F. and De Lorenzo, V. (1999) "Bacterial transcription factors involved in global regulation." Molecular Microbiology **33**(1): 8-17.

Vinué, L., McMurry, L. M. and Levy, S. B. (2013) "The 216-bp *marB* gene of the *marRAB* operon in *Escherichia coli* encodes a periplasmic protein which reduces the transcription rate of *marA*." FEMS Microbiology Letters **345**(1): 49-55.

Wang, Z., Wang, J., Ren, G., Li, Y. and Wang, X. (2015) "Influence of Core Oligosaccharide of Lipopolysaccharide to Outer Membrane Behavior of *Escherichia coli*." Mar Drugs **13**(6): 3325-39.

Warman, E. A., Forrest, D., Guest, T., Haycocks, J. J. R. J., Wade, J. T. and Grainger, D. C. (2021) "Widespread divergent transcription from bacterial and archaeal promoters is a consequence of DNA-sequence symmetry." Nat Microbiol **6**(6): 746-756.

Webber, M. A. and Piddock, L. J. V. (2003) "The importance of efflux pumps in bacterial antibiotic resistance." The Journal of antimicrobial chemotherapy **51**(1): 9-11.

Weber, H., Pesavento, C., Possling, A., Tischendorf, G. and Hengge, R. (2006) "Cyclic-di-GMP-mediated signalling within the σ^S network of *Escherichia coli*." Molecular Microbiology **62**(4): 1014-1034.

Weber, I. T. and Steitz, T. A. (1987) 'Structure of a complex of catabolite gene activator protein and cyclic AMP refined at 2.5 Å resolution." Journal of Molecular Biology **198**(2): 311-326.

Wehrli, W. (1983) "Rifampin: mechanisms of action and resistance." Rev Infect Dis **5**: s407-411.

Weisberg, R. A. and Gottesman, M. E. (1999) "Processive antitermination." Journal of Bacteriology **181**(2): 359-367.

Weiss, A., Moore, B. D., Tremblay, M. H. J., Chaput, D., Kremer, A. and Shaw, L. N. (2017) 'The ω Subunit Governs RNA Polymerase Stability and Transcriptional Specificity in *Staphylococcus aureus*" Journal of bacteriology **199**(2).

Whitfield, C., Heinrichs, D. E., Yethon, J. A., Amor, K. L., Montiero, M. A. and Perry, M. B. (1999) "Assembly of the R1-type core oligosaccharide of *Escherichia coli* lipopolysaccharide. " Journal of Endotoxin Research **5**(3): 151-156.

Wirth, T., Falush, D., Lan, R., Colles, F., Mensa, P., Wieler, L.H., Karch, H., Reeves, P.R., Maiden, M.C., Ochman, H. and Achtman, M. (2006) "Sex and virulence in Escherichia coli: an evolutionary perspective." Mol Microbiol **60**(5): 1136-51.

WHO (2017) Global priority list of antibiotic-resistant bacteria to guide research, discovery, and development of new antibiotics. Available at: https://www.who.int/medicines/publications/WHO-PPL-Short_Summary_25Feb-ET_NM_WHO.pdf?ua=1.

Wigneshweraraj, S., Bose, D., Burrows, P. C., Joly, N., Schumacher, J., Rappas, M., Pape, T., Zhang, X., Stockley, P., Severinov, K. and Buck, M. (2008) "Modus operandi of the bacterial RNA polymerase containing the σ^{54} promoter-specificity factor." Molecular Microbiology **68**(3): 538-546.

William, W., Balaram, G. and Asis, D. (1988) "NusA Protein is Necessary and Sufficient in vitro for Phage λ N Gene Product to Suppress a ρ -Independent Terminator Placed Downstream of nutL." PNAS **85**(8): 2494-2498.

Witz, G. and Stasiak, A. (2010) "DNA supercoiling and its role in DNA decatenation and unknotting." Nucleic acids research **38**(7): 2119-2133.

Wong, G. T., Bonocora, R. P., Schep, A. N., Beeler, S. M., Lee Fong, A. J., Shull, L. M., Batachari, L. E., Dillon, M., Evans, C., Becker, C. J., Bush, E. C., Hardin, J., Wade, J. T. and Stoebel, D. M. (2017) "Genome-Wide Transcriptional Response to Varying RpoS Levels in *Escherichia coli* K-12" Journal of bacteriology **199**(7).

Wood, T. I., Griffith, K. L., Fawcett, W. P., Jair, K. W., Schneider, T. D. and Wolf, R. E. (1999) "Interdependence of the position and orientation of SoxS binding sites in the transcriptional activation of the class I subset of *Escherichia coli* superoxide-inducible promoters." Molecular Microbiology **34**(3): 414-430.

Wu, J. and Weiss, B. (1991) "Two divergently transcribed genes, *soxR* and *soxS*, control a superoxide response regulon of *Escherichia coli*." *Journal of Bacteriology* **173**(9): 2864-2871.

Yang, Y., Darbari, V. C., Zhang, N., Lu, D., Glyde, R., Wang, Y., Winkelman, J., Gourse, R. L., Murakami, K. S., Buck, M. and Zhang, X. (2015) "Structures of the RNA polymerase-σ^{54} reveal new and conserved regulatory strategies." Science **349**(6250): 882-885.

Yang, Z.K., Luo, H., Zhang, Y., Wang, B. and Gao, F. (2019) "Pan-genomic analysis provides novel insights into the association of E.coli with human host and its minimal genome." Bioinformatics **35**(12): 1987-1991.

Yanning, Z. and Susan, G. (1998) "Regulation of Proteolysis of the Stationary-Phase Sigma Factor RpoS." Journal of Bacteriology **180**(5): 1154-1158.

Yarnell, W. S. and Roberts, J. W. (1999) "Mechanism of Intrinsic Transcription Termination and Antitermination." Science **284**(5414): 611-615.

Yethon, J. A., Heinrichs, D. E., Monteiro, M. A., Perry, M. B. and Whitfield, C. (1998) "Involvement of *waaY*, *waaQ*, and *waaP* in the modification of *Escherichia coli* lipopolysaccharide and their role in the formation of a stable outer membrane." J Biol Chem **273**(41): 26310-6.

Yethon, J. A., Vinogradov, E., Perry, M. B. and Whitfield, C. (2000) "Mutation of the lipopolysaccharide core glycosyltransferase encoded by waaG destabilizes the outer membrane of *Escherichia coli* by interfering with core phosphorylation." J Bacteriol **182**(19): 5620-3.

Yousef, M. A., Sylvie, B. and Axel, C. (2008) "*ramR* Mutations Involved in Efflux-Mediated Multidrug Resistance in *Salmonella enterica* Serovar Typhimurium." Antimicrobial Agents and Chemotherapy **52**(7): 2428-2434.

Yuzenkova, Y., Tadigotla, V. R., Severinov, K. and Zenkin, N. (2011) "A new basal promoter element recognized by RNA polymerase core enzyme." The EMBO Journal **30**(18): 3766-3775.

Zhang, G., Campbell, E. A., Minakhin, L., Richter, C., Severinov, K. and Darst, S. A. (1999) "Crystal Structure of *Thermus aquaticus* Core RNA Polymerase at 3.3 Å Resolution." Cell **98**(6): 811-824.

Zheng, D., Constantinidou, C., Hobman, J. L. and Minchin, S. D. (2004) "Identification of the CRP regulon using *in vitro* and *in vivo* transcriptional profiling." Nucleic acids research **32**(19): 5874-5893.

Zhou, P. and Hong, J. (2021) "Structure- and Ligand-Dynamics-Based Design of Novel Antibiotics Targeting Lipid A Enzymes LpxC and LpxH in Gram-negative Bacteria." Acc Chem Res **54**(7): 1623-1634.

Zhou, Y., Kolb, A., Busby, S. J. W. and Wang, Y.-P. (2014) "Spacing requirements for Class I transcription activation in bacteria are set by promoter elements." Nucleic acids research **42**(14): 9209-9216.

Zhu, A. Q. and von Hippel, P. H. (1998) "Rho-dependent Termination within the trp t‘ Terminator. I. Effects of Rho Loading and Template Sequence." Biochemistry **37**(32): 11202-11214.